Geological Survey of Finland

Bulletin 386

1.9 Ga tholeiitic magmatism and related Ni-Cu deposition in the Juva area, SE Finland

by Hannu V. Makkonen

Geological Survey of Finland
Espoo 1996

Geological Survey of Finland, Bulletin 386

1.9 Ga THOLEIITIC MAGMATISM AND RELATED Ni-Cu DEPOSITION IN THE JUVA AREA, SE FINLAND

by

HANNU V. MAKKONEN

with 67 figures, 20 tables, three appendices and an appended map

ACADEMIC DISSERTATION

GEOLOGICAL SURVEY OF FINLAND
ESPOO 1996

Makkonen, Hannu V. 1996. 1.9 Ga tholeiitic magmatism and related Ni-Cu deposition in the Juva area, SE Finland. *Geological Survey of Finland, Bulletin* 386. 101 pages, 67 figures, 20 tables, 3 appendices and an appended map.

The intrusions studied represent magma that for the most part intruded as broadly concordant, sill-like bodies within a predominantly metapelitic sequence derived from turbidites. In spite of subsequent deformation and metamorphism, the age of which constrains the timing of intrusion to around 1.9 Ga, it is thus apparent that the intrusions originally had horizontal or nearly horizontal orientations.

The parent magma to the intrusions was tholeiitic, with MgO abundances of 8 - 11 w-% and an Al_2O_3/TiO_2 ratio of around 10. Considerable variations in CaO/Al_2O_3 exist between intrusions due to variable degrees of contamination by crustal material. Olivine was the earliest and dominant cumulus mineral in all peridotite intrusions, followed by clinopyroxene in magmas relatively richer in CaO, or orthopyroxene and plagioclase in those magmas that were CaO-poor. On the basis of their respective mineralogy, the peridotites are accordingly classified as either wehrlites or lherzolites.

Some of the intrusions record a two-stage history, with crystallization having taken place initially within temporary magma chambers or flow conduits deeper in the crust prior to final emplacement into their present environments. Many of the intrusions contain a Ni-Cu occurrence, which is invariably situated within the stratigraphically basalmost parts of the intrusions. Separation of sulfide melt was presumably promoted by a combination of falling temperature and contamination. Evidence for contamination includes elevated LREE and Zr abundances and relatively low ε_{Nd}(1.88Ga) values between 0.4±0.3 and 2.4±0.4. The mass ratio of silicate melt to sulfide melt (log R) varied from 2.29 - 2.97 with $D_{Ni}^{sul/sil}$ ranging from 243 - 530. Ore compositions are in many cases strongly influenced by whole-rock chemistry of the host intrusions, indicating that ore formation has occurred in situ.

The Ni contents of magmatic olivine with Fo contents ranging from 66.12-84.78 m-% tend to be lower in mineralized intrusions than in barren intrusions. Other potential indicators of mineralization are Cu in olivine, Ni and Cu in orthopyroxene, Ni in chrome spinel, and whole-rock Ni abundances.

The Ni-Cu occurrences of the Juva district closely resemble other Svecofennian occurrences in Finland in terms of both overall composition and mode of occurrence. Most of the presently known occurrences in the Juva district are rather small, which is principally a function of the generally small sizes of the host intrusions themselves.

Key words (GeoRef Thesaurus, AGI): intrusions, igneous rocks, tholeiitic composition, peridotites, gabbros, metavolcanic rocks, geochemistry, olivine, orthopyroxene, chrome spinel, electron probe data, nickel ores, mineral deposits, genesis, magmatic differentiation, Proterozoic, Juva, Finland.

Hannu V. Makkonen, Geological Survey of Finland, P.O. Box 1237, FIN-70211 KUOPIO, FINLAND

ISBN 951-690-630-3
ISSN 0367-522X

Vammala 1996 Vammalan Kirjapaino Oy

CONTENTS

INTRODUCTION

Extensive mafic to ultramafic magmatism of age 1.9 Ga has been documented from many countries and is of particular interest because of its relationship to a number of major nickel provinces. In Finland the Kotalahti and Vammala nickel belts are the most important and best known representatives of such magmatic and ore-forming processes and have therefore accordingly been the traditional focus of exploration activity. The presence of certain geological features, including relatively high grade of metamorphism, with an abundance of schollen migmatites developed from pelitic sedimentary protoliths have long been regarded as enhancing the potential for intrusive-related nickel deposits. There are a number of areas of comparable metamorphic grade and composition elsewhere in the Svecofennian of Finland whose nickel potential has not been adequately assessed, one of these being the Juva district, which has been the subject of this study.

Location of study area and review of previous investigations

The study area is situated within the southern part of the Savo region, centered on the rural municipality of Juva but extending into the surrounding districts of Anttola, Haukivuori, Virtasalmi, Joroinen, Rantasalmi and Sulkava; for brevity the region will be referred to as the Juva district throughout this study.

Most of the study area lies within the borders of the Mikkeli 1:400 000 geological map (Sheet C2), published together with comprehensive explanatory notes by the then Geological Commission of Finland (Frosterus 1900, 1903), although the eastern part of the region extends into the area covered by the adjoining Savonlinna 1:400 000 map (Sheet D2, Hackman and Berghell, 1931; Hackman, 1933). The results of more recent mapping of the region at a scale of 1:100 000 have been published steadily since the 1960's, including the map sheets 3144-Sulkava (Lehijärvi, 1966) and 3142-Mikkeli (Simonen and Niemelä, 1980). Explanatory notes have been published for these two sheets (Korsman and Lehijärvi, 1973; Simonen, 1982), but are not yet available for the 3233-Rantasalmi (Korsman, 1973) or 3231-Haukivuori sheets (Pekkarinen and Hyvärinen, 1984).

Exploration activity in the Juva district commenced during the 1960's, when amateur prospectors discovered a number of samples containing Cu and Ni mineralization. This led to the discovery in 1964 and subsequent exploitation of the Virtasalmi copper deposit (Hyvärinen, 1969). Mining operations at Virtasalmi lasted from 1966 to 1983, while the small Kitula nickel deposit, near Puumala, which was originally discovered in 1951 (Marmo and Hyvärinen, 1951; Marmo, 1954; Hyvärinen, 1967), was mined out during 1970. The finding of numerous mineralized glacial erratics and bedrock showings since then has ensured continuing interest in the potential of the region (Makkonen and Ek-

dahl, 1988; Kontoniemi, 1989), with the Geological Survey of Finland and Outokumpu Exploration conducting most of the exploration activity.

The metamorphic history of the Juva district and surrounding regions has been the subject of intense study, and comprehensive results of metamorphic studies and their implications for bedrock evolution have been published by Korsman (1977), Korsman et al.(1984), Gupta and Johannes (1986), Korsman and Kilpeläinen (1986), Korsman et al. (1988), Kilpeläinen (1988) and Vaasjoki and Sakko (1988). Investigations into the origin of volcanic rocks in the Juva region were also carried out by the Geological Survey of Finland during the 1980's (Kousa, 1985; Viluksela, 1988). Some of the peridotitic rocks occurring in the region also formed the subject of a master's thesis (Pietikäinen, 1986).

Objectives and scope of the present study

The present study deals with the mafic and ultramafic rock units in the Juva district, together with related nickel and copper mineralization. Most of these occurrences have been found during exploration in the 1980's and very little published information is available. In addition to documentation, a major objective of the present study has been to determine the compositions and crystallization histories of the silicate melts and their bearing upon mineralization.

Because not all intrusions are mineralized, a further goal of the study has been to develop practical ways of using geochemistry to discriminate between barren and fertile intrusions, with emphasis being placed on criteria directly applicable in mineral exploration. The characteristics of Ni-Cu mineralization in the Juva district will also be compared with the two main Svecofennian Ni-Cu provinces in Finland, namely the Kotalahti nickel belt to the east, and the Vammala nickel belt to the west (Fig. 1).

Sample material and analytical methods

The material sampled has been collected during the course of ongoing exploration carried out in the region by the Geological Survey of Finland and for this reason drill core material is available for many of the targets. In other cases, sampling has been carried out with portable drilling equipment, or directly from fresh outcrops. Whole rock chemical analyses have been performed on samples from the diamond drill cores, or from samples obtained using the portable drill; in the latter case the upper 5 cm was always removed prior to sample preparation, in order to avoid any possible weathering or leaching effects. Samples were also taken for the purpose of preparing thin sections.

Where drill holes penetrated entire mafic and ultramafic units, samples were systematically analyzed so as to adequately represent the range of lithological variation present, and at intervals of 15-20 m in cases where lithology was more homogeneous. Similar criteria were applied to sampling in outcrop where possible.

A total of 327 whole rock analyses were made during the years 1982-1994. In addition to major elements, Cu, Ni, Zn, Cr and S were analyzed from all samples, along with a variable number of other trace elements. The results of some 1700 analyses from split meter-long intervals of mineralized drill core from various exploration targets were also made available. These all include data for Cu, Ni, Co and S, and in most cases Cr and Zn, while each target was analyzed in at least one place for Pd and Au; Pt was also analyzed

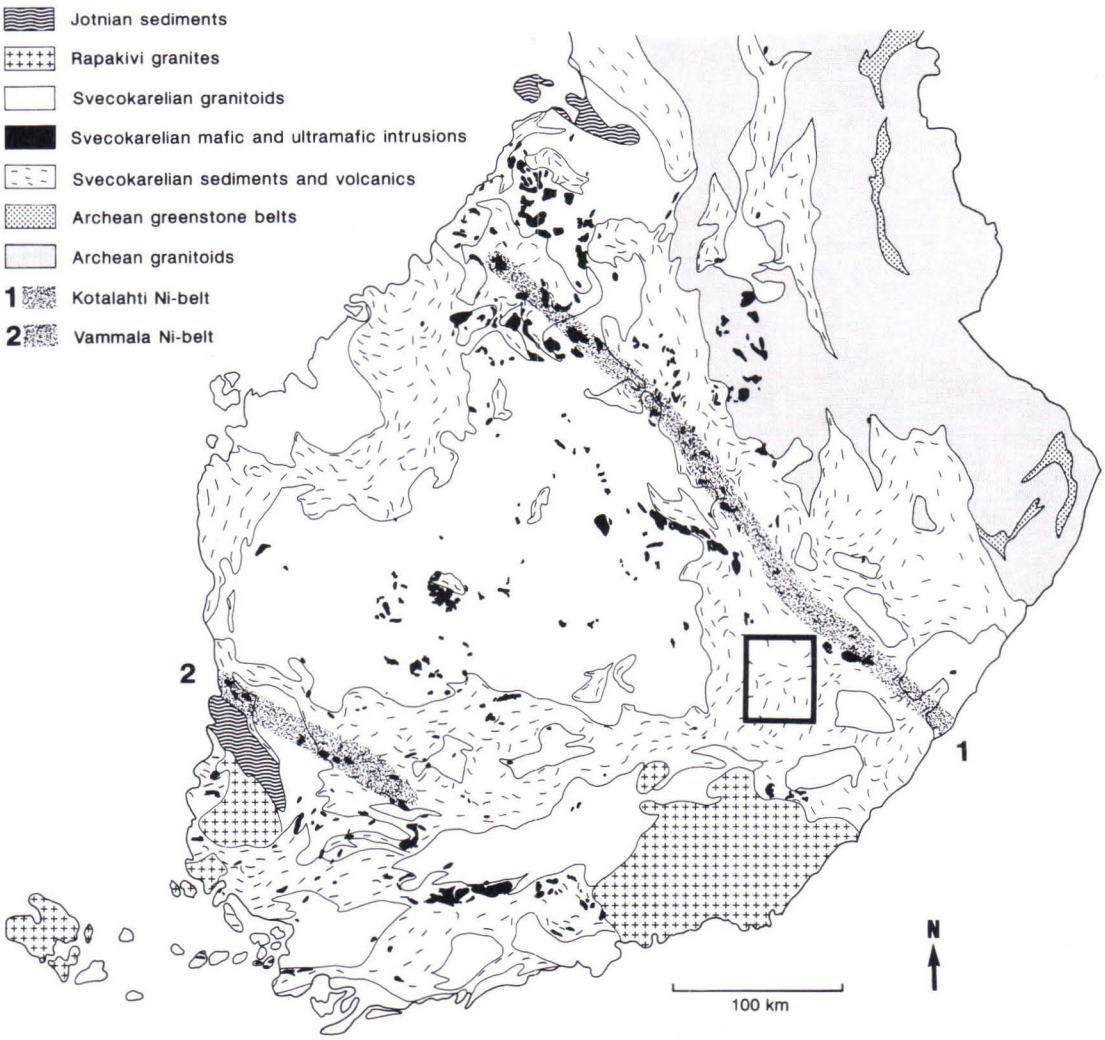

Fig. 1. Location of the study area on the geological map of Finland (outlined by rectangle). The map is modified after Simonen (1980) and Gorbunov and Papunen (1985), with the Kotalahti nickel belt after Gaál (1972) and Vammala nickel belt after Mäkinen (1987).

from selected intervals at each target and in one case PGE were analyzed more comprehensively.

The compositions of silicate minerals were determined quantitatively by electron microprobe studies of polished thin sections, with on average three grains of each mineral per thin section being analyzed. Olivine was analyzed whenever present but pyroxene was analyzed only from selected samples. During the earliest investigations, at the beginning of the 1980's, olivine was only routinely analyzed for Fe and Ni, but subsequently all major components were analyzed, along with Ni, Co and Cu.

In addition to the above mentioned analytical data, the present study has made use of a total of 93 whole rock chemical analyses and

74 microprobe analyses obtained from a number of publications and unpublished master's theses. In addition, results from a study of the Venetekemä intrusion near Pieksämäki (Mänttäri, 1988) have also been utilized.

All chemical analyses have been carried out at the chemical laboratory of the Geological Survey of Finland. Whole rock XRF analyses have been done on both fused beads and pressed powder pellets; Cu, Ni, Co and Zn were principally analyzed by FAAS (with aqua regia leaching), although some were done by a variety of methods including OES, XRF and S by sulfur analyzer. Gold and palladium were analyzed using GAAS (aqua regia leaching) and Au+Pt+Pd together by fire assay in combination with optical emission spectrometry, while REE and PGE were analyzed by ICP-MS (PGE nickel sulfide fire assay preconcentration).

Silicate microprobe analyses have been done on a JEOL Superprobe 733 and more recently on a Cameca Camebax SX 50 electron microprobe operated by the Department of Mineral Resources at the Geological Survey of Finland. Acceleration potential varied from 25-30 kV with a current strength of 50 or 100 nA. Systematic shifts in Ni abundances of silicates were observed between samples from different analytical runs at the beginning of the 1980's and for this reason, reference samples from each locality were reanalyzed in order to allow calculation of correction factors and facilitate comparison of the results. Reference material also included three samples that had previously been analyzed by the Outokumpu Ltd. laboratories in 1981; results were generally found to correlate well with one another although the Ni abundances of olivine tended to be somewhat lower in the Geological Survey analyses with a factor of 0.905.

Because peridotitic samples may contain an abundance of serpentine minerals, total element-oxide sums are commonly as low as 90 w-%, and in one case a total water content of 7.6 w-% was recorded. Therefore, in order that the chemical data might correspond better to the compositions of the protoliths prior to serpentinization, they have been recalculated on a volatile-free basis by normalization to a total sum of 100%, such that $SiO_2 + TiO_2 + Al_2O_3 + FeO_{total} + MnO + MgO + CaO + Na_2O + K_2O + P_2O_5 = 100$.

Some samples contain significant amounts of sulfur, so that it is necessary to consider that considerable amounts of Fe will be bound in sulfides rather than with oxygen in silicate minerals. Accordingly, Fe in sulfides is systematically subtracted from the total using the formula:

$FeO\% = FeO_{total}\% - 1.524*S\%$, assuming that pyrrhotite is the iron sulfide phase.

The results of olivine and pyroxene analyses have been evaluated after being recalculated according to the following procedure. Mean compositions were obtained by averaging the results from at least three grains from each thin section, with analyses being made as close as possible to center of each grain. Laboratory procedures in the early 1980's were such that Fe was the only major element routinely analyzed in olivine and pyroxene and therefore it has been necessary to infer olivine forsterite contents and pyroxene enstatite contents on the basis of respective iron abundances.

Assuming that forsterite + fayalite = 100, the following calculations are made:

$$Fo(m\text{-}\%) = \frac{10000 - 182.4427Fe(w\text{-}\%)}{100 - 0.5648Fe(w\text{-}\%)}$$

or when converted to oxide form:

$$Fo(m\text{-}\%) = \frac{10000 - 141.8127FeO(w\text{-}\%)}{100 - 0.4390FeO(w\text{-}\%)}$$

Likewise, in the case of pyroxene, enstatite + ferrosilite = 100 and hence:

$$En(m\text{-}\%) = \frac{10000\text{-}236.2368Fe(w\text{-}\%)}{100\text{-}0.5648Fe(w\text{-}\%)}$$

or when converted to oxide form:

$$En(m\text{-}\%) = \frac{10000\text{-}183.6269FeO(w\text{-}\%)}{100\text{-}0.4390FeO(w\text{-}\%)}$$

The validity of these formulae has been evaluated by comparing calculated Fo and En compositions against actual Fe and Mg measurements from selected olivine and pyroxene samples, and results of the comparison are shown in Figure 2. It is apparent from this that discrepancies are very small, and become significant only at low En compositions. For the purposes of this study however, samples with low calculated En contents have not been used.

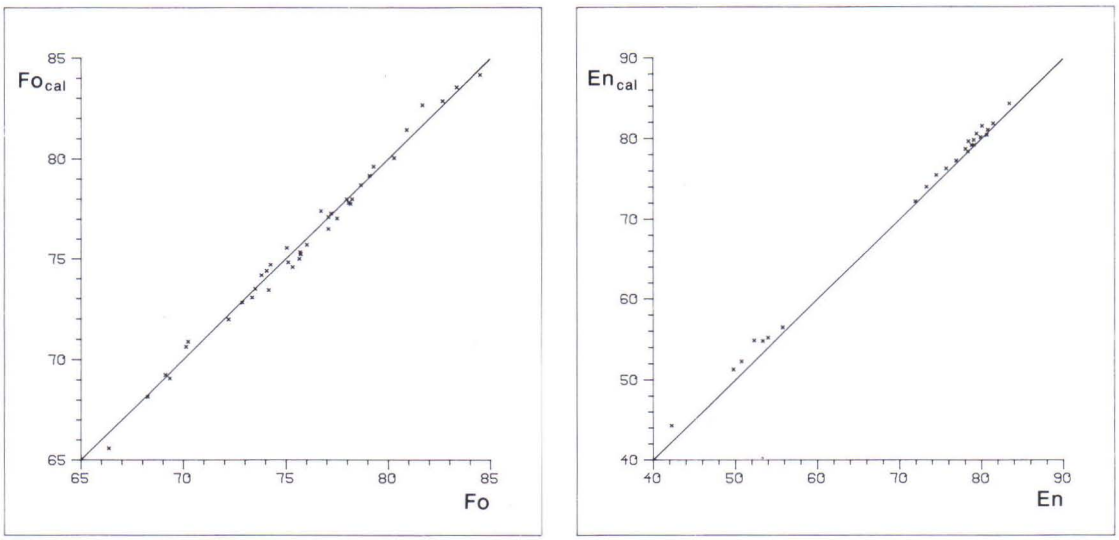

Fig. 2. En and Fo contents (m-%) calculated on the basis of Fe abundances (En_{cal} and Fo_{cal}) compared to those calculated on the basis of both Fe and Mg contents (En and Fo).

REGIONAL GEOLOGICAL SETTING

The supracrustal rocks of the Juva region fall within the broadly defined Svecofennian Supergroup of Luukkonen and Lukkarinen (1986), and lies partly within the southeastern part of the Raahe-Ladoga ore zone of Kahma (1973). According to Gaál (1986, 1990) and Ekdahl (1993), the Raahe-Ladoga zone represents an early Proterozoic collisional suture, in which case the Juva region would lie within the former site of the postulated subduction zone. The Kolkonjärvi shear zone (Gaál, 1972; Korsman et al., 1984), the formation of which was attributed to these processes by Gaál (1986), passes through the eastern part of the Juva district (Figs. 3 and 4). According to Piirainen (1987), the 1.9 Ga Svecofennian magmatism relates to rifting within an island arc setting, in which volcanism gradually progressed from initial felsic or bimodal volcanism to later mafic-dominated magmatism. In contrast, Lahtinen (1994) regarded the Ni-bearing intrusions in the Raahe-Ladoga zone as manifestations of within-plate magmatism post-dating arc-continent collision.

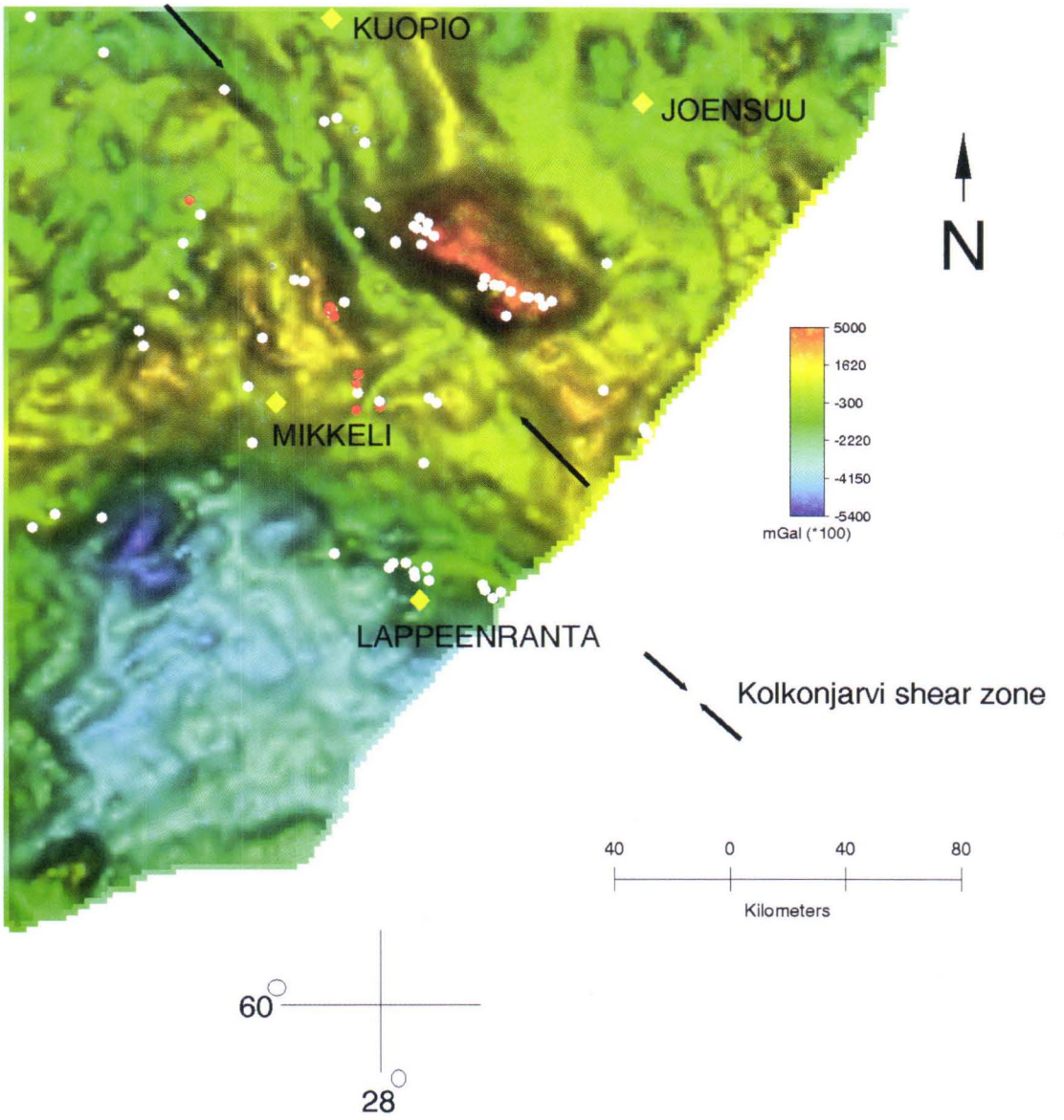

Fig. 3. Svecofennian Ni-Cu occurrences in southeastern Finland (circles, Puustinen et al., 1995). Occurrences with red circle are included in the present study. The map is a shaded relief Bouguer anomaly map made by J.Lerssi using data from the Finnish Geodetic Institute. (for more information on the gravimetric data see Elo, 1992)

The so-called Kotalahti nickel belt (Gaál, 1972) is clearly defined at a distance of some 15km to the northeast of the Kolkonjärvi shear zone, whereas a number of gold occurrences have been documented in closer proximity to the shear zone (Kontoniemi and Makkonen, 1991). The Kotalahti nickel belt is imaged clearly as a positive feature on the regional

Bouguer anomaly map, whereas the gold-bearing zone coincides with a regional negative anomaly. Thus, a major negative gravity anomaly is associated with the Kolkonjärvi shear zone and separates the Kotalahti nickel belt from nickel occurences of the Juva-Pieksämäki region (Fig. 3).

GEOLOGY OF THE JUVA DISTRICT

Lithological descriptions

The following generalized descriptions of the principal rock types in the Juva district are based on both published references and observations made by the author during a number of field seasons throughout the 1980's. A more detailed review of lithologies can be found in Makkonen (1992). Although all rocks in the Juva district, except for the youngest granite intrusions, have been metamorphosed, the prefix "meta-" will be omitted when referring to specific rock types throughout the text. A regional geological map of the Juva area is presented in the appended map.

Mica schists and mica gneisses are the predominant rock types throughout the Juva region. Their appearance and mineralogy vary greatly according to metamorphic grade; in the northern part of the area mica schists predominate and retain many of the primary sedimentary characteristics of turbidites, including grading, cross-bedding and slump structures (Gaál and Rauhamäki, 1971). Discontinuous intercalations of calc-silicate lithologies, sometimes containing scheelite as well as carbonate, are also abundant within the turbiditic sequences but are generally less than ten centimeters thick. Graphite-rich pelitic intercalations are also common.

With increasing metamorphic grade biotite becomes more obvious in pelitic lithologies and muscovite abundance decreases at the expense of andalusite and eventually K-feldspar, sillimanite, cordierite and garnet (Kilpeläinen, 1988); sillimanite in particular can locally be very abundant. Progressive changes in the mineralogy of psammitic rocks lead to the development of quartz-feldspar schists and gneisses. The overall appearance of the pelitic rocks changes radically where granitic and granodioritic dykes and leucosomes are present, with migmatitic veined gneisses locally becoming totally disrupted and forming schollen migmatites and diktyonites.

Some exceptional conglomeratic intercalations displaying cross bedding have also been found within the mica gneisses south of Kolkonjärvi; individual beds are about a meter thick and clasts are generally rounded with diameters less than 10 cm. Conglomerates containing clasts of igneous origin have also been found in the Haukivuori area (Korsman et al., 1988).

Marbles and other metamorphosed equivalents of chemical sediments are characteristic in the transitional zone between sediment-dominated mica gneisses and volcanic-dominated sequences and are particularly abundant in the northern part of the study area, where they can form continuous horizons comprising composite units up to 200 m thick (Makkonen, 1988). Pure carbonate horizons are however uncommon, skarn minerals and quartz-rich intercalations being typically present. Calsic horizons have also been reported from the Mikkeli and Sulkava map sheet areas (Simonen, 1982; Korsman, 1973).

Quartz-rich rocks are conspicuous within the Tutunen sequence (Pekkarinen, 1972), consisting principally of glassy quartz containing only sporadic carbonates but locally abundant sulfides. On the basis of overall appearance and the nature of associated rock

types, namely carbonates and iron formations, these have been interpreted as cherts. Individual layers may attain thicknesses of 10 m and similar lithologies have been reported from elsewhere within the same broad zone along strike from Tutunen, as in the Pirilä area (Makkonen and Ekdahl, 1988).

As noted above, iron formations are also locally present within this calc-silicate and chert association. Oxide facies formations seldom exceed 5 m in thickness and are represented by quartz-magnetite rocks that commonly also contain Fe-rich metamorphic minerals such as grunerite, diopside-hedenbergite and Fa-olivine. Iron formations that differ from the typical oxide facies units in having abundant garnet in addition to grunerite, or consist essentially of quartz and grunerite are considered to represent silicate facies deposits. Sulfide facies iron formations are well-developed within the Tutunen sequence, where compact pyrrhotite-rich layers up to several meters thick occur in association with the cherty layers. The Tutunen and Pirilä areas in general contain the best-developed iron formations in the region.

Volcanogenic rocks are predominantly mafic in composition and comprise elongate zones intruded by granitoids. Hornblende-bearing gneisses that are typically homogeneous, though sometimes banded due to variations in grain size, have generally been interpreted as intermediate volcanics. Primary depositional features are seldom seen because of intense foliation development and metamorphic recrystallization, although relict agglomeratic and porphyritic textures are sporadically preserved.

Clastic fragments within coarse volcaniclastic units are generally elongated, though still less then 10 cm in maximum dimension and are typically lighter in colour than their matrix, consisting mostly of hornblende and plagioclase. Plagioclase and uralitic hornblende after clinopyroxene are the most characteristic phenocrysts in porphyritic volcanogenic rocks and are usually less than 1 cm in size. The groundmass consists of hornblende, biotite, quartz and plagioclase. On the basis of all the above features, the intermediate rocks are regarded as having a predominantly pyroclastic origin.

Mafic volcanics are now represented by amphibolites, including diopside amphibolites. Relict pillow structures are still discernible in numerous places (Korsman, 1973; Kousa, 1985; Pietikäinen, 1986) and it is highly probable that most, if not all of the amphibolites and diopside amphibolites in the Juva district were originally submarine lava flows. Intense deformation has progressively obliterated pillow morphologies in many places however, resulting in a heterogeneous banded appearance. Even so, pillow structures may still be recognizable in highly deformed amphibolites when viewed perpendicular to the principal elongation lineation (cf. Pietikäinen, 1986).

Granoblastic quartz-feldspar gneisses are associated with the mafic volcanics and although no primary features relating to depositional processes have been recognized, local banding may attest to original bedding. Within the same general sequence in the Kolkonjärvi area felsic volcanic units are present and contain relict primary fragmental features that allow them to be interpreted as lapilli tuffs in which elongated felsic clasts generally less than 5 cm in size occur within a felsic to intermediate matrix.

Ultramafic volcanics and concordant sill-like intrusions are commonly associated with the mafic amphibolites. They have previously been described from the Rantasalmi area where they occur as both massive concordant units and discordant intrusions within the amphibolite sequences. Evidence for an extrusive origin for the concordant units is provided by the occasional presence of pillow structures and fragmental features, representing pyroclastic breccias and possibly also autobrecciation processes (Kousa, 1985).

Elongate *granodiorite and quartz diorite*

intrusions occur within the supracrustal rocks, often with broadly concordant contacts, whereas *tonalites* tend to form more equidimensional domal, though still concordant structures. The granodiorites and quartz diorites are typically foliated. Tonalitic intrusions are characteristic of the Kolkonjärvi area, where the largest discrete intrusions, the Tuusmäki and Osikonmäki plutons show mutually similar chemical and petrological features (Kontoniemi and Ekdahl, 1990).

Granites intrude all other rock types and exhibit considerable variations in grain size, with pegmatitic phases being rather common as veins and irregular elongate lenses. The finer grained granites tend to form more coherent rounded intrusions in both the northern and southern parts of the district. The Luonterivesi pluton is rather exceptional since it is of the same age as the granite intrusions even though it corresponds mineralogically to a granodiorite and quartz diorite (Korsman and Lehijärvi, 1973). None of these intrusions are foliated to any great extent.

Stratigraphical relationships and considerations

A number of different stratigraphical interpretations have been presented for the region. According to Hyvärinen (1969) the lowermost rocks at Virtasalmi are mica gneisses with graphitic schist intercalations, overlain successively by diopside- and quartz-feldspar gneisses including calc-silicate intervals, amphibolites, principally diopside amphibolites, and finally by more mica gneisses. A similar stratigraphical sequence was proposed for the Narila area by Pietikäinen (1986). Gaál and Rauhamäki (1971) concluded that in the Haukivesi district pelitic lithologies were lowermost, followed by mafic volcanics, now diopside amphibolites, with turbidites being uppermost. According to Simonen (1982) the quartz-feldspar gneisses and diopside amphibolites lie beneath the mica gneisses.

The present interpretation of the stratigraphical sequence in the Juva district is outlined below.

(youngest)
ultramafic volcanics
mafic volcanics (diopside amphibolites)
felsic volcanics (quartz-feldspar gneisses)
marbles, cherts, iron formations
mica gneisses and mica schists
(oldest)

Consistent transitions through sequence have been mapped at a number of independent locations in throughout the district, of which the more important observations and relationships include:

1: According to observations by Kousa (1985) and the present author, subvolcanic ultramafic rocks that are cogenetic with ultramafic lavas locally intrude the mafic volcanics;

2: The Rautjärvi ultramafic lava overlies mafic volcanics.

Mafic intrusions were clearly emplaced into the mica gneisses. Felsic intrusive rocks are obviously younger than the supracrustal sequence since syntectonic granitoids intrude both mafic and metasedimentary units and granites have intruded all other rock types, including the earlier granitoids.

A number of isotopic age determinations are available for rocks from the study area. Conventional U-Pb multigrain zircon data from metasediments in the mica schist area yield a discordant age falling between 2.2 and 2.3 Ga and nearer to 2.0 Ga within the garnet-cordierite-biotite zone, while in the area of highest metamorphic grade within the so-called Sulkava thermal dome, ages are as young as 1810-1833 Ma (Korsman et al., 1984; Vaasjoki and Sakko, 1988). That is, isotopic ages decrease with increasing metamorphic grade. According to Vaasjoki and Sakko (1988), detrital

zircons are probably ultimately derived from an Archean basement source even though much of the sediment could have been derived from younger rocks whose protoliths separated from the mantle between 2.10-1.91 Ga.

A felsic volcanic unit from near Joroinen has provided a zircon U-Pb age of 1906±4 Ma (Vaasjoki and Sakko, 1988). The U-Pb zircon age for the Tuusmäki tonalite is 1888±15 Ma (Korsman et al., 1984) and for the Osikonmäki tonalite 1887±5 Ma (Vaasjoki and Kontoniemi, 1991). Igneous clasts from the Haukivesi conglomerate also have ages of 1885±6 Ma (Korsman et al., 1988). The Hiltula granodiorite represents a younger age group, having an age of 1840±7 Ma (Vaasjoki and Kontoniemi, 1991). Two of the undeformed post-tectonic granitoids have been dated, the Luonterivesi granodiorite having a zircon U-Pb age of 1822±22 Ma and the Pirilä granite being 1815±7 Ma (Korsman et al., 1984).

Deformation and metamorphic history

The structural and metamorphic evolution of the southern Savo region has been the subject of active investigations, the results of which are highly relevant to the present study and will therefore be reviewed here in some detail.

According to Korsman et al. (1988) the Juva district is characterized by zones of increasing progressive metamorphism, with grade steadily increasing towards the Sulkava thermal dome. In addition to this zonal pattern, differential movement along major fault zones has led to a more complex distribution of blocks of varying metamorphic grade, in places exposing domains that experienced an even earlier granulite facies event. This earlier metamorphic event culminated prior to the end of D_2 deformation (before 1880 Ma), in contrast to the Sulkava zonal metamorphism which culminated during D_3 at 1830-1810 Ma. By this time the tectonometamorphic domains had assumed approximately their present form, although some late-D_3 shear zones locally truncate the metamorphic zonation.

Figure 4 is a tectonometamorphic map of the region showing in addition the style of folding in the different metamorphic blocks after Korsman et al. (1988). The boundaries of the Juva study area are also shown on the map. F_1 folds are tight and typically have amplitudes of 10-20 m with S_1 on fold limbs being almost parallel to lithological layering. F_2 folds also tend to be tight, though with wavelengths of the order of hundreds of meters. The S_2 schistosity is penetrative throughout the K-feldspar-sillimanite zone, while D_3 deformation is much less pervasive and represented by asymmetrical folds of variable wavelength and shear zones that locally disrupt metamorphic zoning. Therefore, D_3 is regarded as a mostly retrogressive event, with the last event recorded in the area being the regularly oriented D_4 crenulation cleavage (Kilpeläinen, 1988).

MAFIC AND ULTRAMAFIC LITHOLOGIES

The mafic and ultramafic rocks of the region fall into two broad categories, namely gabbros, pyroxenites and peridotites within the mica gneisses, and ultramafic lavas and sills that occur within the amphibolite zones. Rocks belonging to the first group have not been identified from the areas of lowest metamorphic grade, characterized by andalusite-muscovite and K-feldspar-sillimanite assemblages and even elsewhere they tend to be

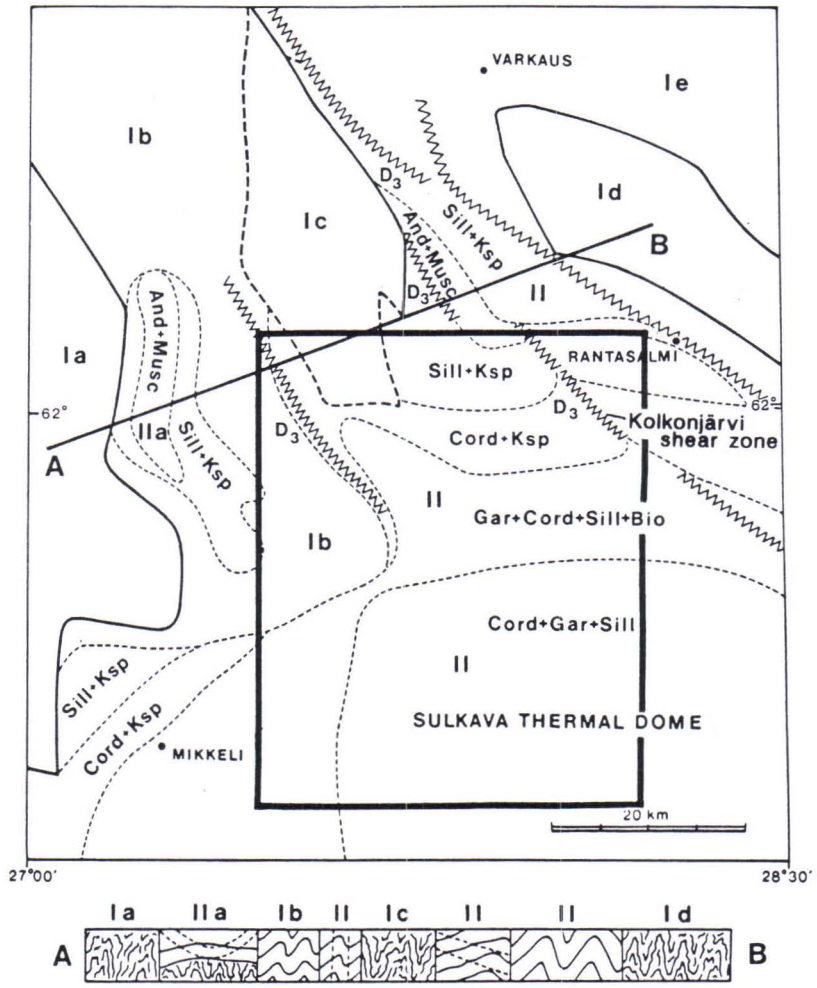

Fig. 4. Location of the study area on the tectonometamorphic map of southern Savo (Korsman et al., 1988).

irregularly distributed, occurring either as elongate zones, such as the gabbroic unit in the Luonterivesi-Heiskalanmäki area, or as local swarms of intrusions, as in the Saarijärvi and Lumpeinen areas (see the appended map).

The distribution of mafic and ultramafic rocks of the second type also tends to correlate broadly with metamorphic grade, since they occur preferentially within regions of lower metamorphic grade and invariably in association with amphibolites. It is reasonable therefore to infer that since these formed originally at high crustal levels and on the seafloor, and that their present metamorphic grade is less than that of the gabbroic and ultramafic intrusions, the two groups of mafic and ultramafic rocks represent different crustal levels juxtaposed during late stages of deformation. The distribution of the gabbroic and pyroxenitic and peridotitic intrusions therefore help in delineate deeper crustal sections, as can be appreciated from inspection of the appended map.

Luonteri-Heiskalanmäki zone

This is a N-trending zone of intrusions some 2 km wide and 15 km long situated on the western margin of the Sulkava thermal dome and consequently has been metamorphosed to granulite facies (Fig. 5). Surrounding gneisses are therefore characterized by garnet-cordierite-sillimanite assemblages. Intrusions at the northern end of the zone are generally larger than those at the southern end. Two intrusions, namely those at Hietajärvi and Rahijärvi, on the eastern side of the zone, are representative of the zone with respect to appearance and composition, despite being somewhat larger than the others. The Hietajärvi intrusion is about 5 km in length and attains a maximum width of 500 m, while the intrusions within the zone proper are elongate and broadly concordant with the regional S_2 schistosity and have maximum lengths of about 1.5 km and thickness invariably less than 200 m.

Compositionally the intrusions correspond predominantly to gabbros but more felsic differentiates are also commonly present, including diorites and quartz diorites. Post-metamorphic faults have typically disrupted the intrusions in many places (Fig. 5), particularly along an ENE trend which is also accentuated by variations in topographical features, with depressions occupied by strings of narrow lakes. This trend corresponds to the orientation of the F_4 fold axis as defined by Kilpeläinen (1988) and it is therefore in principle possible that they are coeval. On the other hand, they might relate instead to a clearly younger set of faults that transect the southern part of the zone with a prevailing orientation of about 030°.

As well as being concordant at outcrop scale, the contacts between the intrusions and the wall-rock gneisses are generally sharp. Sometimes however, gneissic enclaves are present within the gabbro near the contact, which provides direct evidence of their intrusive origin. Moreover, the presence of granitic veins along the contact in many places indicates that the margins of the intrusions were the subject to preferential deformation, a conclusion that is consistent with the generally more intense foliation development in the intrusions approaching their margins. Partly for this reason it has not been possible to establish whether the intrusions originally had chilled margins.

The same deformational events that affected the country rock gneisses can be recognized within the intrusions, with a well-developed S_2 schistosity being the oldest major fabric identified. In the case of very narrow intrusions, the intensity of foliation development is such that the rock has an almost gneissic appearance. These observations demonstrate that the intrusions predate D_2 and hence they cannot have been intruded after 1880 Ma.

Slight differences in mineralogy and appearance occur between different intrusions but in outcrop they all appear rather leucocratic due to the relative abundance of plagioclase and orthopyroxene; on weathered surfaces the latter mineral has a distinctive pale brown colour. Hornblende is therefore readily distinguished from other principal mineral phases because of its contrasting dark colour.

Dominant mineral assemblages consist of plagioclase-orthopyroxene-biotite-hornblende, plagioclase-orthopyroxene-biotite and plagioclase-orthopyroxene-hornblende. Figure 6a shows a typical gabbro from the Luonteri-Heiskalanmäki zone, in which plagioclase occurs as anhedral grains less than 6 mm in size and orthopyroxene forms recrystallized elongate porphyroblasts oriented parallel to the foliation (Fig. 6b). Hornblende is commonly intergrown with orthopyroxene, although not coaxially; usually it is possible to demonstrate that orthopyroxene has grown metamorphically and later than hornblende. Flakes of biotite in turn are oriented discord-

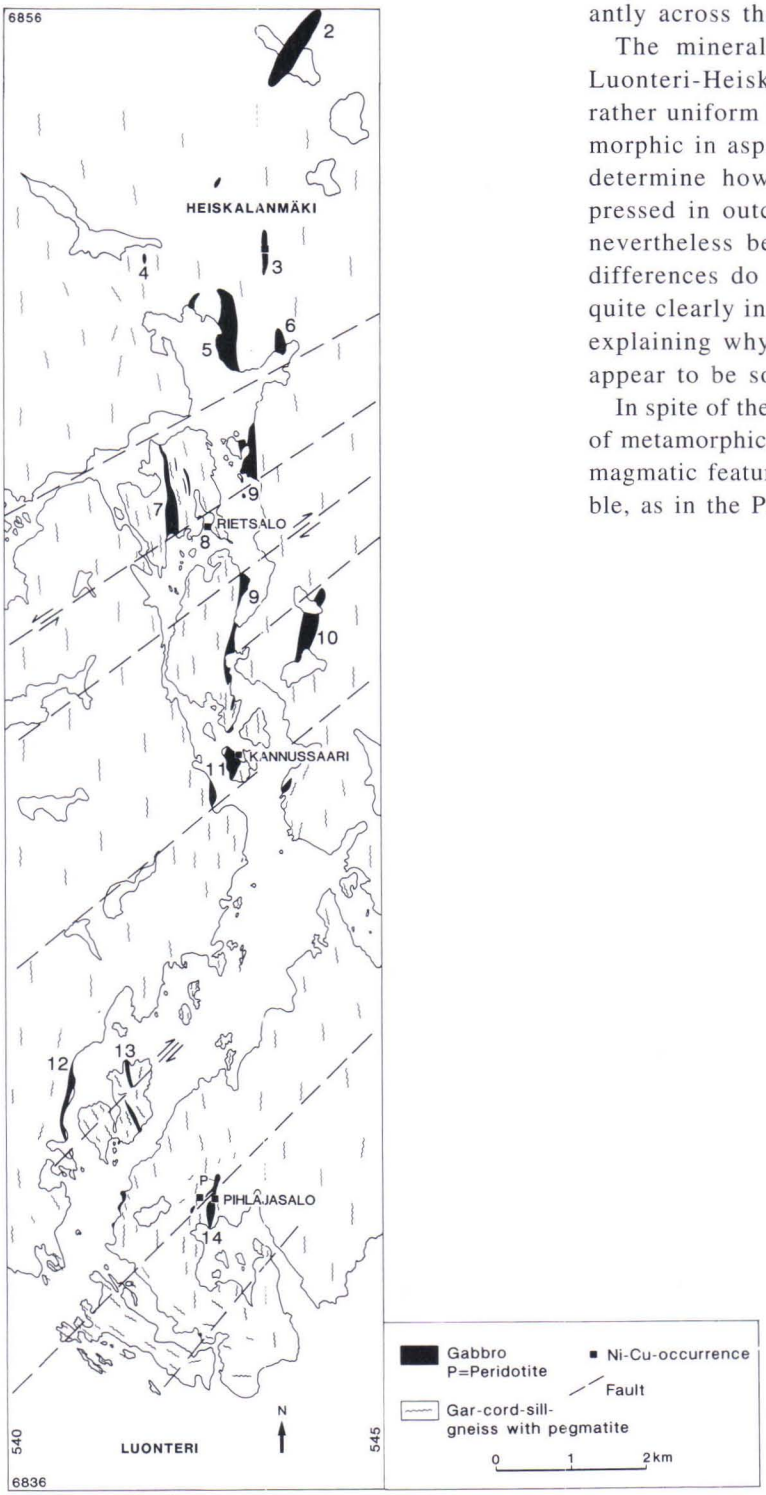

antly across the pyroxene alignement.

The mineralogy of the intrusions in the Luonteri-Heiskalanmäki zone is therefore rather uniform throughout the zone and metamorphic in aspect, making it very difficult to determine how chemical variations are expressed in outcrop or in thin section. It will nevertheless be demonstrated later that such differences do exist and are indeed reflected quite clearly in mineral compositions, thereby explaining why specific mineral assemblages appear to be so widespread.

In spite of the intense deformation and degree of metamorphic recrystallization, relict primary magmatic features are still sometimes discernible, as in the Pihlajasalo gabbro (Fig. 7).

Fig. 5. Luonteri-Heiskalanmäki zone. Intrusions: 2 = Alanen, 3 = Heiskalanmäki, 4 = Syömäjärvi, 5 = Kolkanranta, 6 = Virmaanlahti, 7 = Rietsalo, 8 = Rietsalo BH303, 9 = Kololahdenselkä, 10 = Vekarainen, 11 = Siikavesi, 12 = Rantavuori, 13 = Siikasaari, 14 = Pihlajasalo.

a)

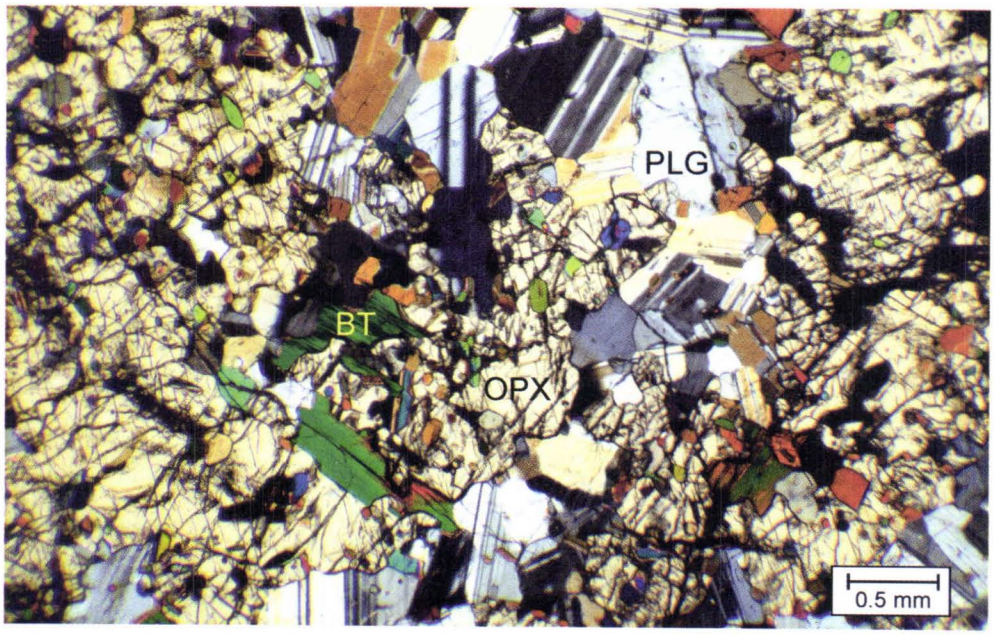

b)

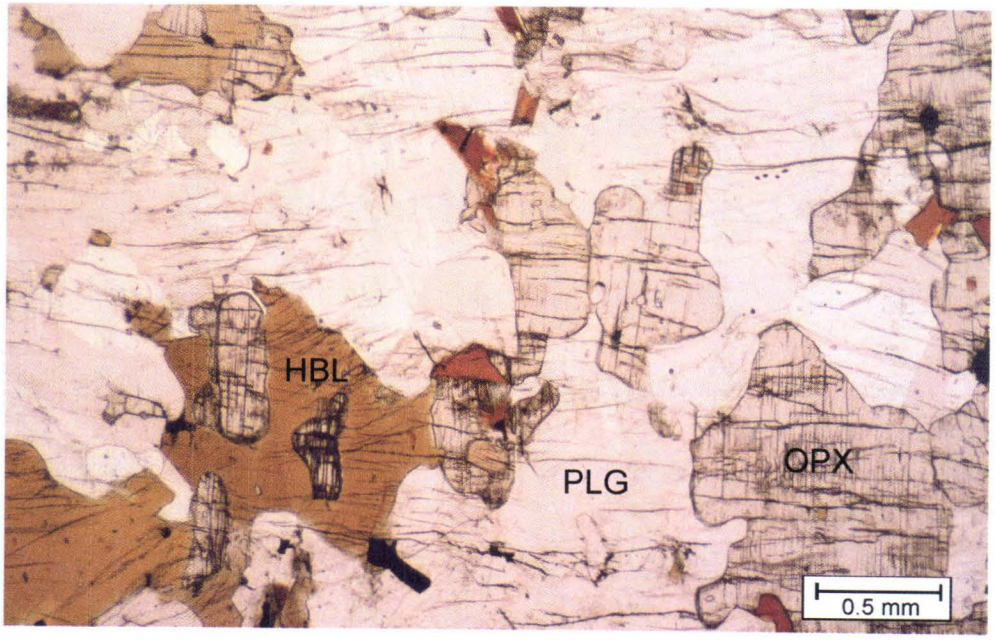

Fig. 6. Representative samples from the Luonteri-Heiskalanmäki zone. a) Typical gabbro, Siikavesi, KJP-83-123.2, crossed nicols. b) Orthopyroxene porphyroblasts oriented parallel to the foliation, Rietsalo, BH301/41.00, single nicol. Photos K.Kojonen. opx = orthopyroxene, bt = biotite, plg = plagioclase, hbl = hornblende.

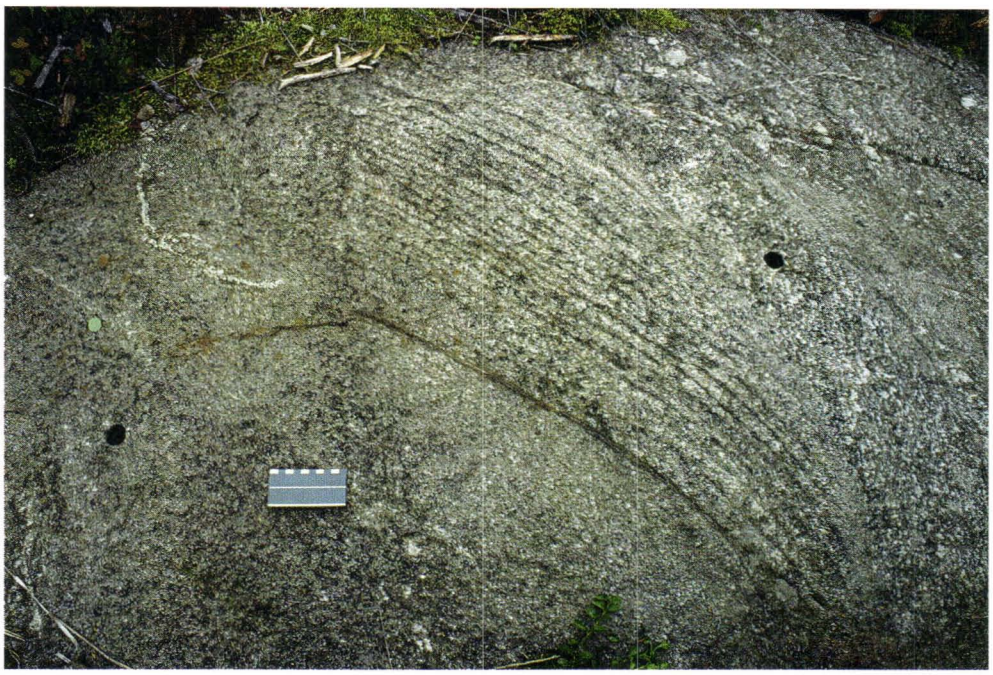

Fig. 7. Cross-bedded layering in the Pihlajasalo gabbro, HVM-92-10. Length of the scale bar is 10 cm. Photo J.Väätäinen.

Peridotites

Peridotitic intrusions consist of weakly differentiated olivine cumulates or olivine-orthopyroxene cumulates that display sharp, commonly tectonic contacts with surrounding mica gneisses or gabbros. They have been deformed together with the enclosing lithologies and the earliest fabric identified in them is the regional S_2 foliation. The intrusions studied are less than 1 km in length and do not exceed 200 m in thickness. Primary mineralogy in some intrusions has been substantially modified by metamorphic recrystallization, with orthopyroxene forming distinct porphyroblasts. Despite this, sufficient relict grains and textures remain to enable classification using the scheme of Streckeisen (1975), on the basis of which the peridotites can be termed *wehrlites* and *lherzolites*. Of the peridotitic intrusions studied, those at Lumpeinen and Turunen are classed as wehrlites.

The main minerals present in the wehrlites are olivine (± serpentine), clinopyroxene and clinoamphibole. Olivine occurs as euhedral or nearly euhedral cumulus grains that display variable amounts of serpentinization (Fig. 8). In addition to olivine, chromite is also sometimes present as a cumulus phase. Clinopyroxene occurs predominantly as an intercumulus mineral although it has generally been almost entirely replaced by clinoamphibole. The Lumpeinen wehrlite body also contains sporadic layers of pyroxenite. On the basis of relative proportions of cumulus and intercumulus minerals most of the wehrlites are classified as orthocumulates using the criteria of Irvine (1982).

The dominant minerals in the lherzolitic intrusions are olivine (± serpentine), orthopyroxene, clinoamphibole and occasionally clinopyroxene as well. Olivine and orthopy-

a)

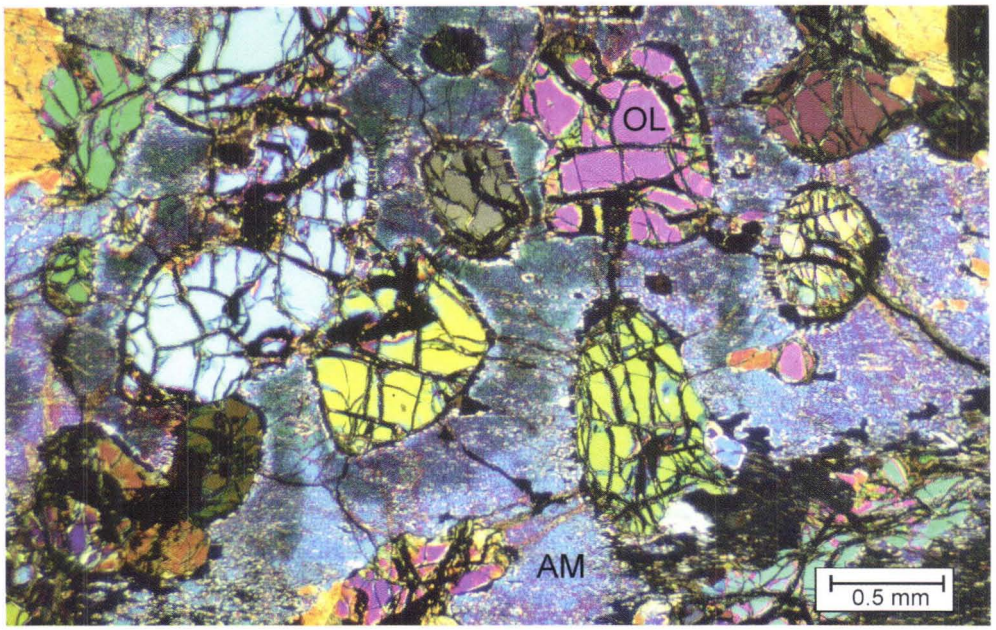

b)

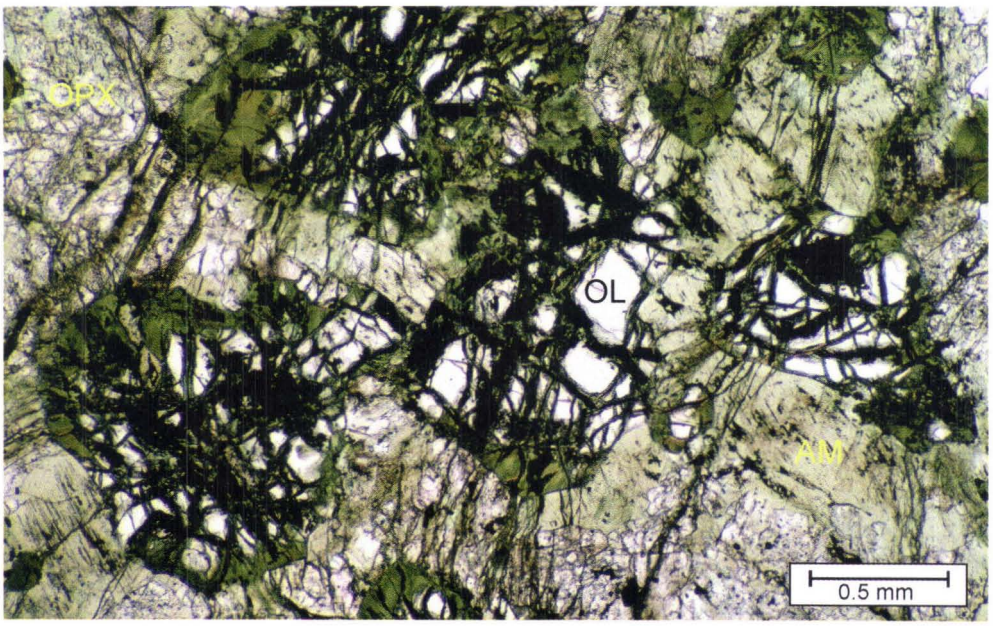

Fig. 8. a) Poikilitic olivine orthocumulate, Turunen, BH14/16.10, crossed nicols. b) Olivine orthocumulate, Lumpeinen, BH373/81.00, single nicol. Photos K.Kojonen.
ol = olivine, am = clinoamphibole, cpx = clinopyroxene.

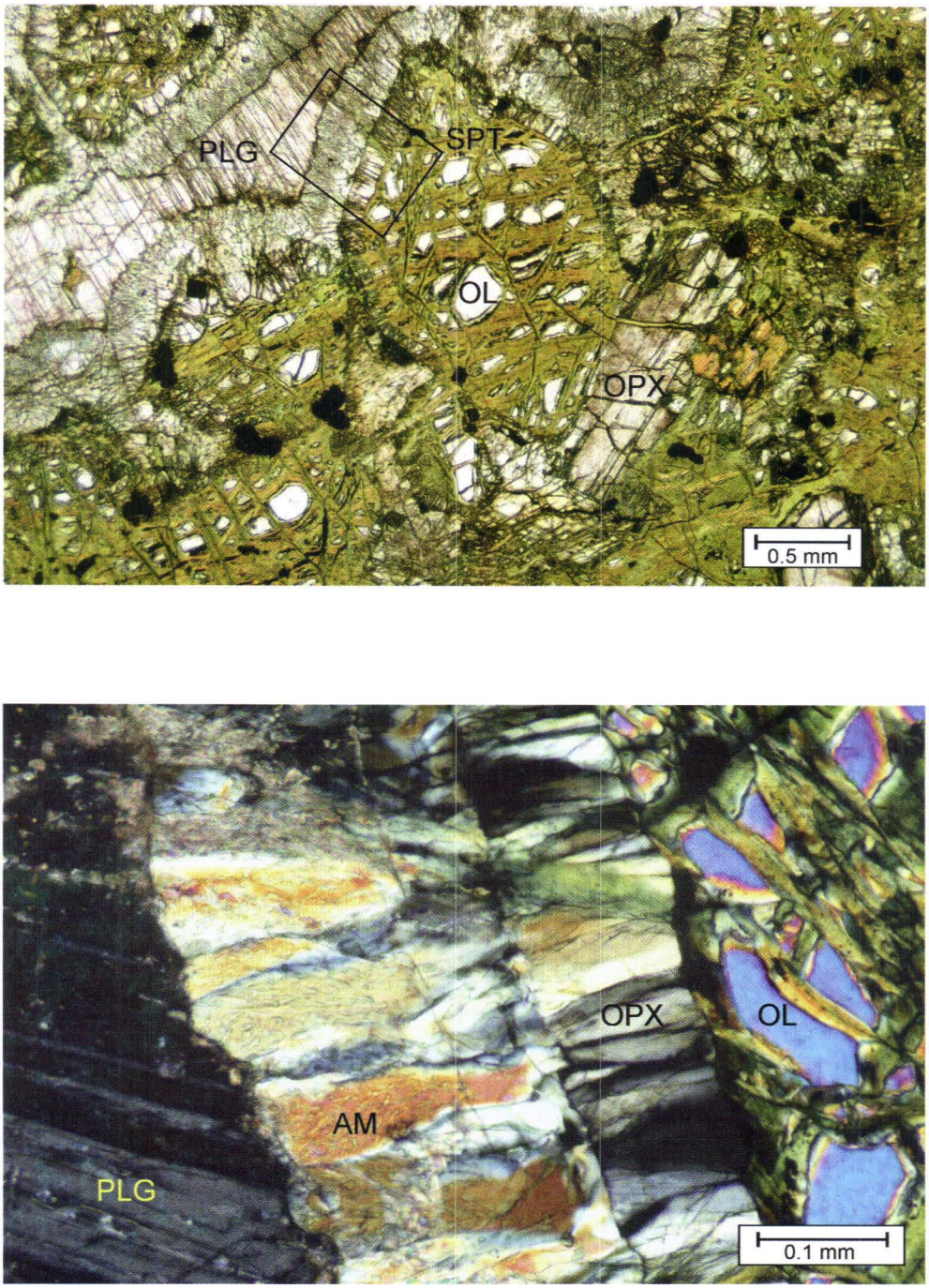

Fig. 9. a) Almost totally serpentinized olivine grain surrounded by a reaction corona of orthopyroxene and clinoamphibole, Saarijärvi, BH359/10.20, single nicol. b) Magnification of the corona (the area outlined by the rectangle in photo a), crossed nicols. Photos K.Kojonen.
spt = serpentine, other abbreviations as in Figures 6 and 8.

roxene occur as primary cumulus phases, as does accessory chromite. The degree of serpentinization of olivine varies just as in the wehrlites. Intercumulus phases are clinoamphibole, which is a replacement product after clinopyroxene, and plagioclase. On the basis of the relative proportions of cumulus and intercumulus phases, the lherzolites can generally be regarded as mesocumulates.

Olivine grains display reaction corona textures when they are in contact with either plagioclase or clinopyroxene (Fig. 9). The coronas are composite, consisting of an inner 0.1-0.2 mm wide zone of orthopyroxene surrounded by an outer zone 0.2-0.4 mm wide consisting of clinoamphibole. In both zones the corona minerals have grown such that their c-axes are oriented towards the centers of the olivine grains. Serpentinization has clearly taken place after the formation of the corona textures since in some cases the orthopyroxene within the inner zone has also been partially serpentinized. Where olivine is in contact with clinopyroxene coronas consist exclusively of orthopyroxene, the outer clinoamphibole corona being absent.

The formation of the corona textures can be explained by the following reaction:

$$\underset{\text{OL}}{2Mg_2SiO_4} + \underset{\text{PLG}}{CaAl_2Si_2O_8} \rightarrow \underset{\text{CPX}}{CaMgSi_2O_6} + \underset{\text{OPX}}{2MgSiO_3} + \underset{\text{SPI}}{MgAl_2O_4}$$

If water is present as a reactant, then amphibole can also form (Deer et al., 1982).

Plagioclase has generally been totally consumed by the corona-forming reactions in these rocks so that the interstices between olivine grains have been filled with intergrowths of the various reaction products (Fig. 10). The corona textures are believed to have

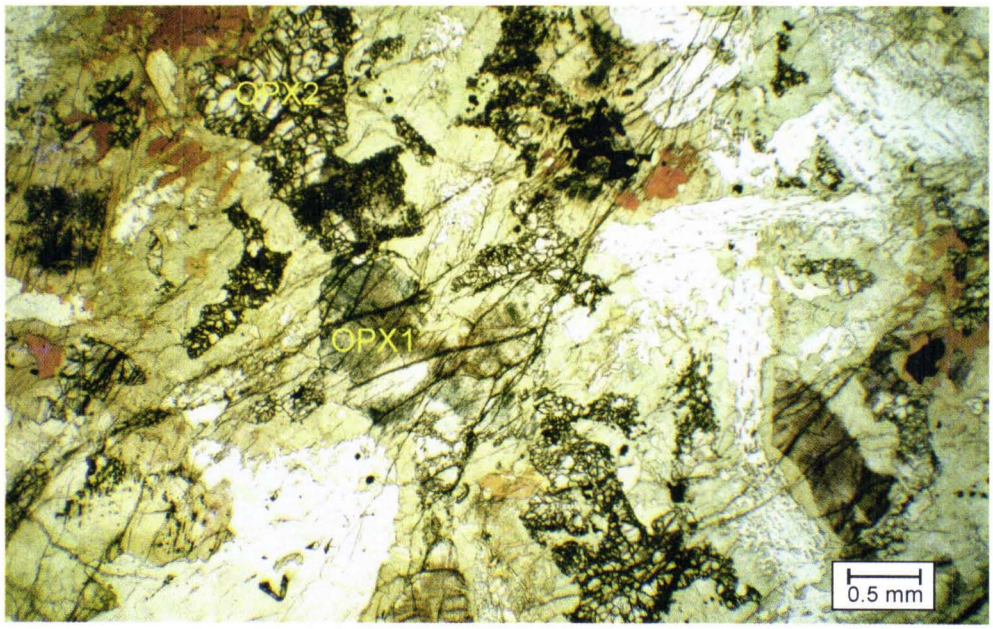

Fig. 10. Intercumulus orthopyroxene (opx 1) and orthopyroxene formed by the reaction between olivine and plagioclase (opx 2), Kekonen, BH346/32.90, single nicol. Photo K.Kojonen.

formed during regional metamorphism at relatively high pressures (6-11 kbar) while the intrusion was cooling under subsolidus conditions. They also provide distinctive evidence in favour of a primary igneous origin for the olivine (Deer et al., 1982).

Intrusions in the study area that can be classified as lherzolites include Saarijärvi N, Saarijärvi S, Niinimäki E, Niinimäki W, Pihlajasalo and Venetekemä.

The Saarijärvi and Niinimäki peridotites outcrop within several different parts of predominantly gabbroic host intrusions, after which they have been named. It is noteworthy that the Saarijärvi peridotites contain exceptionally abundant apatite, up to nearly 5 vol-% of the rock. The Pihlajasalo and Venetekemä peridotites contain appreciably less orthopyroxene than the Saarijärvi and Niinimäki peridotites. The outermost 5-20 m at the margins of the Pihlajasalo and Venetekemä peridotites consist of olivine-bearing orthopyroxene-amphibole rock that is also somewhat finer-grained than the central parts of the intrusions.

Differentiated intrusions

This group of intrusions includes those that vary in composition from peridotitic through to gabbroic as a result of magmatic differentiation processes. Gabbros predominate over peridotites and the intrusions are generally relatively small, being less than 600 m in length and 100 m in thickness. They are typically enclosed within mica gneisses and show the same deformational history, including fabrics related to both D_2 and D_3. Contacts with the mica gneisses are sharp, although gneissic enclaves are sometimes found within the marginal parts of the intrusions.

The differentiation sequence is as follows:

lherzolite - olivine gabbronorite - pyroxene-hornblende-gabbronorite - hornblende gabbro

The peridotites in these intrusions thus correspond to the previously discussed group of peridotites with respect to mineralogy except that olivine is less abundant. Accordingly they are best classified as olivine-orthopyroxene cumulates using the terminology of Irvine (1982). As plagioclase abundances increase the lherzolites progressively change to olivine gabbronorites, pyroxene-hornblende gabbronorites and ultimately hornblende gabbros. Olivine in the lherzolitic parts of the intrusions has often been totally replaced by metamorphic orthopyroxene, due to reaction between olivine and plagioclase (Fig. 10).

Within the Juva district Kekonen and Kiiskilänkangas can be classified as differentiated intrusions.

Ultramafic volcanics and sills

All of the ultramafic rocks in this group occur as concordant sills or lava flows within more extensive amphibolite zones. Individual ultramafic horizons can be traced for distances of several kilometers in some instances and may be up to 100 meters in thickness. In some places it can be demonstrated that they are intrusive into the amphibolites. Ultramafic sills have also been found in association with gabbros. Contacts between ultramafic rocks and adjacent lithologies are generally sharp.

On weathered surfaces the ultramafic rocks tend to be greyish dark green or black, depending upon which of the major minerals predominate. Within the K-feldspar-sillimanite zone, as at Pirilä (Viluksela, 1988), ultramafic rocks are fine-grained and typical metamorphic assemblages include tremolitic or ac-

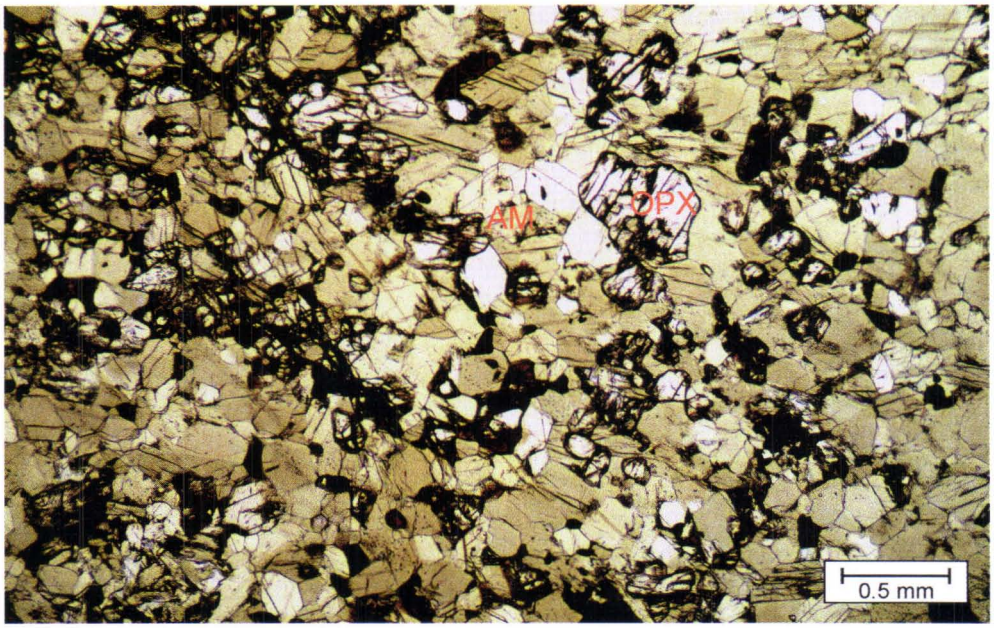

Fig. 11. Ultramafic lava in the garnet-cordierite-sillimanite-biotite zone, Rautjärvi, HVM-83-1.3, single nicol. Photo K.Kojonen. Abbreviations as in Figures 6 and 8.

tinolitic amphibole or hornblende and olivine. In areas of higher metamorphic grade, grain size tends to be larger and orthopyroxene porphyroblasts are ubiquitous, accompanied by olivine and tremolitic-actinolitic amphibole or hornblende (Fig. 11). Green spinel is a typical accessory mineral in the ultramafic rocks.

The ultramafic rocks sometimes exhibit sharply defined layering and the layered Rautjärvi ultramafic lava unit contains individual layers that vary in thickness from 0.4 m to over 10 m. The layers differ from one another with respect to both grain size and texture. Variations in mineralogical and chemical composition are small but nevertheless sufficient as to be reliable indicators of the bases of individual layers. For example Mg-number and MgO systematically increase towards the bases of layers and it can therefore be concluded that the ultramafic rocks stratigraphically overlie the amphibolites (see Makkonen, 1992).

Internal stratigraphy

It is sometimes possible to determine the internal stratigraphy of the intrusions on the basis of relative proportions of relict igneous minerals but in most cases the internal variation is either too small or too much of the primary mineralogy has been destroyed or modified. In the following discussion the internal stratigraphy of selected intrusions has been compared using a combination of MgO (w-%), Mg-number, a modified differentiation index (von Gruenewaldt, 1973) and Fo-content (m-%) (Fig. 12). Intrusions within the

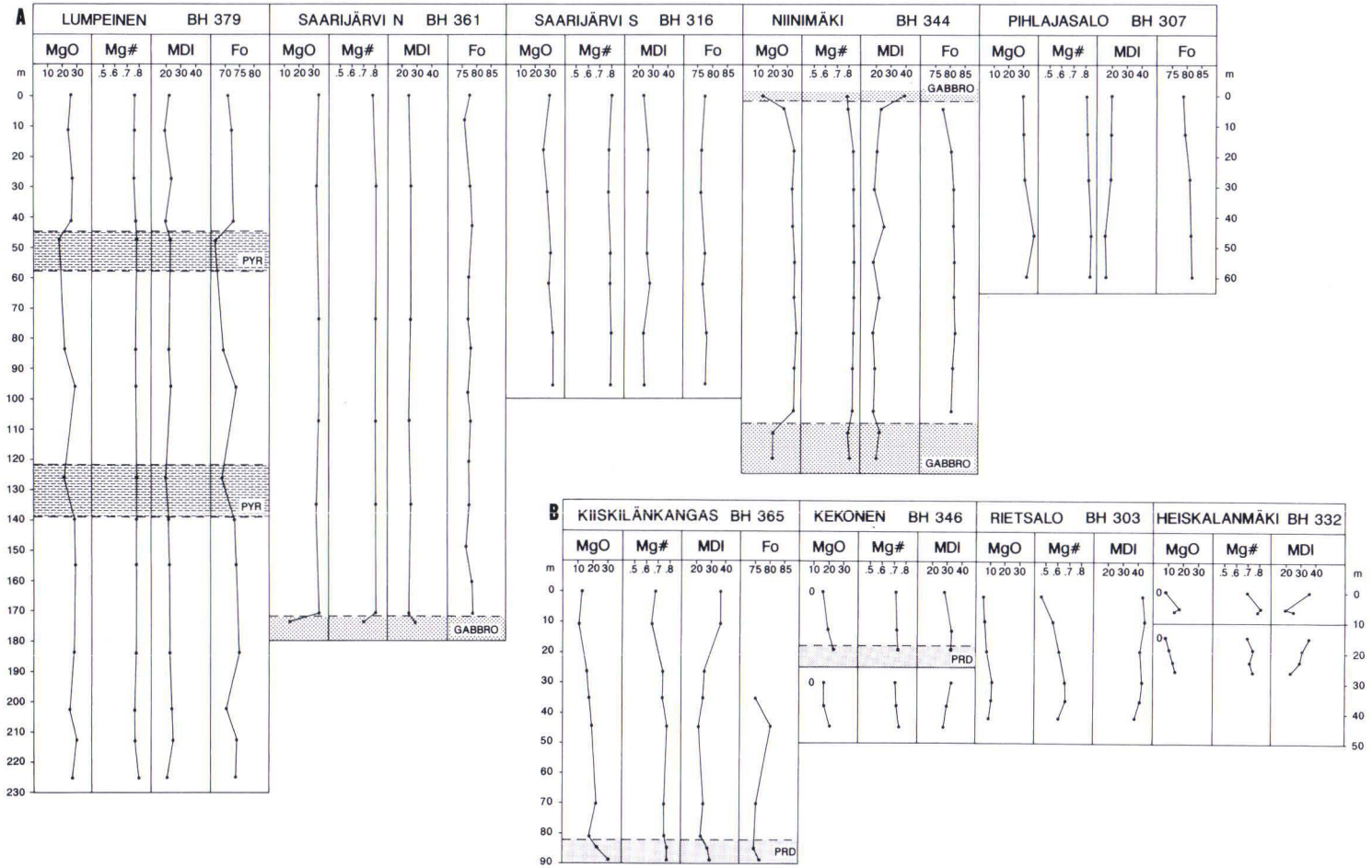

Fig. 12. Chemical composition as a function of stratigraphic level. A = peridotite intrusions; peridotite (no symbol), pyroxenite (pyr) or gabbro. B = differentiated intrusions and intrusions within the Luonteri-Heiskalanmäki zone; gabbro (no symbol) or peridotite (prd). In the cases of Kekonen and Heiskalanmäki both limbs of the folded intrusions have been described separately. Mg# = Mg number ($MgO/(MgO+FeO_{TOT})$) m-%, MDI = modified differentiation index.

Luonteri-Heiskalanmäki zone and the differentiated intrusions show distinct changes in chemical composition as a function of internal stratigraphic level. The basal parts of the intrusions show enrichment in elements that occur preferentially within mafic cumulus mineral phases. In contrast, the peridotitic intrusions are only weakly differentiated although in spite of this, MgO abundances and Fo-content can still reveal differentiation trends. The Pihlajasalo and Niinimäki intrusions are somewhat more strongly differentiated than the Saarijärvi and Lumpeinen intrusions. The abrupt transition from gabbro to peridotite in the Saarijärvi and Niinimäki intrusions is also clearly reflected in the geochemical data.

Ni-Cu OCCURRENCES

Mode of occurrence

Six of the Ni-Cu occurrences in the Juva district have the average Ni contents in excess of 0.50 w-% and have been studied in detail. Mineralization is invariably confined to the basal parts of the intrusions although because they have been affected by complex and multiple deformation, Ni-Cu occurrences can give the impression of occurring in a variety of positions within their respective host intrusions, depending on whether it is right way up, inverted, or tilted on end.

The boundaries of the mineralized horizons are usually readily defined since they coincide with a marked increase in sulfur abundance, from less than 1 w-% to several per cent or more. Sulfides are usually present as disseminations although some compact horizons less than 2 m thick are present at the contact between the intrusion and the country rocks and occasionally as offset ore zones within the gneisses themselves, as at Pihlajasalo. Figure 13 presents cross-sections through the occurrences studied.

Ore mineralogy

The most abundant ore minerals are pyrrhotite, chalcopyrite and pentlandite, with a range of other minerals commonly being present, including ilmenite, Ni-Co arsenides (niccolite, gersdorffite, gersdorffite-cobaltite), pyrite after pyrrhotite, and bravoite and violarite as alteration products after pentlandite. Cubanite, sphalerite, magnetite, millerite and mackinawite are also occasionally present.

The sulfides are generally disseminated throughout the ore, although in places compacted and brecciated ore textures occur. At some occurrences, notably Rantala, the sulfides have been strongly tectonically remobilized during deformation. In contrast primary sulfide droplet textures consisting of pyrrhotite, chalcopyrite and pentlandite have been preserved intact at the Kekonen occurrence. The sulfide droplets are in some cases surrounded by amphibole corona textures resembling those surrounding olivine grains. At the Niinimäki occurrence secondary pyrite is the predominant ore mineral in the upper parts of the mineralized zone (compare Figs. 14 and 15). Pyrrhotite crystals attain sizes of 1 cm, while chalcopyrite is up to 4 mm in size and pentlandite 5 mm. Pentlandite typically occurs as discrete subhedral inclusions within

Fig. 13 (on the right). Cross-sections through the Ni-Cu occurrences.

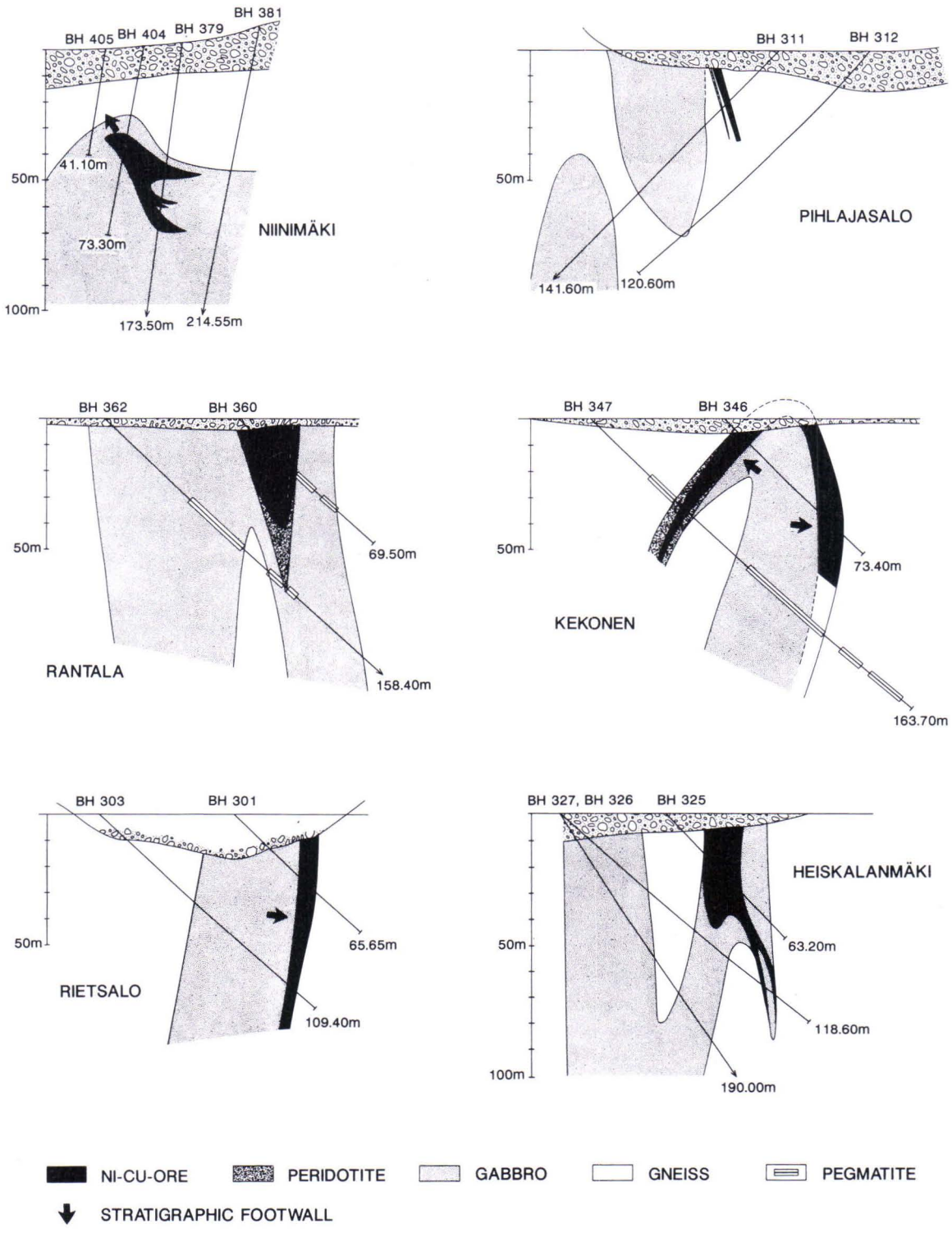
BH 381
BH 405
BH 404
BH 379
41.10m
50m
73.30m
NIINIMÄKI
100m
173.50m
214.55m
BH 311
BH 312
50m
PIHLAJASALO
141.60m
120.60m
BH 362
BH 360
50m
69.50m
RANTALA
158.40m
BH 347
BH 346
50m
73.40m
KEKONEN
163.70m
BH 303
BH 301
50m
65.65m
RIETSALO
109.40m
BH 327, BH 326
BH 325
HEISKALANMÄKI
50m
63.20m
118.60m
100m
190.00m
NI-CU-ORE
PERIDOTITE
GABBRO
GNEISS
PEGMATITE
STRATIGRAPHIC FOOTWALL

Fig. 13.

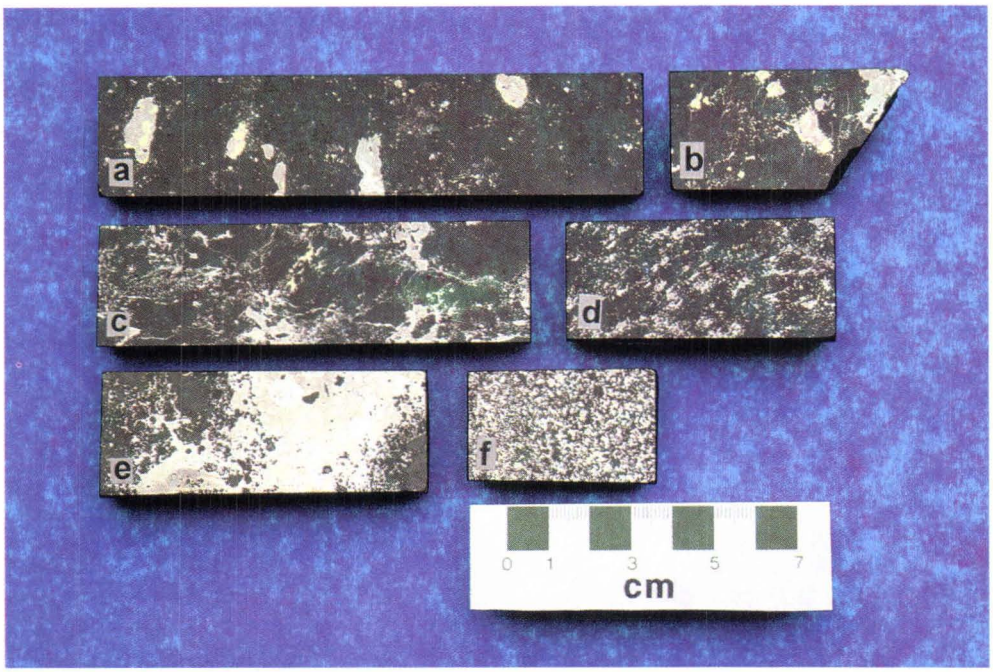

Fig. 14. Representative ore samples. a) Kekonen, BH346/49.60; b) Rietsalo BH305/100.20; c) Rantala, BH360/24.10; d) Heiskalanmäki BH332/66.50; e) Pihlajasalo, BH311/28.30; f) Niinimäki, BH364/26.80. Photo J. Väätäinen.

pyrrhotite but has sometimes been mobilized into fractures within pyrrhotite grains or is intergrown with it, forming flame-like exsolution lamellas. Chalcopyrite likewise often occurs in fractures within other sulfide grains or within silicates.

Metal abundances

Economically significant metals in the occurrences are nickel and copper, and locally cobalt as well; abundances of platinum group elements are low. When evaluating potential reserves, the geological boundaries of the mineralized zones have been defined using a cutoff grade of 0.3-0.5 w-% Ni. As stated earlier, the occurrences that have been studied so far are rather modest but of these, the Niinimäki occurrence is clearly significantly larger in terms of estimated tonnage (Table 1).

Table 1. Ni-Cu occurrences in the Juva area. Ni_{SF} = Ni in 100 % sulfide.

Occurrence	ton	Ni%	Cu%	Ni_{SF}
Pihlajasalo	5000	1.99	0.12	8.78
Rantala	20000	0.53	0.34	3.71
Kekonen	50000	0.54	0.21	6.46
Heiskalanmäki	54000	0.55	0.25	7.17
Rietsalo	56000	0.53	0.53	5.40
Niinimäki	>100000	1.09	0.36	4.95

Fig. 15 (on the right). Photomicrographs from ore samples, single nicol. a) Pentlandite (pn) filling fractures in pyrrhotite (po), Rantala BH360/8.20. b) Zoned Ni-Co arsenide (nic = niccolite, grs = gersdorffite, grs-cob = gersdorffite-cobaltite, cpy = chalcopyrite), Pihlajasalo BH311/28.30. c) Pyrrhotite-pentlandite assemblage, Niinimäki, BH363/20.35. d) Secondary pyrite (py) -violarite (vl) ore, Niinimäki, BH370/23.20. Photos K.Kojonen.

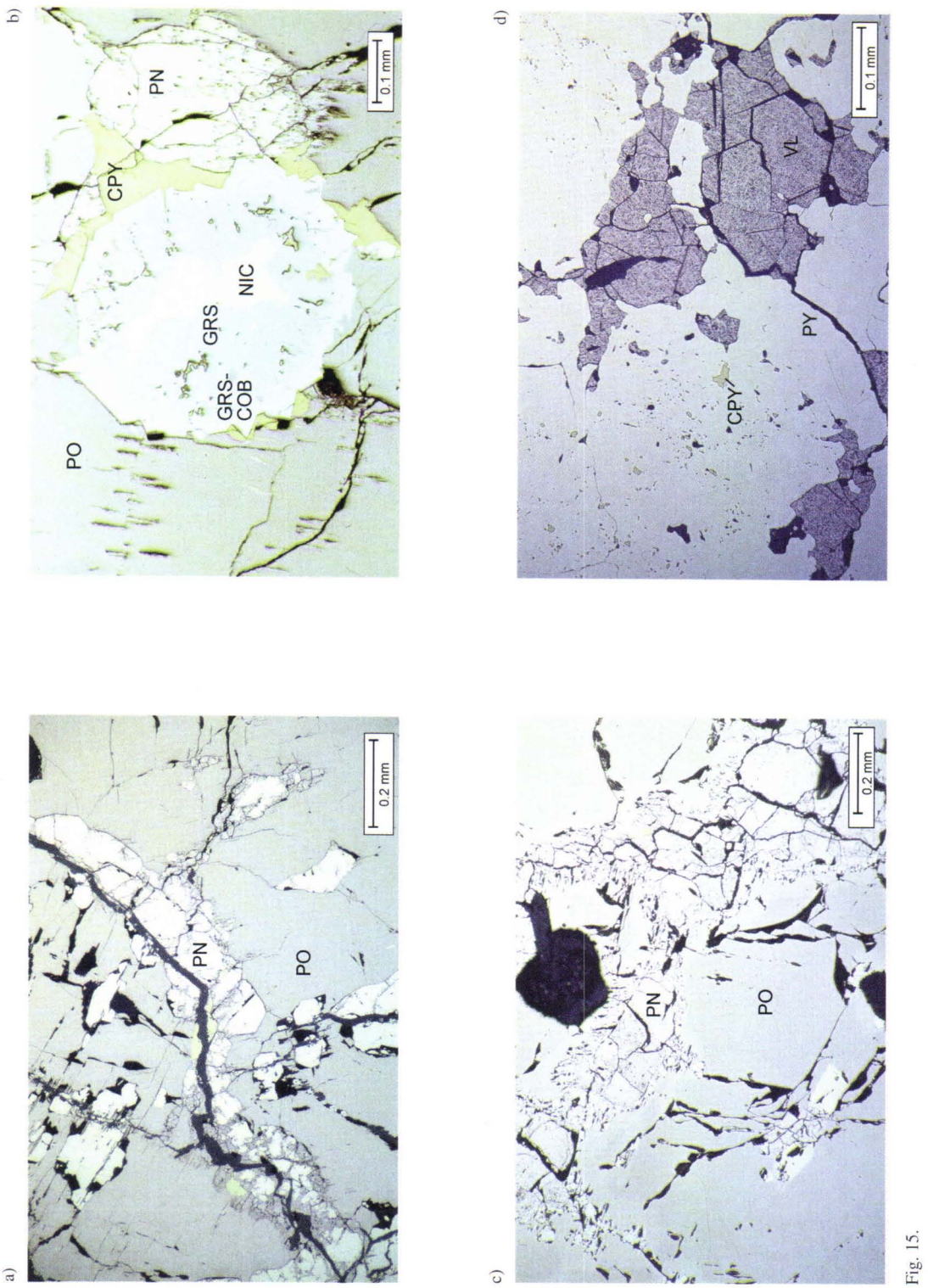
a)
PN
PO
0.2 mm
b)
PO
GRS-COB
GRS
NIC
CPY
PN
0.1 mm
c)
PN
PO
0.2 mm
d)
CPY
PY
VL
0.1 mm

Fig. 15.

WHOLE ROCK GEOCHEMISTRY

Mean chemical compositions for the various rock types will be presented below, while comprehensive data for each of the individual samples analyzed in the course of this study can be found in Appendix 1.

Luonteri-Heiskalanmäki zone

Table 2 lists mean chemical compositions for combined data from the Luonteri-Heiskalanmäki zone intrusions and the spatially associated Hietajärvi, Rasimäki and Niinimäki intrusions, as well as mean data for the individual intrusions (compare Fig. 5 and appended map).

The mean value for SiO_2 is 53.30 w-%, on the basis of which the intrusions are classified as intermediate on average, even though values range from 43.63 - 66.91 w-%, thus encompassing the whole compositional range from ultrabasic (SiO_2<45 w-%) to acidic (SiO_2>66 w-%) (Williams et al., 1982).

This wide variation in composition is also clearly reflected in MgO abundances; the mean MgO value is 8.16 w-% but individual values range from 1.48-24.94 w-%. The Niinimäki intrusion is rather distinctive with respect to its high FeO_{total} abundances and low alkali contents.

The correlation matrix (Table 3) shows some significant features, including a distinct positive correlation between Cr and Mg which can be explained by the incorporation of Cr into pyroxene during crystallization, chromite being absent from these gabbro intrusions. Ni and Cu are clearly associated with sulfur, while Zn is partitioned into both sulfide and silicate phases.

In a general sense the correlation matrix records the effects of magmatic differentiation processes. Those elements that remained within the melt until late during the crystallization history tend to show negative correlations with those that were preferentially partitioned into early crystallizing phases. When comparing correlations between major components however, it is always necessary to bear in mind the potential closure sum problem.

The relative abundance of intermediate and felsic rocks in this zone is also clearly evident in normative calculations (Fig. 16). Almost all of the samples analyzed contain normative quartz, while only a few have normative olivine or diopside.

Peridotites

Table 4 presents averaged analytical data from the peridotitic intrusions, between which some noticeable differences can be recognized. The Lumpeinen and Turunen intrusions have higher CaO abundances than the other peridotites, while SiO_2 values are more or less constant for all intrusions. The Saarijärvi and Kekonen intrusions have conspicuously higher TiO_2 concentrations and the Kekonen intrusion also has elevated P_2O_5 abundances. No analytical data for phosphorus were available from the Saarijärvi intrusions but as noted above, the peridotite contains exceptionally abundant (up to 5 vol-%) apatite; P_2O_5 values accordingly must also be higher than those of the other intrusions.

Normative calculations also reveal that the Saarijärvi, Kekonen, Kiiskilänkangas and Niinimäki peridotites have distinctive compositions compared to the other intrusions, manifesting principally in the relatively small amounts of normative clinopyroxene (Fig. 17). Conversely, the most abundant normative clinopyroxene occurs in the Lumpeinen and

Table 2. Averaged chemical compositions of the intrusions in Luonteri-Heiskalanmäki zone. Number of analyses in parentheses.

	1	2	3	4	5	6	7	8	9	10	11	12	13	14	15	16	17
w-%																	
SiO_2	53.31	54.15	52.78	53.27	59.12	53.79	55.58	52.71	58.44	51.55	52.07	55.19	59.90	54.12	50.71	48.72	50.28
TiO_2	1.17	0.78	0.76	1.09	1.05	0.63	1.48	1.11	1.00	1.00	1.15	1.33	1.05	1.88	1.47	1.42	0.61
Al_2O_3	16.66	18.37	12.28	17.64	15.58	10.60	17.86	15.89	16.38	17.67	17.05	18.52	17.77	16.33	19.29	19.88	12.85
FeO_{tot}	9.47	8.21	8.55	9.36	7.96	11.63	8.67	10.39	7.59	10.81	10.09	7.35	7.21	9.86	9.73	10.46	19.07
MnO	0.13	0.12	0.13	0.15	0.11	0.17	0.11	0.15	0.10	0.15	0.15	0.09	0.09	0.13	0.13	0.14	0.16
MgO	8.16	7.06	13.49	6.95	5.21	15.38	4.90	8.82	5.37	8.41	7.80	3.34	3.68	5.40	5.08	6.55	11.18
CaO	7.04	7.47	9.63	8.92	5.69	5.92	6.29	7.59	6.05	6.81	7.83	5.82	5.09	7.23	7.11	8.98	4.25
Na_2O	2.07	2.21	0.99	1.29	2.82	0.56	2.25	1.91	2.59	1.58	2.06	4.50	3.06	2.37	2.73	2.11	0.73
K_2O	1.58	1.46	1.00	1.04	2.10	1.09	2.32	1.13	2.19	1.59	1.42	2.54	1.85	1.96	1.61	1.35	0.73
P_2O_5	0.41	0.17	0.40	0.26	0.36	0.24	0.55	0.29	0.30	0.43	0.39	1.31	0.29	0.72	0.46	0.38	0.15
ppm																	
Ni	431	75	2750	20	93	397	55	555	74	80	353	16	35	53	61	97	678
Cr	453	235	858	400	196	1439	160	368	193	305	346	33	102	177	179	286	1668
V(n = 97)	210	174	160	n.d.	n.d.	n.d.	n.d.	n.d.	n.d.	n.d.	n.d.	n.d.	n.d.	n.d.	255	258	150
Zr(n = 97)	135	95	89	n.d.	n.d.	n.d.	n.d.	n.d.	n.d.	n.d.	n.d.	n.d.	n.d.	n.d.	128	318	52
Cu	157	38	961	18	69	137	55	237	26	58	69	16	38	41	39	75	167
Co(n = 115)	26	n.d.	n.d.	15	26	36	25	33	21	27	34	16	18	30	n.d.	n.d.	n.d.
Zn	94	111	93	33	70	27	78	30	54	38	42	72	63	91	152	146	148
S(w-%)	0.31	0.09	1.19	0.04	0.07	0.30	0.17	0.34	0.10	0.22	0.36	0.13	0.11	0.16	0.15	0.43	0.33

1 = Mean (212)
2 = Alanen (8)
3 = Heiskalanmäki (21)
4 = Syömäjärvi (4)
5 = Kolkanranta (7)
6 = Virmaanlahti (7)
7 = Rietsalo (20)
8 = Rietsalo BH303 (6)
9 = Kololahdenselkä (17)
10 = Vekarainen (10)
11 = Siikavesi (16)
12 = Rantavuori (5)
13 = Siikasaari (6)
14 = Pihlajasalo (14)
15 = Hietajärvi (35)
16 = Rahijärvi (16)
17 = Niinimäki (19)

Table 3. Correlation matrix for elements in the Luonteri-Heiskalanmäki zone (n = 212).

	SiO_2	TiO_2	Al_2O_3	FeO_{tot}	MnO	MgO	CaO	Na_2O	K_2O	P_2O_5
SiO_2	1.00000									
TiO_2	-0.28030	1.00000								
Al_2O_3	-0.09162	0.33072	1.00000							
FeO_{tot}	-0.70465	0.35774	-0.25504	1.00000						
MnO	-0.67916	0.15580	-0.31989	0.79549	1.00000					
MgO	-0.35133	-0.49836	-0.76496	0.40928	0.48801	1.00000				
CaO	-0.46805	0.18295	0.15715	0.00779	0.26998	-0.10705	1.00000			
Na_2O	0.35288	0.33196	0.62100	-0.42833	-0.53056	-0.79736	-0.13982	1.00000		
K_2O	0.38465	0.26306	0.22726	-0.31789	-0.52366	-0.48536	-0.34606	0.43282	1.00000	
P_2O_5	-0.18406	0.68659	0.10543	0.15332	0.05549	-0.32044	0.19110	0.25225	0.31555	1.00000
Ni	-0.09394	-0.12320	-0.31803	0.18638	0.05149	0.26440	0.07201	-0.24807	-0.11449	0.00478
Cr	-0.21017	-0.48347	-0.77956	0.37192	0.39075	0.94656	-0.26177	-0.70573	-0.42723	-0.32647
Cu	-0.10468	-0.09515	-0.28597	0.13899	0.04761	0.23414	0.14585	-0.23293	-0.13236	0.03714
Zn	-0.29754	0.17182	0.12801	0.25274	0.01632	0.06891	-0.16451	0.09731	0.08605	0.04342
S	-0.14829	-0.03194	-0.24195	0.22354	0.03391	0.20193	0.06305	-0.17642	-0.01121	0.04528

	Ni	Cr	Cu	Zn	S
Ni	1.00000				
Cr	0.22527	1.00000			
Cu	0.94547	0.18483	1.00000		
Zn	0.15656	0.08468	0.15130	1.00000	
S	0.91646	0.16292	0.86594	0.25769	1.00000

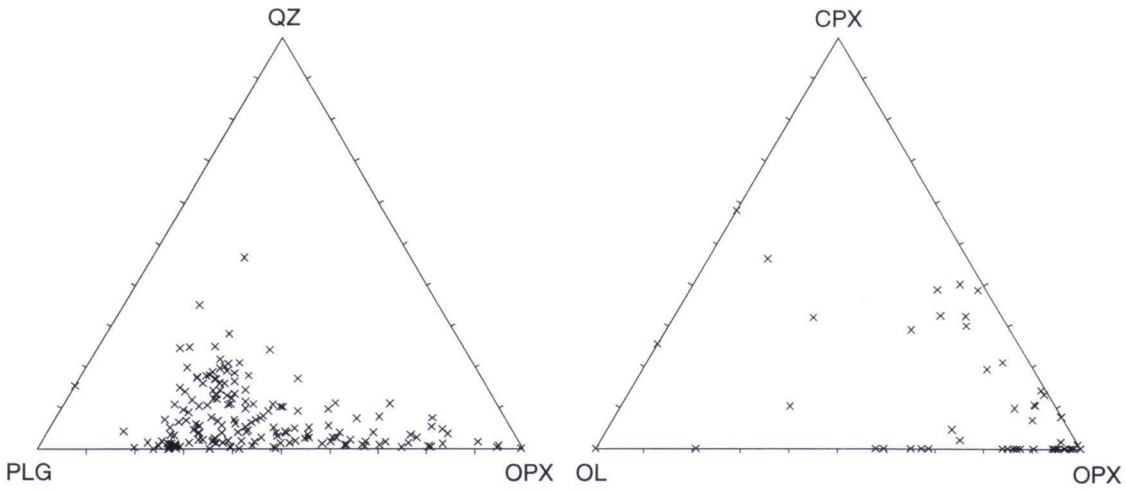

Fig. 16. Normative mineral compositions for samples from the Luonteri-Heiskalanmäki zone. Norms are molecular (Till, 1977).

Table 4. Averaged chemical compositions of peridotites. Number of analyses in parentheses.

	1	2	3	4	5	6	7	8	9	10
w-%										
SiO_2	45.23	44.10	44.24	45.42	42.23	43.15	44.17	46.11	45.72	45.74
TiO_2	0.23	0.29	0.32	0.30	0.67	0.74	0.75	0.35	0.42	0.39
Al_2O_3	3.65	4.90	4.98	3.04	5.60	6.34	8.27	8.50	4.14	4.23
FeO_{tot}	11.78	14.30	14.85	13.86	15.00	14.60	14.91	12.50	13.83	14.44
MnO	0.18	0.18	0.18	0.19	0.19	1.37	0.20	0.18	0.22	0.22
MgO	33.29	33.21	32.43	32.81	31.57	29.95	25.04	24.84	25.84	26.13
CaO	5.18	2.39	2.47	4.27	3.61	3.84	5.05	5.59	9.38	8.52
Na_2O	0.25	0.20	0.22	0.04	0.61	0.82	0.96	0.95	0.25	0.25
K_2O	0.16	0.35	0.22	0.04	0.52	0.43	0.50	0.89	0.15	0.07
P_2O_5	0.04	0.09	0.10	0.02	n.d.	n.d.	0.23	0.09	0.03	0.01
ppm										
Ni	637	1514	1704	n.d.	650	780	2215	618	397	660
Cr	3531	2908	2743	n.d.	n.d.	n.d.	1826	1299	1249	568
V	135	73	79	n.d.	n.d.	n.d.	144	130	221	n.d.
Zr	n.d.	28	33	n.d.	n.d.	n.d.	60	n.d.	13	n.d.
Cu	19	312	415	n.d.	150	65	707	166	147	190
Co	100	n.d.	n.d.	n.d.	n.d.	n.d.	159	94	122	148
Zn	109	151	161	n.d.	n.d.	n.d.	160	67	92	115
S (w-%)	0.11	0.49	0.65	n.d.	n.d.	n.d.	1.47	0.36	0.44	0.27

1 = Pihlajasalo (15)
2 = Niinimäki E (9)
3 = Niinimäki W (7)
4 = Venetekemä (32) (Mänttäri, 1988)
5 = Saarijärvi N (16) (Pietikäinen, 1986)
6 = Saarijärvi S (16) (Pietikäinen, 1986)
7 = Kekonen (9)
8 = Kiiskilänkangas (4)
9 = Lumpeinen (16)
10 = Turunen (4)

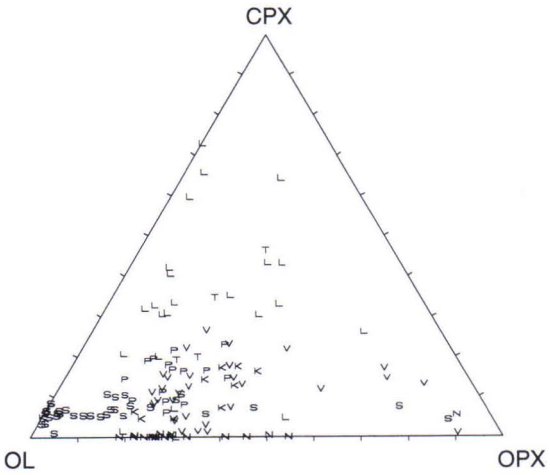

Fig. 17. Normative mineral compositions for peridotite samples. K = Kekonen and Kiiskilänkangas, L = Lumpeinen, N = Niinimäki, P = Pihlajasalo, S = Saarijärvi, T = Turunen, V = Venetekemä.

Turunen peridotites. The normative mineralogies of the Venetekemä and Pihlajasalo peridotites resemble one another closely.

On the basis of normative mineral compositions the different peridotite intrusions are classified, using the nomenclature of Streckeisen (1975), as follows:

Pihlajasalo	- lherzolite
Venetekemä	- dunite + lherzolite
Saarijärvi	- dunite + lherzolite
Kekonen	- lherzolite + harzburgite
Kiiskilänkangas	- lherzolite
Niinimäki	- lherzolite
Lumpeinen	- lherzolite
Turunen	- lherzolite

This classification deviates somewhat from that based on mineralogical investigations,

which classified the Lumpeinen and Turunen intrusions as wehrlites. One reason for this might be that because it is commonly difficult to establish how much amphibole is of primary origin and how much has formed as an alteration product. Nevertheless, the Turunen and Lumpeinen intrusions still plot closer to the wehrlite field on the normative diagram than any of the other peridotites. Therefore the normative calculations are considered to form a reliable basis for classification.

Ultramafic volcanics and sills and amphibolites

The averaged chemical data for the ultramafic volcanics, sills and amphibolites are listed in Table 5. The Pirilä ultramafic rocks clearly have lower MgO abundances than the others. As was also the case for the peridotites, MgO does not show negative correlation with SiO_2; instead, SiO_2 values are locally even higher in some of the other occurrences. Conversely, abundances of Al_2O_3 and CaO are generally higher at Pirilä than in the other occurrences. The Pakinmaa, Myllynkylä and Pirilä results have the highest TiO_2 values, while the highest Ni abundances reported for sulfide-poor lithologies are from Pirilä - that is, from the occurrence having relatively low MgO contents.

The compositions of the chilled margin of the Rantala gabbro and associated dykes correspond to those of amphibolites with respect to a number of major components.

Table 5. Averaged chemical compositions of ultramafic volcanics and sills (1-6) and amphibolites (7) and analyses for Rantala gabbro. Number of analyses in parentheses.

	1	2	3	4	5	6	7	8	9
w-%									
SiO_2	47.97	46.04	50.32	46.02	50.55	46.96	47.91	47.85	48.97
TiO_2	0.49	1.04	0.65	0.96	0.72	0.88	1.16	1.75	1.36
Al_2O_3	7.48	8.67	7.78	9.29	7.63	12.66	15.99	15.03	16.27
FeO_{tot}	11.43	11.81	10.01	11.98	10.18	12.29	13.17	12.72	13.48
MnO	0.20	0.19	0.16	0.19	0.17	0.20	0.20	0.19	0.20
MgO	21.68	21.26	21.35	23.89	20.53	14.72	7.06	10.52	8.45
CaO	9.59	9.55	8.81	6.63	9.01	10.39	11.57	9.53	9.99
Na_2O	0.93	1.17	0.58	0.81	0.62	1.66	2.56	0.53	0.89
K_2O	0.19	0.15	0.19	0.12	0.45	0.16	0.26	1.62	0.26
P_2O_5	0.05	0.11	0.14	0.09	0.15	0.09	0.12	0.26	0.11
ppm									
Ni	1883	600	120	495	409	751	202	187	204
Cr	1879	1500	2400	2000	2071	1013	234	560	370
V	246	n.d.	n.d.	n.d.	n.d.	227	257	333	282
Zr	n.d.	n.d.	n.d.	n.d.	n.d.	n.d.	63	79	150
Cu	831	70	54	72	50	n.d.	n.d.	32	64
Co	112	55	24	43	35	77	50	61	62
Zn	57	20	9	10	11	n.d.	n.d.	131	106
S(w-%)	1.11	0.02	0.01	0.00	0.17	n.d.	n.d.	0.11	0.15

1 = Rantala (6)
2 = Myllynkylä (2)
3 = Levänomainen (1)
4 = Pakinmaa (2)
5 = Rautjärvi (7)
6 = Pirilä (10) (Viluksela, 1988)
7 = Pirilä amfibolites (15) (Viluksela, 1988)
8 = Chilled margin, Rantala, BH363/99.00
9 = Basic dyke, Rantala, BH366/145.80

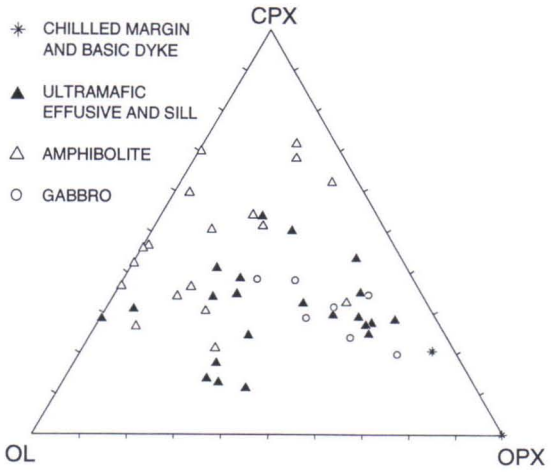

Differences in normative mineral compositions are also evident (Fig. 18), and expressed principally by the greater abundance of normative clinopyroxene in the Pirilä rocks compared to the other ultramafic units. The amphibolites differ from the ultramafic rocks mostly with respect to their relatively low MgO contents and higher Al_2O_3 and Na_2O abundances; this too, is reflected in the normative proportions of clinopyroxene.

Fig. 18. Normative mineral compositions for samples from ultramafic volcanics and sills, amphibolites and Rantala gabbros.

MINERAL CHEMISTRY

Luonteri-Heiskalanmäki zone

Orthopyroxene and hornblende

The En-contents of analyzed orthopyroxenes vary from 42.23-73.31 m-% and show positive correlation with whole rock MgO abundances (Fig. 19). This reflects the relatively uniform mineralogy characteristic of the Luonteri-Heiskalanmäki zone as a whole, even though MgO abundances vary considerably. The only other mineralogical feature associated with this is a tendency for hornblende to become more abundant as MgO increases.

Orthopyroxene has rather low Ni contents, never exceeding 100 ppm in the samples analyzed. Hornblendes in comparison have somewhat higher Ni abundances, namely, 100 ppm, 150 ppm and 170 ppm in the three samples analyzed. According to Häkli (1971) the average Ni content of Finnish pyroxene gabbros is 105 ppm, contrasting with values of 60 ppm in quartz diorites; amphiboles from these rocks have mean Ni contents of 140 ppm and 80 ppm respectively. The Ni contents of orthopyroxenes from the Luonteri-Heiskalanmäki zone are somewhat lower than these quoted values, although corresponding data for hornblende compare very favourably. Although both orthopyroxene and hornblende

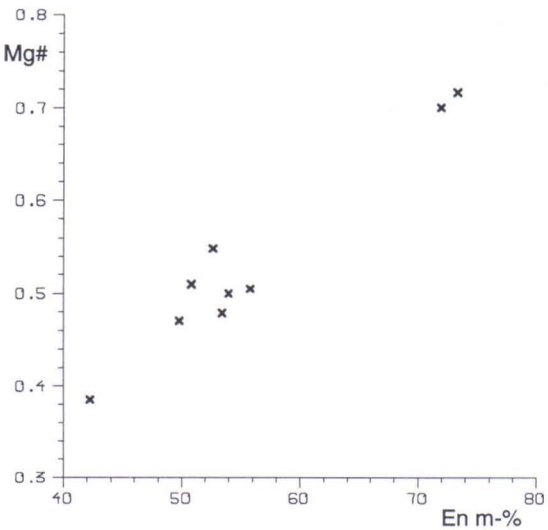

Fig. 19. Orthopyroxene En content (m-%) compared to whole rock Mg-number (Mg#).

are metamorphic in origin, this is not apparent from the Ni data, since compositions overlap with those of magmatic orthopyroxenes studied by Häkli (1971).

The Co contents of the orthopyroxenes are on average 210 ppm, with a range of 150-280 ppm; in contrast, the Co abundances of the three hornblende samples analyzed are, 100 ppm, 130 ppm and 140 ppm. Orthopyroxene Co contents are presumably higher because orthopyroxene contains more Fe than does hornblende, and Co readily substitutes for Fe.

Peridotites

Olivine and orthopyroxene

Table 6 lists averaged mineral compositional data for the different peridotite intrusions, while a list of data containing the results of analyses for all samples studied in the course of this project is presented in Appendix 2. According to the study by Häkli (1971), olivines from Finnish peridotites have an average Ni content of 1330 ppm; most of the olivines in peridotites from the Juva district have Ni contents that lie below this value.

Olivine Fo-contents are highest in the Pihlajasalo peridotites, and lowest in the Kekonen, Lumpeinen and Turunen intrusions. There appears to be no correlation between olivine Ni concentrations and Fo-content, indicating that also other factors than MgO abundance affect the incorporation of Ni into the olivine lattice. In contrast to this, there

Table 6. Averaged chemical compositions of olivine and orthopyroxene in peridotites. Number of samples in parentheses. Detection limit for Ni, Co and Cu 100 ppm.

Occurrence	1	2	3	4	5	6	7	8	9	10	11
Fo	81.44	80.96	79.28	79.69	77.00	77.06	73.11	76.07	77.70	73.87	72.13
m-%	(7)	(9)	(6)	(10)	(32)	(24)	(4)	(4)	(2)	(47)	(4)
Ni_{OLIV}	800	1040	730	1340	1080	1280	1010	470	240	320	760
ppm	(7)	(9)	(6)	(10)	(32)	(24)	(4)	(4)	(2)	(47)	(4)
Co_{OLIV}	230		150		280	290	300	260	320	290	360
ppm	(11)		(2)		(4)	(3)	(2)	(1)	(1)	(8)	(4)
Cu_{OLIV}		210	130		120	220				170	
ppm		(5)	(6)		(2)	(5)				(2)	
En			82.05		80.73	81.49	78.02	80.70	80.84		
m-%			(3)		(28)	(24)	(4)	(4)	(2)		
Ni_{OPX}		240	190		220	270	210	<100	<100		
ppm		(9)	(3)		(28)	(24)	(4)	(4)	(2)		
Co_{OPX}					110	130	150		160		
ppm					(4)	(3)	(2)		(1)		
Cu_{OPX}		200	150		130	180					
ppm		(9)	(3)		(2)	(7)					

1 = Pihlajasalo
2 = Niinimäki E
3 = Niinimäki W
4 = Venetekemä (Mänttäri, 1988)
5 = Saarijärvi N
6 = Saarijärvi S
7 = Kekonen
8 = Kiiskilänkangas, peridotite
9 = Kiiskilänkangas, gabbro
10 = Lumpeinen
11 = Turunen

appears to be a negative correlation between Co and Fo-content. On average Cu concentrations in olivine are slightly lower than those of Co. Within the Saarijärvi and Niinimäki intrusions elevated olivine Cu values correlate spatially with high olivine Ni abundances.

Orthopyroxene analyses are available for samples from the Saarijärvi, Kekonen, Kiiskilänkangas and Niinimäki intrusions. Enstatite contents are higher in the southern part of the Saarijärvi intrusion than in the northern part, even though no differences occur in Fo contents. Orthopyroxenes from the southern part of the intrusion have higher Ni abundances than in the northern part, as was also found to be the case with olivine.

Pyroxenes contain distinctly less Co than olivine, which is consistent with the partition coefficient for cobalt; based on a compilation of data from the literature (Hanski, 1983), basaltic compositions have partition coefficients for cobalt in olivine of 2-5, while for orthopyroxene corresponding values are only 1-2. Furthermore, it is reasonable to expect lower concentrations of cobalt in pyroxene where olivine has crystallized first, since the Co content of the melt will be already somewhat depleted before orthopyroxene starts to crystallize. Olivine and orthopyroxene have broadly similar Cu abundances, even though Cu has a lower partition coefficient for olivine (1) than for orthopyroxene (10) (data compilation by Hanski, 1983). This too can be explained by the fact that olivine begins to crystallize earlier.

Chrome spinel

Chrome spinels were analyzed from the Pihlajasalo, Niinimäki, Lumpeinen and Saarijärvi peridotites and averaged analytical data for each intrusion are given in Table 7.

Analyses were made preferably from near the grain centers, which means that it is not possible to use this data set to examine any spinel zonation that might be present. Three grains from the Lumpeinen intrusion were nevertheless analyzed at their margins as well as their centers, revealing somewhat higher Al, Mg and Zn abundances in the cores and conversely, higher Fe and V approaching the margins. Zonation is not usually optically discernible except in the case of the chrome spinels from the Saarijärvi peridotites, which commonly display dark brown cores and greenish rims (Pietikäinen, 1986). Chromite grains are generally euhedral, although often somewhat rounded, and in serpentinized rocks they are often altered along fractures.

Table 7. Averaged chemical compositions of chrome spinel in different intrusions. Number of samples in parentheses. Fe_2O_3 and FeO calculated from total iron content according to Carmichael (1967).

	1	2	3	4
w-%				
SiO_2	0.04	0.05	0.11	0.02
TiO_2	0.06	0.55	0.05	0.12
Al_2O_3	33.69	23.19	48.33	39.32
Fe_2O_3	5.31	8.72	2.86	1.78
FeO	23.96	26.98	18.40	21.19
MnO	0.25	0.45	0.14	0.28
MgO	8.12	4.84	13.39	10.27
CaO	n.d.	n.d.	0.01	0.01
Na_2O	n.d.	n.d.	n.d.	n.d.
K_2O	n.d.	n.d.	n.d.	n.d.
Cr_2O_3	27.35	32.63	15.34	24.67
NiO	0.11	0.04	0.11	0.07
ZnO	0.70	1.01	0.62	0.75
Total	99.59	98.47	99.36	98.48
Structural formula based on 32 oxygens				
Si	0.0101	0.0137	0.0255	0.0048
Ti	0.0116	0.1120	0.0079	0.0212
Al	9.6410	7.0250	12.707	10.925
Fe^{3+}	0.9802	1.7652	0.4779	0.3172
Fe^{2+}	4.8971	5.9752	3.4473	4.2131
Mn	0.0520	0.1027	0.0266	0.0572
Mg	2.9413	1.8495	4.4528	3.6219
Ca	n.d.	n.d.	0.0020	0.0031
Na	n.d.	n.d.	n.d.	n.d.
K	n.d.	n.d.	n.d.	n.d.
Cr	5.3087	6.8816	2.7383	4.6920
Ni	0.0209	0.0078	0.0187	0.0132
Zn	0.1258	0.1958	0.1028	0.1307

1 = Saarijärvi (8), 2 = Lumpeinen (6)
3 = Niinimäki (20), 4 = Pihlajasalo (6)

When chrome spinels from the Juva district are compared with chrome spinels in general, they appear to define their own distinct group (Fig. 20), characterized by low Mg/(Mg + Fe^{2+}) ratios and relatively high Al abundances. Compositionally similar chrome spinels have also been documented from a number of other mafic and ultramafic intrusions within the Svecofennian of Finland (Lehto, 1987; Lamberg, 1990; Peltonen, 1995a), and also from ultramafic units within the Lapland and West-Inari granulites (Idman, 1980). Ultramafic cumulates from the Outokumpu assemblage also contain some chrome spinels with low Mg/(Mg + Fe^{2+}) ratios, although in some cases this may be due to alteration (Vuollo

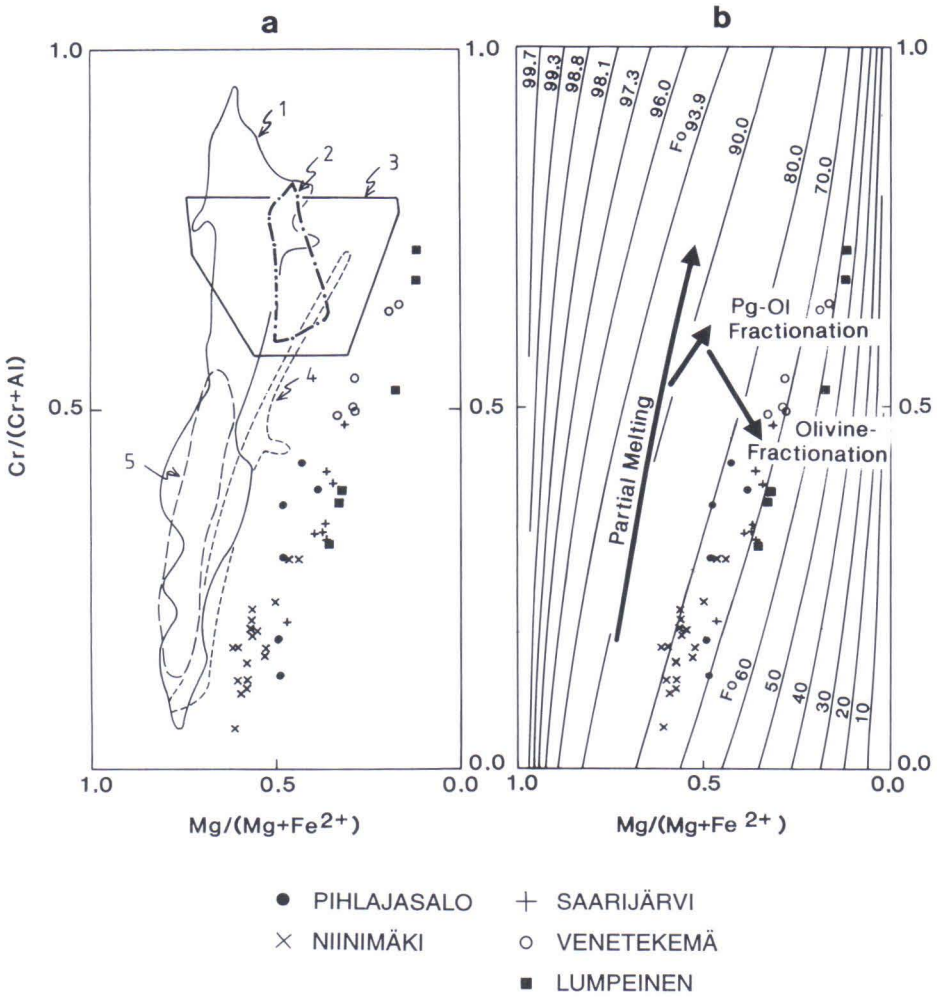

Fig. 20. Composition of chrome spinel in Juva peridotites compared to that in a wide variety of rocks (a) and to composition of olivine in equilibrium with chrome spinel when T = 1200° C (b). In (b) the changes in the composition of chrome spinel due to partial melting of peridotite and fractional crystallization of plagioclase and olivine are also shown (Dick and Bullen, 1984). 1 = Alpine-type peridotites (Irvine, 1967), 2 = S.E.Alaskan intrusions (Irvine, 1977), 3 = Layered intrusions (Irvine, 1967), 4 = Alpine Alpine-type peridotites (Dick and Bullen, 1984), 5 = Abyssal peridotites (Irvine, 1967).

and Piirainen, 1989).

According to Irvine (1965) low Mg/(Mg + Fe^{2+}) ratios in chrome spinels can result from progressive equilibration with surrounding Fe-Mg silicate phases during cooling. Pietikäinen (1986) considered this to be one possible explanation for the low Mg/(Mg + Fe^{2+}) ratios in spinels from the Saarijärvi peridotites.

Figure 20b shows equilibrium chrome spinel compositions as a function of olivine composition, although according to Dick and Bullen (1984) the calculated olivine compositional lines are not quantitatively exact. Average olivine Fo-contents for the Pihlajasalo, Niinimäki, Saarijärvi, Venetekemä and Lumpeinen peridotites range between 73.87 - 81.44 m-% (Table 6) and the chrome spinels from the Juva district follow the compositional lines on the diagram rather closely. Analytical data fall between the Fo_{60} and Fo_{80} lines, which agree well with the known compositions of olivines from these intrusions. Therefore, on the basis of this diagram it seems that the Juva chrome spinels are almost in equilibrium with associated olivines, even though they are slightly enriched in Fe with respect to ideal compositions. Peltonen (1995a) attributed similar features in the olivine cumulates of the Vammala belt to continual subsolidus equilibration between chrome spinel and olivine and pyroxene, reflecting the relatively slow cooling history of the intrusions. Marked variations in the Cr/Al ratio, common to both the Vammala and Juva districts (Fig. 20), are considered to reflect changing melt compositions due to combination of fractional crystallization and assimilation of wall rock sediments (Peltonen, 1995a).

Table 8. Averaged chemical compositions of apatite in Saarijärvi (1 - 3), Lumpeinen (4) and Pihlajasalo (5) peridotites.

Sample	1 (n = 7)	2 (n = 8)	3 (n = 13)	4 (n = 4)	5 (n = 4)
P_2O_5	42.46	42.58	42.78	42.10	42.08
CaO	54.27	54.90	54.67	52.80	54.57
SrO	0.49	0.44	0.45	0.33	0.17
FeO	0.40	0.17	0.17	0.31	0.46
MnO	0.05	0.07	0.06	0.01	0.07
SiO_2	0.56	0.14	0.16	0.08	0.19
La_2O_3	0.13	0.13	0.13	0.09	0.04
H_2O	1.05	1.00	0.92	1.00	0.34
F	1.20	1.48	1.39	1.39	2.28
Cl	0.69	0.39	0.86	0.37	1.43
Sum	101.30	101.28	101.59	98.48	101.62

Apatite

Apatite is abundant in some of the lherzolites and is present in lesser amounts in the wehrlites. Analyses of apatite were made from five peridotite samples and average compositions are presented in Table 8. All analyzed grains were fluorapatite and Cl and F values are highest in the sample from the Pihlajasalo intrusion. Apatites from peridotites rich in orthopyroxene (Saarijärvi) have higher La and Sr concentrations than those from intrusions poor in orthopyroxene (Lumpeinen and Pihlajasalo).

Ultramafic volcanics and sills

Olivine and orthopyroxene

Table 9 lists average compositions for olivines and orthopyroxenes, while the results for individual analyses are given in Appendix 2.

The Fo-contents of metamorphic olivine from the ultramafic rocks are rather low. In contrast however, metamorphic olivines have consistently higher Ni abundances than primary magmatic olivines (see Table 6). The only exception to this is the Rantala ultramafic rock which is also distinctive in being closely associated with Ni-Cu mineralization. It is probable that Ni at Rantala became en-

Table 9. Averaged chemical copmpositions of olivine in ultramafic lavas and sills. Number of samples in parentheses.

Occurrence	Rautjärvi	Rantala	Pakinmaa	Myllynkylä	Levänomainen
Fo (m-%)	70.50 (4)	71.49 (6)	75.07 (2)	69.63 (2)	73.27 (1)
Ni_{OLIV} (ppm)	1100 (4)	660 (6)	2310 (2)	1880 (2)	2510 (1)
Co_{OLIV} (ppm)	350 (1)	220 (2)	290 (1)	330 (1)	
En (m-%)	76.06 (7)	78.98 (3)	79.28 (2)		78.67 (1)
Ni_{OPX} (ppm)	260 (7)	120 (3)	380 (2)		500 (1)
Co_{OPX} (ppm)	120 (1)	160 (1)	140 (1)		

riched preferentially in sulfide phases during regional metamorphism whereas at other localities where sulfur was less abundant, Ni was mostly incorporated within olivine.

The Fo and Ni contents of metamorphic olivine in the sulfide-poor occurrences are very similar to those reported for metamorphic olivine in the Rantasalmi district by Peltonen (1990), who concluded that olivine formed from chlorite-dominated hydrous phyllosilicates and also attributed the high Ni contents in olivine to the relative scarcity of sulfur.

Petrographic observations indicate that the orthopyroxene is metamorphic rather than primary in origin and its Ni contents correlate in a positive manner with those of metamorphic olivine. That is, metamorphic orthopyroxene has on average higher Ni abundances than primary orthopyroxene. The Co abundances in both olivine and orthopyroxene are very comparable with their respective abundances in the peridotites.

CHEMISTRY OF SULFIDE FRACTION

The compositions of sulfide fractions (SF) from different intrusions are shown in Table 10. Values have been calculated on the basis of those samples that contain in excess of 0.1 w-% Ni. The proportion of Ni in silicates has been calculated according to the amount of olivine present and its respective Ni concentration in each case. S_{SF} has been calculated according to the relative proportions of Ni, Cu and S in the sulfide fractions assuming the presence of pyrrhotite, pentlandite and chalcopyrite. The value thus obtained is then used further in calculating Ni_{SF} and Cu_{SF}. Ratios shown represent ratios of the arithmetic means. When examining the Ni/Co ratios it should be realized that some of the Co might be partitioned into silicate minerals (see Table 6). Nevertheless, the whole-rock Ni/Co ratio relates effectively to that of pentlandite alone since this is the principal Co-bearing phase (see Table 10). Hence the whole-rock Ni/Co ratio accurately reflects the sulfide-fraction Ni/Co ratio as well, except in the case of the Niinimäki intrusion, for which the whole-rock Ni/Co ratio is clearly lower than that of pentlandite.

The Ni content of the sulfide fraction (Ni_{SF}) is highest within the Pihlajasalo peridotite, while the Rantala ultramafic rock and the nearby Kiiskilänkangas intrusion clearly have the lowest sulfide-fraction Ni abundances. The Ni/Co ratio of the Pihlajasalo occurrence is high while that for Kiiskilänkangas is distinctly lower than that of the other intrusions. The Cu/(Cu+Ni) ratio generally seems to increase from the peridotites to gabbros (the latter being represented by the Heiskalanmäki and Rietsalo intrusions).

Table 10. Compositions of sulfide fractions in different intrusions.

Occurrence	S_{SF}	Ni_{SF}	Cu_{SF}	Zn_{SF}	Ni/Co	Ni/Cu	$\frac{Cu}{Cu+Ni}$
Pihlajasalo	37.87	8.90	0.68	0.34	51.72	13.10	0.07
Niinimäki W	38.00	4.90	1.59	0.07	25.41	3.08	0.25
Niinimäki E	37.89	5.21	2.00	0.14	32.60	2.61	0.28
Venetekemä	36.05	5.69	3.82		21.33	1.49	0.40
Saarijärvi	37.25	6.34	2.26		23.49	2.80	0.26
Kekonen	37.12	6.94	2.57		26.52	2.70	0.27
Kiiskilänkangas	37.97	3.34	1.39		10.59	2.41	0.29
Rantala	37.93	4.21	2.50	1.81	16.85	1.69	0.37
Heiskalanmäki	37.31	7.23	3.34	0.12	33.21	2.17	0.32
Rietsalo	37.70	5.54	5.40		30.82	1.03	0.49

According to Papunen et al. (1979) the sulfide fraction in weakly mineralized mafic and ultramafic intrusions in Finland is richer in Co than that occurring in economic and subeconomic deposits. The same general conclusion seems to be applicable to the Ni-Cu occurrences of the Juva district as well (Fig. 21). At low Ni abundances (Ni < 0.1 w-%) the relative proportion of Co is greater than at ore-grade abundances. In other words, the abundance of cobalt within an individual occurrence correlates in a negative manner with degree of mineralization. However it is not possible to use Co content to directly evaluate ore potential, since a sample containing abundant Co (with respect to Ni and Cu) may actually correspond to the marginal part of an ore body.

Cu-Ni-Co diagrams for each of the occurrences are presented in Figure 22. The Kiiskilänkangas occurrence which has the lowest sulfide-fraction Ni contents is clearly distinguishable from the others on the basis of its markedly higher Co contents. The Rantala ultramafic unit also has low sulfide-fraction Ni contents and relatively high Co abundances. At Rietsalo on the other hand, the sulfide

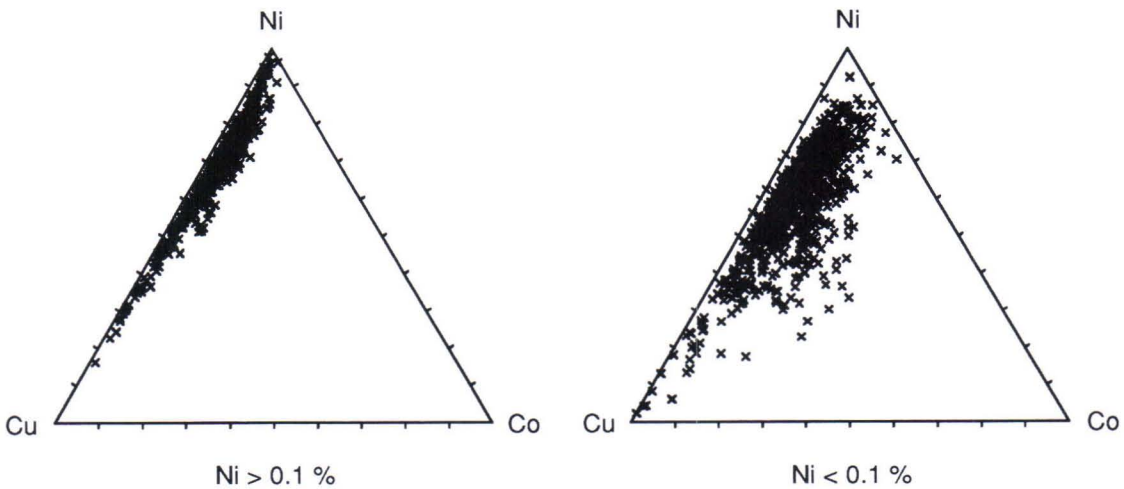

Fig. 21. Composition of the sulfide fraction in weakly mineralized samples (Ni < 0.1 w-%) and in moderately mineralized samples (Ni > 0.1 w-%).

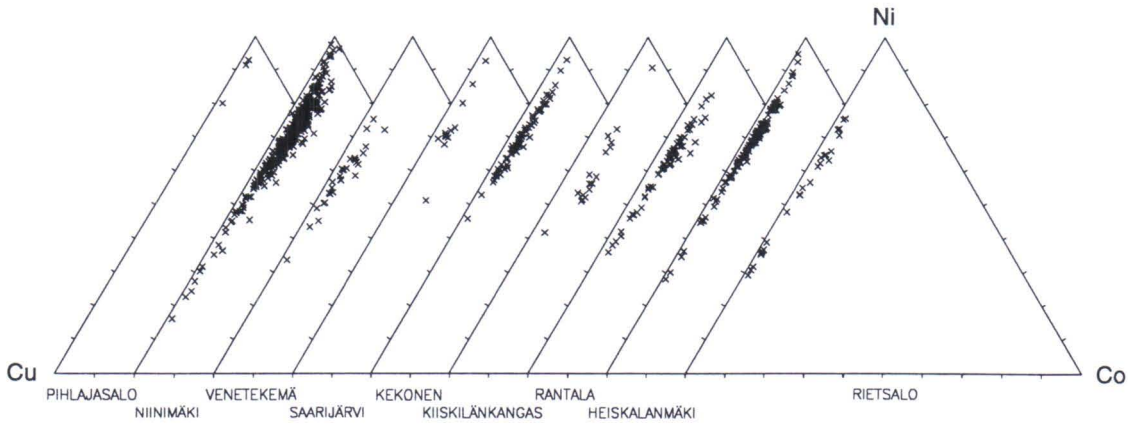

Fig. 22. Composition of sulfide fractions in the different occurrences (Ni> 0.1 w-%).

fraction contains abundant Cu.

Each occurrence has its own characteristic sulfide-fraction Ni abundances, although differences only become readily apparent when whole-rock Ni contents exceed 0.5 w-%; at lower concentrations the differences between occurrences are masked by internal variation within each occurrence, so that they cannot be discriminated on the basis of single samples (Fig. 23).

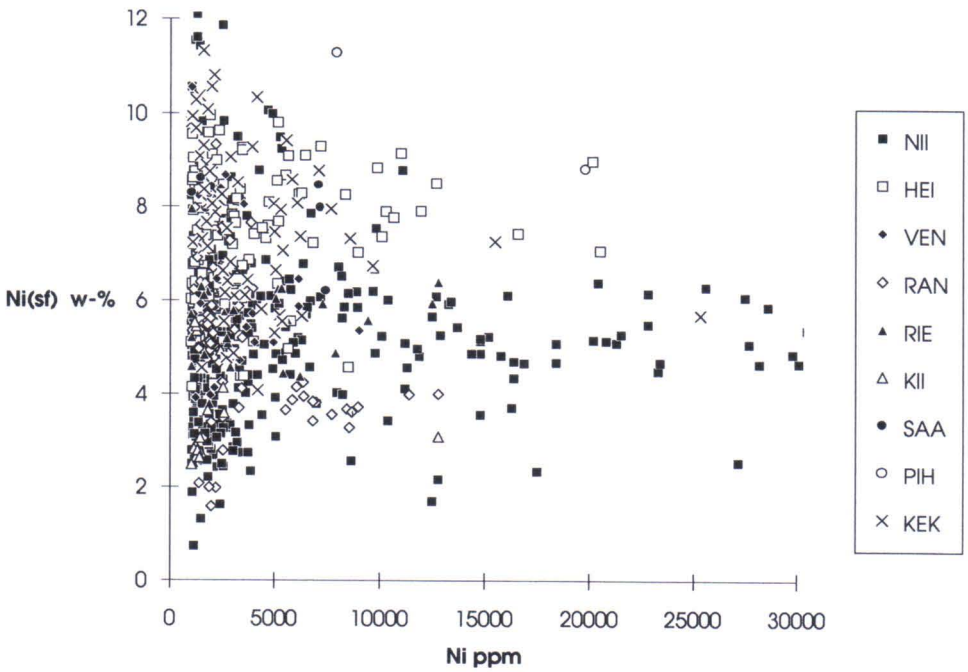

Fig. 23. Variation in sulfide-fraction nickel content as a function of whole rock nickel content. NII = Niinimäki, HEI = Heiskalanmäki, VEN = Venetekemä, RAN = Rantala, RIE = Rietsalo, KII = Kiiskilänkangas, SAA = Saarijärvi, PIH = Pihlajasalo, KEK = Kekonen.

Pyrrhotite and pentlandite

Pyrrhotite has been analyzed from all Ni-Cu occurrences with the exception of those at Saarijärvi and Heiskalanmäki and the results of averaged analyses are presented in Table 11.

According to Ramdohr (1980), when the iron deficit ($Fe_{1-x}S$) increases above the value 0.100, pyrrhotite undergoes a transition from its hexagonal polymorph to monoclinic form. Hexagonal pyrrhotite is antiferromagnetic while monoclinic pyrrhotite is ferromagnetic. All of the Ni-Cu occurrences in the Juva district are associated with prominent magnetic anomalies and therefore it is concluded that the predominant form of pyrrhotite in the intrusions is monoclinic. This conclusion is also supported by the results of chemical analyses. Within the Kekonen intrusion, pyrrhotite composition varies according to prevailing lithology such that the pyrrhotite Fe deficit in peridotite is <0.1 while in gabbro it is >0.1. Pyrrhotite Ni contents are highest in the Pihlajasalo intrusion, which also displays the highest sulfide-fraction Ni abundances.

The Fe/Ni ratio of pentlandite varies between 0.802 - 0.971 and the lowest ratio is present in the Pihlajasalo occurrence. Each occurrence has its own distinctive pentlandite Ni/Co ratio, with the Kiiskilänkangas having

Table 11. Averaged chemical compositions of pyrrhotite and pentlandite. x = the iron deficit ($Fe_{1-x}S$) in pyrrhotite.

PYRRHOTITE

Occurrence	Rietsalo	Pihlaja-salo	Kekonen	Rantala	Kiiski-länk.	Niini-mäki
n	11	5	15	12	10	11
S	39.35	39.41	38.53	39.05	38.70	39.06
Fe	60.65	59.57	61.41	60.82	61.08	59.88
Ni	0.48	0.89	0.26	0.35	0.22	0.82
Cu	0.02	0.06	0.01	0.03	0.03	0.03
Co	0.04	0.07	0.06	0.07	0.06	0.06
As	0.12	0.09	0.04	0.07	0.05	0.07
Sum	100.66	100.09	100.31	100.39	100.14	99.92
X	0.120	0.132	0.085	0.106	0.094	0.120

PENTLANDITE

Occurrence	Rietsalo	Pihlaja-salo	Kekonen	Rantala	Kiiski-länk.	Niini-mäki
n	9	4	20	9	9	22
S	33.79	33.47	33.00	32.62	33.33	32.96
Fe	30.58	29.43	31.63	30.61	30.71	29.72
Ni	34.21	36.68	34.40	34.00	31.62	35.03
Cu	0.08	0.09	0.04	0.06	0.05	0.06
Co	1.18	0.62	1.19	2.12	4.70	0.94
As	0.16	0.05	0.06	0.03	0.09	0.11
Sum	100.00	100.34	100.32	99.44	100.50	98.82
Ni/Co	28.99	59.16	28.91	16.03	6.73	37.27
Fe/Ni	0.894	0.802	0.919	0.900	0.971	0.848

the highest Co abundances. Rantala also has relatively high Co, which is consistent with these two occurrences being situated quite close to one another within the same overall lithological association. The highest As contents in pentlandite are found in the Rietsalo occurrence, which also contains abundant arsenides.

Arsenides and sulfoarsenides

A variety of arsenides are present in small amounts in all of the Ni-Cu occurrences studied, with the Rietsalo occurrence containing them in greatest abundance. The results of analyses (Table 12) indicate that niccolite, gersdorffite and gersdorffite-cobaltite are present. Ni-Co arsenides have also been reported as accessory phases in many other Svecofennian Ni-Cu occurrences in Finland (Papunen, 1980; Grundström, 1980; Isohanni, 1985; Isohanni et al., 1985).

Table 12. Chemical compositions of arsenides.

	ARSENIDES					
Sample	1a	1b	1c	2a	2b	3
n	2	3	1	1	1	2
S	0.23	19.62	20.18	19.90	20.17	17.89
Fe	0.34	2.45	5.73	0.56	4.99	5.91
Ni	43.07	32.20	18.97	34.96	10.42	16.26
Cu	0.06	0.02	0.00	0.06	0.16	0.03
Co	0.04	0.79	9.83	0.71	19.40	13.46
As	56.21	45.36	45.59	44.93	46.49	47.54
Sum	99.98	100.44	100.30	101.12	101.63	101.09

1a) BH301/37.70, Rietsalo
$(Ni_{0.99}Fe_{0.01})_{0.98}(As_{0.99}S_{0.01})_1$(niccolite)
1b) BH301/37.70, Rietsalo
$(Ni_{0.91}Fe_{0.07}Co_{0.02})_{1.00}(As_{0.50}S_{0.50})_2$(gersdorffite)
1c) BH301/37.70, Rietsalo
$(Ni_{0.55}Fe_{0.17}Co_{0.28})_{0.96}(As_{0.49}S_{0.51})_2$ (gers.cobaltite)

2a) BH311/28.80, Pihlajasalo
$(Ni_{0.96}Fe_{0.02}Co_{0.02})_{1.01}(As_{0.49}S_{0.51})_2$ (gersdorffite)
2b) BH311/28.80, Pihlajasalo
$(Ni_{0.30}Fe_{0.14}Co_{0.56})_{0.95}(As_{0.50}S_{0.50})_2$ (gers.cobaltite)
3) BH360/24.30, Rantala
$(Ni_{0.45}Fe_{0.17}Co_{0.38})_{1.03}(As_{0.53}S_{0.47})_2$(gers.cobaltite)

Platinum group elements (PGE)

Abundances of PGE in the Ni-Cu occurrences of the Juva district tend generally to be rather low (Pd<50 ppb), with the highest value analyzed (from meter long drill core sections) being 1.2 ppm Pt at the Rietsalo occurrence; a total of 10 samples were analyzed from this locality.

On the chondrite-normalized diagram the Rietsalo PGE contents plot near to those of Sudbury, while on the Ni/Cu versus Pd/Ir diagram they fall within the MORB and calc-alkaline fields. In other words, PGE characteristics reflect the basaltic character of the silicate melt (Figs. 24 and 25).

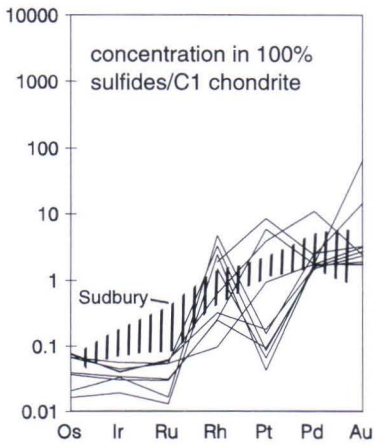

Fig. 24. Chondrite normalized (Barnes et al., 1985) metal patterns for samples from the Rietsalo gabbro.

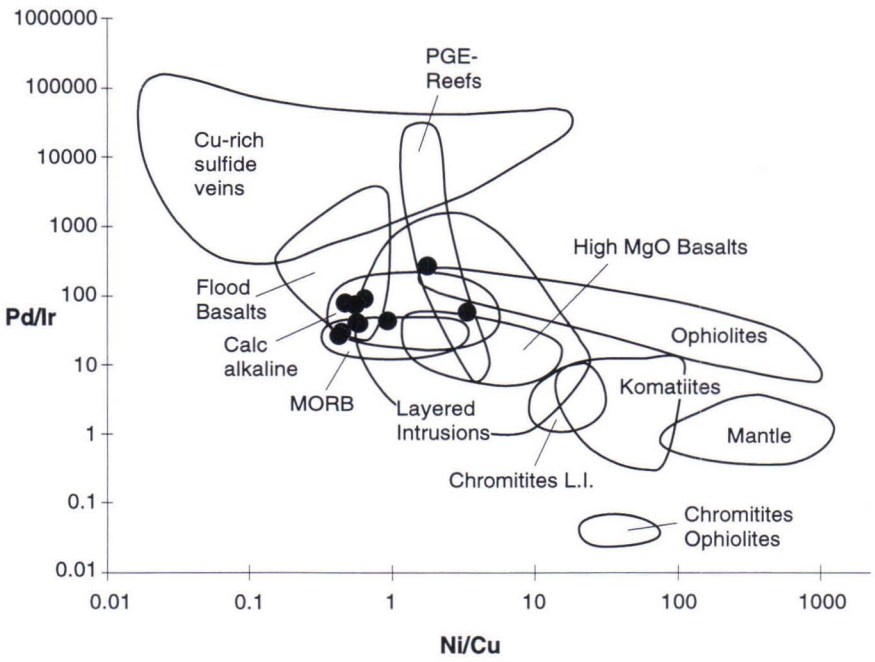

Fig. 25. Pd/Ir versus Ni/Cu diagram for samples from the Rietsalo gabbro. Fields for the different rock types after Barnes et al. (1993).

MAGNESIUM CONTENT OF THE SILICATE MELT

Methods for determining

Petrographic studies indicate that in many instances the rocks examined represent cumulates and therefore formed by fractional crystallization processes. That being the case, the present compositions of such rocks does not correspond to that of the primary silicate melt from which they differentiated.

If it were possible to systematically sample a whole intrusion, the weighted mean could be used to approximate the overall bulk composition of the original melt, assuming that crystallization took place in situ, with no loss or replenishment of material. The chilled margins of intrusions where present have traditionally been regarded as representative of the primary melt composition, although the effects of possible wall rock contamination should be kept in mind.

While taking the above caveats into consideration, the above two methods provide direct estimates of the whole-rock silicate melt composition. If for some reason however it is not possible to use this approach, partial information concerning the melt composition can be obtained by determining the Mg/Fe cation ratio.

The Mg/Fe cation ratio of a silicate melt can be determined from the earliest cumulus mineral phases using the following relation (Roeder and Emslie, 1970):

$$K_D = \frac{(MgO/FeO)_{melt}}{(MgO/FeO)_{mineral}} \qquad (1)$$

According to the experimental studies by Roeder and Emslie (1970) K_D is 0.30 for olivine and 0.23 for orthopyroxene and is independent of temperature. Subsequent refinements have led to a revised K_D for olivine of 0.30-0.36 (Roeder, 1974; Duke, 1976; Longhi

et al., 1978; Bickle et al., 1977 and Bickle 1982). An value of 0.33 has been chosen for application to the present study.

If it is not possible to analyze cumulus minerals, the whole-rock analytical data must be used instead. The Mg/Fe ratio for Fe-Mg silicate cumulus minerals corresponds effectively to the cumulate Mg/Fe ratio, from which it is possible to calculate the Mg/Fe ratio of the bulk silicate melt. It is also possible to use normative calculations for the same purpose.

From the silicate melt Mg/Fe ratio it is then possible estimate the MgO content of the bulk melt. For comparison chemical data from rapidly cooled or quenched weakly fractionated material can be used, such as glass, chilled margins and spinifex-textured zones in komatiites and picrites. Although such comparative material can also be used to determine abundances of other elements, for the purposes of this study, only Mg and Ni need be determined.

Chemical data obtained from the literature (references available from author on request) for spinifex-textured komatiites have been plotted in Figure 26 in order to estimate the MgO content of the silicate melt, applying the formula:

$$\text{Mg-number} = MgO/(MgO+FeO_{TOT}) \text{ m-\%}.$$

The regression line passing through the analytical data will be used later to determine the correlation between the MgO content and the Mg-number of the melt.

The results of experimental studies on melts of basaltic composition enable the MgO content of the parent magma to be determined as long as the MgO/FeO ratio is known. Based on the results of Roeder (1974) the partitioning of MgO between melt and olivine is temperature dependent according to the relation:

$$\log \frac{MgO_{OL}}{MgO_{LIQ}} = \frac{3252}{T} - 1.460 \qquad (2)$$

$(T = °K)$, $(MgO = w\text{-}\%)$

(= regression line equation, r = 0.77, calculated from Table 1 in Roeder, 1974).

The relationship between temperature and MgO content of the melt can be obtained using the results of Roeder (1974) as follows:

$$T = \frac{1000}{0.8100 - 0.1660 \log MgO_{LIQ}} \qquad (3)$$

(= regression line equation, r = 0.94, calculated from Table 1 in Roeder, 1974)

By combining equations (2) and (3) we obtain:

$$\log MgO_{OL} = 0.4602 \log MgO_{LIQ} + 1.174 \qquad (4)$$

from which

$$\log MgO_{LIQ} = \frac{\log MgO_{OL}}{0.4602} - 2.551 \qquad (5)$$

By using the additional relation:

$$Fo = 100 - \frac{10000 - 174.5285 MgO_{OL}}{100 + 0.7825483 MgO_{OL}} \qquad (6)$$

the MgO content (w-%) of the melt can be obtained using the known Fo-content (m-%) according to:

$$\log MgO_{LIQ} = \frac{\log Fo - \log(252.7833 - 0.7825 Fo)}{0.4602} + 1.795 \qquad (7)$$

and the En content (m-%) of orthopyroxene ($K_D = 0.23$) according to:

$$\log MgO_{LIQ} = \frac{\log En - \log(36268.9182 - 188.1602En)}{0.4602} + 6.1409 \qquad (8)$$

Because the experimental investigations referred to above were performed at temperatures between 1150-1300°C and the maximum MgO content in the experimental runs was about 12 w-%, it is not possible to use the calculated curve for melts of ultramafic composition. Instead, for magmas with MgO >12 w-% it is possible to use the correlation between Mg-number and MgO content of spinifex-textured komatiites (Fig. 26). Expressed in terms of the Fo content ($K_D = 0.33$) we obtain the following relation:

$$MgO_{LIQ} = \sqrt[0.2588]{\frac{0.9554}{100 - 0.67Fo}} \qquad (9)$$

The mean FeO content of the Rantala gabbro chilled marginal phase and mafic dyke, and of the Pirilä amphibolites, is 13 w-% (Table 5). Figure 27 shows a comparison of the correlation between the calculated Mg number and MgO abundance for the above rock composition using both Equation 7 and an assumed FeO content of 13 w-%. The compositions of the amphibolites and the Rantala intrusion correspond rather well with the correlation based on Equation 7, which is hence suitable for the rocks of the Juva district. The ultramafic rocks however deviate markedly from the curve of Equation 7 where MgO exceeds 12 w-% . This is because

$$\frac{(MgO/FeO)_{MELT}}{(MgO/FeO)_{OL}}$$

either changes significantly as MgO contents increase above 12 w-%, or because the proportion of cumulus olivine increases markedly. The calculated curve for 13 w-% FeO also agrees closely with the analyzed compo-

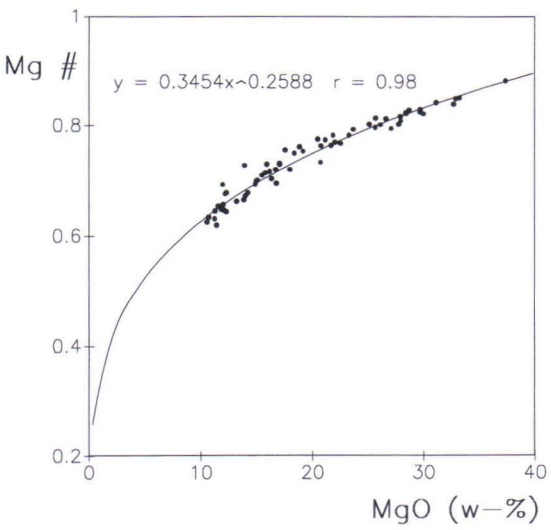

Fig. 26. Correlation between Mg-number (Mg#) and MgO content in spinifex textured komatiites.

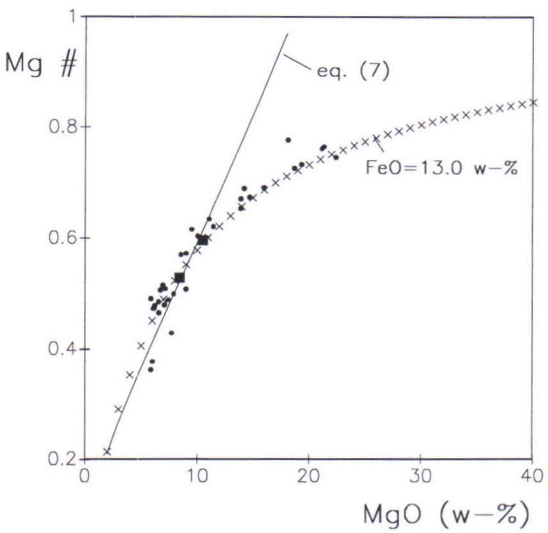

Fig. 27. Correlation between Mg-number and MgO content calculated from Equation (7) compared to that for Pirilä volcanics (dots) as well as Rantala chilled margin and basic dyke (squares). The correlation calculated on the basis of 13 w-% FeO_{TOT} is also shown.

sitions. Equations 7 and 9 will be used later to determine MgO abundances. The curves calculated on this basis intersect at an MgO abundance of 11.18 w-% on the MgO - Mg# diagram, which corresponds to a Fo content of 84.6 m-%. Therefore, equation 9 is used for Fo abundances greater than this value.

Luonteri-Heiskalanmäki zone

Neither primary cumulus minerals nor chilled margins have been recognized within intrusions of the Luonteri-Heiskalanmäki zone, so that primary magmatic compositions can only be deduced using bulk rock chemistry. The intrusions are however, rather well exposed and a comprehensive range of samples have been analyzed. Therefore, the mean chemical data shown in Table 2 are considered to be reliable and representative estimates of true melt compositions. On this basis the MgO content of the silicate melt should have been 8.16 w-%. On the Mg# versus MgO diagram (Fig. 28a) the samples plot on the low-MgO side above the curve of comparative data (Equations 7 and 9), possibly due to segregation and loss of olivine prior to the final stages of emplacement (compare with data for peridotites in Fig. 31a); this is consistent with the presence of discrete olivine cumulates throughout the Luonteri-Heiskalanmäki zone.

The MgO/FeO ratios of Fe-Mg minerals in equilibrium with the silicate melt have been calculated using the FeO/TiO_2 - MgO/TiO_2 molar ratio diagram (Fig. 28b), which is based on the theory of Pearce (1968).

Molecular proportions of Fo or En are obtained from the MgO/FeO ratio as follows:

$$\begin{cases} b = \dfrac{MgO(m\text{-}\%)}{FeO(m\text{-}\%)} \\ Fo,En = \dfrac{100MgO(m\text{-}\%)}{MgO(m\text{-}\%) + FeO(m\text{-}\%)} \end{cases}$$

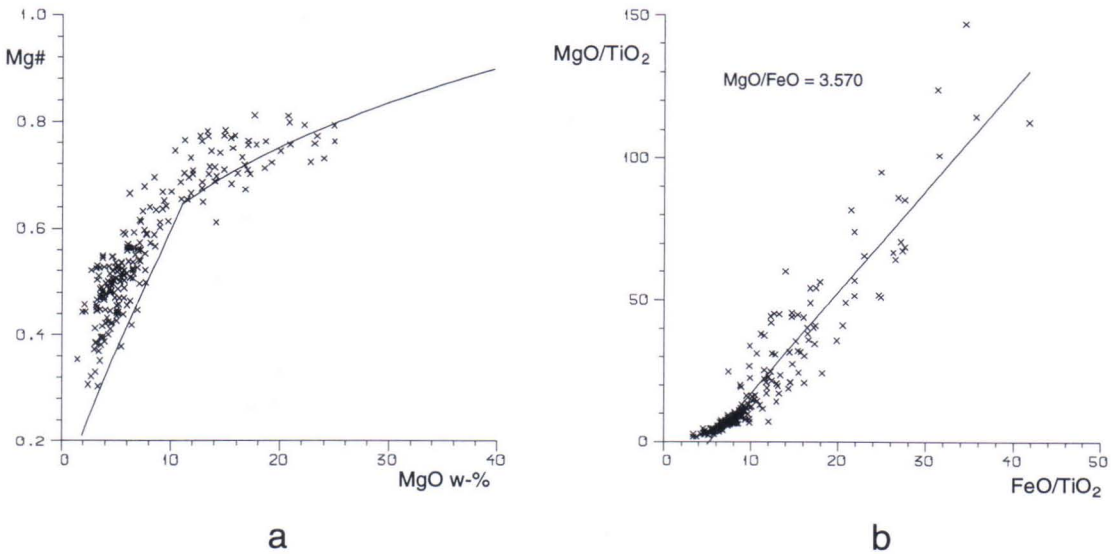

Fig. 28. a) Mg-number versus MgO diagram for samples from the Luonteri-Heiskalanmäki zone. Curves for Equation (7) and (9) are also shown as in similar plots later. b) Molar ratio diagram for determining the MgO/FeO ratio of the silicate melt in the Luonteri-Heiskalanmäki zone.

$$\Rightarrow \quad Fo,En = 100 \frac{b}{1 + b}$$

The Fo abundance calculated from the MgO/FeO ratio is 78.12, which would correspond to the olivine Fo content had this mineral been present in abundance; it will be seen below however that in this case the principal Fe-Mg phase that crystallized was in fact orthopyroxene, so that the MgO/FeO ratio relates instead to the En content. Accordingly, on the basis of Equation 8, the MgO content of the magma is calculated to be 6.86 w-%.

On the molar ratio diagram samples from Rietsalo gabbro represent a silicate melt in equilibrium with orthopyroxene having an En content of between 78.19 and 82.30 (the small number of samples has resulted in a discrepancy between the diagrams in Fig. 29). Using the mean of these two values (80.25), the MgO composition of the silicate melt is calculated at 7.58 w-%. Based on the same procedure, the corresponding MgO content of the Heiskalanmäki intrusion is 9.36 w-%.

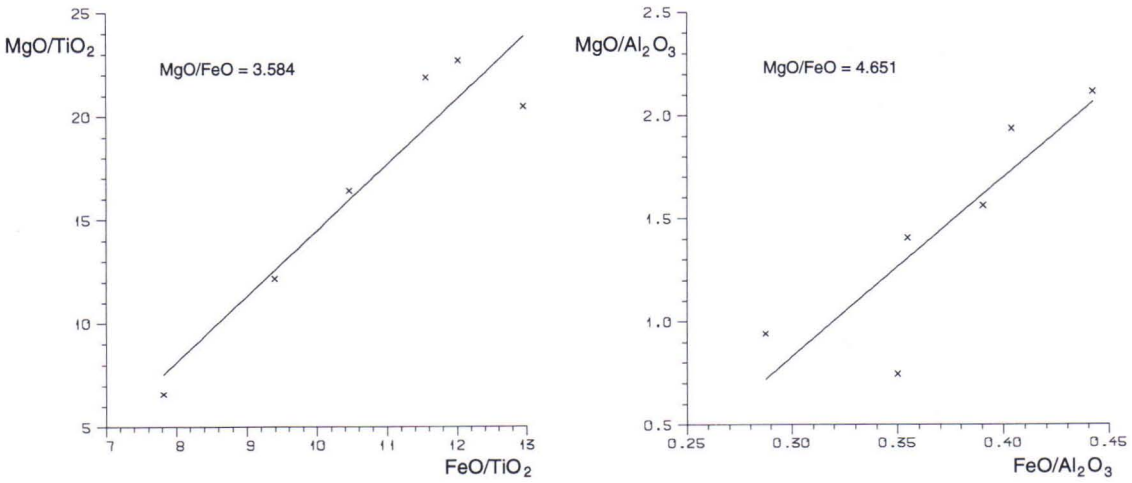

Fig. 29. Molar ratio diagrams for determining the MgO/FeO ratio of the silicate melt in Rietsalo gabbro.

Peridotites

Because all of the peridotites examined correspond to Mg-rich cumulates, their average calculated composition does not represent that of the silicate melt, which must therefore be determined using different parameters.

Olivine, being the first Fe-Mg silicate to crystallize from the melt, reflects the composition of the magma and all peridotites investigated contain primary olivine. Therefore, in contrast to the gabbroic cumulates, which formed via fractional crystallization, the chemical compositions of the peridotitic magmas can be considered as reliable estimates of their respective parent magmas. Table 13 lists the highest Fo contents (m-%) recorded for each peridotite intrusion, together with forsterite compositions as calculated from the molar ratio diagrams (Fig. 30), and also the highest CIPW normative forsterite contents.

Analyzed forsterite contents and the mean calculated forsterite contents from the molar ratio diagrams for the various intrusions are all mutually comparable, with the biggest variations being recorded by the Kiiskilänkangas

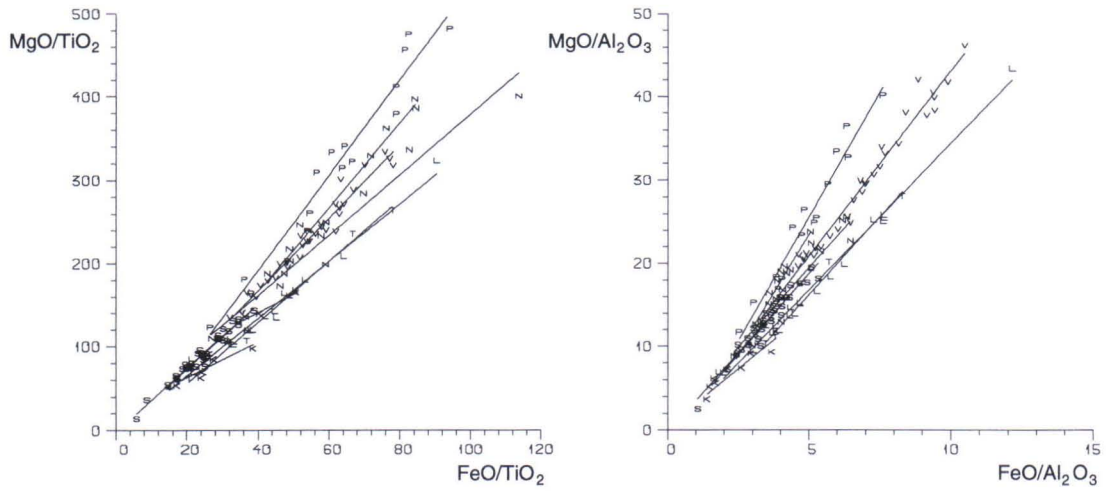

Fig. 30. Molar ratio diagrams for determining the MgO/FeO ratio of the parent magmas in peridotites. The steeper the regression line the higher the MgO content in melt (cf. Table 17). Symbols as in Figure 17.

Table 13. Analyzed (Fo_{MAX}) and calculated (Fo_{CALC} Fo_{CIPW}) Fo-contents (m-%) in peridotites.

Occurrence	Fo_{MAX}	Fo_{CALC}	Fo_{CIPW}
Pihlajasalo	84.63	85.77	84.24
Niinimäki E	82.11	84.24	82.54
Niinimäki W	80.32	80.64	81.74
Venetekemä	81.70	81.77	81.64
Kiiskilänkangas	80.27	82.10	79.22
Saarijärvi N	79.45	79.28	81.85
Saarijärvi S	78.66	79.91	79.23
Lumpeinen	77.95	78.10	81.45
Turunen	75.69	78.99	77.22
Kekonen	75.40	76.97	81.67

Table 14. MgO contents for the parent magmas in peridotites calculated on the basis of Fo contents.

Occurrence	Fo (m-%)	$Mg\#_{LIQ}$	MgO_{LIQ} (w-%)
Pihlajasalo	84.63	0.645	11.17
Niinimäki E	82.11	0.602	10.25
Niinimäki W	80.32	0.574	9.61
Venetekemä	81.70	0.596	10.10
Kiiskilänkangas	80.27	0.573	9.59
Saarijärvi N	79.45	0.561	9.31
Saarijärvi S	78.66	0.549	9.05
Turunen	78.99	0.554	9.16
Lumpeinen	77.95	0.538	8.82
Kekonen	75.40	0.503	8.02

and Turunen peridotites; in the latter case however this may be an artefact of the relatively small number (4) of samples analyzed. Those olivines that were richest in forsterite were not analyzed. In many cases the normative forsterite contents correspond to those that were analyzed, with notable differences being found only for the Lumpeinen and Kekonen intrusions. In summary, the results of these comparisons indicate that the molar ratio diagrams and the CIPW norms are both reliable in determining forsterite contents from whole rock analytical data.

The Mg-number of magma in equilibrium with olivine has been calculated using Equation 1 in Table 14. Forsterite contents have been approximated to maximum analyzed contents. The Turunen olivine compositions were however determined from the bulk peridotite composition. The MgO abundances of the parent magmas have been calculated with Equation 7, except in the case of Pihlajasalo, for which Equation 9 was used.

When the data are plotted on the Mg# - MgO diagrams (Fig. 31a), variations in parent magma compositions and degrees of fraction-

ation become apparent. Analytical data for almost all peridotites define horizontal trends at a given Mg-number which in each case corresponds to respective maximum analyzed forsterite contents.

The horizontal part of these trends lie to the right hand side of the curve for spinifex-textured rocks, indicating that the peridotites have been strongly enriched in Mg-rich cumulus minerals with respect to the residual melt. The Pihlajasalo and Kiiskilänkangas samples deviate least from this trend, while the Kekonen peridotites broadly follow the trend, even though they are displaced to the right of it. It

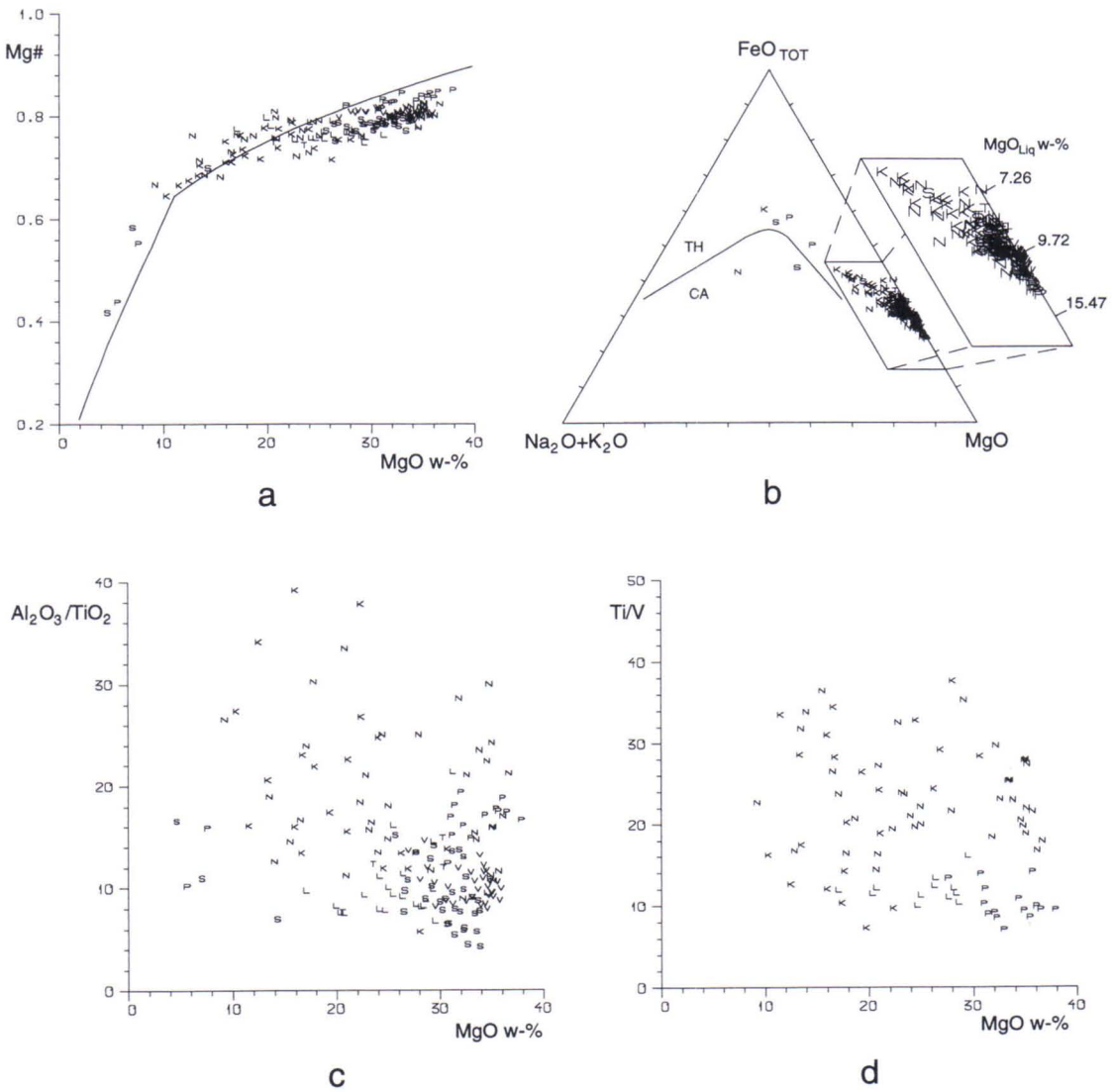

Fig. 31. Diagrams describing the composition of parent magmas in peridotites. Associated gabbros (MgO < 16 w-%) are also shown. Tholeiitic (TH) and calc-alkaline (CA) fields on the AFM diagram after Irvine and Baragar (1971), as in all AFM-diagrams in this work. MgO_{Liq} = MgO content of silicate melt calculated on the basis of MgO/FeO ratio (K_D = 0.33). Symbols as in Figure 17.

is therefore possible to argue that peridotites from the three latter occurrences had larger proportions of residual melt with respect to Mg-rich cumulus minerals than did the other peridotites. In the Kekonen and Kiiskilänkangas intrusions this is also evident petrographically, since both are clearly differentiated from peridotitic to gabbroic; the other peridotites are represented exclusively by Mg-rich cumulates and contain no gabbros.

The Al_2O_3/TiO_2 ratio of the magma has been used to describe how primitive the magma is, since it increases proportionally with degree of mantle melting. For most known komatiite series and chondritic meteorites this ratio is about 20, while for basalts values increase steadily from about 10 as MgO contents increase (Nesbitt et al., 1979). Because olivine does not contain significant amounts of either Ti or Al, the Al_2O_3/TiO_2 ratio of the the olivine-rich cumulates effectively represents the Al_2O_3/TiO_2 ratio of the parent magma as a whole. Figure 31c presents Al_2O_3/TiO_2 for the peridotites. For those samples richest in olivine (with MgO> 30w-%) it is typically around 10, except for the somewhat higher values for samples from the Pihlajasalo and Niinimäki peridotites. On the basis of their Al_2O_3/TiO_2 ratios the parent magma would have been basaltic in composition, which is consistent with calculated MgO contents for the magma.

The Ti/V ratio for both the Lumpeinen and the Pihlajasalo peridotites is around 10, while those of the Niinimäki and Kekonen peridotites are significantly higher (Fig. 31d). According to Nesbitt and Sun (1976) spinifex-textured komatiites have Ti/V ratios of around 12-15, compared to 15-20 for MgO-rich tholeiites and 20-30 for MgO-poor tholeiites. The Ti/V ratio of chondrites is 8.4 (Wänke et al., 1974), so that of the Lumpeinen and Pihlajasalo peridotites is near chondritic and deviates markedly from tholeiitic values, this being however a consequence of pyroxene crystallization. The D values of both orthopyroxene and clinopyroxene are less than one for Ti and greater than one for V, according to the results of numerous investigations (data compilation by Hanski, 1983) and for this reason pyroxene-bearing peridotites have lower Ti/V ratios than their parent magmas.

On the AFM diagrams the peridotites fall within a tight cluster towards the Mg-Fe tieline, with the proportion of alkalies being very small compared to that of Fe and Mg (Fig 31b). Because the peridotites are olivine-rich cumulates, they have Mg/Fe ratios very similar to those of olivine itself and hence the parent magma compositions can also be inferred directly from the AFM diagrams. For this reason the Mg-Fe side of the diagrams shows corresponding MgO melt values, assuming that the whole-rock Mg/Fe ratio indeed corresponds to that of olivine. For each intrusion, the peridotitic samples richest in Mg plot on the AFM diagram close to their respective calculated MgO compositions based on their forsterite contents (Table 14). Thus the AFM diagram is a very simple and effective indicator of the parent magma composition for olivine-rich cumulates.

All peridotites plot within the tholeiitic field on the AFM diagrams, indicating that the parent magma to the peridotites must have been a tholeiitic basalt with an MgO content of between 8-11 w-%.

Ultramafic volcanics and sills and amphibolites

The mean MgO content of the ultramafic rocks varies between 14.72-23.89 w-% (Table 5) and because primary textures indicate that at least some of these rocks represented lava flows, those having MgO > 18 w-% would be classified as komatiites, while those with less than 18 w-% MgO are classsified as komatiitic basalts (Arndt and Nisbet, 1982). On the

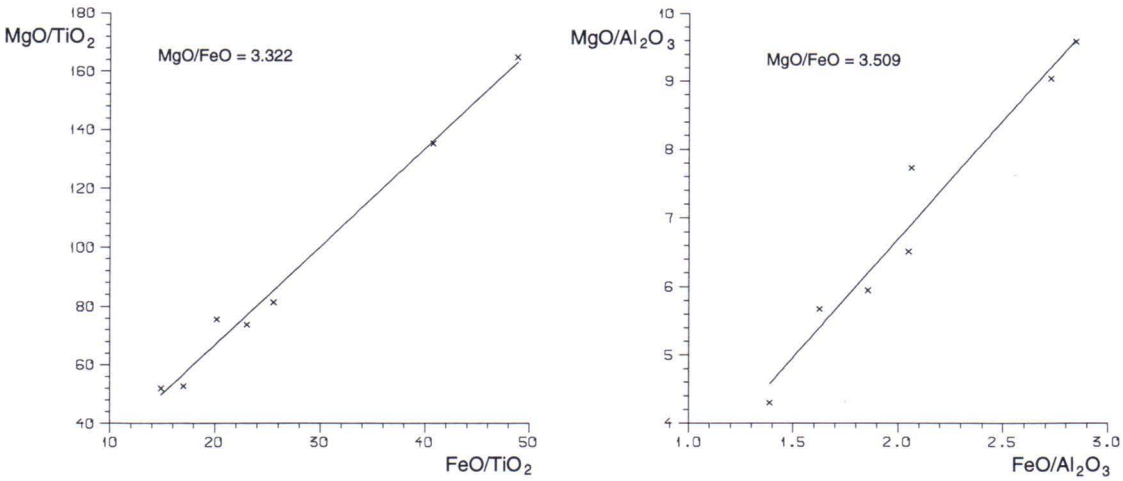

Fig. 32. Molar ratio diagrams for determining the MgO/FeO ratio of the parent magma in the Rantala ultramafic sill.

basis of the following analysis it is however, apparent that the MgO content of the parent magma to the ultramafic rocks was considerably less than that of the analyzed samples.

The ultramafic rocks do not contain any primary olivine or orthopyroxene and therefore estimates of the Mg/Fe ratio of the magma must be inferred from whole-rock geochemistry. Scatter on the molar ratio diagrams is in many cases so large that reliable estimates cannot be made but the correlation coefficient for the Rantala samples is sufficiently high as to allow calculation of a forsterite composition of 77.34 m-% (Fig. 32, mean).

On the Mg# - MgO diagrams the Pirilä ultramafic rocks and amphibolites plot close to the curve for spinifex-textures rocks, whereas those samples richer in Mg tend to form a cluster near the field for peridotites, slightly below a value of 0.8 on the Mg# axis. The mean Mg-number for the Rautjärvi ultramafic rock is 0.78, according to which its forsterite content should be 78 m-% (Fig. 33a).

The CIPW normative forsterite contents and those calculated from the molar ratio diagrams are presented in Table 15 together with the calculated Mg-numbers and MgO contents. Forsterite contents for the Rantala and Rautjärvi samples have been calculated directly from the molar ratio data but because of the small number of analyses available for the other occurences it has also been necessary to use CIPW normative forsterite contents.

The MgO contents of the chilled margin of the Rantala gabbro vary between 8.45 w-% and 10.52 w-% (Table 5). The calculated MgO content of the parent magma to the Rantala ultramafic rocks is very close to these values, suggesting that the gabbro and ultramafic rocks are indeed comagmatic.

Even though the estimated MgO abundances of the parent magma to the ultramafic rocks are not as reliable as for the peridotites, the results for each ultramafic occurrence are nevertheless of the same order of magnitude. The inferred MgO content of the parent magma is appreciably lower than the mean analyzed MgO contents and is approximately the same as that of the peridotites. The Al_2O_3/TiO_2 ratios of many of the ultramafic units, as well as that of the Rantala gabbros is close to 10, which is also comparable with the peridotite values (Fig. 33c). This too indicates a common

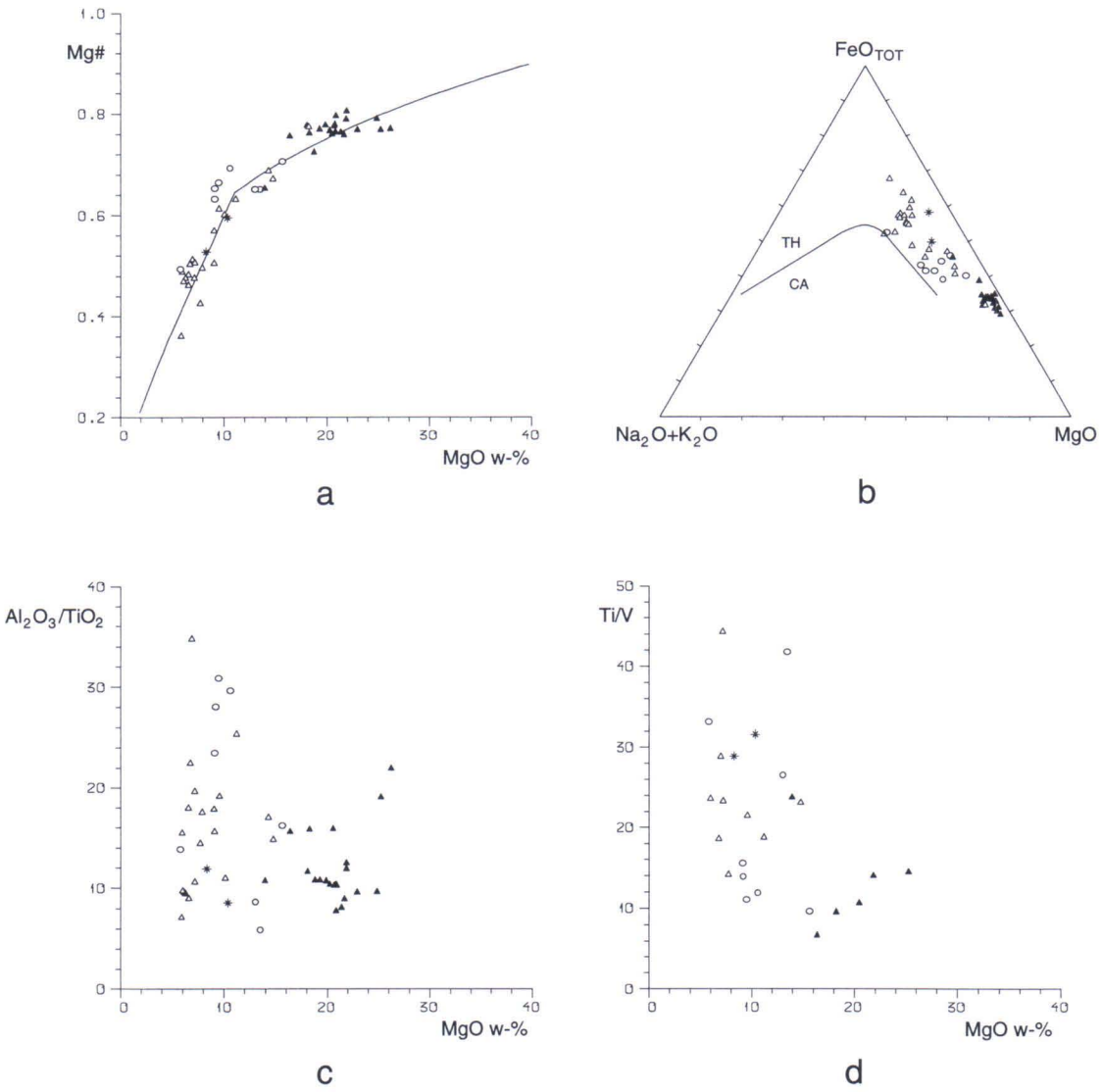

Fig. 33. Diagrams describing the composition of parent magmas in ultramafic volcanics and sills, amphibolites and Rantala gabbro. Symbols as in Figure 18.

tholeiitic parent magma. The low Ti/V ratio of the Rantala ultramafic rocks, which is also similar to that of the peridotites, furthermore suggests that the former crystallized via the same kind of fractionation processes as the peridotites. The Pirilä samples that are richest in MgO were not analyzed for V although the Ti/V ratios of the MgO-poor ultramafic rocks are the same as those of the amphibolites (Fig 33d).

How can the higher MgO abundances of the ultramafic volcanics compared to those of the parent magma be explained? One plausible interpretation is that crystallization took place along the walls of feeder channels prior to intrusion or eruption. In this case olivine ac-

Table 15. MgO contents for the parent magmas in ultramafic volcanics and sills calculated on the basis of Fo contents.

Occurrence	Fo_{CIPW}	Fo_{CALC}	$Mg\#_{LIQ}$	MgO_{LIQ} (w-%)
Pirilä	79.52		0.562	9.34
Rantala	83.80	77.34	0.530	8.62
Rautjärvi	81.20	78.00	0.539	8.83
Myllynkylä	77.34		0.530	8.62
Pakinmaa	79.41		0.560	9.30
Levänomainen	79.40		0.560	9.30

cumulation could have led to the intrusion of olivine-enriched sills or eruption of olivine-rich lavas. If for instance, 20 w-% of olivine Fo_{80} were added to a magma with an original MgO content of 11 w-% (which corresponds to about 18% on a volume basis), then the total MgO content would increase to 17.2 w-%, which is broadly the same as that of the mean values for the ultramafic sills and volcanics (14.72-23.89 w-%, Table 5).

On the AFM diagrams the ultramafic rocks and amphibolites plot clearly within the tholeiitic field, as do the data for the marginal phases of the Rantala gabbroic intrusion (Fig. 33b). According to the classification diagrams presented by Viljoen et al. (1982) the Rantala samples tend to generally plot as Mg-tholeiites. Both Kousa (1985) and Viluksela (1988) classsified the amphibolites as tholeiitic basalts. The hornblende amphibolites of the Virtasalmi area also have compositions corresponding to tholeiitic basalts (Suvanto, 1983; Lawrie, 1992).

The MgO contents of the parent magmas to the studied units (including the gabbro-peridotite intrusions and ultramafic sills and volcanics) overlap with those of the amphibolites, whilst the composition of the chilled margin to the Rantala gabbro corresponds to the mean composition of the amphibolites (see Table 5). It is therefore reasonable to conclude that the amphibolites represent the extrusive equivalents of the intrusive tholeiitic magmatism.

GEOTECTONIC SETTING OF MAGMATIC ROCKS

The geotectonic setting of the magmas has been inferred from the discrimination diagrams presented in Figures 34a-j. Although these diagrams were originally devised for volcanic rocks that are assumed to have undergone relatively limited fractional crystallization, they can nevertheless be extended with some confidence to discrimination between different kinds of cumulate compositions.

On the MgO/10 - CaO/Al_2O_3 - $SiO_2/100$ triangular plot (Fig. 34a), the more felsic differentiates lie principally within the field of unaltered magmatic rocks. This contrasts with the data for the ultramafic differentiation products, which are scattered along a trend close to the MgO/10 - CaO/Al_2O_3 side of the diagram; this is attributed to relative variations in the abundances of clinopyroxene and orthopyroxene. Some of the Pirilä amphibolites have slightly higher CaO/Al_2O_3 ratios than those of unaltered magmatic rocks. Metasomatic changes are indicated for rocks of the Luonteri-Heiskalanmäki zone, based on the molar ratio diagrams (Fig. 36) and this probably accounts for their relatively broad scatter on the discrimination diagrams in Figure 34.

On the MgO-Fe_2O_{3TOT} diagram (Fig. 34b), both the Pirilä amphibolites and the Rantala mafic dyke and chilled margin follow fractionation trends for oceanic and continental tholeiites, whereas the gabbros of the Luonteri-Heiskalanmäki zone lie along island-arc tholeiitic trends. On the MgO - FeO_{TOT} - Al_2O_3 triangular plot (Fig. 34c), the gabbros mostly fall within the ocean ridge or floor and orogenic fields, the latter being represented in particular by the more felsic differentiates of the Luonteri-Heiskalanmäki zone. Most sam-

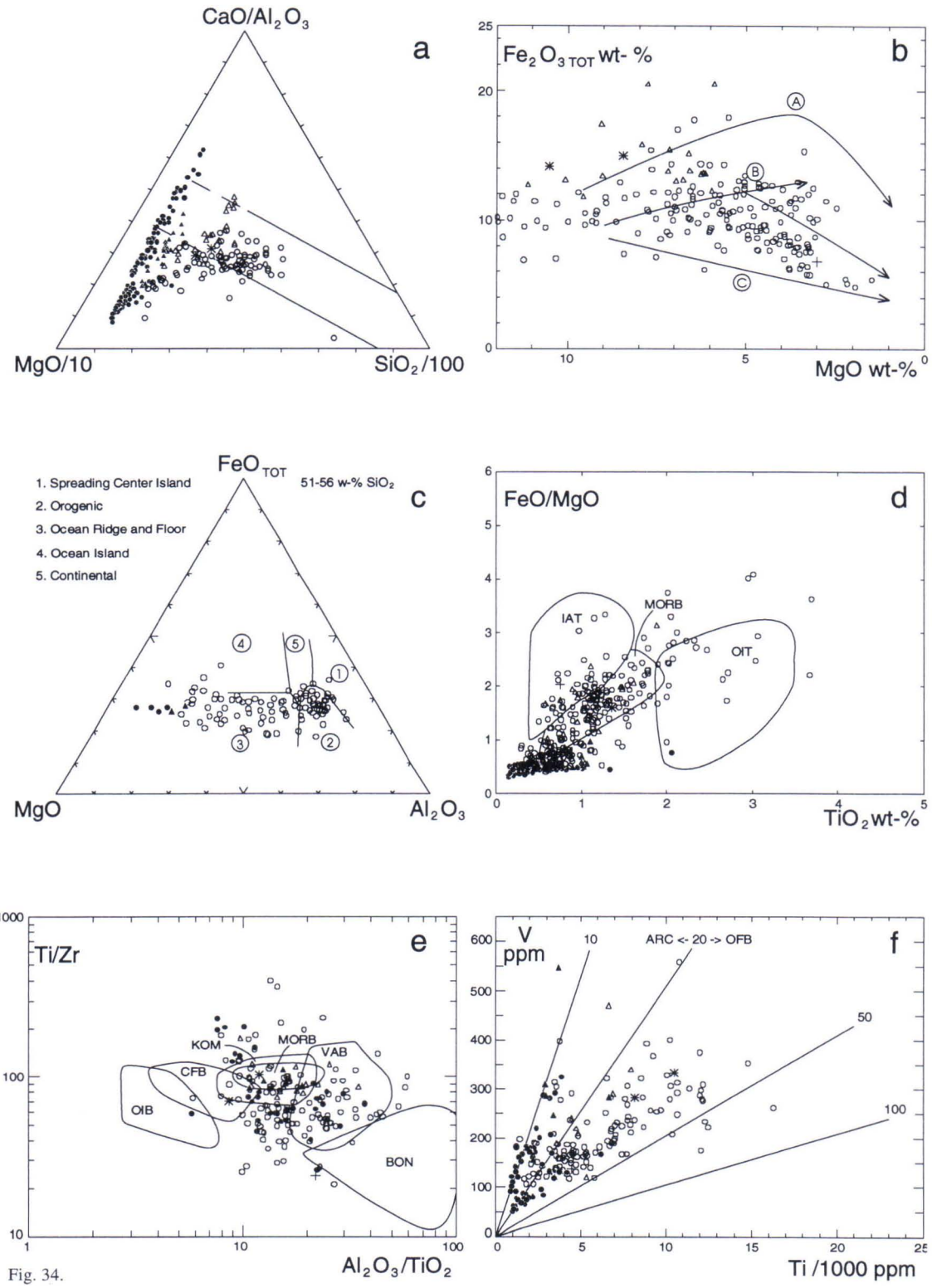
CaO/Al2O3
a
MgO/10
SiO2/100
Fe2O3 TOT wt- %
b
A
B
C
MgO wt-%
FeO TOT
51-56 w-% SiO2
1. Spreading Center Island
2. Orogenic
3. Ocean Ridge and Floor
4. Ocean Island
5. Continental
c
MgO
Al2O3
FeO/MgO
d
IAT
MORB
OIT
TiO2 wt-%
Ti/Zr
e
KOM
MORB
VAB
CFB
OIB
BON
Al2O3/TiO2
V
ppm
ARC <- 20 -> OFB
10
50
100
f
Ti /1000 ppm

Fig. 34.

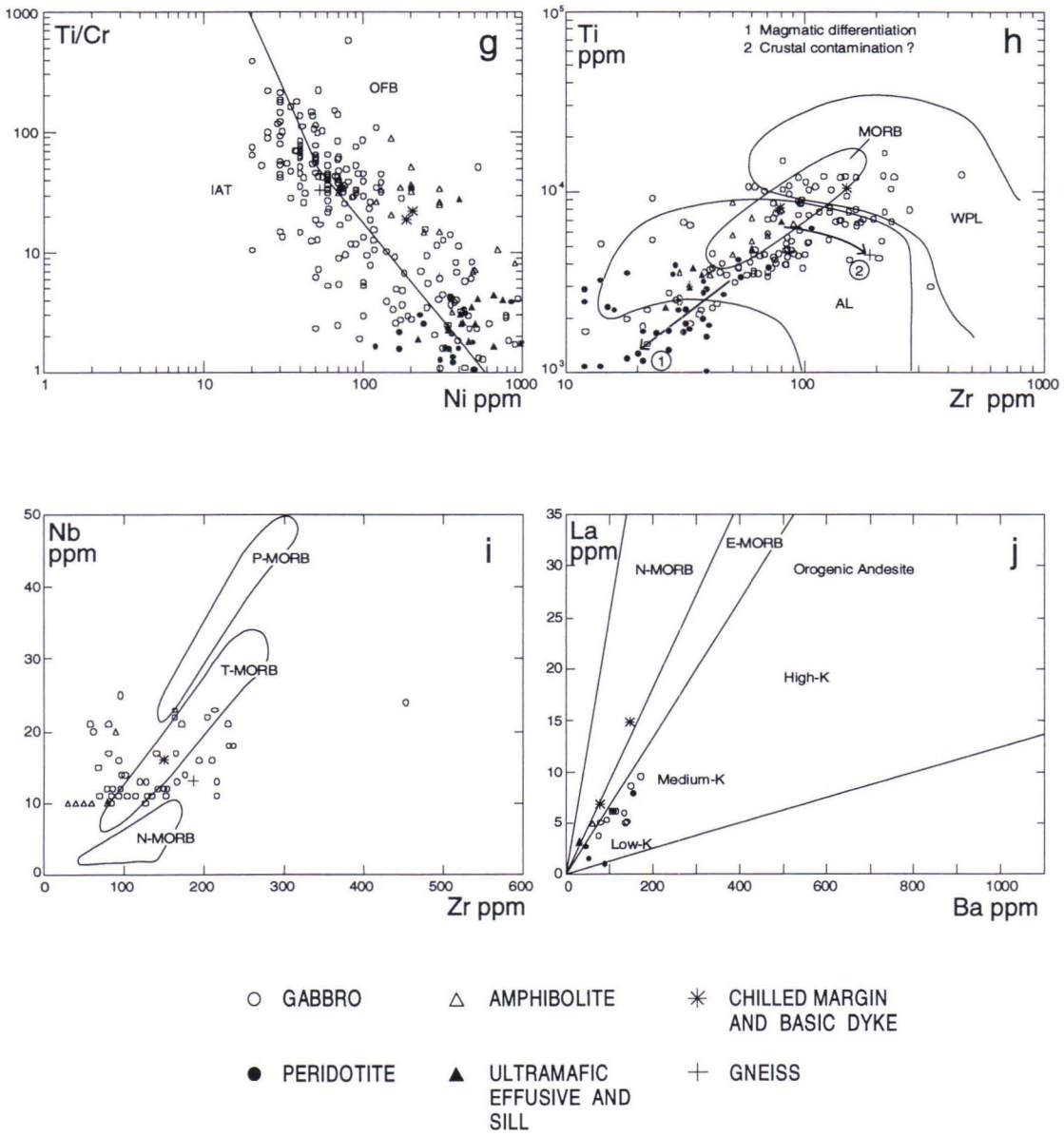

Fig. 34. Composition of different rock types on tectonomagmatic discrimination diagrams. a) Field for unaltered magmatic rocks (Davis et al., 1978). b) Trend lines for oceanic and continental tholeiites (A), island arc tholeiites (B) and island arc calc-alkaline rocks (C) after Pharoah and Pearce (1984). c) Diagram for basaltic andesites (Pearce et al., 1977). d) Oceanic volcanics after Jelinek et al. (1980), IAT = island arc tholeiites, MORB = mid ocean ridge basalts, OIT = ocean island tholeiites. e) Fields for volcanics after Cattel and Taylor (1990), OIB = oceanic island basalts, CFB = continental flood basalts, KOM = komatiitic basalts and Archaean tholeiitic basalts, MORB = mid ocean ridge basalts, VAB = volcanic arc basalts, BON = boninites. f) Arc volcanics (ARC) and ocean floor basalts (OFB) after Shervais (1982). g) Island arc tholeiites (IAT) and ocean floor basalts (OFB) after Beccaluva et al. (1979). h) Mid ocean ridge basalts (MORB), within plate basalts (WPB) and arc lavas (AL) after Pearce (1982); arrow 1 describes the increase in the amount of mafic cumulus minerals and arrow 2 possible trend of contamination in Juva area. i) Fields for N-MORB (normal), T-MORB (transitional) and P-MORB (plume-enriched) after LeRoex et al. (1983). j) Fields for orogenic andesites, N-MORB (normal) and E-MORB (enriched) after Gill (1981).

ples lie within the MORB field on the FeO/MgO - TiO_2 diagram (Fig. 34d), while on the Ti/Zr - Al_2O_3/TiO_2 diagram (Fig. 34e), data fall within both the MORB + komatiite and island arc fields. Nevertheless, almost all of the samples that are considered to be most representative of primary melt compositions, namely the amphibolites and rapidly chilled marginal phases of the Rantala intrusion, plot within the MORB + komatiite field. The V/(Ti/1000) diagram effectively discriminates between island arc volcanics and ocean floor basalts (Fig. 34f) and shows that in the present case, most gabbro samples fall within the ocean floor field, with a tendency for the peridotites to plot within the island arc volcanic field; similar results are also obtained when the data are plotted on the Ti/Cr - Ni diagrams (Fig. 34g). On the Ti - Zr plot (Fig. 34h), samples best approximating primary melt compositions tend to fall within the MORB field, while other samples lie typically within the island arc volcanic field. However, the MgO-rich cumulates, which are characterized by low Ti and Zr abundances, fall outside the island arc volcanic field, thus indicating that at least some of the other samples only plot as arc volcanics because of magmatic differentiation processes. The gabbros that have MgO contents overlapping with those of the amphibolites are nevertheless typically richer in Zr than the amphibolites and thus still plot within the island arc field. Whether or not this relative enrichment in Zr can be attributed to crustal contamination, is a problem that will be addressed later. There is a lack of suitable and abundant data for plotting on MORB type discrimination diagrams although the Nb - Zr and La - Ba plots (Figs. 34 i and j) suggest that in most cases the rocks analyzed can be classified as either T-MORB or E-MORB. The samples corresponding to primary melt compositions also fall generally within the MORB field, whereas the cumulates plot in the orogenic andesite field.

In conclusion, the discrimination diagrams indicate that the rocks investigated have both MORB (E- and T-types) and IAB characteristics. Magmatic differentiation processes have nevertheless led to dispersion of data such that more analyses plot within the IAB field than would be expected from the unfractionated compositions. Even though magmas are thus best classified as E-type and T-type MORB, it is still not possible to draw definitive conclusions about geotectonic setting since these rock types are found in diverse environments, such as elevated ocean ridge segments (Wood et al., 1979), seamounts (Taras and Hart, 1987), passive margins (Fodor and Vetter, 1984), back arc basins (Marsh et al., 1980; Saunders and Tarney, 1984; Volpe et al., 1988) and intraplate continental flood basalts (Ewart et al., 1989). Lawrie (1992) concluded that the metatholeiites of the Virtasalmi area, which lies immediately to the west of the Juva district, were formed in a passive plate margin setting.

On the MORB-normalized element abundance diagrams (Fig. 35), rock types have been subdivided as follows:

a) those corresponding to primary melt compositions (amphibolites and the rapidly chilled marginal phases of the Rantala gabbroic intrusion);
b) ultramafic sills and lavas;
c) gabbros, and
d) peridotites.

All of these display elevated Rb and Ba abundances, which is a characteristic feature of 1.9 Ga Svecofennian basalts (Ekdahl, 1993; Lahtinen, 1994; Kähkönen and Nironen, 1994; Viluksela, 1994) as well as within ultramafic intrusions of similar age (Peltonen, 1995b). A wide variety of modern basalts are also enriched in these elements, including island arc tholeiites, within plate basalts (such as E-MORB) and both oceanic and continental calc-alkaline basalts (Pearce, 1983; Pearce et al., 1984); it is accordingly very difficult to

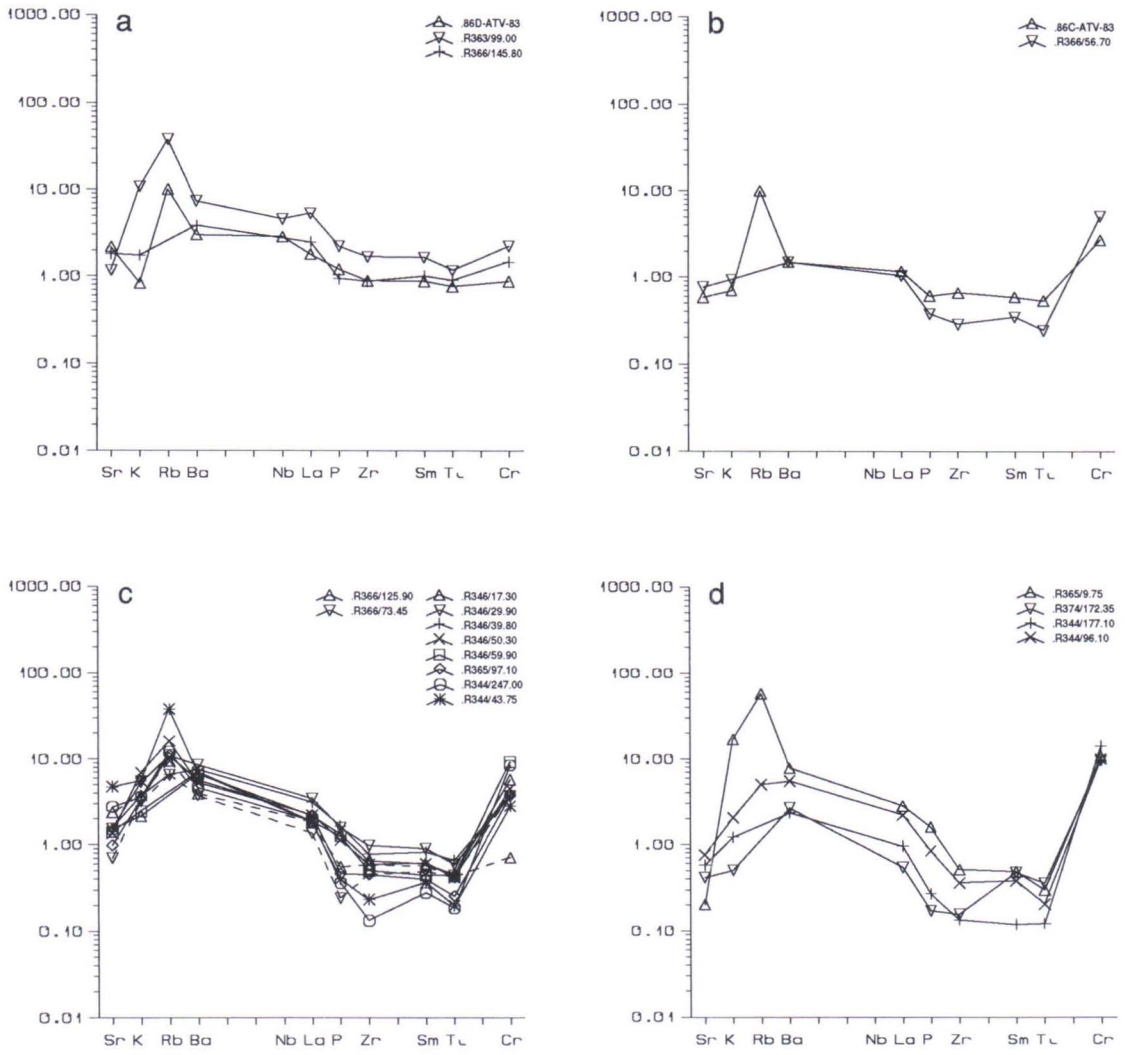

Fig. 35. MORB normalized (Pearce, 1982) element patterns for the different rock types. a) amphibolite and Rantala gabbro; b) ultramafic sills and lavas; c) gabbros; d) peridotites.

use these observations in determining tectonic setting of magmatism. Furthermore, because analytical data are not available for all of the elements normally used in tectonomagmatic classification, no firm conclusions can be made. However, the general increase in disparity between La and Cr abundances when progressing from amphibolite to ultramafic sills and lavas to gabbros and peridotites appears to reflect a corresponding increase in the abundance of mafic cumulus minerals. Similarly, the generally uniform element variation trends for different rock types suggests that all are derived from a common parent magma.

FRACTIONAL CRYSTALLIZATION AND MAGMATIC DIFFERENTIATION

Luonteri-Heiskalanmäki zone

Changes in chemical composition within intrusions of this zone are not reflected in their mineralogy and therefore differentiation processes have been assessed on the basis of whole rock chemistry alone; essential features are summarized in the diagrams in Figure 36.

An estimate of 6.86 w-% was obtained for the MgO content of the primary silicate melt for the Luonteri-Heiskalanmäki zone. On the AFM diagram, samples containing this amount of MgO plot close to the culmination of the cluster of data points; analyses plotting between here and the MgO apex thus represent MgO-rich cumulates, while those trending towards the alkali corner represent residual melts containing late-stage plagioclase and quartz. It is also noteworthy that this residual melt is actually calc-alkaline in character, which could be a result of contamination by country rock sediments, or else addition of alkali elements during metamorphism.

Molar ratio diagrams based on the theory of Pearce (1968) show that the crystallizing Mg-rich mineral has been orthopyroxene. Another fractionation trend can be identified on the same diagram as a nearly vertical line corresponding to an $(FeO+MgO)/SiO_2$ ratio of around zero and representing the crystallization of plagioclase and quartz.

It is also evident from the CMA diagram that the Mg-rich cumulus mineral has been orthopyroxene rather than clinopyroxene since if significant amounts of clinopyroxene had existed, the data points would be located closer to the CaO apex. There is also a marked change in the trend appproaching the Al_2O_3 apex, which is attributed to the onset of extensive plagioclase crystallization.

Differentiation processes are also well displayed on the MgO-DI diagram. The orthopyroxene cumulates define their own trend which intersects the trend of the more felsic differentiates along the MgO axis at a value of around 6 w-%, which is close to the inferred composition of the melt.

The steady increase in Cr within silicate phases as a function of MgO content is also apparent from the Cr-MgO diagram, which is also consistent with the absence of chromite from the gabbros. This also indicates that the crystallization of pyroxene was dominant since no such correlation would be expected if olivine had been crystallizing, Cr being less readily incorporated into the olivine lattice.

Some samples do however show normative olivine. The diagram (plagioclase) - (clinopyroxene) - (orthopyroxene + 4 x quartz) represents the basalt tetrahedron (plagioclase) - (clinopyroxene) - (orthopyroxene) plane, onto which the olivine-bearing samples have been projected. The boundary lines on the diagram have been drawn from the liquidus curves compiled by Irvine (1970), according to which orthopyroxene and plagioclase commenced crystallization after olivine (Fig. 37).

Scatter on both the AFM and molecular ratio diagrams is rather large and is considered to reflect metasomatic processes. This is quite likely given the small size of the intrusions and the high grade of regional metamorphism, which was accompanied by the emplacement of widespread potassic granitoids.

In conclusion, the crystallization history of the Luonteri-Heiskalanmäki zone can be summarized as follows. The mean MgO content of the melt was about 6-7 w-% and the early

Fig. 36 (on the right). Diagrams depicting magmatic differentiation in Luonteri-Heiskalanmäki zone. FM = FeO_{TOT} + MgO; cpx = clinopyroxene, opx = orthopyroxene, ol = olivine; DI = differentiation index (Till, 1977).

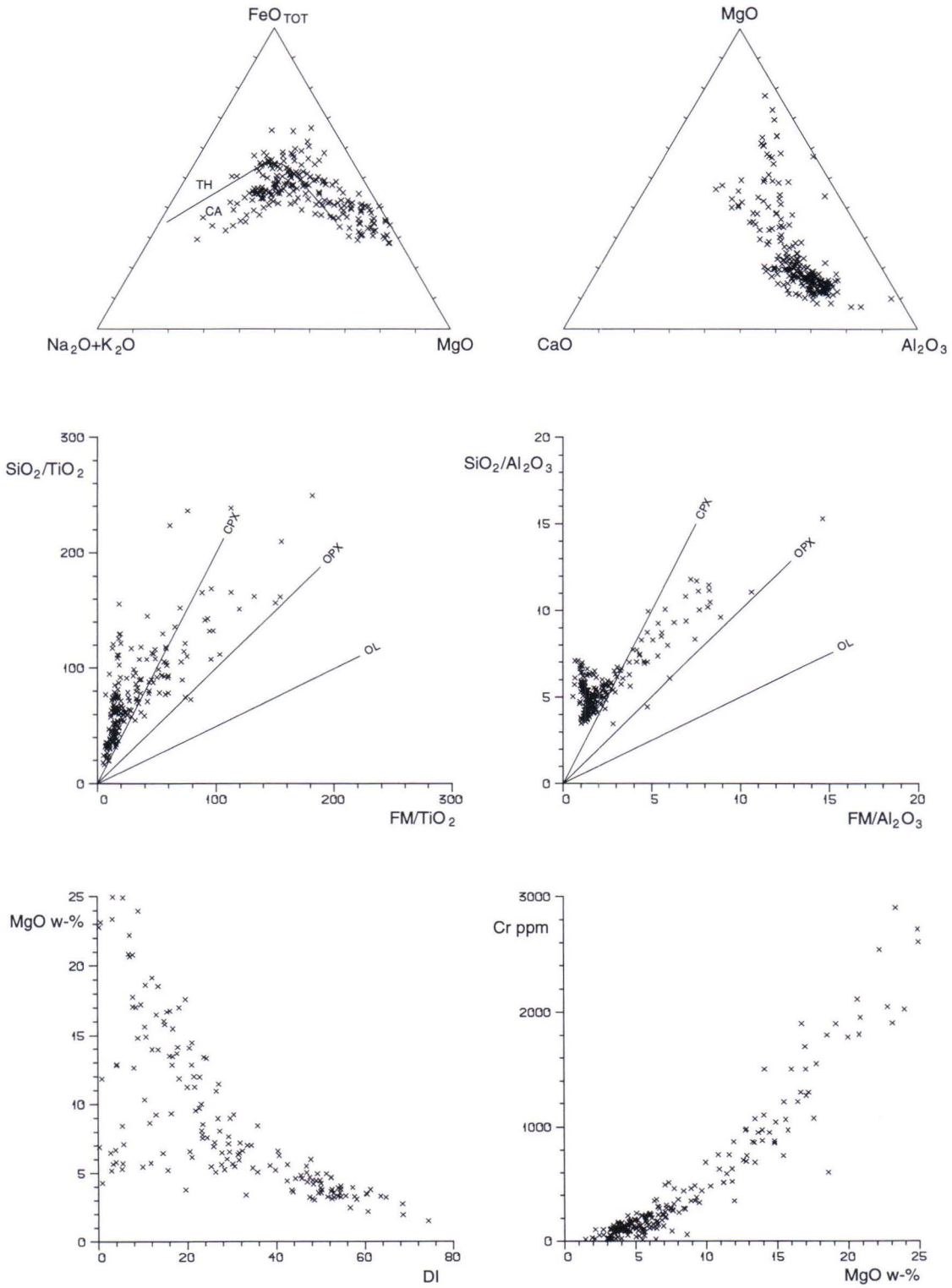
FeO TOT
TH
CA
Na2O+K2O
MgO
MgO
CaO
Al2O3
SiO2/TiO2
CPX
OPX
OL
FM/TiO2
SiO2/Al2O3
FM/Al2O3
MgO w-%
DI
Cr ppm
MgO w-%

Fig. 36.

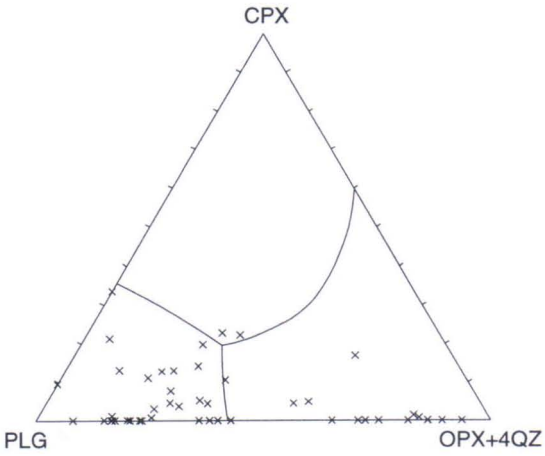

Fig. 37. Olivine normative samples on the plagioclase-clinopyroxene-orthopyroxene+4xquartz projection of basalt tetrahedron. Liquidus curves after Irvine (1970).

stages of crystallization were dominated by the formation of orthopyroxene. The intrusions in the northern part of the zone tend to have the cumulates richer in Mg, with values locally exceeding 18 w-% MgO. With continued crystallization, the Mg and Fe contents of the remaining melt fell to levels where plagioclase and quartz were the main phases to crystallize, with the MgO content of the most felsic differentiates being less than 2 w-%.

Peridotites

The molar ratio diagrams in Figure 38 show that the predominant Mg-Fe-bearing cumulus phase in the peridotites was olivine, except in the case of Lumpeinen, where pyroxene was also crystallizing in notable amounts. The diagrams do not show very much scatter, indicating that chemical compositions have not been significantly affected by post-magmatic processes.

Crystallization trends subsequent to olivine crystallization have been deduced from the basalt tetrahedron (plagioclase) - (clinopyroxene) - (orthopyroxene + 4 x quartz) plane (Fig. 39a). Clinopyroxene and orthopyroxene crystallization took place at the Lumpeinen, Turunen, Venetekemä and Pihlajasalo occurrences, in contrast to the crystallization of orthopyroxene and plagioclase in the Niinimäki, Saarijärvi, Kekonen and Kiiskilänkangas intrusions. Differences in respective normative

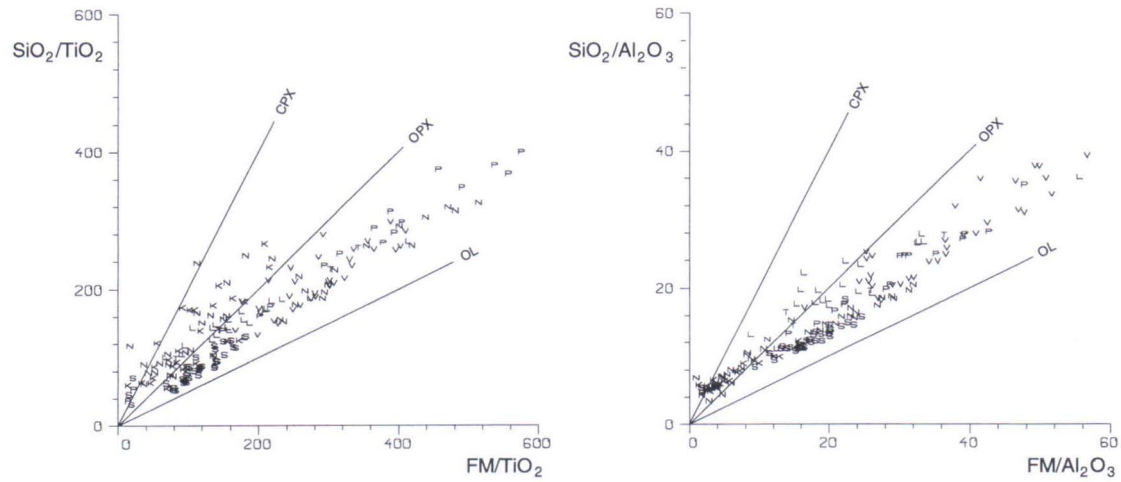

Fig. 38. Molar ratio diagrams indicating crystallizing phases in peridotites. FM = FeO_{TOT} + MgO. Symbols as in Figure 17.

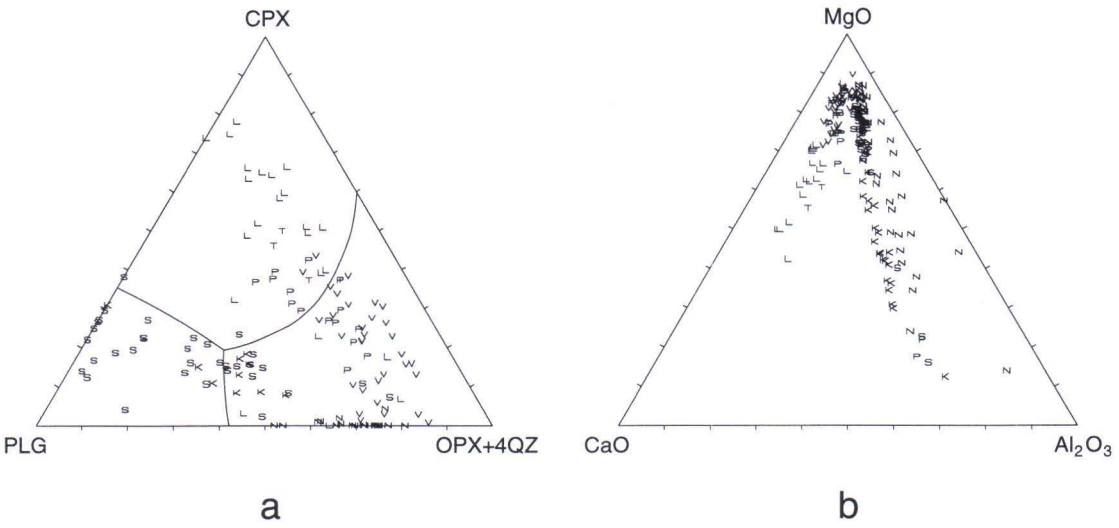

Fig. 39. Peridotite samples and samples of associated gabbros on the plagioclase-clinopyroxene-orthopyroxene+4xquartz projection of basalt tetrahedron (a) and on CMA diagram (b). Liquidus curves after Irvine (1970). Symbols as in Figure 17.

mineral compositions are also consistent with modal mineralogy. Only the Saarijärvi, Kekonen and Kiiskilänkangas peridotites contain intercumulus plagioclase. These conclusions can also be made from inspection of the CMA diagram (Fig. 39b). Those peridotites with abundant clinopyroxene show increasing Ca/Al ratios with decreasing Mg abundances, whereas the converse applies to those rich in orthopyroxene. Gabbros from the Luonteri-Heiskalanmäki zone plot in the Mg-rich parts of the CMA diagrams, together with the gabbros rich in orthopyroxene (compare with Fig. 36). There is a distinct compositional gap between the peridotites and gabbros of the Pihlajasalo, Niinimäki and Saarijärvi intrusions, but continuous compositional variations are observed for the Kekonen and Kiiskilänkangas intrusions.

Mäkinen (1987) classified Svecofennian mafic and ultramafic intrusions in Finland into Vammala-type and Kotalahti-type intrusions, the latter containing abundant normative orthopyroxene, in contrast to clinopyroxene in the former group. These differences were then attributed to differences in the origin of the magmas, the Kotalahti intrusions being regarded as derived from a deeper level primary magma than the Vammala magmas. Melting at deeper levels would be more extensive and result in a magma poorer in Ca than that formed at higher levels, where melting of clinopyroxene would predominate.

The possibility of contamination provides an alternative explanation for the differences between the Kotalahti and Vammala magma types since the assimilation of country-rock sediments leads to an increase in Si content, allowing orthopyroxene to crystallize directly after olivine, even though the primary melt composition would favour the crystallization of clinopyroxene (Schiffries and Rye, 1989). The CaO/Al_2O_3 ratio of the magma would also approach that of the Kotalahti-type intrusions by progressive sediment contamination and hence the orthopyroxene-rich Kotalahti intrusions would represent more contaminated magmas than the Vammala-type intrusions. Moreover, because intrusions of both type are present in the Juva district, they are not necessarily restricted to distinct magmatic provinces.

A further possibility is that of mantle heterogeneity, in which case the Kotalahti-type would represent enriched mantle and the Vammala-type would correspond to depleted mantle, as proposed by Lahtinen (1994). The merits of each of these possibilities will be considered later.

Ultramafic volcanics and sills and amphibolites

It is evident from the molar ratio diagrams that the ultramafic rocks record olivine fractionation trends while the amphibolites reflect crystallization of clinopyroxene (Fig. 40). On the basis of the (plagioclase) - (clinopyroxene) - (orthopyroxene + 4 x quartz) projection, the ultramafic rocks crystallized orthopyroxene and clinopyroxene after olivine. Only the Pirilä ultramafic rocks plot partly within the plagioclase field, while the Pirilä amphibolites and the gabbros of the Rantala intrusion fall within both the plagioclase and clinopyroxene fields. The chilled margin of the Rantala gabbro and the Rantala mafic dyke have compositions within the orthopyroxene field, according to which the crystallization sequence should have been olivine - orthopyroxene - (clinopyroxene) - plagioclase (Fig. 41a).

In comparison to the peridotites, the ultramafic volcanics and sills lie closer to the liquidus curves, principally because the amount of intercumulus melt in these rocks was greater than in the peridotites. They also plot differently to the peridotites on the CMA diagrams, lying along the olivine crystallization trend between CaO-poor and CaO-rich peridotites, and thus resembling Archean komatiites (Green and Naldrett, 1981). The Pirilä amphibolites deviate somewhat from this trend because of their higher CaO/Al_2O_3 ratios (Fig. 41b).

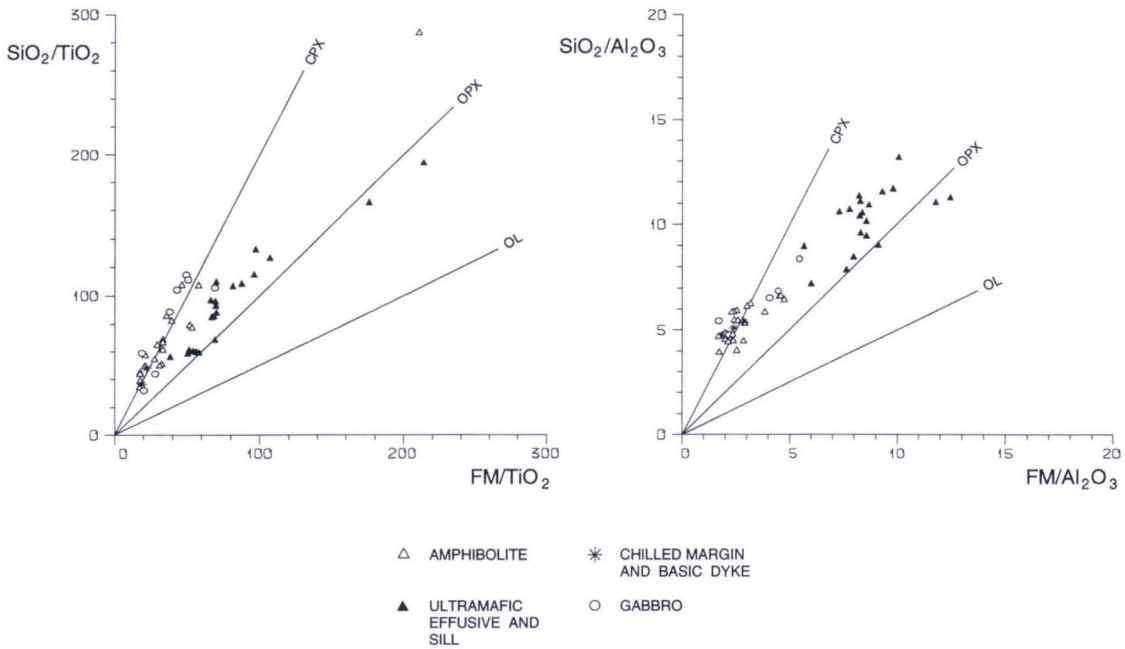

Fig. 40. Molar ratio diagrams indicating crystallizing phases in ultramafic volcanics and sills, amphibolites and Rantala gabbros. FM = FeO_{TOT} + MgO.

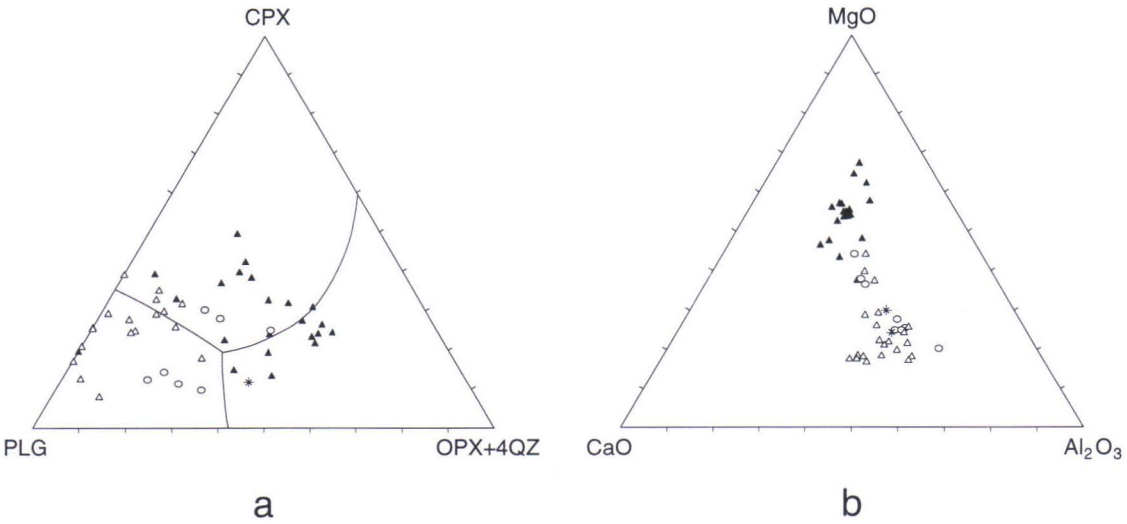

Fig. 41. Samples of ultramafic volcanics and sills, amphibolites and Rantala gabbros on the plagioclase-clinopyroxene-orthopyroxene+4xquartz projection of basalt tetrahedron (a) and on CMA diagram (b). Liquidus curves after Irvine (1970). Symbols as in Figure 40.

REE INVESTIGATIONS

Rare earth elements have been analyzed for 37 samples (App. 3) and chondrite-normalized results overall resemble those of continental, island arc, plate margin tholeiites and tholeiitic intrusions (Fig. 42). The intrusions of the Juva district deviate from N-type MORB in having higher LREE abundances and generally falling or slightly increasing LREE trends. There are nevertheless similarities with E-type and transitional MORB.

Fractional crystallization results in up to ten times difference in REE abundances between the more felsic and mafic differentiates (Fig. 43), which should be kept in mind when comparing REE data from different occurrences. Figure 44 compares stratigraphic variations in REE abundances throughout the Rietsalo gabbro. As MgO contents increase from 5.25 w-% to 11.47 w-%, La_{cn} decreases

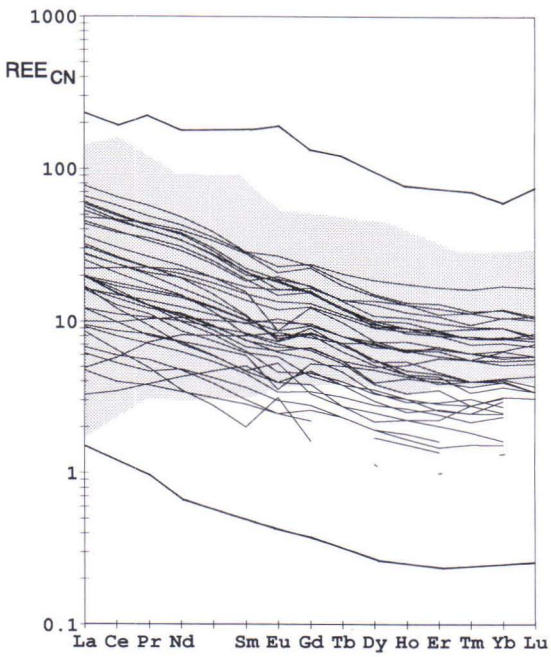

Fig. 42 (on the right). Chondrite normalized REE patterns for the mafic and ultramafic rocks of the Juva area. Chondritic REE concentrations after Boynton (1984) as elsewhere in this work. For comparison REE patterns for tholeiitic intrusions (between the thick lines) and continental, island arc and back arc basin tholeiites (stippled area) are shown (Cullers and Graf, 1984, Figures 7.7 and 7.8).

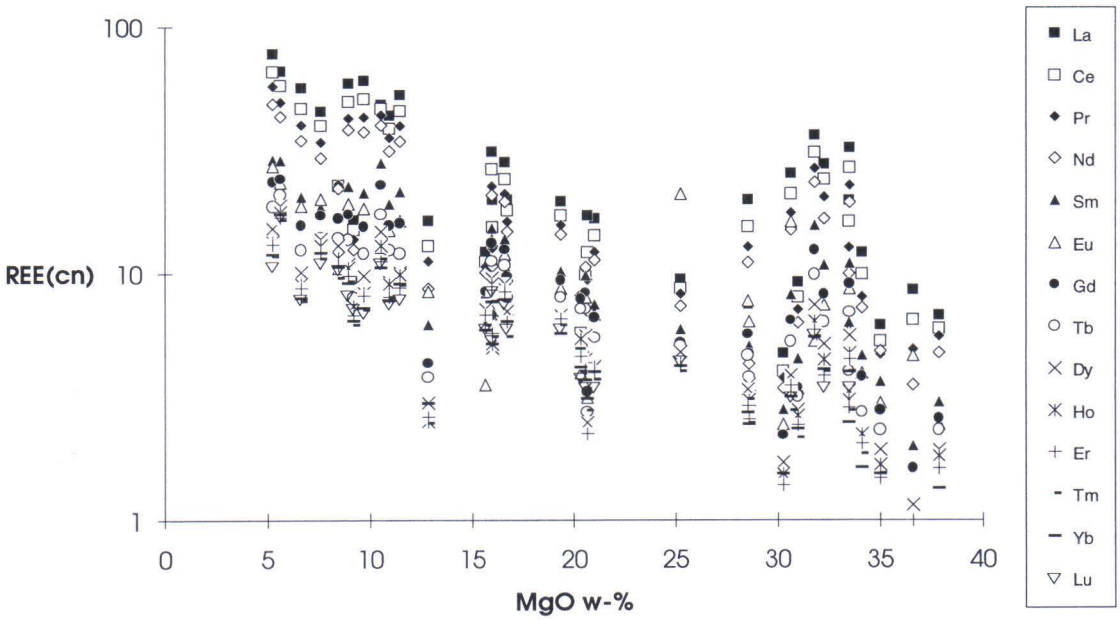

Fig. 43. Chondrite normalized REE contents as a function of MgO content.

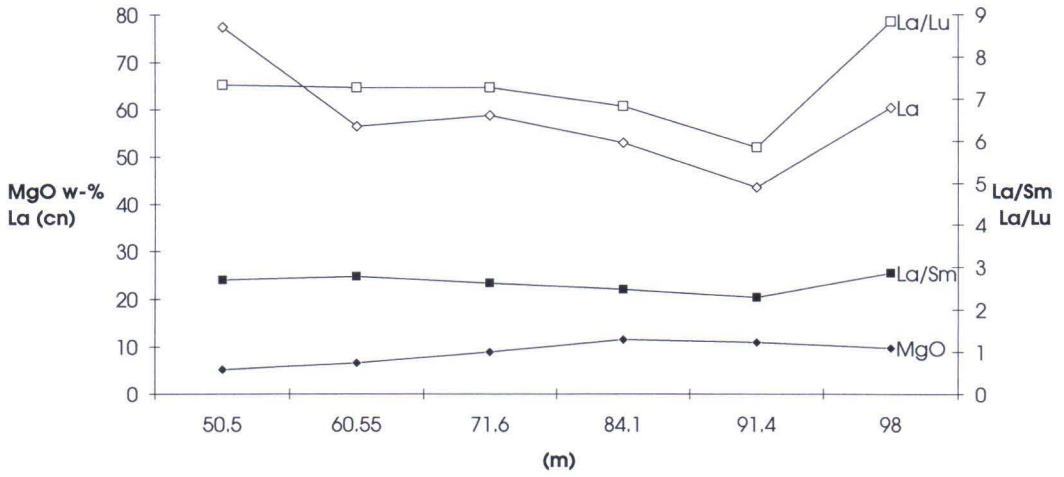

Fig. 44. Variation of chondrite normalized REE contents and MgO content in BH303 from the Rietsalo gabbro.

from 77.4 to 52.9, while La_{cn}/Sm_{cn} and La_{cn}/Lu_{cn} ratios remain almost constant. The sample from a depth of 98 m represents the marginal phase of the intrusion about 9 m from the contact with the country-rock gneisses. The results clearly show elevated La abundances and chondrite-normalized La/Sm and La/Lu ratios that are probably a result of contact contamination processes.

Comparison of REE data from different intrusions reveals the following features:

1) gabbros tend to have higher REE abun-

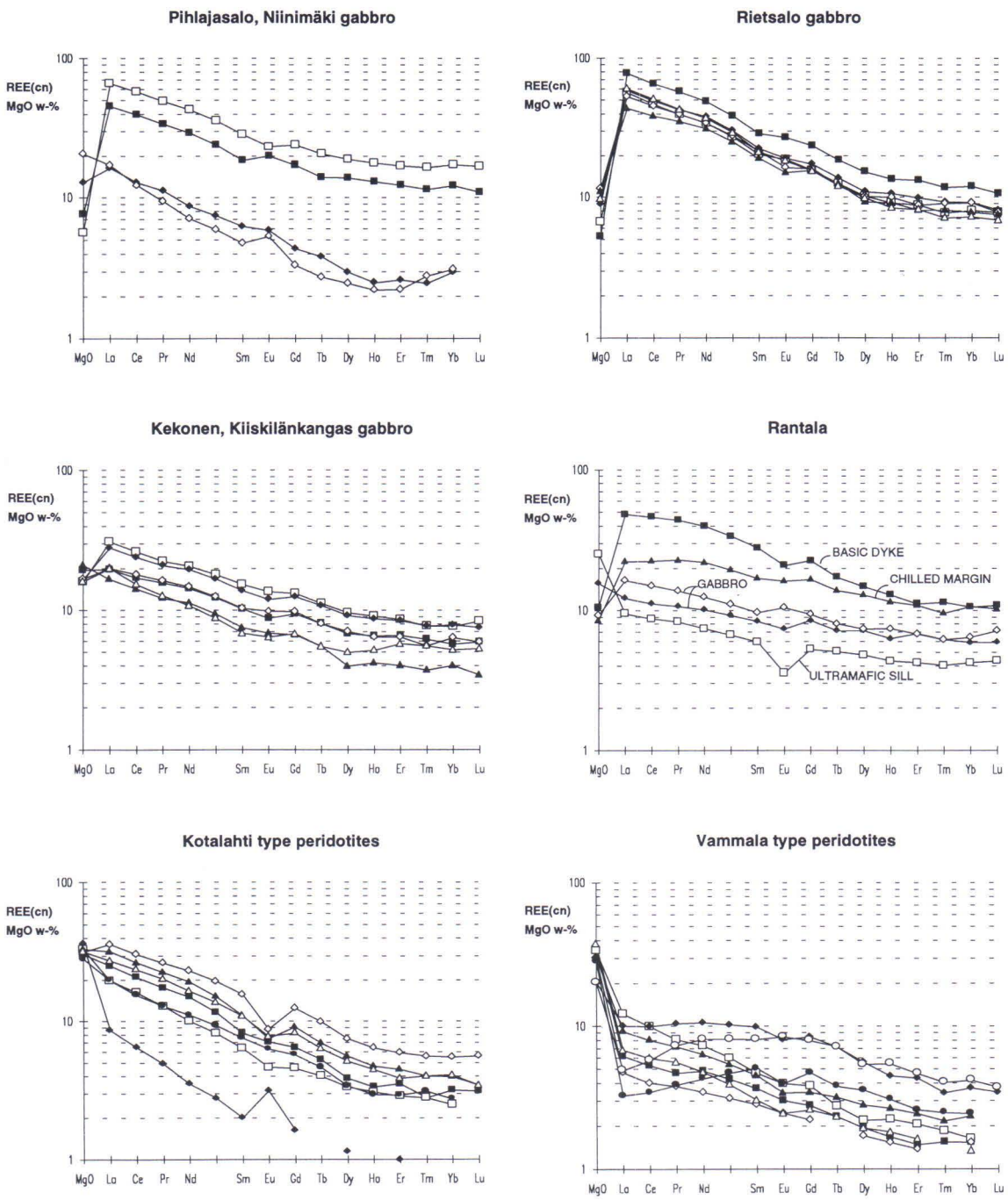

Fig. 45. Chondrite normalized REE patterns for the different rock types.

dances than peridotites;

2) Kotalahti-type (orthopyroxene-rich) and Vammala-type (clinopyroxene-rich) peridotites are clearly separate from one another, with the Kotalahti-type being characterized by higher LREE abundances and a falling trend. In contrast, the Vammala-type samples have gently decreasing or increasing LREE trends. The chondrite-normalized La/Sm ratios of the Kotalahti-type peridotites range from 2.30-3.08 and for the Vammala-type peridotites from 0.61-2.61.

3) Many of the peridotites that are serpentinized have either negative or positive Eu anomalies (Fig. 45).

The first of the above features can be explained in terms of normal fractional crystallization since the REE content of the melt increases progressively with crystallization. This cannot be the case for the second feature however, since MgO and other variables that describe differentiation processes, including Fo content, Mg-number and MDI are very similar for the Vammala-type and Kotalahti-type intrusions. The third feature, namely irregularities in Eu abundance, is likely to result from Eu^{2+} mobility during the serpentinization process itself (Sun and Nesbitt, 1978), especially since the anomalous values are essentially restricted to the serpentinized lithologies.

Sm-Nd INVESTIGATIONS

Seven of the samples were analyzed for Sm and Nd isotopic ratios at the Geological Survey of Finland Isotope Laboratory (Table 16). Two samples of Kotalahti-type peridotite were selected (Saarijärvi BH361/170.05 and Niinimäki BH344/177.10), as were three Vammala-type peridotites (Turunen BH13/54.25, Lumpeinen BH374/142.35 and Pihlajasalo BH307/61.50), of which the Pihlajasalo sample has a chemistry transitional between the Vammala and Kotalahti types, and finally, a sample from an ultramafic sill (Rantala BH366/56.70) and a gabbro (Rietsalo BH303/84.10).

Nd-epsilon values have been calculated using an age of 1.88 Ga, which is considered to be a representative age for Svecofennian Ni-bearing intrusions in Finland. Values for ε_{Nd}(1.88Ga) are between 0.4-2.4, with the values for Vammala-type intrusions being higher than those for the Kotalahti-type intrusions. All samples however have ε_{Nd}(1.88Ga) values

Table 16. Isotope compositions for samarium and neodymium.

Sample	Sm ppm	Nd ppm	$^{147}Sm/^{144}Nd$	$^{143}Nd/^{144}Nd$ ($\pm 2\sigma m$)	ε_{Nd} (1880 Ma)	T(DM) Ma
BH361/170.05 prd(k)	3.37	15.82	0.1289	0.511823±10	0.4±0.3	2193
BH344/177.10 prd(k)	0.56	3.12	0.1091	0.511609±14	1.0±0.4	2088
BH307/61.50 prd(v)	0.68	3.01	0.1374	0.511968±13	1.2±0.4	2145
BH374/142.35 prd(v)	0.89	2.62	0.2058	0.512825±16	1.4±0.5	
BH13/54.25 prd(v)	1.92	6.71	0.1733	0.512472±10	2.4±0.4	
BH366/56.70 umaf	1.20	4.60	0.1574	0.512252±28	1.9±0.7	2146
BH303/84.10 gb	4.27	20.89	0.1235	0.511816±8	1.6±0.3	2072

Error in $^{147}Sm/^{144}Nd$ is 0.4%. $^{143}Nd/^{144}Nd$ ratio is normalized to $^{146}Nd/^{144}Nd = 0.7219$. Average value for LaJolla standard was 0.51185±1(SD,N = 11). T(DM) is calculated according to DePaolo (1981). prd(k) = Kotalahti type peridotite, prd(v) = Vammala type peridotite, umaf = ultramafic sill, gb = gabbro.

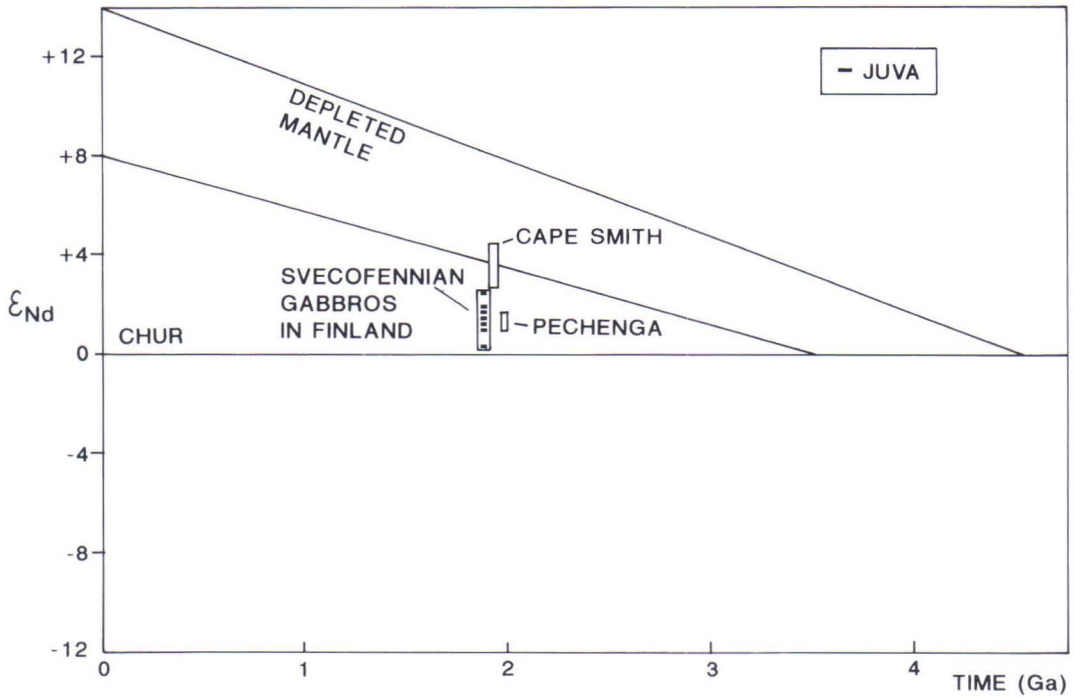

Fig. 46. Samples from Juva plotted on ε_{Nd}(T)-T diagram compared to other Svecofennian gabbros in Finland (Huhma, 1986; Patchett and Kouvo, 1986), Cape Smith (Hegner and Bevier, 1991) and Pechenga (Hanski, 1993). Depleted mantle field after Cousens and Ludden (1991).

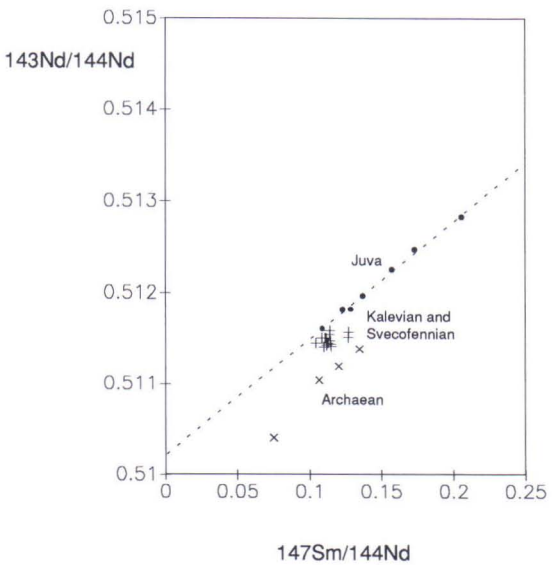

Fig. 47. $^{143}Nd/^{144}Nd$ versus $^{147}Sm/^{144}Nd$ diagram for samples from Juva (dots), Kalevian and Svecofennian metasediments (crosses, Huhma, 1987) and Archean metasediments and granitoids (ticks, Huhma, 1987).

lower than the depleted mantle figure of 3.74 (calculated according to DePaolo, 1981), indicating either derivation from heterogeneous mantle or variable contamination of magma derivated from depleted mantle with crustal material (Fig. 46).

When the data are plotted on a $^{143}Nd/^{144}Nd$ versus $^{147}Sm/^{144}Nd$ diagram they define an array providing an initial $^{143}Nd/^{144}Nd$ ratio of 0.51019 and a magmatic age estimate of 1.970±133 Ma. The large scatter and high MSWD value of 10.3 nevertheless indicates that they form a heterogeneous population and little significance should be attached to the result. Although the data make reliable conclusions difficult, the Rantala ultramafic sample (BH366/56.70) nevertheless plots within the array and indicates that it does not belong to a separate magmatic event or source. The Kotalahti-type peridotite samples plot at the lower end of the array, while the Vammala-

type samples plot at the upper end, thereby indicating that the Kotalahti-type samples had a lower initial Sm/Nd ratio than the Vammala-type samples. This difference cannot be explained by variations in the relative proportions of clinopyroxene and orthopyroxene since both minerals have relatively uniform D_{Sm}/D_{Nd} ratios of around 1.6. The abundance of plagioclase is higher in the Kotalahti-type rocks and because plagioclase has a D_{Sm}/D_{Nd} ratio of around 1, addition of plagioclase will tend to lower the whole-rock Sm/Nd ratio of the peridotite. Increasing apatite abundance ($D_{Sm}/D_{Nd} = 0.8$) produces the same effect (data compilation by Jacobsen and Wasserburg, 1979).

It is possible that the chord in Figure 47 represents the mixing of older crustal material with mafic magmas. If Svecofennian or Kalevian sedimentary material were added to the Juva samples, the array would become steeper and the initial $^{143}Nd/^{144}Nd$ ratio would become correspondingly smaller.

A CONTAMINATION MODEL

Because the Vammala and Kotalahti-type intrusions are both present in the Juva district and have similar olivine compositions and Mg-numbers, as well hosting in general ore deposits of similar compositions (Papunen and Gorbunov, 1985; Ekdahl, 1993), it is therefore most likely that their differences relate to processes after magma genesis rather than representing different degrees of mantle melting or sources. Secondary phenomena, such as early metamorphic metasomatic changes are however, considered unlikely, since the intrusions are spatially associated and have experienced the same metamorphic events. The degree of serpentinization of the Vammala-type and Kotalahti-type intrusions is also very similar and furthermore, the higher CaO content in olivines of the Vammala-type intrusions indicates that the different CaO/Al_2O_3 ratios reflect differences in melt

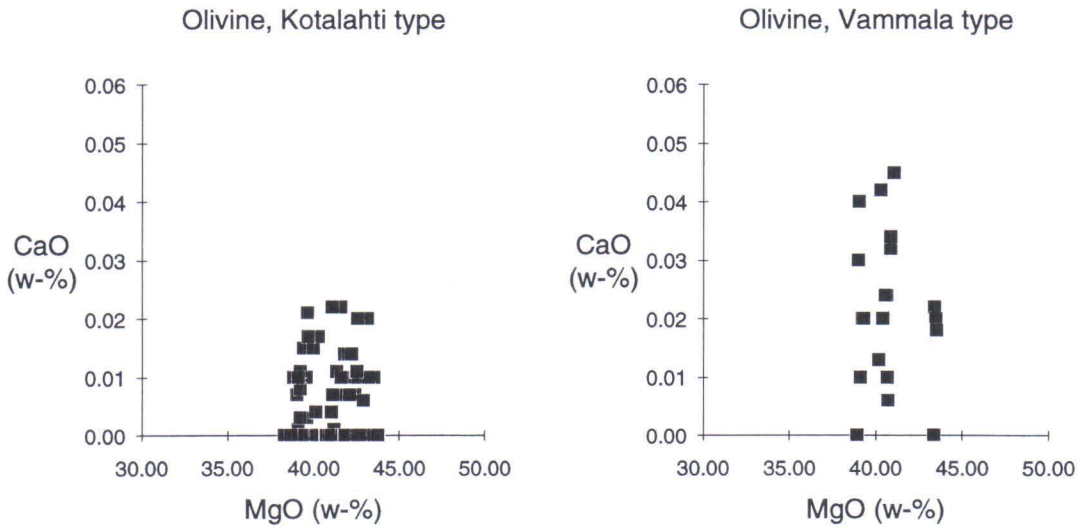

Fig. 48. CaO content in olivine of Kotalahti type (Niinimäki, Saarijärvi) and Vammala type (Lumpeinen, Pihlajasalo). Detection limit for CaO is 0.0060 w-%.

composition rather than post-crystallization alteration (Fig. 48). It should be kept in mind however, that olivine CaO abundances are rather close to the analytical detection limit of the microprobe.

The chilled margin of the Rantala gabbro, together with the nearby mafic dyke and Pirilä amphibolites most closely approximate the parent magma composition of the intrusions studied. All of these samples have chondritic normalized La/Sm ratios of < 2 (Fig. 45 and Viluksela, 1988), which corresponds to the composition of the Vammala-type intrusions. The REE abundances of the Rantala gabbro chilled margin and mafic dyke are nevertheless high with respect to those of the amphibolites, which strongly implicates the role of contamination (compare Rietsalo gabbro in Figure 44). For this reason, the Pirilä amphibolite is considered to best represent the composition of the primary melt, and has a chondritic normalized La/Sm ratio of 1.08 (Viluksela, 1988).

During fractional crystallization the chondritic normalized La/Sm ratio should steadily decrease in mafic cumulates compared to that of the parent magma, principally due to preferential incorporation of Sm into cumulus olivine and pyroxene (data compilation by Hanski, 1983). An increasing LREE trend is apparent only for some of the Vammala-type peridotites, so that the Vammala-type intrusions are considered to more reliably represent primary melt compositions.

In order to obtain rocks with the REE characteristics of the Kotalahti-type intrusions from an initial composition corresponding to that of the Vammala-type magmas, it is necessary to either increase the proportion of melt containing higher and negative sloping REE - and particularly LREE - abundances, or to selectively remove from the melt those components that contain low abundances of REE with positive sloping patterns. Whichever solution is correct, it must be compatible with the difference in CaO/Al_2O_3 ratios of the Vammala- and Kotalahti-type intrusions.

In the case of the first alternative, crustal contamination is a likely possibility, since assimilation of the present country rocks, as well as any Archean granitic basement at depth, could shift the REE characteristics of the Vammala-type magmas towards that of the Kotalahti intrusions. Both the Archean basement and Svecofennian (so-called Upper Kaleva) sediments are suitably enriched in REE and have negatively sloping LREE patterns, as shown in Figure 49 (O'Brien et al., 1993;

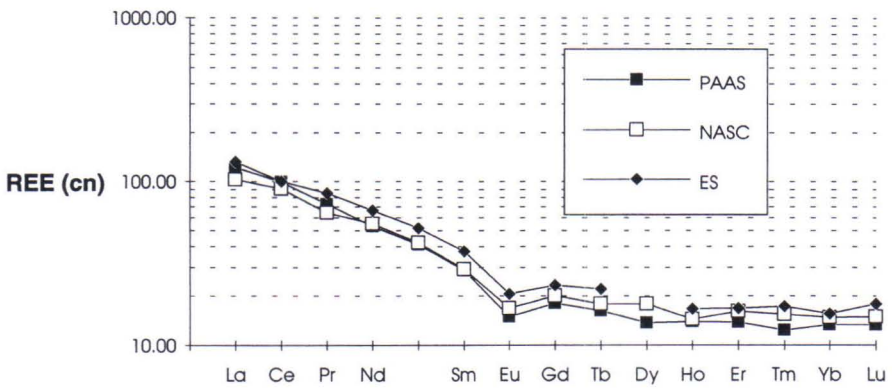

Fig. 49. Chondrite normalized REE pattern for upper crust. PAAS = Post-Archean average Australian shale (Nance and Taylor, 1976), NASC = North American shale composite (Haskin et al., 1968), ES = European shale composite (Haskin and Haskin, 1966).

Huhma, 1987; Asko Kontinen, personal communication). This kind of contamination could also explain the different CaO/Al_2O_3 ratios of the Vammala-type and Kotalahti-type intrusions since the CaO/Al_2O_3 ratio could be expected to drop dramatically as sediments are assimilated.

In the case of the second alternative, the crystallization conditions of the melt are critical, since at moderately high (> 3 kbar) to high (> 10 kbar) pressures, clinopyroxene commences crystallization at an earlier stage, corresponding to higher MgO contents, than at lower pressures (Elthon, 1993). If fractional crystallization occurs, then the CaO content of the melt decreases and LREE increases (Elthon, 1993; Cullers and Graf, 1984). According to this model, Kotalahti-type magmas would have undergone fractional crystallization of clinopyroxene at high pressures before emplacement to their present levels. This too could in principle explain the observed differences in REE abundances and CaO/Al_2O_3 ratios of the Vammala-type and Kotalahti-type intrusions.

If clinopyroxene is removed from a magma having a chondritic normalized La/Sm ratio of 1 by fractional crystallization such that the degree of crystallization (= residual melt amount/ original melt amount) is 0.5, then according to D-values after Henderson (1984), the residual chondritic normalized La/Sm ratio would be 1.76; note however that according to D-values after most authors, (data compilation by Hanski, 1983; Prinzhofer and Allegre, 1985), the resulting change in La/Sm ratio would be somewhat smaller. The chondritic normalized La/Sm ratio of the Kotalahti-type peridotites is, however around 2.30-3.08, which could not even be achieved by extreme fractional crystallization of clinopyroxene. Furthermore, the chondritic normalized La/Sm ratio of the Kotalahti-type *magmas* should be even higher than that of the olivine and olivine-orthopyroxene cumulates formed via fractional crystallization since the chondritic normalized La/Sm ratio of both olivine and orthopyroxene is, according to many studies, less than unity (data compilation by Hanski, 1983). With the same degree of crystallization the CaO/Al_2O_3 ratio of the magma changes radically from 0.72 to 0.10 (with clinopyroxene CaO/Al_2O_3 ratio of 10). Even at a degree of crystallization of 0.9 the CaO/Al_2O_3 ratio decreases from 0.72 to 0.60, which compares closely with the CaO/Al_2O_3 ratios of 0.61 and 0.63 for the Rantala chilled margin and mafic dyke respectively. These rocks plot in the orthopyroxene field on the plagioclase - diopside - orthopyroxene + 4 x quartz projection of the basalt tetrahedron (compare with Fig. 41a), whereas the Pirilä amphibolites (CaO/Al_2O_3 ratio of 0.72) fall within the clinopyroxene or plagioclase field. Therefore, even a small degree of clinopyroxene fractionation can shift the CaO/Al_2O_3 ratio of a Vammala-type magma to that characteristic of Kotalahti magmas.

The contamination interpretation given above explains the difference in REE abun-

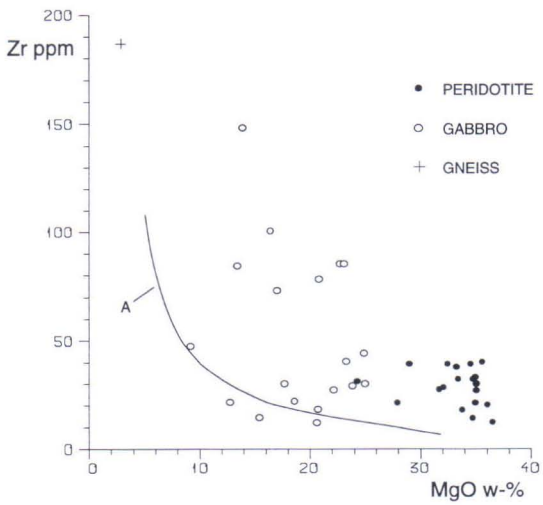

Fig. 50. MgO versus Zr diagram for samples from the Niinimäki intrusion. Curve A indicates the compositions of Vammala type peridotites and Pirilä amphibolites (cf. Fig. 65).

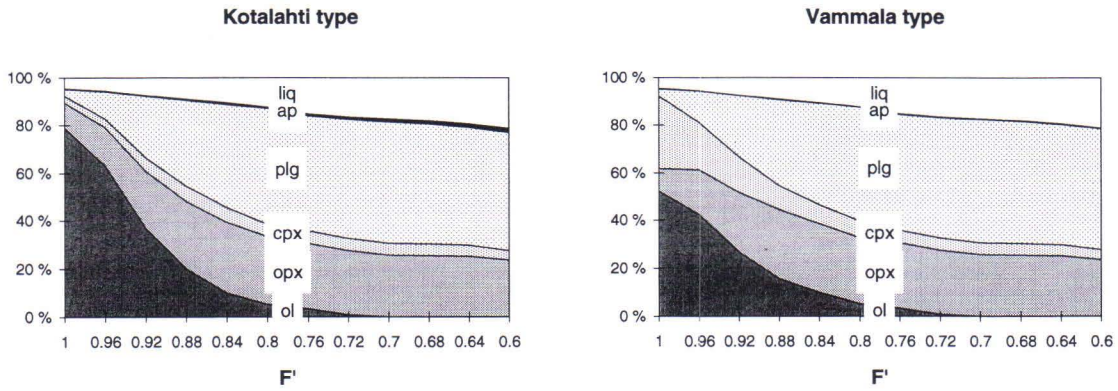

Fig. 51. Mineral composition for Kotalahti and Vammala types as a function of degree of crystallization (F'). ol = olivine, opx = orthopyroxene, cpx = clinopyroxene, plg = plagioclase, ap = apatite, liq = intercumulus liquid.

dances between the Vammala and Kotalahti intrusive types more effectively, while the different CaO/Al_2O_3 ratios are consistent with either interpretation.

Clear evidence for contamination by crustal material is provided by comparative Zr abundances in gabbros and peridotites. An example of this is the Niinimäki intrusion, in which peridotites have a sharp contact against the enclosing gabbro. Diagrams showing magmatic differentiation (Figs. 38 and 39) indicate that the peridotite and gabbro represent the same parent magma, even though they were intruded as separate batches at different times. If the high Zr content of the peridotite had been inherited from the source, then a gabbroic differentiate should have even more enrichment in Zr. This is not the case at Niinimäki, where the peridotites can actually have more Zr than the gabbro (Fig. 50), indicating that the peridotite is the more contaminated, and has been affected independently from the gabbro. Although this evidence for contamination is compelling, it still does not exclude the possibility of a different primary source for the Kotalahti-type and Vammala-type magmas. Contamination is nevertheless regarded as a more probable explanation since the Vammala-type peridotites of the Juva district (Lumpeinen and Turunen) are generally barren, while the Kotalahti-type magmas contain ore deposits, which may be related to different degrees of assimilation.

In the following discusssion, the inferred parent magma and its variably contaminated olivine cumulate derivatives will be compared with the obtained analytical data. Major element data will be evaluated using the CaO/Al_2O_3 ratio, which is the most significant discriminant between the Kotalahti-type and Vammala-type intrusions, while La, Sm and Zr are considered to be immobile trace elements. Crystallization calculations have been performed using the FRAKIT program (Hanski and Koivumaa, 1983). The mean composition of the Pirilä amphibolites has been taken as equivalent to the parent magma (n = 15, Viluksela, 1988), while that of the potential upper crustal contaminant has the La and Sm abundances of NASC (Haskin et al., 1968) and the mean Ca, Al and Zr compositions of schollen migmatites from the Kotalahti Ni-belt (n = 72, Mäkinen, 1995). The chosen compositions also closely resemble the mean values for Upper Kalevian sediments (Asko Kontinen, personal communication) and are thus suitably representative of country rock chemistry in the area surrounding the intrusions.

For the purpose of the FRAKIT program

calculations, mineral compositions of the Vammala-type and Kotalahti-type intrusions were compiled as a function of degree of crystallization (Fig. 51). The degree of crystallization was determined on the basis of differentiation indices, with respective mineralogical compositions corresponding to CIPW normative mineralogy. The degree of crystallization of the analyzed peridotites is seen to be 0.99-0.85 and it is significant that in both types of intrusions the normative abundance of plagioclase exceeds 10% at an early stage of crystallization. In most cases however, peridotite samples are devoid of plagioclase since it has typically been consumed by reaction with olivine or affected by uralitization. The partition coefficients used (principally after Bedard, 1994, Table 1) are

	La	Sm	Zr
olivine	0.00044(1)	0.00018(1)	0.003(2)
orthopyroxene	0.016(3)	0.0.054(3)	0.16(3)
clinopyroxene	0.0536(4)	0.291(4)	0.1234(4)
plagioclase	0.042(3)	0.022(3)	0.09(5)
apatite	8.5(6)	12(6)	0.1(6)

1) Prinzhofer and Allegre (1985), 2) Johnson and Dick (1992), 3) Bedard (1994), 4) Hart and Dunn (1993), 5) LeMarchand et al. (1987), 6) The value used by Hanski and Koivumaa (1983).

Table 17 presents the initial compositions used in the model calculations, as well as the compositions for various degrees of mixing and, for comparative purposes, the composition of the chilled margin of the Rantala gabbro. The CaO/Al_2O_3 ratio of the mixtures decreases markedly even at small degrees of contamination and indicates that the Rantala chilled margin records about 20% contamination. Calculations based on Zr, La and Sm abundances suggest contamination of between 5-15 %. Of the other intrusions, the Rietsalo gabbro has a mean CaO/Al_2O_3 ratio of 0.48, which corresponds to about 40% contamination.

The model calculations generate REE abundances comparable with analyzed values based on contamination of parent magma with a starting composition corresponding to that of the Vammala-type peridotites (Fig. 52). The calculated Zr abundances also match the analytical data rather well (Tables 4 and 18), which confirms the conclusion that the mean Pirilä amphibolite compositions are reliable approximations to those of the parent magma.

Because the Kotalahti-type peridotites have less clinopyroxene than the Vammala-type peridotites, REE abundances are accordingly less and therefore any elevated REE contents observed in the former must be attributed to the composition of the initial melt. Analyzed REE and Zr abundances for the Kotalahti-type peridotites are:

La_{cn}	8.6 - 36.1	mean 19.0
Sm_{cn}	2.0 - 15.7	mean 8.8
Zr ppm	12 - 46	mean 30

On the basis of the model calculations the mean chondrite normalized La abundances represent at least 40% contamination, with the maximum value of 36.1 being impossible to obtain with the modelling used. The same applies to the higher Sm abundances, even though the general shape of the REE profiles follows the results of modelling quite well (Fig. 52). The negative slopes of the LREE profiles correspond to contamination of about 10%, while Zr abundances suggest up to at least 40% contamination (Table 18).

The model calculations are affected by both the choice of partition coefficients and the proportion of intercumulus melt, which is dependent upon the degree of crystallization. If the amount of melt is increased, then the La, Sm and Zr abundances of the cumulates increase and the above mentioned contamination percentages would accordingly decrease. Variations in element ratios are in fact more important in the contamination modelling than changes in absolute abundances.

The high REE abundances and negatively

Table 17. Changes in the composition of parent magma contaminated by upper crust.

Composition	CaO/Al_2O_3	Zr ppm	La_{cn}	Sm_{cn}	La_{cn}/Sm_{cn}
Magma	0.72	63	16.13	14.87	1.08
Upper crust	0.17	184	103.23	29.23	3.53
Cont. 5%	0.70	69	20.49	15.59	1.31
Cont. 10%	0.67	75	24.84	16.31	1.51
Cont. 15%	0.64	81	29.20	17.02	1.72
Cont .20%	0.62	87	33.55	17.74	1.89
Cont. 25%	0.59	93	37.91	18.46	2.05
Cont. 30%	0.56	99	42.26	19.18	2.20
Cont. 35%	0.54	105	46.62	19.90	2.34
Cont. 40%	0.50	111	50.97	20.61	2.47
Cont. 50%	0.45	124	59.68	22.05	2.71
Rantala chilled margin	0.61	79	22.30	17.00	1.31

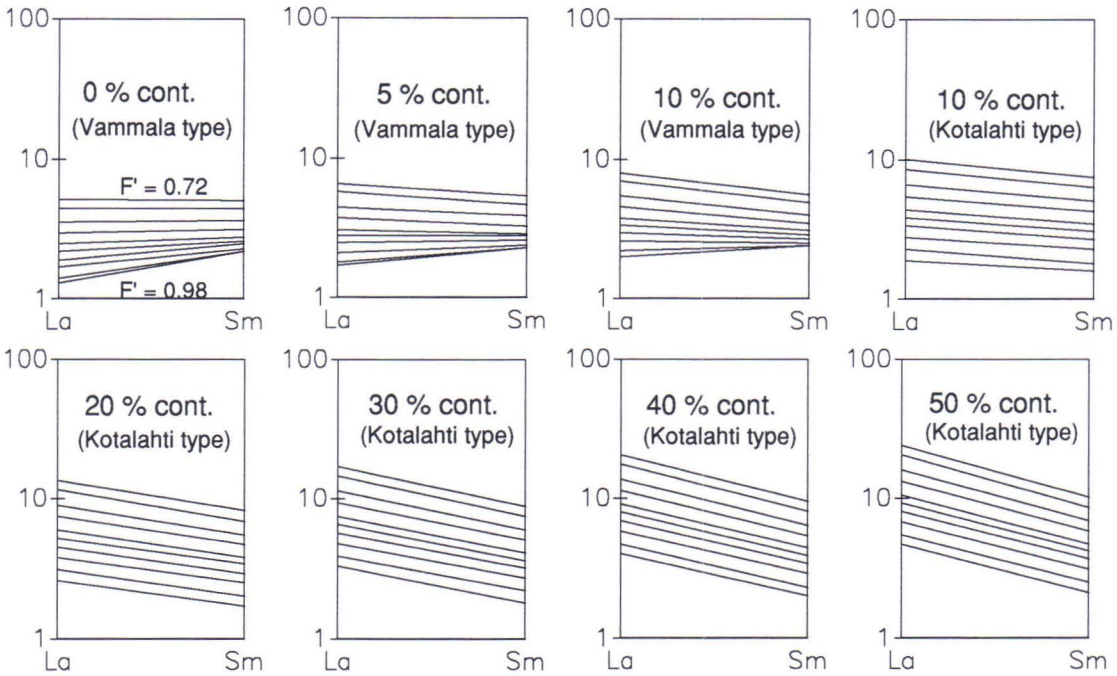

Fig. 52. Calculated chondrite normalized LREE pattern for Vammala and Kotalahti type peridotites as a function of contamination percentage and degree of crystallization (F'). F' = 0.98, 0.96, 0.94, 0.92, 0.90, 0.88, 0.84, 0.80, 0.76, 0.72.

sloping LREE trends of the Kotalahti-type peridotites are consistent with the presence of abundant apatite in these rocks, since the analyzed concentrations of La in apatite (1100 ppm) are high enough to explain the whole-rock content of this element. On this basis, the high REE contents can be attributed to the abundance of phosphorus and therefore

Table 18. Zr content (ppm) of parent magma as a function of degree of crystallization (F') and contamination percentage (%) in Vammala (VAMM) and Kotalahti (KOTA) types.

F'	0.98	0.96	0.94	0.92	0.88	0.84	0.80	0.76	0.72
VAMM 0%	7	8	10	11	13	16	18	21	24
KOTA 10%	7	8	10	12	16	19	21	25	28
KOTA 20%	8	9	11	14	18	22	25	29	33
KOTA 30%	9	11	13	16	21	25	28	34	38
KOTA 40%	10	12	15	18	23	28	32	38	43
KOTA 50%	11	13	17	20	26	31	35	42	47

it is necessary to consider the reason for this element in the Kotalahti-type peridotites. One possibility is contamination by gabbroic rocks, since peridotites containing abundant phosphorus have commonly intruded gabbros, as at Niinimäki. The mean P_2O_5 content in the Luonteri - Heiskalanmäki zone is 0.41 w-% (Table 2), which is appreciably higher than that of metapelites (0.13 w-%), although some phosphorite layers have been found in association with carbonate rocks throughout the Juva district (Makkonen, 1988).

Table 19 shows the results of Nd isotopic shifts that would be anticipated by modelling the effects of contamination where an initial magma derived from depleted mantle and having $\varepsilon_{Nd}(1.88Ga) = 3.74$, and Nd = 6.39 - 11.75 ppm was contaminated with Rantasalmi mica schists having $\varepsilon_{Nd}(1.9Ga) = -2.5$ and Nd = 30 ppm (Hannu Huhma, personal communication). The $\varepsilon_{Nd}(T)$ of the magma has been calculated according to DePaolo (1981) and the estimated Nd value has been taken from analytical data for the Pirilä amphibolites

Table 19. The change in $\varepsilon_{Nd}(T)$ in the contamination model.

Nd_{MAGMA} = 6.39 ppm		Nd_{MAGMA} = 11.75 ppm	
Cont.%	$\varepsilon_{Nd}(1.9Ga)$	Cont.%	$\varepsilon_{Nd}(1.9Ga)$
5	2.5	10	2.4
6	2.3	15	1.8
10	1.6	20	1.3
15	0.9	25	0.9
20	0.4	30	0.5

(Jukka Kousa, personal communication).

The analyzed samples thus yield $\varepsilon_{Nd}(T)$ values that correspond to 5 - 30% contamination, depending on both the sample itself and the Nd value assigned to the magma (taking error margins into consideration, a range in contamination from 3 - 35% is obtained). For low Nd abundances the effect of contamination on the $\varepsilon_{Nd}(T)$ value is significant, even for a change in degree of contamination of only one per cent. Patchett and Kouvo (1986) used a magmatic Nd value of 10 ppm when modelling contamination for 1.9 - 1.7 Ga Svecofennian rocks in Finland although they assumed the magmas to be of island arc basalt affinity that presumably has higher Nd abundances than those of the ocean floor basalts considered to correspond to the source magmas in the present study. However, even though the lowest possible Nd value of 6.39 ppm is chosen for modelling, the degree of contamination must still be in excess of 5%.

In summary, the results of the contamination modelling indicate that:

1) both the Vammala-type and Kotalahti-type intrusions were contaminated to variable degrees between 5 - 40% by mass;

2) contamination can adequately explain the observed differences in mineral composition, REE profiles and $\varepsilon_{Nd}(T)$ isotopic characteristics between the two types of intrusions;

3) the high phosphorus and related high REE abundances in the Kotalahti-type peridotites demand contamination by a source that contains more phosphorus than most su-

pracrustal rocks, and

4) the peridotites can be more highly contaminated than the gabbros.

The model presented above describes a simple bulk contamination process that took place prior to fractional crystallization of the magma. In reality however, it is likely that contamination processes were more complex, since several phases of contamination could have occurred during passage of the magma through feeder channels before reaching its final site of emplacement. Contamination could also have been somewhat selective, in which case the contaminant might have been a eutectic wall-rock melt, or represent anatexis associated with regional metamorphism. This latter possibility could explain the observed high REE and Zr abundances of the Kotalahti-type intrusions with a lower degree of contamination than that required by the bulk contamination model. Peltonen (1995c) adopted such a selective contamination explanation for the Vammala area, arguing that S and Zn were transferred by C-O-H-S fluids from graphitic wall-rock schists into the cooling magma. In the present case however, this explanation does not account for the observed variations in CaO/Al_2O_3 ratios between the various intrusions.

ORIGIN OF THE JUVA DISTRICT Ni-Cu DEPOSITS

Intrusive processes

The emplacement and eruption of magma requires a suitable extensional magmatic setting, such as at mid-ocean ridges and continental margins. Because the intrusions and lavas of the Juva district are surrounded principally by metamorphosed turbidites (Gaál and Rauhamäki, 1971), a mid-ocean ridge setting seems unlikely in the present case. According to Viluksela (1988) the amphibolites and ultramafic rocks of the Pirilä area have geochemical characteristics resembling that of back arc magmatism. Piirainen (1987) also considered the 1.9 Ga Svecofennian magmatism to be of back arc origin, whereas Lahtinen (1994) regarded the Ni-bearing intrusions of the Raahe-Ladoga zone as the products of within-plate magmatism.

At the present erosion level the intrusions of the Luonteri-Heiskalanmäki zone are elongate and narrow, which suggests that they originally formed as sills. Other groups of more irregular intrusions could also represent disrupted and boudinaged sills, although it is possible that considerable primary thickness variations existed as well.

Because all of the intrusions studied show evidence for magmatic differentiation, indicated by systematic variations in both mineralogy and geochemistry, with layering being concordant with that in the enclosing sediments, it is concluded that the intrusions must have originally had horizontal planar orientations. This is also consistent with the presence of early foliations, such as S_2, within the intrusions as well as their wall rocks and suggests that intrusion took place prior to, if not during the earliest stages of D_2 deformation. Because recumbent folds developed during both D_1 and D_2 (Koistinen, 1981), it is still possible that intrusion took place during D_2. However, no D_1 structures have been truncated by gabbros or peridotites in the Juva district, indicating that intrusion probably took place before D_2.

The intrusions investigated can be classified as either single-stage or two-stage intrusions. The former have been emplaced directly into their present environment, while the two-stage intrusions underwent partial crystallization within a temporary magma cham-

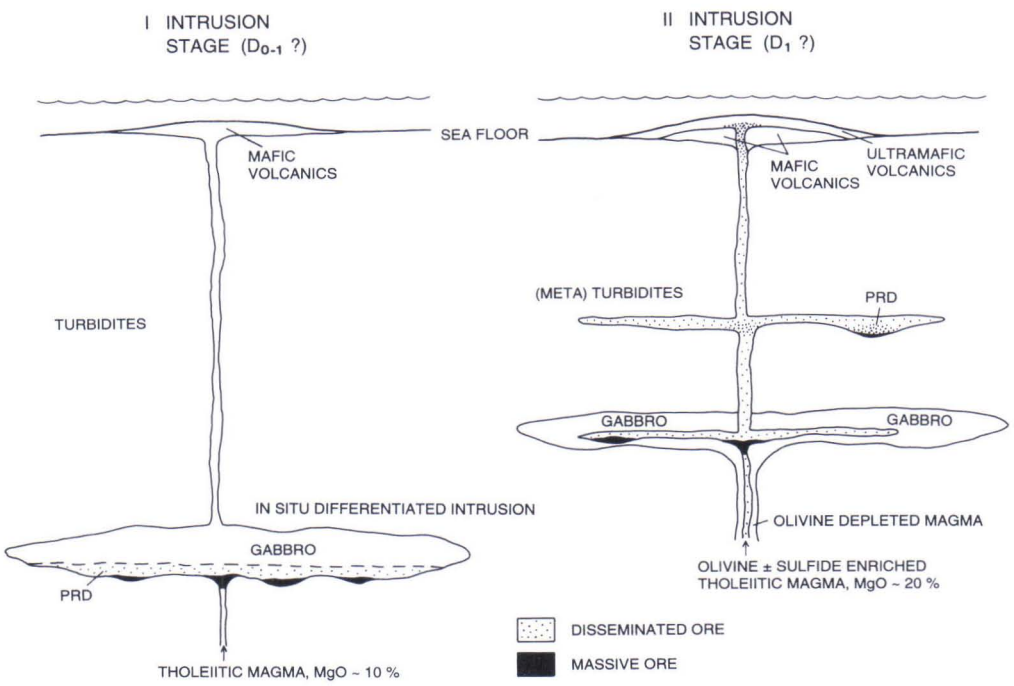

Fig. 53. A model for the intrusion of tholeiitic magma in the Juva area.

ber or flow conduit prior to final emplacement.

Kekonen and Kiiskilänkangas intrusions represent single stage emplacement, with gradational contacts and a continuous compositional trend from peridotite to gabbro, while the Saarijärvi, Niinimäki, Pihlajasalo and Rantala intrusions are two-stage intrusions with a distinct compositional gap and sharp intrusive contacts between gabbroic and peridotitic phases.

Because peridotites also occur as discrete intrusions separate from the gabbros, as at Lumpeinen and Venetekemä, residual melts and olivine-rich melt must have become separated from one another within either the flow conduits or temporary magma chambers, allowing the formation of olivine-cumulates from the olivine-rich melt. As discussed previously, this can also explain the origin of the ultramafic volcanics and sills, if they are interpreted as olivine-rich melts extruded at or near the surface. According to Huppert and Sparks (1984), convective fractionation can cause significant compositional heterogeneity between different parts of a magma chamber. As a consequence, magmas derived from such a chamber can vary in composition as a function of time and provides a possible mechanism for generating olivine-rich melts. Magmatic compositions may also become more mafic by the physical removal of plagioclase due to density contrasts between phenocrysts and residual melt; in this case ultramafic lavas and sills could represent melt that was depleted in plagioclase. Evidence for convection within magma chambers in the Juva district is provided by the cross-bedded layering observed in the Pihlajasalo gabbro intrusion (Fig. 7). The banding in the gabbro could have

formed by double-diffusive convection (Huppert and Sparks, 1984).

In the case of the two-stage intrusions it is natural to ask whether the gabbro was earlier or later than the peridotite, since in the case of eruptive rocks, the ultramafic lithologies are younger than the mafic rocks. By analogy therefore it might be expected that the peridotite intrusions are younger than the gabbros. No intrusive field relations have been found to confirm this since although the two rock types are juxtapozed with sharp boundaries, mutual intrusive relations have not been seen. The gabbroic part of the Niinimäki intrusion is highly altered in close proximity to the peridotite, with plagioclase being altered to saussurite and mafic minerals replaced by chlorite, thereby indicating that the peridotite is younger than the gabbro. Density differences also indicate the same intrusive relationships since the less dense gabbroic melt would be expected to ascend at an earlier stage than the denser olivine-rich magma.

Because mineralization is restricted to the basal parts of the intrusions, it follows that ore formation also predates the reorientation of the intrusions into steep attitudes. Figure 53 presents a schematic model of the intrusive processes.

Separation of sulfide melt

If magma is intruded into sediments on or beneath the sea-floor, then a number of factors can influence the separation of sulfide melt, including:

1) rapid drop in temperature;
2) increase in oxygen fugacity
3) contamination (SiO_2, Al_2O_3, Na_2O)
4) assimilation of sediment-derived sulfur by the magma.

Magma temperature falls rapidly as a result of intrusion into wet sediments, while according to Haughton et al., (1974), the oxygen fugacity of a magma can increase as it incorporates water, which becomes dissociated, with diffusive loss of hydrogen from the system. An increase in oxygen fugacity causes an increase in the abundance of ferric iron, which in turn decreases the solubility of sulfur in the melt. If intrusion took place later, during metamorphism associated with D_1, then wall rock temperatures could have been in excess of 500°C, precluding a rapid drop in magma temperature; wall rocks would also have been less hydrous under these conditions.

Evidence for contamination of the magmas by country rock sediments is provided by the available trace element, REE and Sm-Nd data. Because the differences in mineralogy between the Vammala-type and Kotalahti-type intrusions can be explained by contamination, this should also be considered as a likely cause of sulfide separation, even though there would only be a relatively small amount of contamination in the case of the Vammala-type intrusions.

If the magma were emplaced into sediments, sulfide separation from the melt could be caused by assimilation of sedimentary sulfur. Peltonen (1995c) considered sulfur assimilation in the Vammala district to one of the most critical factors in ore formation. In the Juva district however, Ni-Cu mineralization is associated with sulfur-poor as well as graphitic and sulfide-rich schists and therefore sulfur assimilation is less likely to have been the primary cause of sulfide separation, even though it has presumably affected R values (silicate melt/sulfide melt). Sulfur isotopic studies of Finnish Svencofennian Ni-Cu ore deposits indicate that most of the sulfur is of magmatic origin (Papunen and Mäkelä, 1980). On the other hand, sulfur isotopic compositions of Svecofennian metapelites vary widely, from $\delta^{34}S_{\Sigma S}$ = -7.1 - +2.8 (Peltonen, 1995c), so that addition of sedimentary sulfur might not necessarily cause noticeable changes to magmatic values

(+0.5±1.5; Ohmoto and Rye, 1979), even at high levels of contamination.

An important question from the point of view of ore formation is whether the separation of sulfide melt took place in a single step (batch equilibration), or occurred progressively by fractional segregation. In the case of batch equilibration, the metal ratios of the magma would have been constant and dependent upon total metal contents and respective partitioning coefficients between the silicate and sulfide melts. If fractional segregation occurred however, then the composition of the ore varies in time as a function of different partition coefficients for different metals and as a function of silicate and sulfide crystallization. Because $D_{Co}^{sul/sil}$ is smaller than $D_{Ni}^{sul/sil}$ and $D_{Cu}^{sul/sil}$ (Naldrett, 1989), the Ni/Co and Cu/Co ratio of the sulfide melt decreases continually while the Ni/Cu ratio nevertheless remains almost unchanged. Crystallization of olivine and pyroxene also causes a decrease in the Ni/Cu and Ni/Co ratios of the sulfide melt, but does not significantly affect the Cu/Co ratio.

The Ni-Cu deposits of the Juva district all display remarkably uniform and consistent Ni/Co ratios, which suggests that sulfide separation would have been mainly a single-stage process. It is unclear however when this occurred with respect to silicate crystallization, although the fact that the ore deposits are consistently located towards the bases of the intrusions indicates that they formed relatively early. In general Ni/Cu ratios are more variable than Ni/Co ratios, which may be a consequence of Cu mobility during metamorphism.

Separation of sulfides could have taken place at deeper levels prior to final emplacement, or alternatively in situ at their present crustal level. The former alternative would require that sulfide droplets remained entrained in the magma during ascent, but settled to the floor of the intrusion when the magma reached its final emplacement level, the final result being effectively the same as for in situ sulfide separation and ore formation. However, would the overall metal distribution be similar in both cases? If, for example, the sulfide droplets were thoroughly mixed during ascent, it is unlikely that the ore deposit would display the same kind of stratigraphical zonation of metals that would occur within an intrusion that underwent fractional segregation in situ. On the other hand, if sulfides formed in situ during a single stage process, they would not necessarily display such zonation either. As noted above, sulfide separation in the Juva district intrusions was presumably mainly a single-stage process and therefore metal ratios and zonation cannot directly reveal information concerning the timing of sulfide separation.

Crystallization of sulfide melt

Fractional crystallization of sulfide melt can also lead to zonation of ore bodies since metals are preferentially incorporated into crystallizing phases in the sequence Co>Ni>Cu (+Pt+Pd+Au). This means that the Cu/(Cu+Ni), Ni/Co and Cu/Co and also (Pt+Pd)/(Ru+Ir+Os) ratios of the residual melt increase progressively with time (Naldrett, 1989).

Two of the intrusions, namely Kekonen and Rietsalo, contain ore bodies that are large enough to permit the presence of metal zonation to be assessed (Fig. 54). In the Kekonen deposit Ni/Co, Cu/Co and Au+Pd all decrease towards the base of the ore, with one exceptionally high Ni/Co observation representing compact ore. The Rietsalo intrusion does not display such marked zonation, at least with respect to these ratios, although the Pd/Ir ratio does decrease towards the base of the ore. It may nevertheless be concluded that the upper parts of the ore deposits are enriched in those

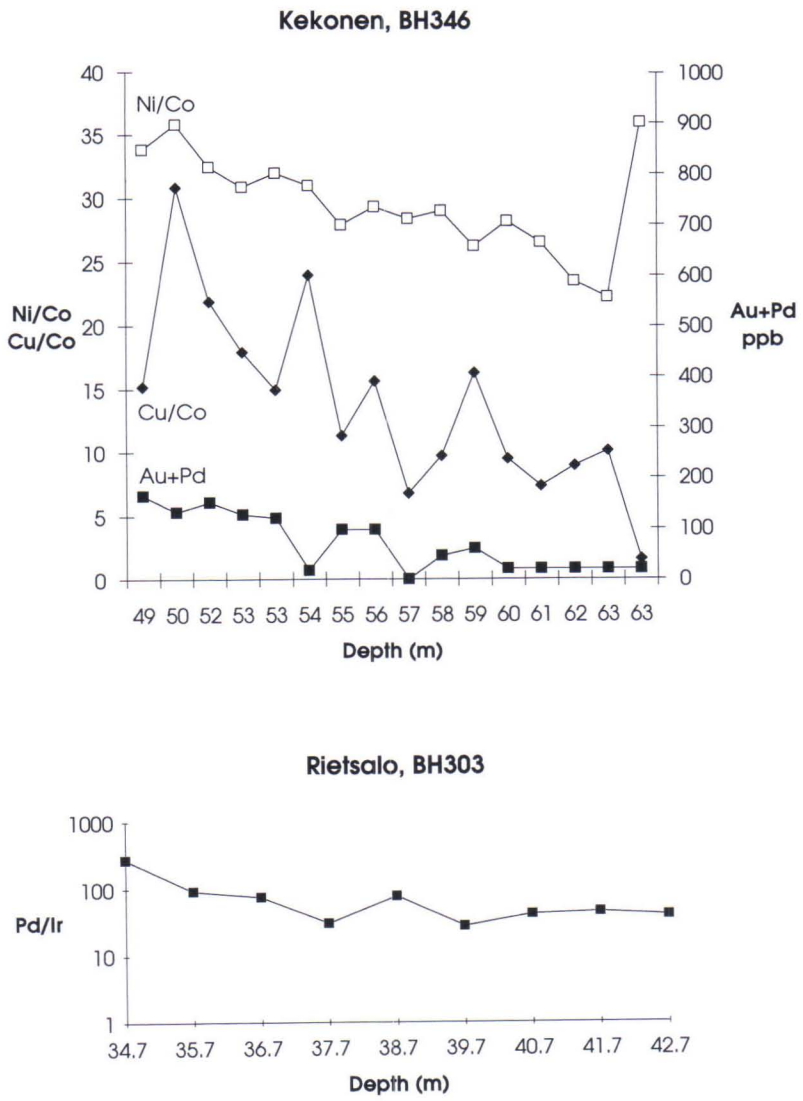

Fig. 54. Zonation of metals at the Kekonen and Rietsalo occurrences. For location of bore holes see Figure 13.

metallic elements that tend to be the last to crystallize from sulfide melts. This provides strong evidence for fractional crystallization of the sulfide melts and also confirms the interpretation favouring single-stage sulfide separation; if separation had taken place by progressive segregation, the opposite zonation trends would have been expected, with Ni/Co and Cu/Co ratios being highest at the base of the ore deposits, Ni and Cu having crystallized from the earliest sulfide melt (assuming that sulfide droplets settled immediately to the floor of the intrusions).

Ore composition and silicate melt chemistry

The composition of the silicate magma exerts the greatest influence on the metal ratios of Ni-Cu ore deposits (Naldrett, 1989). Table 20 is a compilation of calculated values of

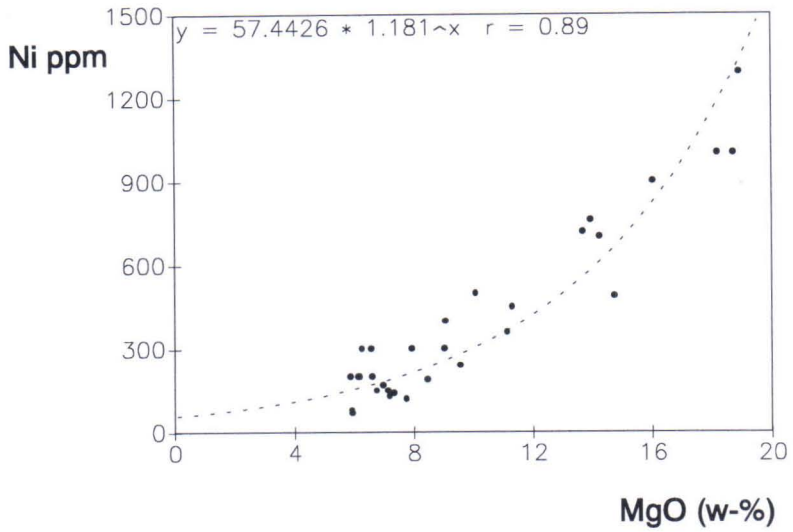

Fig. 55. Correlation of Ni and MgO contents in Pirilä mafic and ultramafic volcanics.

those factors considered important in influencing the Ni and Cu abundances of the investigated intrusions in the Juva district. The original Ni content of the silicate melt X_{ONi} has been determined from the data presented in Figure 55, in which only the amphibolite Ni contents are considered to be representative of the magma as a whole. The ultramafic rocks have high Ni abundances because of their high proportion of cumulus olivine and therefore the curves in Figure 55 should not be used to infer Ni abundances where MgO exceeds 12 w-%. The Ni content of the melt during olivine crystallization (X_{Ni}) can be calculated from the following equation using the highest olivine Ni value analyzed for each respective intrusion:

$$D_{Ni}^{Ol/Liq} = e^{(4.961-1.266 \ln MgOLiq)}$$

(Duke and Naldrett, 1978)

Log R has been calculated according to Campbell and Naldrett (1979). Because no primary Ni analytical data are available for the Rantala, Rietsalo and Heiskalanmäki intrusions, they have been assigned $D_{Ni}^{sul/sil}$ value of 380, which represents the mean of the range of calculated $D_{Ni}^{sul/sil}$ values. X_{OCu} has been determined after Campbell and Naldrett (1979) using a $D_{Cu}^{sul/sil}$ value of 250.

The calculated $D_{Ni}^{sul/sil}$ values based on melt Ni concentrations (X_{Ni}) inferred from olivine Ni abundances are generally somewhat higher than the figure of 275 quoted for basaltic melts by Rajamani and Naldrett (1978), al-

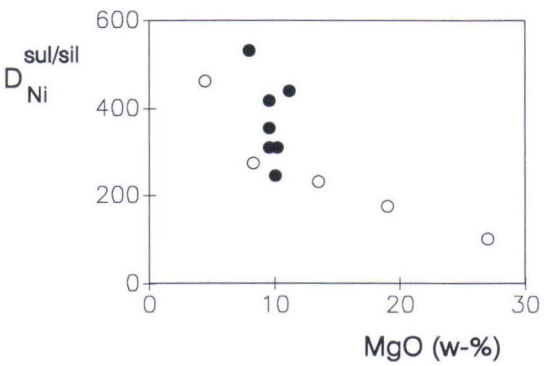

Fig. 56. $D_{Ni}^{sul/sil}$ as a function of MgO content in silicate liquid. Filled circles: Ni-Cu occurrences in Juva area, open circles: experimental results after Rajamani and Naldrett (1978) (MgO ≤ 13.5 w-%) and values after Naldrett (1989) (MgO > 13.5 w-%).

Table 20. Distribution of Ni and Cu in different occurrences.

Occurrence	Ni_{SF} w-%	Cu_{SF} w-%	logR	X_{Ni} ppm	$D^{sul/sil}_{Ni}$	X_{oNi} ppm	X_{oCu} ppm
Pihlajasalo	8.90	0.68	2.76	203	438	353	39
Saarijärvi	6.34	2.26	2.80	179	354	278	126
Kekonen	6.94	2.57	2.89	131	530	220	136
Rantala	4.21	2.50	2.51		380	240	176
Kiiskilänkangas	3.34	1.39	2.29	108	309	278	126
Rietsalo	5.54	5.40	2.96		380	206	274
Venetekemä	5.69	3.82	2.93	234	243	300	197
Heiskalanmäki	7.23	3.34	2.97		380	268	169
Niinimäki W	4.90	1.59	2.48	118	415	279	116
Niinimäki E	5.21	2.00	2.58	169	308	307	132

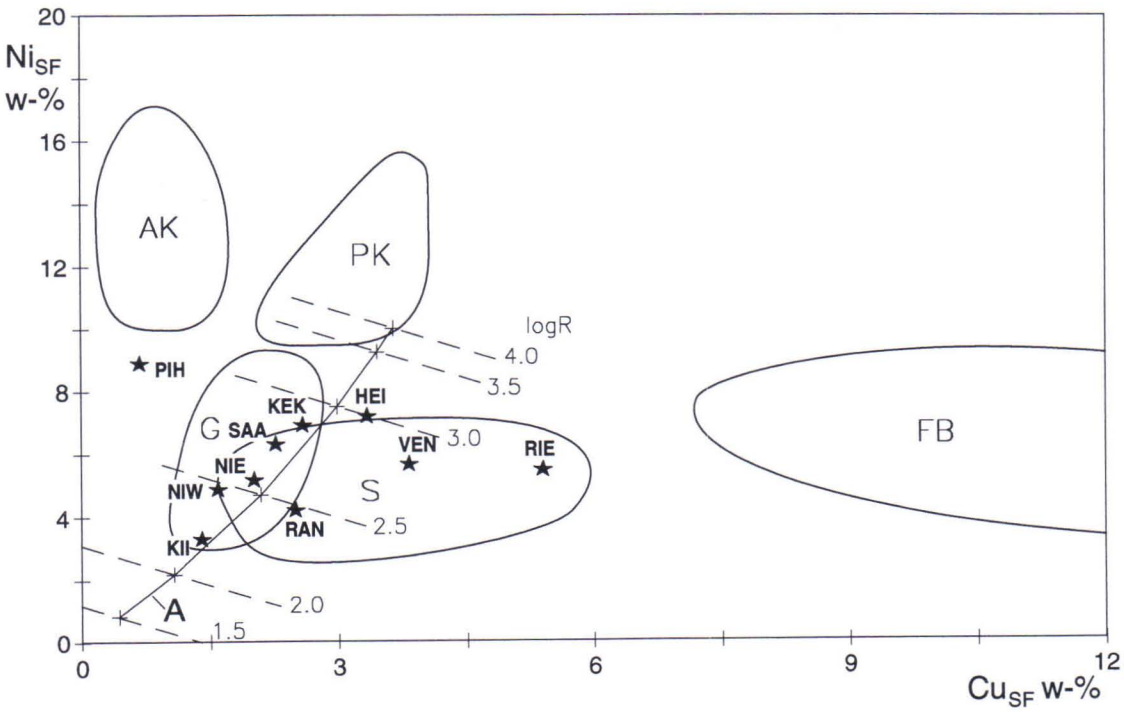

Fig. 57. Ni and Cu contents of sulfide fractions indicating the mass ratio (R) between silicate melt and sulfide melt. Line A depicts the change in the composition of sulfide fraction as a function of R, based on the following values. The nickel content in silicate melt is the average in Table 20, 273 ppm. For copper the value is 149 ppm, calculated on the basis of $D^{sul/sil}_{Cu} = 250$. The $D^{sul/sil}_{Ni}$ value is the mean, 380, of calculated values. The lines for different R values have been drawn on the basis of the Pihlajasalo and Rietsalo data. Fields for different rock types after Naldrett (1989): AK = Archaean komatiites, PK = Proterozoic komatiites, S = Sudbery, G = Gabbros, FB = Flood basalts. PIH = Pihlajasalo, NIE = Niinimäki E, NIW = Niinimäki W, SAA = Saarijärvi, KEK = Kekonen, RAN = Rantala, KII = Kiiskilänkangas, VEN = Venetekemä, RIE = Rietsalo, HEI = Heiskalanmäki.

though they are broadly of the same magnitude (Fig. 56). Furthermore, similar results between 370 - 770 have been obtained for sulfide globules and glass from basalts (Czamanske and Moore, 1977), showing that the $D_{Ni}^{sul/sil}$ data in Table 20 can be considered as reliable.

There is considerable variation in the calculated R values between the different intrusions and this could be responsible for the ranges in metal abundances in different ore deposits, since the uniformity of silicate melt compositions otherwise suggests that the ores should all be rather similar. It is also noteworthy that the Rietsalo and Heiskalanmäki occurrences have both the highest R values and the greatest abundances of Pt and Pd. This is in agreement with the study by Campbell and Naldrett (1979), who concluded that an increase in R leads to a radical increase in the abundance of metals with high partition coefficients ($D^{sul/sil}$) in sulfide melts. On the other hand, the Rietsalo silicate melt represents one of the most felsic differentiates in the study area and platinum group elements could have become enriched in the melt via normal fractional crystallization processes prior to sulfide separation. Moreover, if the gabbros of the Luonteri-Heiskalanmäki zone crystallized from a melt that was strongly depleted in Fe and Mg due to fractional crystallization of olivine prior to final emplacement, then the PGE content of the melt would have been greater than that of in situ differentiated magmas having the same MgO abundances.

It is apparent from Figure 57 that the Ni and Cu concentrations of sulfide fractions from the various deposits correlate well with the calculated model. Deposits with low R values plot towards the lower left corner of the diagram. Furthermore, the Juva district Ni-Cu deposits plot within the field for gabbro-hosted mineralization, which is in agreement with the primary magma having been basaltic in composition. Because the ore composition at each occurrence is dependent upon the silicate melt chemistry, it can be safely assumed that ores were derived from magmas corresponding to each respective intrusion; in other words ore deposits formed in situ.

The Venetekemä intrusion has lower Ni_{SF} than would be expected from the MgO content of the parent magma. In contrast to the Rantala and Kiiskilänkangas intrusions, the R value is also relatively high and hence cannot explain the low Ni concentrations in the sulfide fraction. Therefore, in addition to the known Ni-Cu mineralization, the Venetekemä intrusion should be associated with a further deposit in which Ni_{SF} is around 8 w-%.

The influence of deformation and metamorphism

The peak regional metamorphic conditions in the Juva district have been rather high, with temperatures around 680-750°C (Korsman et al., 1984) , which are sufficient, at least in principle, for the mobilization of sulfides. The most obvious evidence that this has indeed occurred is the presence of chalcopyrite within fractures and breccia matrix in the ores. The preferential migration or concentration of ore in F_3 hinge zones also indicates sulfide mobilization following the metamorphic peak, when temperatures were already declining. However, because primary metallic zonation can be discerned in the ore deposits, mobilization did not necessarily take place on a large scale. Primary compositional layering has also been preserved in the ore deposits, just as in other rock types.

An interesting problem concerns the nature and origin of the so-called offset ore deposits, which may represent either primary or later syntectonic mobilization. If the lower chilled margin of an intrusion becomes fractured, then basal sulfide cumulate aggregates can penetrate into the underlying sediments, thus forming a primary offset ore body. During

metamorphic and tectonic processes it is also possible that sulfides will migrate and become concentrated as offset ore bodies outside the intrusion.

The metamorphic mobilization of sulfide as a function of temperature can also be assessed as the converse of the sulfide melt crystallization process. During crystallization, the residual melt tends to become enriched in Cu, Pt, Pd and Au and these elements are consequently the first to become remobilized if the sulfide fraction begins melting during metamorphism. Intense metamorphic remobilization can therefore potentially cause marked changes in metal ratios compared to their distribution in the original ore deposit. Mobilization is typically expressed for example by a relatively low Ni/Cu ratio compared to the primary ore deposits. The abundances of Pt and Pd should also be enriched with respect to those of primary magmas.

Pihlajasalo is the only Ni deposit in the Juva district that is clearly within the country rocks rather than hosted by the intrusions and in this case the Ni/Cu ratio is exceedingly high (12.36). The basal part of the Kekonen Ni-Cu deposit also comprises a narrow massive ore horizon that has higher Ni/Cu ratios than those in the rest of the ore. These ore bodies are therefore classified on the basis of respective metal abundances as primary.

There are nevertheless offset ore bodies in some Svecofennian Ni-Cu deposits in Finland in which Ni/Cu ratios are somewhat lower than the mean value, as at Kotalahti (Papunen and Koskinen, 1985) and Enonkoski (Grundström, 1985); these ores are more readily interpreted as late mobilized deposits compared to those of the Juva district.

DISCRIMINATION BETWEEN BARREN AND MINERALIZED ROCK UNITS

Olivine

Because olivine commences crystallizing early and is effective in selectively removing Ni from the melt, the Ni content of this mineral provides a reliable estimate of the original concentration of Ni in the parent melt. Furthermore, if it is assumed that the silicate and sulfide melts are in mutual chemical equilibrium, then olivine Ni abundances should also reflect the Ni concentration in the sulfide melt.

According to Duke and Naldrett (1978), Ni concentrations are higher in olivine that crystallized from a sulfide-undersaturated melt than in olivine from a melt that was saturated with respect to sulfides. However, in order to observe the difference in Ni abundances, log R must be <3 (Naldrett, 1989). The separation of a small amount of sulfide causes only minimal decreases in Ni concentration such that the Ni concentrations in crystallizing olivine are effectively the same as those from olivine progressively crystallizing in a sulfide-undersaturated melt.

All of the intrusions investigated have log R values of less than 3 so that the presence of sulfide melt should be discernible in the Ni concentrations in olivine. Large differences in olivine Ni contents have been observed between the various intrusions and this have been related directly to forsterite compositions in most, though not all cases (Fig. 58). The mean Ni concentration for olivine with a forsterite composition of 78 - 80 varies widely between the intrusions studied and this can be explained by variations in respective R values for each intrusion since a positive correlation exists between R values and olivine Ni concentrations (Fig. 59). In these intrusions, where large amounts of sulfide melt were generated compared to the proportion of silicate melt, the silicate melt is conspicuously depleted in Ni and olivine crystallizing

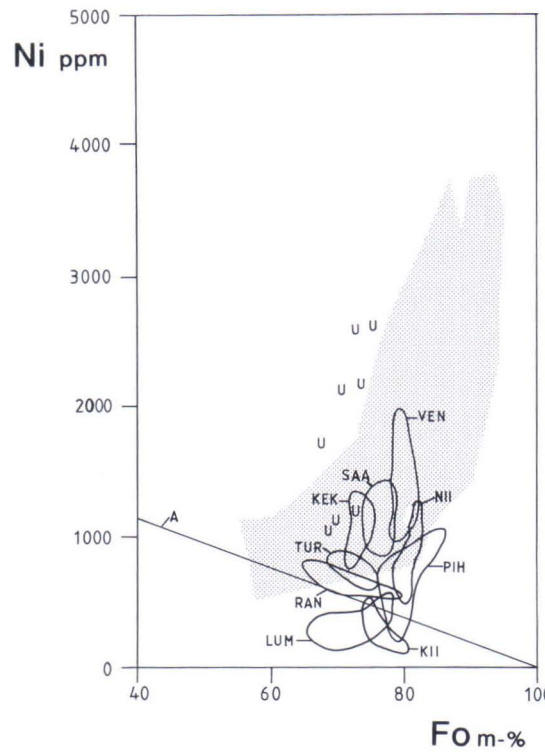

from such melts will contain very little Ni. The Saarijärvi peridotite illustrates this process well on the scale of an individual intrusion. In the northern part of the intrusion, where evidence for mineralization has been found, the Ni concentrations in olivine are lower than those in the barren southern part of the intrusion, even though forsterite abundances are similar in both cases (Table 6). In Venetekemä and Niinimäki intrusions a marked decrease in olivine Ni concentrations is concomitant with a decrease in Fo content and records the onset of sulfide separation (Fig. 58). These observations also indicate that olivine was crystallizing throughout the sulfide separation process and also demon-

Fig. 58. Composition of olivine in Juva area compared to the field for olivines in peridotites of upper mantle, Archean komatiites, basalts and layered intrusions. A = composition of olivine in equilibrium with a sulfide melt having 10 m-% NiS (Fleet et al., 1977). U = ultramafic lava and sill, other abbreviations as in Figure 57 (NII = Niinimäki).

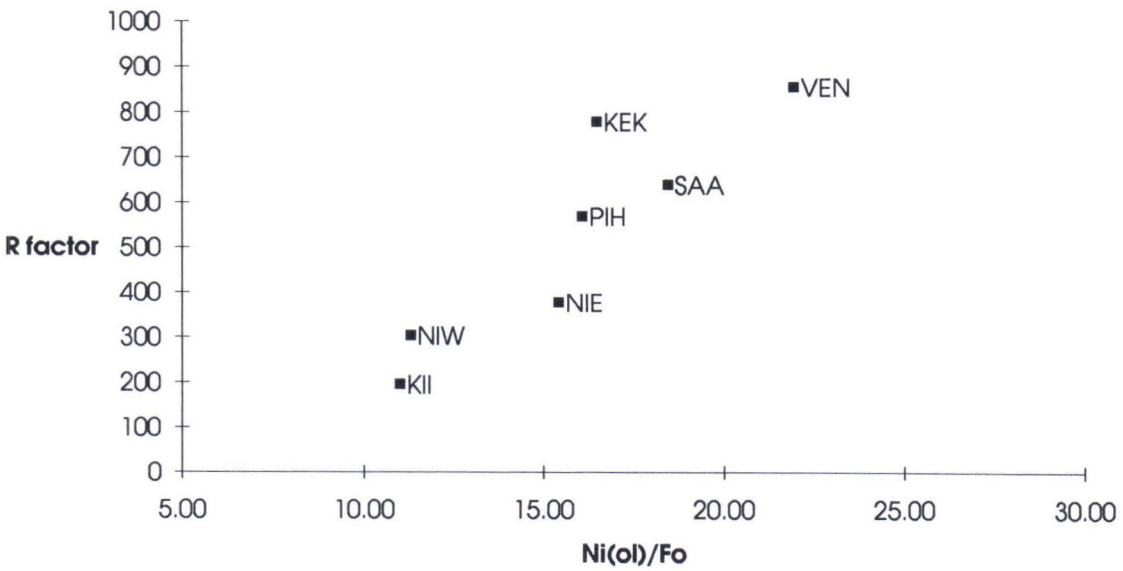

Fig. 59. Mass ratio (R) between silicate melt and sulfide melt as a funtion of nickel content in olivine. To avoid the effect of positive correlation between olivine forsterite and nickel contents Ni/Fo has been used. Abbreviations as in Figure 57.

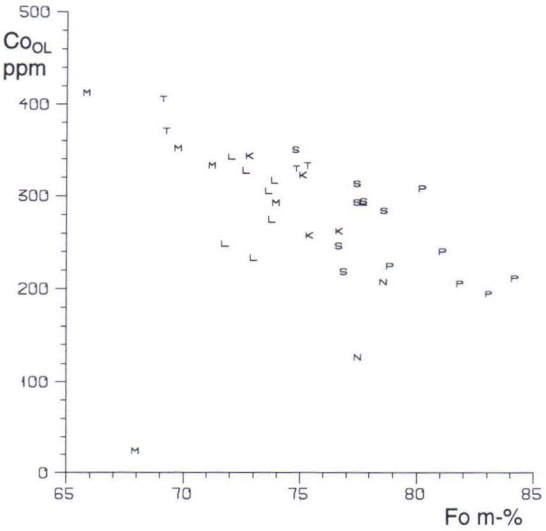

Fig. 60. Olivine cobalt content as a function of forsterite content. M = metamorphic olivine, other symbols as in Figure 17. Detection limit for cobalt is 100 ppm.

strates how suitable these intrusions were for the formation of Ni mineralization. The steeply descending trend from relatively high (> 1000 ppm) olivine Ni concentrations clearly indicates that sulfide separation has taken place within the intrusion itself and not at deeper crustal levels. Thus, olivines with high Ni contents represent crystallization during the earliest stages of sulfide separation.

A comparison of the olivine data for the Juva district intrusions with the general olivine compositional field (Fig. 58) indicates that the Pihlajasalo, Kiiskilänkangas and Lumpeinen olivines are Ni-poor, while the Saarijärvi, Venetekemä, Kekonen and to some extent also the Niinimäki and Turunen intrusions represent more usual olivine compositions. Metamorphic olivines from the ultramafic lavas and sills tend to plot both within and outside the magmatic field, so that olivine Ni abundance alone is not a diagnostic criterion for determining whether or not olivine is primary.

It is noteworthy that the composition of the Rantala olivines corresponds almost exactly to that of experimentally determined data for a melt NiS concentration of 10 mole %, which according to Fleet et al. (1977), corresponds to the composition of most naturally occurring Ni deposits. On this basis it can be concluded that the Rantala metamorphic olivines crystallized in equilibrium with sulfides in the same rocks (Fig. 58). The olivines from the Kiiskilänkangas intrusion shows similar characteristics to those from Rantala, with Ni concentrations increasing sympathetically with fayalite content. Because the Kiiskilänkangas intrusion contains abundant sulfides throughout, it is possible that chemical reequilibration between olivine and sulfides has taken place during regional metamorphism.

According to investigations by Häkli (1963), there is a positive correlation between the Ni content of olivine and that of the sulfide fraction in Svecofennian Ni-bearing intrusions. Because the samples studied are all sulfide bearing, it is nevertheless possible that equilibration has taken place during metamorphism. On the other hand, as noted earlier, if the R value is low, then the Ni contents of both the olivine and the sulfide fraction can also be low, and consequently, positive correlations could still be primary in origin.

Olivine Co concentrations as a function of forsterite content is considered in Figure 60, where the Co content of primary olivine is seen to be of the same order of magnitude in each of the occurrences. A negative correlation between Co and Fo contents is nevertheless discernible and indicates that Co can substitute for Fe in the olivine lattice. In contrast to Ni there is no correlation between R values and Co concentration in olivine, so that Co abundances in olivine cannot be used as a reliable indicator of mineralization potential. In contrast there is a positive correlation between the Cu and Ni concentrations of olivine (Table 6), such that Cu concentration can also be used as a general indicator of sulfide separation and hence mineralization.

Orthopyroxene

The Ni concentration of orthopyroxene shows positive correlation with olivine Ni abundances (Fig. 61) and therefore it too has potential as an indicator of sulfide separation. The partition coefficient between melt and orthopyroxene for Cu is around 1 (data compilation by Hanski, 1983), which is significantly less than that betweeen sulfide and silicate melt (about 250), so that the Cu content of orthopyroxene should also reveal whether or not sulfide separation has taken place. In the southern part of the Saarijärvi peridotite, olivine and orthopyroxene have higher Ni concentrations than in the northern part of the intrusion; the same applies to the Cu concentration in orthopyroxene (Fig. 62). Although the difference is not great, the results nevertheless indicate that Cu should be measured as a possible indicator of mineralization.

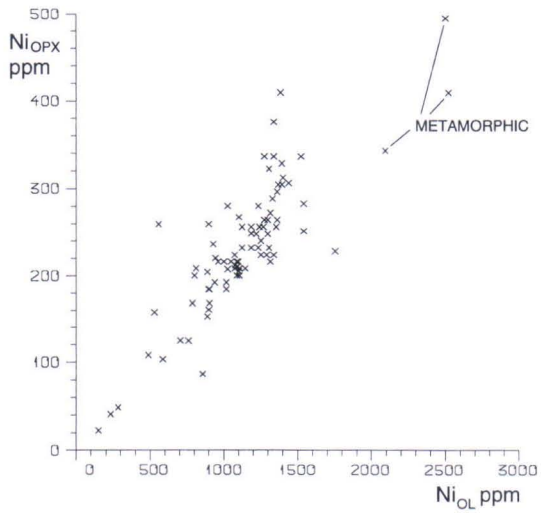

Fig. 61. Correlation between the nickel contents of orthopyroxene and olivine in Saarijärvi and Niinimäki intrusions and in ultramafic rocks from Rantala and Levänomainen (= metamorphic). Detection limit for nickel is 100 ppm.

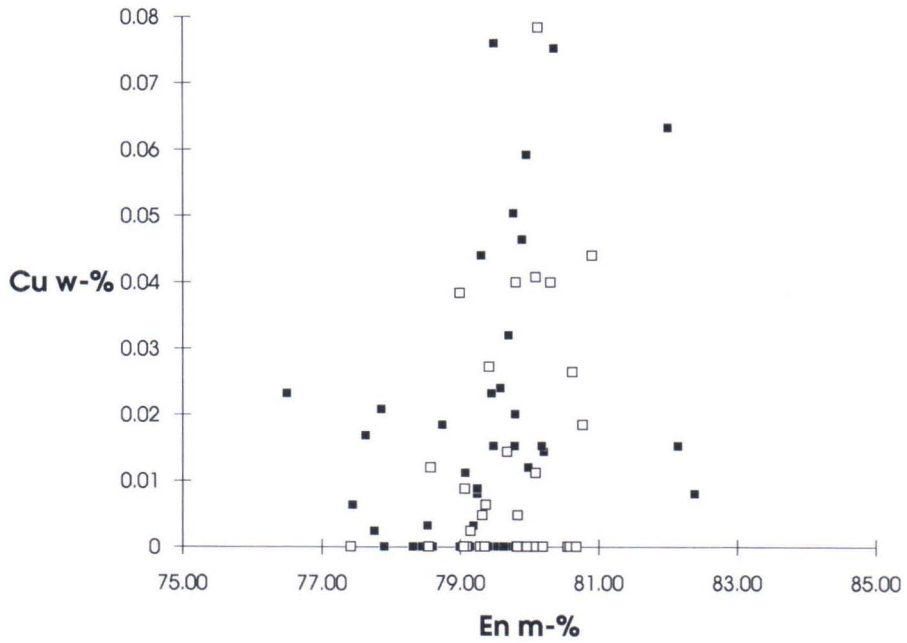

Fig. 62. Orthopyroxene copper contents in the southern (filled squares) and northern (open squares) parts of the Saarijärvi intrusion. Detection limit for copper is 0.01 w-%.

Chrome spinel

According to Groves et al. (1977), the ZnO content of chrome spinels is higher (>1 w-%) in mineralized ultramafic rocks from Western Australia than in barren lithologies. Lamberg and Peltonen (1991) and Peltonen (1995c) found similar features in the ultramafic intrusions of the Vammala district - chrome spinel ZnO contents are indeed higher in the mineralized intrusions.

The ZnO concentrations in the chrome spinels of the Juva district seem to have been principally controlled by magmatic differentiation since the lowest ZnO abundances are found in rocks having the highest MgO contents (Fig. 63). Neither does it seem possible to discriminate between mineralized (Niinimäki, Pihlajasalo, Venetekemä) and barren intrusions on the basis of ZnO in spinel. The Venetekemä samples differ from the trend defined by the other intrusions because of their distinctly lower ZnO contents although comparison of results is hindered by the fact that the analyses were made using different techniques. The Venetekemä data nevertheless suggest that the ZnO contents of chrome spinel are not critical indicators of mineralization, at least in this intrusion, and possible throughout the Juva district as a whole. Hanski (1993) came to similar conclusions with respect to the deposits of the Pechenga district in the northern part of the shield.

It also seems that the Ni contents of chrome spinels follow magmatic differentiation trends. However, the mineralized Niinimäki and Pihlajasalo intrusions have somewhat lower Ni concentrations in spinel than those from the barren to weakly mineralized Saarijärvi intrusion at equivalent MgO abundances (Fig.63). Therefore, the Ni content of chrome spinel may be used as an indicator of mineralization in the same way as Ni in olivine, as advocated by Hanski (1993). Peltonen (1995d) arrived at similar conclusions with regard to the intrusions of the Vammala district.

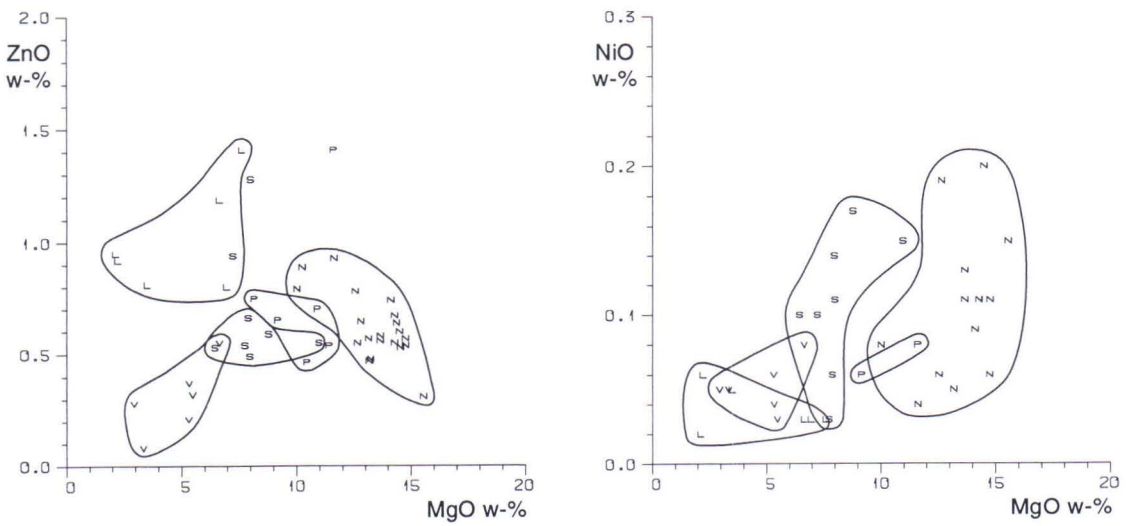

Fig. 63. ZnO and NiO contents of chrome spinel as a function of MgO content in different intrusions. Symbols as in Figure 17.

Whole rock analytical data

If sulfide separation occurred at deep crustal levels, then single stage intrusions should have higher mineralization potential since the sulfide melt will be intimately associated with the intrusion itself. For two-stage intrusions emplaced higher in the crust, it is possible that the sulfide melt does not continue to ascend with the olivine-rich silicate melt to the final site of emplacement. However, the Rantala ultramafic sill demonstrates that in some cases a sulfide melt can accompany the silicate melt to the final emplacement level.

Whole-rock Ni abundances appear to be reliable indicators of ore potential since the Ni content of a sulfide-poor rock effectively corresponds to the abundance of Ni in mafic minerals. Figure 64 illustrates the Ni concentrations of the Luonteri-Heiskalanmäki zone intrusions as a function of MgO; Ni contents are conspicuously lower than in comagmatic mafic volcanics, thereby indicating that a part of the Ni has been removed with the sulfide fraction.

If contamination is considered to be a significant factor in separation of sulfides, then the diagrams showing different degrees of contamination are also effective in indicating ore potential. Figure 65 presents such potentially useful diagrams, based on the results of the Juva district investigations. In addition to using the general results of REE analyses, it appears that an olivine cumulate could be re-

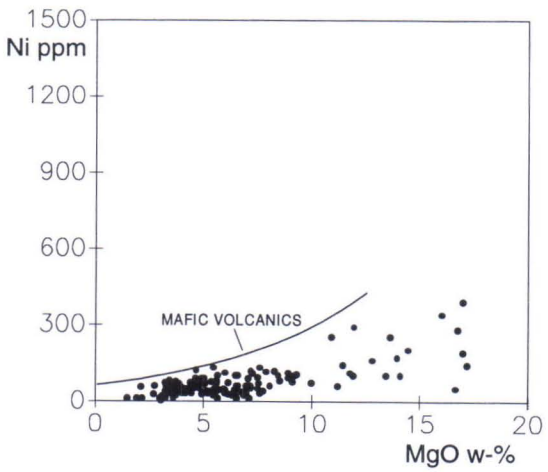

Fig. 64. Whole rock Ni content as a function of MgO content in Luonteri-Heiskalanmäki zone.

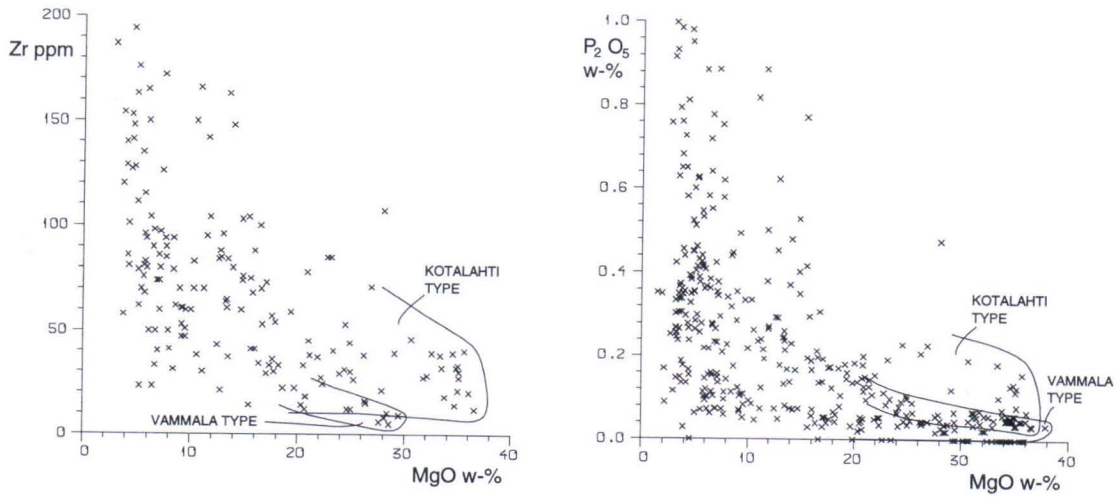

Fig. 65. Kotalahti and Vammala type samples in Zr-MgO and P_2O_5-MgO diagrams.

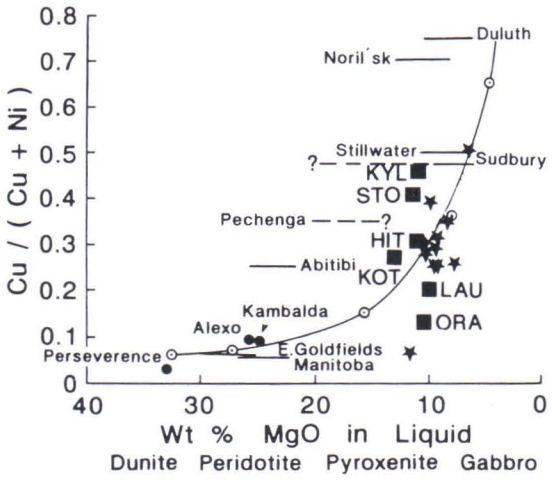

Fig. 66. Compositions of several Ni-Cu deposits and the parent magmas to their host rocks compared to Ni-Cu occurrences in the Juva area (stars). HIT = Hitura, KOT = Kotalahti, KYL = Kylmäkoski, ORA = Oravainen, STO = Stormi, LAU = Laukunkangas. Other data after Rajamani and Naldrett (1978). Composition of sulfide fractions for Finnish deposits after Papunen and Vorma (1985, Table 3).

garded as ore-critical if the chondritic normalized La/Sm ratio is greater than unity, which corresponds to a negative sloping LREE pattern.

A COMPARISON BETWEEN Ni-Cu OCCURRENCES OF THE JUVA DISTRICT AND OTHER SVECOFENNIAN OCCURRENCES IN FINLAND

Based on Fo contents the estimated MgO concentration of the parent magmas to the Juva district intrusions appears to have been broadly similar to that of the host rocks to other Svecofennian Ni-Cu deposits in Finland (compare with Mäkinen, 1987). The similarities in chrome spinel compositions also suggest a similar kind of parent magma and the Juva district apparently contains both the Vammala-type and Kotalahti-type intrusions.

The Ni-Cu occurrences of the Juva district are invariably associated with the basal stratigraphic parts of the intrusions, a feature which has also been recognized elsewhere, including Enonkoski (Grundström, 1985) and Stormi (Häkli et al., 1979).

The occurrences of the Juva district tend to be mineralogically simple, the dominant sulfide minerals being pyrrhotite, pentlandite and chalcopyrite, as in numerous other Svecofennnian intrusions in Finland (Papunen and Gorbunov, 1985).

The country rocks to the Ni-Cu occurrences of the Juva district are gneisses derived from predominantly turbiditic protoliths, which is also typical of other Svecofennian Ni-Cu ore provinces in Finland (Häkli et al.,1979).

Figure 66 shows a comparison of the Juva district Ni-Cu occurrences to the most important Svecofennian Ni-Cu deposits in Finland, and to some deposits outside Finland. Parent magma MgO contents for Finnish deposits have been calculated based on the highest Fo values listed in the available literature for each intrusion, using Equations 7 and 9. On these diagrams the Juva deposits are indistinguishable from those elsewhere in Finland.

If R values are high, then sulfide melts should contain more PGE than if R is low . Of all the Svecofennian deposits, only Hitura has been found to have significant enrichment in PGE (Häkli et al., 1976). On this basis R could be inferred as being greater at Hitura than in the other intrusions. Some of the deposits in the Juva district have typical Pt-Pd abundances between 0.1-1 ppm, which could be attributed

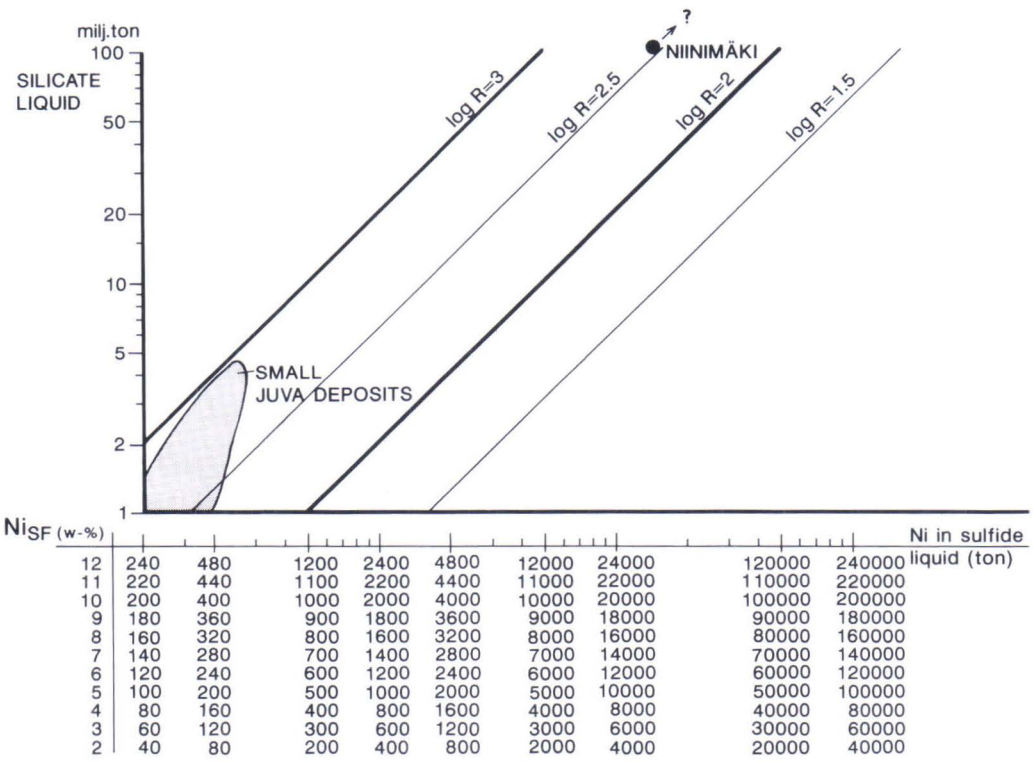

Fig. 67. Correlation between the nickel content in sulfide liquid and the amount of silicate liquid as a function of different mass ratios (R) between silicate and sulfide liquids and nickel contents in 100 % sulfides (Ni_{SF}). Juva occurrences fall between R values of log 2 and log 3.

to higher than average R values. Papunen (1989) regarded low R values as one potential explanation for the generally low PGE concentrations in Svecofennian Ni-Cu deposits.

Contamination has been invoked in the intrusions of the Vammala district with descending LREE trends observed (Peltonen, 1995b), and similar features are present in the Juva district. The low ε_{Nd}(1.9Ga) value of +0.2±0.5 for the Laukunkangas intrusion (Huhma, 1986) is also consistent with contamination.

Overall the Ni-Cu occurrences of the Juva district resemble those of the Kotalahti and Vammala districts with respect to both composition and mode of occurrence. For this reason it is considered that exploration outside these traditionally defined zones should be continued.

Because the ore metals are ultimately derived from the same magma as the host intrusions, a positive correlation exists between the sizes of ore deposits and the host intrusions (Fig. 67). This correlation is nevertheless somewhat obscured by the random and variable nature of the present erosion level. The small sizes of the presently known Juva district deposits can therefore be explained by the generally small sizes of the intrusions themselves.

SUMMARY

The mafic and ultramafic intrusions of the Juva district represent magma that was intruded as predominantly concordant bodies into metapelitic sediments, prior to deformation

and reorientation into their present steeply dipping attitudes. Isotopic age constraints on the timing of deformation and metamorphism indicate that intrusion took place at about 1.9 Ga. Some of the magma reached the sea-floor, where it erupted as pillow lavas, now mainly represented by amphibolites.

The intrusions can be classified into single-stage and two-stage types, the former being the result of intrusion directly to their present position, while the latter underwent initial crystallization in a temporary magma chamber or flow conduit prior to final crystallization at higher crustal levels. The single-stage intrusions record a continuum of compositional trends, typically with differentiates ranging from peridotites through to gabbros. The two-stage intrusions usually consist of gabbros and younger peridotites with sharp mutual intrusive contacts. The ultramafic volcanics represent the eruption of magmas that became progressively enriched in cumulus olivine.

The MgO content of the parent magmas varied between 8 - 11 w-% and corresponded to tholeiitic basalt in composition, with Al_2O_3/TiO_2 ratios of around 10. Variable contamination by crustal material resulted in differences in the CaO/Al_2O_3 ratios between intrusions prior to the commencement of silicate crystallization. Evidence for such contamination includes elevated LREE abundances and low $\varepsilon_{Nd}(T)$ values. Wehrlitic rocks crystallized from the CaO-rich magmas, and lherzolites from CaO-poor magmas and olivine was the first and dominant cumulus mineral in all of the peridotites.

The Ni-Cu deposits formed by separation of the sulfide melt from silicate melt, with sulfide separation being responsible for both lowering of temperature and contamination. The sulfide melts accumulated towards the bases of the intrusions, so that ore deposits invariably occur near basal contacts. However, because of subsequent deformation, ore bodies may presently be located within both footwall and hanging wall positions with respect to their host rocks. Some offset deposits have been identified and these can be of either primary or tectonic origin.

The initial metal abundances in the silicate melts strongly influenced the ultimate composition of the sulfide melts, as did the R values (proportion of silicate melt to sulfide melt), and the partition coefficients between the silicate and sulfide melts for various elements. $D_{Ni}^{sul/sil}$ varied between 243 - 530 and log R ranged between 2.29 - 2.97. The highest PGE abundances occur in intrusions where R is greatest and where sulfide separation occurred within a highly differentiated magma. Ore formation evidently took place in situ.

The sulfide melt underwent fractional crystallization, which explains the development of metal zonation within some of the ore deposits, the upper parts being enriched in residual melt and containing preferential concentrations of Cu, Pt, Pd and Au. The predominant sulfide minerals are pyrrhotite, pentlandite and chalcopyrite. All deposits contain Ni-Co arsenides although these are at their most abundant in intrusions that have elevated Pt and Pd concentrations. Pentlandite also has high As contents in such Pt-Pd enriched intrusions.

The single stage intrusions have greater mineralization potential than the two-stage intrusions. Mineralized intrusions also have higher abundances of elements associated with contamination processes, including REE, P_2O_5 and Zr. Similarly, the results of Sm-Nd isotopic investigations indicate that mineralized intrusions tend to have lower $\varepsilon_{Nd}(T)$ than do barren intrusions.

Mineralized intrusions also tend to have lower Ni concentrations in olivine, whilst a positive correlation has been found between the R value and olivine Ni contents. Nevertheless, the possibility of metamorphic equilibration between primary olivine and sulfide minerals means that the Ni contents in olivine should be treated with caution when using them to infer mineralization potential. Other potential mineralization indicators include Cu

in olivine, Ni and Cu in orthopyroxene, Ni in chrome spinel and whole-rock Ni abundances.

The Ni-Cu deposits of the Juva district correlate well with other Svecofennian deposits in terms of both composition and general mode of occurrence, although R values in some Juva district deposits tend to be somewhat higher. It is therefore concluded that areas outside the traditionally defined Vammala and Kotalahti Ni belts should be considered as prospective from the point of view of Ni-Cu mineralization.

ACKNOWLEDGEMENTS

I wish firstly to thank Associate Professor Tauno Piirainen of Oulu University who supervised the project. His enthusiastic attitude towards the work and his relevant and constructive criticism helped considerably in defining problems and developing solutions. Associate Professors Tuomo Alapieti of Oulu University and Jaakko Siivola of Helsinki University, who were the official reviewers, have provided many constructive comments and suggestions for improvement. Numerous valuable comments and advice were given also by those colleaques, who read various versions of the manuscript, including Eero Hanski, Pertti Hautala, Hannu Huhma, Jukka Jokela, Olavi Kontoniemi, Jukka Kousa, Pertti Lamberg and Jari Mäkinen. I am also grateful to Professor Kauko Laajoki of Oulu University, Director of the Geological Survey, Dr Veikko Lappalainen, Professor Jouko Talvitie, Dr Anssi Lonka and Dr Elias Ekdahl for their encouragement and continuing interest in the project. The microprobe data form an important part of this study and I am therefore very apprecaitive of the efforts of Bo Johansson, Kari Kojonen and Lassi Pakkanen. Field work was particularly important during the early stages of the project and I thank my colleagues for their company and co-operation, especially Kimmo Pietikäinen, Heikki Karvonen, Veikko Autio, Rauli Lempiäinen, Erkki Niskanen, Toivo Pienräihä and Martti Saastamoinen. The diagrams have been drafted by Helinä Moberg, Terttu Muraja and Raija Väänänen, while assisted with computing has been provided by Anne Kousa and Matti Partanen. Numerous other staff at the Geological Survey have contributed in various ways to the success of the project and I express my warm thanks to them all. I also thank Outokumpu Finnmines Co. for permission to publish data of Niinimäki occurrence. The manuscript was translated into English by Dr Peter Sorjonen-Ward. This study represents the results of many years work, for which I can only say thankyou to my wife Sinikka and my son Antti for your support and understanding.

REFERENCES

Arndt, N.T. & Nisbet, E.G. 1982. What is a komatiite? In: Arndt, N.T. & Nisbet, E.G.(eds.) Komatiites. London: George Allen & Unvin, 19 - 27.

Barnes, S.-J., Naldrett, A.J. & Gorton, M.P. 1985. The origin of the fractionation of platinum-group elements in terrestial magmas. Chemical Geology 53, 303 - 323.

Barnes, S.-J.,Couture, J.-F.,Sawyer, E.W. & Bouchaib, C. 1993. Nickel-copper occurrences in the Belleterre-Angliers Belt of the Pontiac Subprovince and the use of Cu-Pd ratios in interpreting Platinum-Group Element Distributions. Economic Geology 88, 1402 - 1418.

Beccaluva, L.,Ohnenstetter, D. & Ohnenstetter, M. 1979. Geochemical discrimination between ocean - floor and island-arc tholeiites - application to some ophiolites. Canadian Journal of Earth Sciences 16, 1874 - 1882.

Bedard, J.H. 1994. A procedure for calculating the equilibrium distribution of trace elements among the minerals of cumulate rocks, and the concentration of trace elements in the coexisting liquids. Chemical Geology 118, 143 - 153.

Bickle, M.J. 1982. The magnesium contents of komatiitic liquids. In: Arndt, N.T. & Nisbet, E.G. (eds.) Komatiites. London: George Allen & Unvin, 479 - 494.

Bickle, M.J., Ford, C.E. & Nisbet, E.G. 1977. The petrogenesis of peridotitic komatiites: evidence from high-pressure melting experiments. Earth and Planetary Science Letters 37, 97 - 106.

Boynton, W.V. 1984. Cosmochemistry of the rare earth elements: meteorite studies. In: Henderson, P. (ed.) Rare earth element geochemistry. Amsterdam: Elsevier, 63 - 114.

Campbell, I.H. & Naldrett, A.J. 1979. The influence of silicate: sulfide ratios on the geochemistry of magmatic sulfides. Economic Geology 74, 1503 -1505.

Carmichael, Ian,S.E. 1967. The iron-titanium oxides of salic volganic rocks and their associated ferromagnesian silicates. Contributions to Mineralogy and Petrology 14, 36 - 64.

Cattel, C.A. & Taylor, R.N. 1990. Archaean basic magmas. In: Hall,R.P. & Hughes, D.J. (eds.) Early Precambrian basic magmatism. Glasgow: Blackie & Sons, 11 - 39.

Cousens, B.L. & Ludden, J.N. 1991. Radiogenic isotope studies of oceanic basalts: a window into the mantle. In: Heaman, L. & Ludden, J.N. (eds.) Applications of Radiogenic Isotope Systems to Problems in Geology. Mineralogical Association of Canada. Short Course Handbook, 19, 225 - 257.

Cullers, R. & Graf, J.L. 1984. Rare earth elements in igneous rocks of the continental crust: predominantly basic and ultrabasic rocks. In: Henderson, P.(ed.) Rare earth element geochemistry. Amsterdam: Elsevier, 237 - 274.

Czamanske, G.K. & Moore, J.G. 1977. Composition and phase chemistry of sulfide globules in basalt from the Mid-Atlantic Ridge rift valley near 37 N lat. Geological Society of America, Bulletin 88, 587 - 599.

Davis, A.,Blackburn, W.H.,Brown, W.R. & Ehmann, W.D. 1978. Trace element geochemistry and origin of late Precambrian - early Cambrian Catoctin greenstones of the Appalachian Mountains. Unpublished report, University of California, Davies.

Deer, W.A.,Howie, R.A. & Zussman, J. 1982. Rock forming minerals. Vol 1A: Orthosilicates. London: Longman. 919 p.

DePaolo, D.J. 1981. Neodymium isotopes in the Colorado Front Range and crust-mantle evolution in the Proterozoic. Nature 291, 193 - 196.

Dick, H.J.B. & Bullen, T. 1984. Chromian spinel as a petrogenetic indicator in abyssal and alpine type peridotites and spatially associated lavas. Contributions to Mineralogy and Petrology 86, 54 - 76.

Duke, J.M. 1976. Distribution of the period four transition elements among olivine, calcic clinopyroxene and mafic silicate liquid: experimental results. Journal of Petrology 17, 499 - 521.

Duke, J.M. & Naldrett, A.J. 1978. A numerical model of the fractionation of olivine and molten sulfide from komatiite magma. Earth and Planetary Science Letters 39, 255 - 266.

Ekdahl, E. 1993. Early Proterozoic Karelian and Svecofennian formations and the evolution of the Raahe-Ladoga Ore Zone, based on the Pielavesi area, central Finland. Geological Survey of Finland, Bulletin 373. 137 p.

Elo, S. 1992. Painovoima-anomaliakartat - Gravity anomaly maps. In: Koljonen, T. (ed.) Suomen geokemian Atlas, osa 2: moreeni - The Geochemical Atlas of Finland, Part 2: Till. Espoo: Geological Survey of Finland, 70 - 75.

Elthon, D. 1993. The crystallization of mid-ocean ridge basalts at moderate and high pressures. European Journal of Mineralogy 5, 1025 - 1037.

Ewart, A.,Chapell, B.W. & Menzies, M.A. 1989. An overview of the geochemical and isotopic characteristics of the Eastern Australian Cainozoic volcanic provinces. Journal of Petrology, Special Lithosphere Issue, 225 - 273.

Fleet, M.E.,MacRae, N.D. & Herzberg, C.T. 1977. Partition of nickel between olivine and sulfide: A test for immiscible sulfide liquids.Contributions to Mineralogy and Petrology 65, 191 - 197.

Fodor, R.V. & Vetter, S.K. 1984. Rift-zone magmatism:Petrology of basaltic rocks transitional from CFB to MORB, southeastern Brazil margin. Contributions to Mineralogy and Petrology 88, 307 - 321.

Frosterus, B. 1900. Mikkeli. General Geological Map of Finland 1:400 000, Pre-Quaternary Rocks, Sheet C2. Geological Commission.

Frosterus, B. 1903. Vuorilajikartan selitys. General Geological Map of Finland 1:400 000, Pre-Quaternary Rocks, Sheet C2, Mikkeli. Geological Commission. 102 p.

Gaál, G. 1972. Tectonic control of some Ni-Cu deposits in Finland. In: Gill, J.E. (ed.) International Geological Congress, 24th session, Montreal 1972, Section 4, Mineral Deposits, 215 - 224.

Gaál, G. 1986. 2200 years of crustal evolution:The Baltic shield.Bulletin of the Geological Society of Finland 58 (1), 149 - 68.

Gaál, G. 1990. Tectonic styles of Early Proterozoic ore deposition in the Fennoscandian Shield. Precambrian Research 46, 83 - 114.

Gaál, G. & Rauhamäki, E. 1971. Petrological and structural analysis of the Haukivesi area between Varkaus and Savonlinna, Finland. Bulletin of the Geological Society of Finland 43 (2), 265 - 337.

Gill, J.B. 1981. Orogenic andesites and plate tectonics. Berlin: Springer-Verlag. 399 p.

Gorbunov, G.J. & Papunen, H. 1985 (eds.). General geological map of the Baltic Shield. Geological Survey of Finland, Bulletin 333. (appended map)

Green, A.H. & Naldrett, A.J. 1981. The Langmuir volcanic peridotite associated nickel deposits: Canadian equivalents of the Western Australian occurrences. Economic Geology 76, 1503 - 1523.

Groves, D.I.,Barret, F.M.,Binns, R.A. & McQueen, K.G. 1977. Spinel phases associated with metamorphosed volcanic type iron nickel sulfide ores from Western Australia. Economic Geology 72, 1224 - 1244.

Gruenewaldt, G. von 1973. The modified differentiation index and the modified crystallization index as parameters of differentation in layered intrusions. Transactions of the Geological Society of South Africa 76, 53 - 61.

Grundström, L. 1980. The Laukunkangas nickel copper occurrence in southeastern Finland. Bulletin of the Geological Society of Finland 52 (1), 23 - 53.

Grundström, L. 1985. The Laukunkangas nickel copper deposit. In: Papunen, H. & Gorbunov, G.I.(eds.) Nickel-copper deposits of the Baltic Shield and Scandinavian Caledonides. Geological Survey of Finland, Bulletin 333, 240 - 256.

Gupta, L.N. & Johanssen, W. 1986. Genetic model for the stromatic migmatites of the Rantasalmi Sulkava Area, Finland. Journal of Petrology 27, 521 - 539.

Hackman, V. 1933. Kivilajikartan selitys. General Geological Map of Finland 1:400 000, Pre-Quaternary Rocks, Sheet D2, Savonlinna. Helsinki: Geological Commission of Finland. 175 p.

Hackman, V. & Berghell, H. 1931. Savonlinna. General Geological Map of Finland 1:400 000, Pre-Quaternary Rocks, Sheet D2. Geological Commission of Finland.

Häkli, A. 1963. Distribution of nickel between the silicate and sulphide phases in some basic intrusions in Finland. Bulletin de la Commission géologique de Finlande 209, 54 p.

Häkli, T.A. 1971. Silicate nickel and its application to the exploration of nickel ores. Bulletin of the Geological Society of Finland 43 (2), 247 - 263.

Häkli, T.A., Hänninen, E., Vuorelainen, Y. & Papunen, H. 1976. Platinum group minerals in the Hitura nickel deposit, Finland. Economic Geology 71, 1206 - 1213.

Häkli, T.A., Vormisto, K. & Hänninen, E. 1979. Vammala, a nickel deposit in layered ultramafite, Southwest Finland. Economic Geology 74, 1166 - 1182.

Hanski, E.J. 1983. Alkuaineiden jakautuminen mine-raalien ja silikaattisulan kesken: jakautumis-kertoimet.Arkeeisten alueiden malmiprojekti, report 15. University of Oulu, Department of Geology. 179 p.

Hanski, E.J. 1993. Petrology of the Pechenga ferropicrites and cogenetic, Ni-bearing gabbro-wehrlite intrusions, Kola Peninsula, Russia. Geological Survey of Finland, Bulletin 367. 192 p.

Hanski, E.J. & Koivumaa, S.S. 1983. Ohjelma alkuaineiden käyttäytymisen laskemiseksi fraktioivassa kiteytymisprosessissa. Arkeeisten alueiden malmiprojekti, report 10A. University of Oulu, Department of Geology. 29 p.

Hart, S.R. & Dunn, T. 1993. Experimental cpx/melt partitioning of 24 trace elements. Contributions to Mineralogy and Petrology 113, 1 - 8.

Haskin, L.A.,Haskin, M.A.,Frey, F.A. & Wildeman, T.R. 1968. Relative and absolute terrestial abundances of the rare earths. In: Ahrens, L.H. (ed.) Origin and Distribution of the Elements 1. Oxford: Pergamon, 889 - 911.

Haskin, M.A. & Haskin, L.A. 1966. Rare earths in European shales: a redetermination. Science 154, 507 - 509.

Haughton, D.R.,Roeder, P.L. & Skinner, B.J. 1974. Solubility of sulfur in mafic magmas. Economic Geology 69, 451 - 467.

Hegner, E. & Bevier, M.L. 1991. Nd and Pb isotopic constrains on the origin of the Purtuniq ophiolite and Early Proterozoic Cape Smith belt, northern Quebec, Canada. Chemical Geology 91, 357 - 371.

Henderson, P. 1984. General geochemical properties and abundances of the rare earth elements. In: Henderson, P. (ed.) Rare earth element geochemistry. Amsterdam: Elsevier, 1 - 32.

Huhma, H. 1986. Sm-Nd, U-Pb and Pb-Pb isotopic evidence for the origin of the Early Proterozoic Svecokarelian crust in Finland. Geological Survey of Finland, Bulletin 337. 48 p.

Huhma, H. 1987. Provenance of early Proterozoic and Archaean metasediments in Finland: a Sm-Nd isotopic study. Precambrian Research 35, 127 - 143.

Huppert, E.H. and Sparks, R.S.J. 1984. Double-diffusive convection due to crystallization in magmas. Annual Review of the Earth and Planetary Sciences 12, 11 - 37.

Hyvärinen, L. 1967. Puumalan Kitulan nikkeli kupariesiintymän geologiasta ja mineralogiasta. Unpublished Licentiate thesis. University of Helsinki, Department of Geology. 65 p.

Hyvärinen, L. 1969. On the geology of the copper ore field in the Virtasalmi area, eastern Finland. Bulletin de la Commission géologique de Finlande 240. 82 p.

Idman, H. 1980. Lapin ultramafiittien oksidifaasista. Unpublished master's thesis, University of Turku, Department of Geology. 147 p.

Irvine, T.N. 1965. Chromian spinel as a petrogenetic indicator. Part 1 Theory. Canadian Journal of Earth Sciences 2, 648 - 672.

Irvine, T.N. 1967. Chromian spinel as a petrogenetic indicator, Part 2: petrologic applications. Canadian Journal of Earth Sciences 4, 71 - 103.

Irvine, T.N. 1970. Crystallization sequences in the Muskox intrusion and other layered intrusions.1. Olivine pyroxene plagioclase relations. Geological Society of South Africa Special Publications 1, 441 - 476.

Irvine, T.N. 1977. Origin of chromitite layers in the Muskox intrusion and other stratiform intrusions: a new interpretation. Geology 5, 273 - 277.

Irvine, T.N. 1982. Terminology for layered intrusions. Journal of Petrology 23, 127 - 162.

Irvine, T.N. & Baragar, W.R.A. 1971. A guide to the classification of the common volcanic rocks. Canadian Journal of Earth Sciences 8, 523 - 548.

Isohanni, M. 1985. The Oravainen nickel occurrence in western Finland.In: Papunen, H. & Gorbunov, G.I. (eds.) Nickel-copper deposits of the Baltic Shield and Scandinavian Caledonides. Geological Survey of Finland, Bulletin 333, 189-210.

Isohanni, M., Ohenoja, V. & Papunen, H. 1985. Geology and nickel-copper ores of the Nivala area. In: Papunen, H. & Gorbunov, G.I. (eds.) Nickel-copper deposits of the Baltic Shield and Scandinavian Caledonides. Geological Survey of Finland, Bulletin 333, 211 - 227.

Jakobsen, S.B. & Wasserburg, G.J. 1979. Nd and Sr isotopic study of the Bay of Islands ophiolite complex and the evolution of the source of mid-ocean ridge basalts. Journal of Geophysical Research 84, 7429 - 7445.

Jelinek, E.,Soucek, J.,Bluck, B.J.,Bowes, D.R. & Treloar, P.J. 1980. Nature and significance of beerbachlites in the Ballantrae ophiolite SW Scontland. Transactions of the Royal Society of Edinburgh: Earth Sciences 71, 159 - 179.

Johnson, K.T.M. & Dick, H.J.B. 1992. Open system melting and temporal and spatial variation of peridotite and basalt at the Atlantis-II fracture zone. Journal of Geophysical Research 97, 9219 - 9241.

Kähkönen, Y. & Nironen, M. 1994. Supracrustal rocks around the Paleoproterozoic Haveri Au-Cu deposit, southern Finland: evolution from a spreading center to a volcanic arc environment. In: Nironen, M. & Kähkönen, Y. (eds.) Geochemistry of Proterozoic supracrustal rocks in Finland. Geological Survey of Finland, Special Paper 19, 141 - 159.

Kahma, A. 1973. The main metallogenic features of Finland.Geological Survey of Finland, Bulletin 265. 29 p.

Kilpeläinen, T. 1988. Evolution of deformation and metamorphism as afunction of time in the Rantasalmi-Sulkava area, southeastern Finland. Geological Survey of Finland, Bulletin 343, 77 - 87.

Koistinen, T. 1981. Structural evolution of an early Proterozoic strata-bound Cu-Co-Zn deposit, Outokumpu, Finland. Transactions of the Royal Society of Edinburgh: Earth sciences 72, 115 - 158.

Kontoniemi, O. 1989. The Osikonmäki gold occurrence at Rantasalmi, southeastern Finland. In: Autio, S. (ed.) Current Research 1988. Geological Survey of Finland, Special Paper 10, 107 - 110.

Kontoniemi, O. & Ekdahl, E. 1990. Tonalite hosted early Proterozoic gold deposit at Osikonmäki, southeastern Finland. Bulletin of the Geological Society of Finland 62, 61 - 70.

Kontoniemi, O. & Makkonen, H. 1991. Etelä Savon kultapotentiaali Rantasalmen tutkimusten

valossa. Summary: Southern Savo - A gold potential area in Finland. Vuoriteollisuus 1 (48), 31 - 34.

Korsman, K. 1973. Rantasalmi. Geological Map of Finland 1:100 000, Pre-Quaternary Rocks, Sheet 3233. Geological Survey of Finland.

Korsman, K. 1977. Progressive metamorphism of the metapelites in the Rantasalmi-Sulkava area, southeastern Finland. Geological Survey of Finland, Bulletin 290. 82 p.

Korsman, K. & Lehijärvi, M. 1973. Sulkavan kartta-alueen kallioperä. Summary: Precambrian rocks of the Sulkava map-sheet area. Geological Map of Finland 1:100 000, Pre-Quaternary Rocks, Sheet 3144. Geological Survey of Finland. 24 p.

Korsman, K., Hölttä, P., Hautala, T. & Wasenius, P. 1984. Metamorphism as an indicator of evolution and structure of the crust in eastern Finland. Geological Survey of Finland, Bulletin 328. 40 p.

Korsman, K. & Kilpeläinen, T. 1986. Relationship between zonal metamorphism and deformation in the Rantasalmi Sulkava area, southeastern Finland. Geological Survey of Finland, Bulletin 339, 33 - 42.

Korsman, K.,Niemelä, R. & Wasenius, P. 1988. Multistage evolution of the Proterozoic crust in the Savo schist belt, eastern Finland.Geological Survey of Finland, Bulletin 343, 89 - 96.

Kousa, J. 1985. Rantasalmen tholeiittisista ja komatiittisista vulkaniiteista. Summary: The tholeiitic and komatiitic metavolcanics in Rantasalmi, southeastern Finland. Geologi 37 (2), 17-22.

Lahtinen, R. 1994. Crustal evolution of the Svecofennian and Karelian domains during 2.1 - 1.79 Ga, with special emphasis on the geochemistry and origin of 1.93 - 1.91 Ga gneissic tonalites and associated supracrustal rocks in the Rautalampi area, central Finland. Geological Survey of Finland, Bulletin 378. 128 p.

Lamberg, P. 1990. Porrasniemen intruusio, sen rakenne ja petrologia - 1.9 Ga magmatismi ja Ni-malmit. Unpublished master's thesis, University of Oulu, Department of Geology. 151 p.

Lamberg, P. & Peltonen, P. 1991. Chromian spinels in barren and fertile (Ni-Cu) Svecofennian 1.9 Ga ultramafic intrusions. In: Biennial meeting of the European Union of geosciences, EUG VI, Strasbourg.Abstracts.

Lawrie, K.C. 1992. Geochemical characterisation of a polyphase deformed, altered, and high grade metamorphosed volcanic terrane: implications for the tectonic setting of the Svecofennides, south-central Finland. Precambrian Research 59, 171 - 205.

Lehijärvi, M. 1966. Sulkava. Geological Map of Finland 1:100 000, Pre-Quaternary Rocks, Sheet 3144. Geological Survey of Finland.

Lehto, K. 1987. Kylmälahden, Markkavuoren ja Vetkaimen emäksisten - ultraemäksisten intruusioiden petrografia, mineralogia ja geokemia. Unpublished master's thesis, University of Oulu, Department of Geology. 88 p.

LeMarchand, F.,Villemant, B. & Calas, G. 1987. Trace element distribution coefficients in alkaline series. Geochimica et Cosmochimica Acta 51, 1071 - 1081.

LeRoex, A.P.,Dick, H.J.B.,Erlank, A.J.,Reid, A.M.,Frey, F.A. & Hart, S.R. 1983. Geochemistry, mineralogy and petrogenesis of lavas erupted along the Southwest Indian Ridge between Bouvet triple junction and 11 degrees east. Journal of Petrology 24, 267 - 318.

Longhi, J.,Walker, D. & Hayes, J.F. 1978. The distribution of Fe and Mg between olivine and lunar basaltic liquids. Geochimica et Cosmochimica Acta 42, 1545 - 1558.

Luukkonen, E. & Lukkarinen, H. 1986. Explanation to the stratigraphic map of Middle Finland. Geological Survey of Finland, Report of Investigation 74. 47 p.

Mäkinen, J. 1987. Geochemical characteristics of Svecokarelidic mafic-ultramafic intrusions associated with Ni-Cu occurrences in Finland. Geological Survey of Finland, Bulletin 342. 109 p.

Mäkinen, J. 1995. Migmatiittien geokemiallinen koostumus Leppävirran ja Varkauden ympäristössä. Geological Survey of Finland, unpublished report, S/42/3241/1/95. 3 p.

Makkonen, H. 1988. Tutusen kalkkikiviesiintymän tutkimukset Juvan Nääringissä vuosina 1987 - 1988. Geological Survey of Finland, unpublished report, M19/3231/88/1/10. 13 p.

Makkonen, H. 1992. 1.9 Ga tholeiittinen magmatismi ja siihen liittyvä Ni-Cu-malminmuodostus Juvan alueella, Kaakkois-Suomessa. Unpublished licentiate thesis, University of Oulu, Department of Geology. 200 p.

Makkonen, H. & Ekdahl, E. 1988. Petrology and structure of the early Proterozoic Pirilä gold deposit in southeastern Finland. Bulletin of the Geological Society of Finland 60, 55 - 6.

Mänttäri, I. 1988. Venetekemän serpentiiniytynyt peridotiitti ja siihen liittyvä Ni-Cu mineralisaatio Pieksämäen maalaiskunnassa. Unpublished master's thesis, University of Helsinki, Department of Geology. 82 p.

Marmo, V. & Hyvärinen, L. 1951. Selostus tutkimuksista Puumalan Kitulassa kesällä 1951. Geological Survey of Finland, unpublished report, M17/Puu51/1. 3 p.

Marmo, V. 1954. A small nickeliferous subsilicic cluster at Puumala in Southern Finland. Geological Survey of Finland, Bulletin 168, 1 - 12.

Marsh, N.G., Saunders, A.D.,Tarney, J. & Dick, H.J.B. 1980. Geochemistry of basalts from the Slukoku and Daito Baisins, Deep Sea Drilling Project Leg 58. In: DeVries Klein,G. et al. (eds.) Initial Report Deep Sea Drilling Project, 58. Washington: U.S. Government Printing Office, 805 - 842.

Naldrett, A.J. 1989. Magmatic sulfide deposits. Oxford monographs on geology and geophysics, n:o 14. New York: Oxford University Press.186 p.

Nance, W.B. & Taylor, S.R. 1976. Rare earth element patterns and crustal evolution - I. Australian post-Archean sedimentary rocks. Geochimica et Cosmochimica Acta 40, 1539 - 1551.

Nesbitt, R.W. & Sun, S.S. 1976. Geochemistry of Archaean spinifex textured peridotites and magnesian and low magnesian tholeiites. Earth and Planetary Science Letters 31, 433 - 453.

Nesbitt, R.W.,Sun, S.S. & Purvis, A.C. 1979. Komatiites: geochemistry and genesis. Canadian Mineralogist 17, 165 - 186.

O'Brien, H.E., Huhma, H. & Sorjonen-Ward, P. 1993. Petrogenesis of the late Archean Hattu schist belt, Ilomantsi, eastern Finland. In: Nurmi, P.A. & Sorjonen-Ward, P.(eds.) Geological development, gold mineralization and exploration methods in the late Archean Hattu schist belt, Ilomantsi, eastern Finland. Geological Survey of Finland, Special Paper 17, 147 - 184.

Ohmoto, H. & Rye, R.O. 1979. Isotopes of sulfur and carbon. In: Barnes, H.L. (ed.) Geochemistry of hydrothermal ore deposits, 2nd ed. New York: Wiley, 509 - 567.

Papunen, H. 1980. The Kylmäkoski nickel-copper deposit in southwestern Finland. Bulletin of the Geological Society of Finland 52, 129 - 145.

Papunen, H. 1989. Platinum group elements in metamorphosed Ni-Cu deposits in Finland. In: Prendergast, M.D. & Jones, M.J.(ed.) Magmatic sulphides: the Zimbabwe volume. London: Institution of Mining and Metallurgy, 165 - 176.

Papunen, H., Häkli, T.A. & Idman, H. 1979. Geological, geochemical and mineralogical features of sulfide bearing ultramafic rocks in Finland. Canadian Mineralogist 17, 217 - 232.

Papunen, H. & Mäkelä, M. 1980. Sulfur isotopes in Finnish nickel-copper occurrences. Bulletin of the Geological Society of Finland 52 (1), 55 - 66.

Papunen, H. & Gorbunov, G.I. (eds.) 1985. Nickel-copper deposits of the Baltic Shield and Scandinavian Caledonides. Geological Survey of Finland, Bulletin 333. 394 p.

Papunen, H. & Koskinen, J. 1985. Geology of the Kotalahti nickel-copper ore. In: Papunen, H. & Gorbunov, G.I. (eds.) Nickel-copper deposits of the Baltic Shield and Scandinavian Caledonides. Geological Surey of Finland, Bulletin 333, 229 - 240.

Papunen, H. & Vorma, A. 1985. Nickel deposits in Finland. In: Papunen, H. & Gorbunov, G.I. (eds.) Nickel-copper deposits of the Baltic Shield and Scandinavian Caledonides. Geological Survey of Finland, Bulletin 333, 123 - 143.

Patchett, P.J. & Kouvo, O. 1986. Origin of continental crust of 1.9 - 1.7 Ga age: Nd isotopes and U-Pb ages in the Svecokarelian Terrain of South Finland. Contributions to Mineralogy and Petrology 92, 1 - 12.

Pearce, J.A. 1982. Trace element chracteristics of lavas from destructive plate margins. In: Thorpe, R.S. (ed.) Andesites. Orogenic Andesites and Related Rocks. Chichester: Wiley and Sons, 525 - 548.

Pearce, J.A. 1983. Role of sub-continental lithosphere in magma genesis at active continental margins. In: Hawkesworth, C.J. & Norry, M.J. (eds.) Continental basalts and mantle xenoliths. Cheshire: Shiva Publishing Ltd, 111 - 138.

Pearce, T.H. 1968. A contribution to the theory of variation diagrams. Contributions to Mineralogy and Petrology 19, 142 - 157.

Pearce, T.H.,Gorman, B.E. & Birkett, T.C. 1977. The relationship between major element chemistry and tectonic environment of basic and intermediate volcanic rocks. Earth and Planetary Science Letters 36, 121 - 132.

Pearce, J.A.,Lippard, S.J. & Roberts, S. 1984. Characteristics and tectonic significance of suprasubduction zone ophiolites. In: Kokelaar, B.P. & Howells, M.F. (eds.) Marginal Basins Geology. Geological Society of London, Special Publication 16, 77 - 94.

Pekkarinen, J. 1972. Selostus Juvan tutkimusprojektin malmitutkimuksista vuosina 1962 - 1971 (X=6880.0 eteläpuoli). Geological Survey of Finland, unpublished report, M19/3231/ -72/1/10. 48 p.

Pekkarinen, J. & Hyvärinen, L. 1984. Haukivuori. Geological Map of Finland 1:100 000, Pre-Quaternary Rocks, Sheet 3231. Geological Survey of Finland.

Peltonen, P. 1990. Metamorphic olivine in picritic metavolcanics from Southern Finland. Bulletin of the Geological Society of Finland 62 (2), 99 - 114.

Peltonen, P. 1995a. Crystallization and re-equilibration of zoned chromite in ultramafic cumulates, Vammala Ni-belt, southwestern Finland. Canadian Mineralogist 33, 521 - 535.

Peltonen, P. 1995b. Petrogenesis of ultramafic

rocks in the Vammala Nickel Belt: Implications for crustal evolution of the early Proterozoic Svecofennian arc terrane. Lithos 34, 253 - 274.

Peltonen, P. 1995c. Magma-country rock interaction and the genesis of Ni-Cu deposits in the Vammala Nickel Belt, SW Finland. Mineralogy and Petrology 52, 1 - 24.

Peltonen, P. 1995d. Petrology, geochemistry and mineralogy of ultramafic rocks and associated Ni-Cu deposits in the Vammala Ni-belt, southwestern Finland. Academic dissertation. Espoo: Geological Survey of Finland. 24 p.

Pharoah, T. & Pearce, J.A. 1984. Geochemical evidence for the tectonic setting of early Proterozoic metavolcanic sequences in Lapland. Precambrian Research 25, 283 - 308.

Pietikäinen, K. 1986. Juvan Saarijärven peridotiittien malmipotentiaalista. Unpublished master's thesis, University of Turku, Department of Geology. 72 p.

Piirainen, T. 1987. Malmigeologisesti potentiaalisimmat kohdealueet Suomessa. In: Ekdahl.E. & Kontoniemi.O.(eds.) Malmiosaston geologien kokous, Rovaniemi, 25 - 27.11.1987. Geological Survey of Finland, unpublished report, M10.2/87/1.

Prinzhofer, A. & Allegre, C.J. 1985. Residual peridotites and the mechanism of partial melting. Earth and Planetary Science Letters 74, 251 - 265.

Puustinen, K.,Saltikoff, B. & Tontti, M. 1995. Distribution and metallogenic types of nickel deposits in Finland. Geological Survey of Finland, Report of Investigation 132. 38 p.

Rajamani, V. & Naldrett, A.J. 1978. Partitioning of Fe, Co, Ni, and Cu between sulfide liquid and basaltic melts and the composition of Ni-Cu sulfide deposits. Economic Geology 73, 82 - 93.

Ramdohr, P. 1980. The ore minerals and their intergrowths. Oxford: Pergamon Press. 1207 p.

Roeder, P.L. 1974. Activity of iron and olivine solubility in basaltic liquids. Earth and Planetary Science Letters 23, 397 - 410.

Roeder, P.L. & Emslie, R.F. 1970. Olivine liquid equilibrium. Contributions to Mineralogy and Petrology 29, 275 - 289.

Saunders, A.D. & Tarney, J. 1984. Geochemical characteristics of basaltic volcanism within back-arc basins. In: Kokelaar, B.P. & Howells, M.F. (eds.) Marginal Basins Geology. Geological Society of London, Special Publication 16, 59 - 76.

Schiffries, C.M & Rye, D.M. 1989. Stable isotopic systematics of the Bushveld coplex: I Constraints of magmatic processes in layered intrusions. American Journal of Science 289, 841 - 873.

Shervais, J.W. 1982. Ti-V plots and the petrogenesis of modern and ophiolitic lavas. Earth and Planetary Science Letters 59, 101 - 118.

Simonen, A. 1980. Pre-Quaternary Rocks of Finland 1:1 000 000. Espoo: Geological Survey of Finland.

Simonen, A. 1982. Mäntyharjun ja Mikkelin kartta - alueiden kallioperä. Summary: Pre-Quaternary rocks of the Mäntyharju and Mikkeli map-sheet areas. Geological Map of Finland 1:100 000, Explanation to the Maps of Pre-Quaternary Rocks, Sheets 3123 and 3142. Espoo: Geological Survey of Finland. 36 p.

Simonen, A. & Niemelä, R. 1980. Mikkeli. Geological Map of Finland 1:100 000, Pre-Quaternary Rocks, Sheet 3142. Geological Survey of Finland.

Streckeisen, A. 1975. To each plutonic rock its proper name. Earth Science Reviews. 12, 1 - 33.

Sun, S-S. & Nesbitt, R.W. 1978. Petrogenesis of Archean ultrabasic volcanics: evidence from rare-earth elements. Contributions to Mineralogy and Petrology 65, 301 - 325.

Suvanto, J. 1983. Virtasalmen alueen karsikivijaksoista. Unpublished master's thesis, University of Helsinki, Department of Geology. 54 p.

Taras, B.D. & Hart, S.R. 1987. Geochemical evolution of the New England Seamount Chain: isotopic and trace-element constrains. Chemical Geology 64, 35 - 54.

Till, R. 1977. The hardrock package, a series of Fortran IV computer programs for performing and plotting petrochemical calculations. Computer Geosciences 3, 185 - 243.

Vaasjoki, M. & Sakko, M. 1988. The evolution of the Raahe - Ladoga zone in Finland: isotopic constrains. Geological Survey of Finland, Bulletin 343, 7 - 32.

Vaasjoki, M. & Kontoniemi, O. 1991. Isotopic studies from the Proterozoic Osikonmäki gold prospect at Rantasalmi, southeastern Finland. In: Autio, S. (ed.) Current Research 1989 - 1990. Geological Survey of Finland, Special Paper 12, 53 - 57.

Viljoen, M.J.,Viljoen, R.P. & Pearton, T.N. 1982. The nature and distribution of Archaean komatiite volcanics in South Africa. In: Arndt, N.T. & Nisbet, E.G. (eds.) Komatiites. London: George Allen & Unwin, 53 - 79.

Viluksela, A. 1988. Rantasalmen ja Parikkalan - Punkaharjun vulkaniittien petrografia, geokemia ja tektonomagmaattinen luonne. Unpublished master's thesis, University of Helsinki, Department of Geology. 96p.

Viluksela, A. 1994. Geochemistry of calc-alkaline metavolcanic rocks in the Parikkala-Punkaharju area, southeastern Finland. In: Nironen,M. & Kähkönen, Y. (eds.) Geochemistry of Proterozoic supracrustal rocks in Finland. Geological Survey of Finland, Special Paper 19, 61 - 69.

Volpe, A.M.,Macdougall, J.D. & Hawkins, J.W. 1988. Lau Basin basalts (LBB): trace element and Sr-Nd isotopic evidence for heterogeneity in backarc basin mantle. Earth and Planetary Science Letters 90, 174 - 186.

Vuollo, J. & Piirainen, T. 1989. Mineralogical evidence for an ophiolite from the Outokumpu serpentinites in North Karelia, Finland. Bulletin of the Geological Society of Finland 61, 95 - 112.

Wänke, H., Baddenhausen, H., Palme, H. & Spettel, B 1974. On the chemistry of the Allende inclusions and their origin as high temperature condensates. Earth and Planetary Science Letters 23, 1 - 7.

Williams, H.,Turner, F.J. & Gilbert, C.M. 1982. Petrography: An introduction to study of rocks in thin sections. 2.ed. San Francisco: Freeman and Co. 625 p.

Wood, D.A.,Joron, J.L.,Treuil, M.,Norry, M. & Tarney, J. 1979. Elemental and Sr isotope variations in basic lavas from Iceand and the surroundings ocean floor. Contributions to Mineralogy and Petrology 70, 319 - 339.

Appendix 1. Whole rock chemical data for the Juva area. Oxides and S in weight %, others in ppm. GB=gabbro and more felsic differentiates, PRD=peridotite, UMAF=ultramafic rock, GN=gar-cord-gneiss, M.DYKE=mafic dyke, MARG.=chilled margin, n.d.=not determined, <=below detection limit, >=minimum content.

Occurrence	ALANEN								HEISKALANMÄKI								
Sample	1	2	3	4	5	6	7	8	9	10	11	12	13	14	15	16	17
Lithology	GB	GB	GB	GB	GB	GB	GB	GB	GB	GB	GB	GB	GB	GB	GB	GB	GB
SiO2	51.82	52.16	49.80	53.73	53.47	54.24	54.01	63.83	53.03	54.14	52.48	54.27	51.55	52.99	51.21	52.59	54.59
TiO2	0.53	0.61	0.80	0.90	0.76	0.79	1.14	0.70	0.58	0.65	0.75	0.70	1.24	0.67	0.73	0.87	0.44
Al2O3	17.83	17.53	20.18	17.56	18.72	19.76	19.33	16.08	7.61	8.26	9.61	9.14	11.82	10.86	10.47	10.20	13.24
FeOtot	9.46	8.88	8.86	7.65	9.05	7.20	8.97	5.65	7.28	14.61	8.24	9.32	8.27	7.35	10.85	7.72	9.03
MnO	0.15	0.15	0.14	0.12	0.14	0.11	0.11	0.07	0.14	0.21	0.13	0.14	0.12	0.13	0.17	0.15	0.15
MgO	9.52	9.32	8.64	7.39	6.56	5.79	5.55	3.78	17.59	16.77	15.78	15.62	15.43	14.90	14.82	14.81	14.47
CaO	7.38	7.84	9.83	7.97	7.79	8.40	5.70	4.90	12.77	3.85	11.23	9.42	8.14	11.16	10.06	11.92	5.78
Na2O	2.11	2.07	0.82	2.65	2.14	2.27	2.77	2.79	0.46	0.48	0.78	0.55	0.53	0.83	0.71	0.63	1.07
K2O	1.09	1.33	0.77	1.73	1.22	1.31	2.35	1.88	0.37	0.72	0.71	0.64	2.13	0.76	0.59	0.58	1.07
P2O5	0.11	0.11	0.18	0.30	0.16	0.11	0.07	0.34	0.17	0.31	0.30	0.20	0.77	0.35	0.40	0.53	0.17
Cr	56	166	511	176	380	335	98	154	1073	1900	971	1064	750	1042	874	857	950
Ni	99	76	117	42	77	105	37	43	411	280	1995	1620	1236	371	10226	300	200
V	161	126	164	186	187	178	219	172	173	n.d.	170	187	167	174	166	181	n.d.
Cu	80	<20	42	25	38	56	<20	27	85	80	674	506	444	148	4649	89	80
Pb	<20	21	22	<20	<20	21	29	23	<20	n.d.	26	21	21	<20	31	<20	n.d.
Zn	93	92	98	115	121	125	139	105	78	20	135	116	114	80	159	87	20
Co	n.d.	n.d.	n.d.	n.d.	n.d.	n.d.	n.d.	n.d.	n.d.	30	n.d.	n.d.	n.d.	n.d.	n.d.	n.d.	30
Sn	<20	<20	<20	<20	<20	<20	<20	<20	<20	n.d.	<20	<20	<20	<20	<20	<20	n.d.
Mo	<10	<10	<10	<10	<10	<10	<10	<10	<10	n.d.	<10	<10	<10	<10	<10	<10	n.d.
S	0.12	0.03	0.08	0.10	0.12	0.14	0.07	0.08	0.13	0.16	0.90	0.79	0.44	0.12	3.89	0.12	0.15
As	<30	<30	<30	<30	<30	<30	<30	<30	<30	n.d.	<30	<30	<30	<30	<30	<30	n.d.
Rb	32	75	54	48	58	36	79	42	10	n.d.	29	37	80	29	18	13	n.d.
Ba	147	502	476	313	221	242	418	287	140	n.d.	302	192	506	304	264	285	n.d.
Sr	322	822	496	418	390	459	404	506	425	n.d.	597	265	944	910	560	962	n.d.
Ga	<20	25	21	26	20	20	28	25	<20	n.d.	<20	<20	<20	<20	<20	<20	n.d.
Nb	<10	12	<10	<10	<10	<10	11	<10	<10	n.d.	<10	<10	11	<10	<10	<10	n.d.
Zr	62	154	126	90	61	51	135	83	57	n.d.	68	75	104	76	74	103	n.d.
Y	17	18	17	15	17	10	15	14	15	n.d.	14	15	26	17	23	21	n.d.
Th	<10	<10	<10	<10	<10	<10	<10	<10	<10	n.d.	<10	<10	<10	<10	<10	<10	n.d.
La	<30	39	36	<30	<30	<30	33	<30	30	n.d.	<30	<30	51	<30	35	48	n.d.
Ce	32	78	49	41	41	31	70	43	49	n.d.	51	49	127	61	74	96	n.d.
Cl	93	246	160	90	184	89	100	93	116	n.d.	104	60	193	116	199	126	n.d.

Appendix 1. Continued 2/22.

Occurrence	HEISKALANMÄKI												HIETAJÄRVI		
Sample	18	19	20	21	22	23	24	25	26	27	28	29	30	31	32
Lithology	GB	GB	GB	GB	GB	GB	GB	GB	GB	GB	GB	GB	GB	GB	GB
SiO2	56.62	52.01	52.13	49.99	52.23	53.67	51.88	50.67	52.17	53.36	53.35	53.54	50.94	50.65	48.60
TiO2	0.55	0.59	0.59	0.93	0.79	0.66	0.88	1.16	0.60	1.12	0.66	0.74	1.13	1.13	2.00
Al2O3	9.67	13.31	13.57	12.08	11.51	13.55	15.08	13.94	15.51	13.94	16.16	18.31	16.77	17.02	16.63
FeOtot	8.37	7.03	6.64	12.39	11.00	6.62	7.75	9.09	6.18	8.90	6.30	6.63	9.08	10.51	13.82
MnO	0.14	0.12	0.12	0.11	0.13	0.12	0.10	0.12	0.10	0.11	0.12	0.09	0.13	0.16	0.18
MgO	13.68	13.39	13.31	12.87	12.79	12.64	11.83	11.63	11.25	10.87	10.33	8.43	7.53	8.42	7.68
CaO	10.00	11.16	10.76	8.81	9.04	10.32	8.64	9.96	11.21	8.43	10.49	8.99	8.65	9.43	6.64
Na2O	0.00	1.51	1.77	0.93	0.98	0.83	2.00	1.12	2.05	0.72	1.33	1.44	3.24	0.72	2.38
K2O	0.81	0.65	0.88	1.26	1.08	1.31	1.35	1.43	0.68	1.73	0.94	1.37	1.78	1.65	1.45
P2O5	0.17	0.25	0.24	0.62	0.45	0.29	0.50	0.89	0.24	0.82	0.33	0.44	0.75	0.32	0.62
Cr	950	862	870	749	968	710	634	758	513	758	479	284	293	438	264
Ni	250	939	298	19179	11478	254	479	3798	230	3590	380	244	109	116	93
V	n.d.	135	139	139	131	160	167	189	138	184	134	149	214	282	375
Cu	100	456	202	4636	3208	94	493	1892	172	1688	300	186	116	<20	64
Pb	n.d.	32	33	34	26	22	46	41	30	30	23	24	<20	<20	21
Zn	<10	75	73	111	143	88	111	123	70	177	79	97	147	132	194
Co	20	n.d.	n.d.	n.d.	n.d.	n.d.	n.d.	n.d.	n.d.	n.d.	n.d.	n.d.	n.d.	n.d.	n.d.
Sn	n.d.	<20	<20	<20	<20	<20	<20	<20	<20	<20	<20	<20	<20	<20	<20
Mo	n.d.	<10	<10	<10	<10	<10	<10	<10	<10	<10	<10	<10	<10	<10	<10
S	0.21	0.33	0.08	7.90	5.12	0.10	0.43	1.87	0.14	1.63	0.20	0.19	0.19	0.01	0.13
As	n.d.	<30	<30	<30	<30	<30	<30	<30	<30	<30	<30	<30	<30	<30	<30
Rb	n.d.	21	25	37	38	71	48	51	21	78	46	63	84	147	53
Ba	n.d.	304	399	477	497	423	637	697	369	898	447	620	476	689	360
Sr	n.d.	1453	1435	761	737	988	1561	1305	1777	1132	1498	1767	1305	597	556
Ga	n.d.	<20	<20	<20	<20	<20	<20	<20	<20	<20	<20	22	28	<20	23
Nb	n.d.	<10	<10	<10	<10	<10	<10	12	<10	13	<10	11	21	<10	16
Zr	n.d.	61	64	85	88	84	104	142	70	166	83	94	172	31	94
Y	n.d.	16	13	15	14	13	20	25	12	26	13	18	33	20	24
Th	n.d.	<10	<10	<10	<10	<10	<10	<10	<10	<10	<10	<10	<10	<10	<10
La	n.d.	34	42	38	40	41	36	74	31	74	42	45	73	<30	<30
Ce	n.d.	57	57	89	75	60	85	152	63	127	64	87	165	43	76
Cl	n.d.	87	134	88	172	137	175	262	133	235	161	328	675	115	114

Appendix 1. Continued 3/22.

Occurrence	HIETAJÄRVI														
Sample	33	34	35	36	37	38	39	40	41	42	43	44	45	46	47
Lithology	GB	GB	GB	GB	GB	GB	GB	GB	GB	GB	GB	GB	GB	GB	GB
SiO2	52.55	49.49	48.89	49.63	50.73	50.35	50.21	53.40	51.12	53.68	50.85	53.32	49.26	50.50	51.20
TiO2	1.52	1.19	1.32	1.09	0.63	1.58	1.45	1.29	1.68	1.72	1.27	1.17	1.54	1.78	1.30
Al2O3	16.81	19.52	19.10	21.12	20.53	19.17	20.25	18.68	19.04	16.59	20.29	19.00	20.71	18.88	20.29
FeOtot	10.11	9.44	9.68	9.73	8.16	9.35	10.20	9.43	10.72	11.50	9.67	9.47	10.68	11.70	9.74
MnO	0.15	0.13	0.18	0.15	0.13	0.14	0.17	0.13	0.14	0.15	0.14	0.14	0.15	0.14	0.14
MgO	7.20	7.11	6.95	6.70	6.64	6.11	5.76	5.73	5.73	5.71	5.67	5.45	5.29	5.21	5.17
CaO	6.87	9.53	8.50	8.52	9.49	8.90	7.60	6.53	6.92	5.84	7.83	7.63	8.64	6.41	7.40
Na2O	2.53	1.78	2.75	2.12	2.66	2.24	2.94	2.61	2.48	2.71	3.08	2.62	2.57	2.97	3.18
K2O	1.88	1.47	2.36	0.66	0.75	1.81	0.99	1.78	1.64	1.54	0.76	0.81	0.55	1.78	1.13
P2O5	0.38	0.35	0.27	0.27	0.28	0.37	0.42	0.41	0.53	0.54	0.44	0.39	0.63	0.62	0.46
Cr	314	252	237	285	299	226	191	226	205	173	214	220	133	141	181
Ni	87	35	72	61	51	42	100	75	78	69	76	75	38	90	67
V	256	232	227	322	142	254	223	236	328	306	280	226	368	292	243
Cu	40	<20	73	<20	<20	<20	54	42	58	28	29	<20	23	174	30
Pb	22	<20	<20	<20	<20	<20	<20	21	20	25	<20	20	23	20	<20
Zn	146	111	182	118	102	128	154	152	155	193	141	138	148	232	147
Co	n.d.	n.d.	n.d.	n.d.	n.d.	n.d.	n.d.	n.d.	n.d.	n.d.	n.d.	n.d.	n.d.	n.d.	n.d.
Sn	<20	<20	43	<20	<20	<20	<20	<20	<20	<20	<20	<20	<20	<20	<20
Mo	<10	<10	<10	<10	<10	<10	<10	<10	<10	<10	<10	<10	<10	<10	<10
S	0.12	0.06	0.82	0.05	0.01	0.10	0.14	0.16	0.16	0.03	0.12	0.02	0.12	0.49	0.13
As	<30	<30	<30	<30	<30	<30	<30	<30	<30	<30	<30	<30	<30	<30	<30
Rb	117	139	193	33	34	114	37	87	79	76	28	37	23	90	35
Ba	369	365	877	437	283	639	313	642	477	485	298	383	279	429	438
Sr	414	553	508	623	687	522	595	477	590	491	642	517	550	513	627
Ga	24	28	28	26	20	27	26	28	25	25	26	26	27	34	27
Nb	14	<10	<10	<10	<10	12	12	11	15	17	<10	11	<10	20	12
Zr	97	74	275	33	98	150	96	115	68	81	76	70	23	62	79
Y	24	26	15	<10	13	25	19	22	21	24	18	32	19	21	21
Th	<10	<10	<10	<10	<10	<10	<10	<10	<10	<10	<10	<10	<10	<10	<10
La	35	<30	34	<30	30	<30	<30	36	<30	45	<30	30	<30	<30	49
Ce	73	66	63	44	47	62	63	72	71	74	62	75	42	75	88
Cl	151	70	66	57	82	141	85	114	79	185	75	64	76	196	97

Appendix 1. Continued 4/22.

Occurrence	HIETAJÄRVI														
Sample	48	49	50	51	52	53	54	55	56	57	58	59	60	61	62
Lithology	GB	GB	GB	GB	GB	GB	GB	GB	GB	GB	GB	GB	GB	GB	GB
SiO2	54.55	53.02	52.38	55.18	46.37	48.66	49.67	50.21	49.54	58.88	48.37	56.39	49.32	51.08	51.80
TiO2	1.17	1.33	1.36	1.18	2.01	1.29	2.47	1.90	1.62	1.14	1.71	1.16	2.08	1.78	2.03
Al2O3	18.59	19.28	20.02	18.50	21.83	21.86	19.55	20.66	21.53	17.69	22.04	18.87	21.65	20.36	19.65
FeOtot	8.47	8.61	9.27	8.23	11.24	11.44	11.40	10.31	9.78	7.33	9.84	7.89	11.15	10.23	10.31
MnO	0.12	0.10	0.13	0.12	0.13	0.18	0.15	0.14	0.12	0.10	0.12	0.11	0.12	0.12	0.10
MgO	5.09	4.95	4.79	4.70	4.59	4.47	4.27	4.27	4.17	4.06	4.03	4.03	3.96	3.77	3.73
CaO	6.08	5.84	7.04	6.40	8.28	8.29	7.09	7.62	8.20	5.31	9.96	5.86	6.61	6.50	7.29
Na2O	3.40	3.27	3.11	3.26	2.42	2.60	3.24	3.08	3.11	3.07	2.47	2.97	3.45	3.47	2.85
K2O	2.12	3.00	1.46	2.04	2.15	0.97	1.37	1.24	1.27	2.06	0.75	2.27	1.64	2.01	1.49
P2O5	0.40	0.60	0.45	0.39	0.98	0.24	0.81	0.58	0.65	0.36	0.73	0.44	0.03	0.68	0.76
Cr	243	187	154	184	83	222	84	93	97	159	88	128	90	101	76
Ni	85	69	60	69	47	73	38	30	31	52	29	48	69	49	35
V	199	212	237	207	297	306	353	301	257	190	279	195	223	248	276
Cu	25	<20	31	26	65	61	34	39	24	<20	55	37	47	33	86
Pb	24	27	25	21	22	<20	24	25	23	30	21	20	25	29	29
Zn	149	162	143	136	138	183	153	147	162	122	132	146	172	156	159
Co	n.d.	n.d.	n.d.	n.d.	n.d.	n.d.	n.d.	n.d.	n.d.	n.d.	n.d.	n.d.	n.d.	n.d.	n.d.
Sn	<20	<20	<20	<20	<20	<20	<20	<20	<20	<20	<20	<20	<20	<20	<20
Mo	<10	<10	<10	<10	<10	<10	<10	<10	<10	<10	<10	<10	<10	<10	<10
S	0.05	0.05	0.10	0.06	0.17	0.20	0.10	0.15	0.14	0.05	0.44	0.12	0.13	0.12	0.46
As	<30	<30	<30	<30	<30	<30	<30	<30	<30	<30	<30	<30	<30	<30	<30
Rb	100	144	68	100	51	43	63	64	72	137	39	130	56	97	94
Ba	526	559	614	661	3318	598	452	597	612	596	626	499	1085	1068	1555
Sr	504	482	587	510	908	622	567	664	716	415	720	499	669	550	798
Ga	26	33	31	28	29	29	30	29	35	23	33	28	33	30	33
Nb	14	22	13	16	<10	10	21	14	12	18	11	17	24	21	13
Zr	176	163	128	194	141	127	81	101	86	231	129	140	453	58	120
Y	23	23	23	31	16	12	18	18	24	32	35	29	<10	36	20
Th	<10	<10	<10	<10	<10	<10	<10	<10	<10	<10	<10	<10	<10	<10	<10
La	37	48	41	44	80	<30	37	<30	37	47	38	43	<30	50	64
Ce	96	85	74	94	170	44	86	67	81	97	83	87	50	99	125
Cl	121	250	149	130	96	83	116	170	199	108	144	242	65	120	338

Appendix 1. Continued 5/22.

Occurrence	HIETAJÄRVI			KEKONEN											
Sample	63	64	65	66	67	68	69	70	71	72	73	74	75	76	77
Lithology	GB	GB	GB	PRD	PRD	PRD	PRD	PRD	GB	GB	PRD	GB	GB	GB	GB
SiO2	50.98	49.17	65.02	43.12	43.49	41.67	44.16	48.05	46.79	44.90	46.86	45.79	46.72	47.14	47.45
TiO2	1.73	2.05	0.72	1.04	0.63	0.53	0.70	0.46	0.67	0.68	0.56	0.63	0.98	0.89	0.37
Al2O3	21.18	20.52	19.32	5.99	7.45	7.13	8.36	10.36	10.38	11.83	12.37	14.49	13.21	14.18	16.31
FeOtot	10.50	11.64	4.89	16.16	15.50	18.49	15.50	10.86	13.22	13.60	12.19	11.29	11.99	11.57	10.09
MnO	0.13	0.13	0.03	0.21	0.20	0.22	0.22	0.18	0.19	0.20	0.18	0.15	0.18	0.17	0.17
MgO	3.62	3.53	2.19	28.01	26.85	26.22	24.47	21.09	20.99	19.34	17.88	16.71	16.60	15.97	13.52
CaO	6.14	7.46	0.53	4.03	4.20	4.35	5.07	7.03	6.12	7.30	7.97	8.41	7.94	8.02	9.37
Na2O	3.75	3.47	1.83	0.62	0.62	0.91	0.95	1.03	1.13	1.67	1.27	1.35	1.63	1.08	0.82
K2O	1.81	1.23	5.39	0.34	0.83	0.25	0.33	0.85	0.37	0.32	0.60	1.04	0.55	0.80	1.82
P2O5	0.15	0.79	0.09	0.48	0.23	0.21	0.23	0.09	0.15	0.16	0.12	0.14	0.20	0.19	0.08
Cr	102	70	101	2130	2054	1791	1678	990	2315	1436	865	1120	964	921	501
Ni	55	30	55	1394	1110	6253	6702	1769	1118	794	869	2457	475	435	314
V	208	234	117	166	129	131	128	145	165	154	167	133	171	171	127
Cu	62	<20	<20	163	93	1102	3263	1219	298	179	121	2082	132	112	60
Pb	31	20	61	<20	<20	26	31	<20	<20	<20	<20	<20	<20	<20	<20
Zn	164	154	167	133	145	172	203	135	169	117	117	83	102	94	101
Co	n.d.	n.d.	n.d.	126	120	257	251	92	109	104	115	124	83	86	75
Sn	<20	<20	<20	<20	<20	<20	<20	<20	<20	<20	<20	<20	<20	<20	<20
Mo	<10	<10	<10	<10	<10	<10	<10	<10	<10	<10	<10	<10	<10	<10	<10
S	0.17	0.05	0.02	0.20	0.12	3.34	3.81	0.93	0.41	0.16	0.14	1.27	0.10	0.10	0.06
As	<30	<30	<30	<30	<30	<30	<30	<30	<30	<30	<30	<30	<30	<30	<30
Rb	63	66	153	14	23	<10	<10	17	<10	<10	18	32	13	22	55
Ba	1227	798	746	177	173	104	126	99	140	134	133	105	149	171	123
Sr	606	636	135	119	114	124	140	100	168	183	181	162	187	187	248
Ga	29	28	34	n.d.	n.d.	n.d.	n.d.	n.d.	n.d.	n.d.	n.d.	n.d.	n.d.	n.d.	n.d.
Nb	21	23	22	<10	<10	<10	<10	<10	<10	<10	<10	<10	<10	<10	<10
Zr	230	213	204	107	71	38	53	38	45	59	54	53	70	88	37
Y	13	20	<10	19	11	11	<10	11	11	17	11	12	14	18	10
Th	<10	<10	20	<10	<10	<10	<10	<10	<10	<10	<10	<10	<10	<10	<10
La	31	40	69	32	<30	<30	<30	<30	<30	<30	<30	<30	<30	<30	<30
Ce	53	88	152	41	30	<30	<30	<30	30	<30	<30	32	<30	31	<30
Cl	71	121	70	350	273	465	138	126	112	127	101	160	132	122	144

Appendix 1. Continued 6/22.

Occurrence	KEKONEN		KIISKILÄNKANGAS											KOLOLAHDENS.	
Sample	78	79	80	81	82	83	84	85	86	87	88	89	90	91	92
Lithology	GB	GB	PRD	PRD	PRD	PRD	GB	GB	GB	GB	GB	GB	GB	GB	GB
SiO2	48.37	48.74	42.09	46.96	48.52	46.87	48.15	46.36	48.50	49.15	52.15	51.73	57.77	49.48	46.55
TiO2	0.74	1.02	0.45	0.34	0.34	0.27	0.24	0.35	0.31	0.38	0.40	0.57	1.28	0.85	0.67
Al2O3	15.23	16.43	6.14	8.47	9.24	10.14	12.89	14.79	14.02	15.04	13.59	15.50	16.83	8.94	18.25
FeOtot	10.95	10.28	14.65	12.42	10.75	12.20	10.06	11.27	9.59	9.41	10.69	10.10	10.80	13.14	9.15
MnO	0.16	0.15	0.19	0.19	0.17	0.18	0.16	0.15	0.16	0.15	0.17	0.16	0.15	0.21	0.13
MgO	13.38	11.53	30.64	24.01	22.39	22.33	19.70	17.62	17.40	15.99	12.51	10.32	3.24	17.22	11.99
CaO	8.32	9.29	3.01	6.04	6.71	6.58	7.59	7.61	8.55	8.11	7.81	8.74	5.89	8.65	9.36
Na2O	0.77	1.77	0.13	1.25	1.30	1.13	0.87	1.32	1.00	1.20	1.96	1.76	2.72	0.43	0.00
K2O	1.96	0.59	2.51	0.26	0.52	0.28	0.32	0.48	0.45	0.51	0.65	1.05	1.02	1.03	3.64
P2O5	0.13	0.19	0.19	0.06	0.05	0.04	0.03	0.05	0.04	0.06	0.07	0.08	0.30	0.05	0.27
Cr	648	487	2651	680	950	918	1324	785	970	926	714	473	69	1300	350
Ni	387	318	1082	230	170	990	304	1569	95	69	153	52	41	140	290
V	155	182	94	n.d.	n.d.	166	198	147	182	191	189	209	168	n.d.	n.d.
Cu	105	88	35	99	60	485	173	1159	42	39	<20	66	47	70	<10
Pb	<20	<20	<20	n.d.	n.d.	<20	<20	28	<20	<20	<20	<20	22	n.d.	n.d.
Zn	104	91	156	13	<10	92	77	86	77	80	102	91	109	20	40
Co	69	69	121	55	36	164	84	268	69	69	71	60	38	30	40
Sn	<20	<20	<20	n.d.	n.d.	<20	<20	<20	<20	<20	<20	<20	<20	n.d.	n.d.
Mo	<10	<10	<10	n.d.	n.d.	<10	<10	<10	<10	<10	<10	<10	<10	n.d.	n.d.
S	0.09	0.12	0.08	0.15	0.10	1.13	0.39	2.15	0.11	0.07	0.03	0.24	0.08	0.24	0.02
As	<30	<30	<30	n.d.	n.d.	<30	<30	<30	<30	<30	<30	<30	<30	n.d.	n.d.
Rb	65	17	115	n.d.	n.d.	11	13	15	21	22	27	31	40	n.d.	n.d.
Ba	174	201	155	n.d.	n.d.	70	80	117	94	115	141	200	672	n.d.	n.d.
Sr	222	274	24	n.d.	n.d.	70	82	101	92	118	134	151	423	n.d.	n.d.
Ga	n.d.	n.d.	n.d.	n.d.	n.d.	n.d.	n.d.	n.d.	n.d.	n.d.	n.d.	n.d.	n.d.	n.d.	n.d.
Nb	<10	<10	<10	n.d.	n.d.	<10	<10	<10	<10	<10	<10	<10	13	n.d.	n.d.
Zr	65	95	46	n.d.	n.d.	24	22	36	33	41	43	70	216	n.d.	n.d.
Y	17	19	11	n.d.	n.d.	<10	<10	<10	<10	<10	16	16	25	n.d.	n.d.
Th	<10	<10	<10	n.d.	n.d.	<10	<10	<10	<10	<10	<10	<10	<10	n.d.	n.d.
La	<30	<30	<30	n.d.	n.d.	<30	<30	<30	<30	<30	<30	<30	38	n.d.	n.d.
Ce	31	43	<30	n.d.	n.d.	<30	<30	<30	<30	31	<30	<30	59	n.d.	n.d.
Cl	131	135	1704	n.d.	n.d.	84	79	125	88	78	124	130	273	n.d.	n.d.

Appendix 1. Continued 7/22.

Occurrence	KOLOLAHDENSELKÄ														
Sample	93	94	95	96	97	98	99	100	101	102	103	104	105	106	107
Lithology	GB	GB	GB	GB	GB	GB	GB	GB	GB	GB	GB	GB	GB	GB	GB
SiO2	50.40	46.12	53.23	55.25	60.32	60.14	61.23	62.33	62.73	64.04	64.88	60.51	63.47	65.85	66.91
TiO2	0.90	3.04	1.30	1.19	0.87	1.08	0.79	0.75	0.77	0.66	0.66	1.07	0.67	0.56	1.15
Al2O3	18.24	16.14	17.94	17.44	16.30	17.42	16.80	16.48	16.66	16.38	16.07	17.67	15.91	15.81	16.04
FeOtot	8.13	15.96	9.98	8.33	6.91	7.53	6.28	5.53	5.62	5.20	5.75	7.00	5.18	4.50	4.84
MnO	0.13	0.21	0.12	0.10	0.08	0.09	0.08	0.07	0.07	0.07	0.08	0.06	0.06	0.06	0.00
MgO	7.21	6.44	5.94	5.21	4.68	4.23	3.92	3.77	3.49	3.29	3.26	3.24	3.21	2.74	1.48
CaO	11.07	9.91	7.74	7.65	5.25	5.09	4.71	4.44	4.46	4.03	4.86	5.07	4.45	3.65	2.44
Na2O	1.91	0.63	1.28	2.30	3.16	2.45	3.43	4.51	3.29	3.97	2.74	2.67	4.39	4.07	2.80
K2O	1.68	0.83	2.10	2.23	2.07	1.85	2.39	1.82	2.56	2.12	1.54	2.43	2.39	2.50	3.98
P2O5	0.34	0.72	0.36	0.30	0.35	0.13	0.35	0.31	0.35	0.26	0.15	0.27	0.27	0.25	0.35
Cr	290	14	140	90	150	110	120	120	110	110	110	47	100	100	18
Ni	50	40	50	30	120	50	60	70	60	60	60	40	70	60	10
V	n.d.	n.d.	n.d.	n.d.	n.d.	n.d.	n.d.	n.d.	n.d.	n.d.	n.d.	n.d.	n.d.	n.d.	n.d.
Cu	50	60	20	20	60	30	<10	<10	20	<10	40	60	<10	<10	20
Pb	n.d.	n.d.	n.d.	n.d.	n.d.	n.d.	n.d.	n.d.	n.d.	n.d.	n.d.	n.d.	n.d.	n.d.	n.d.
Zn	30	40	50	60	60	60	60	50	60	50	50	80	40	50	120
Co	20	30	20	20	20	20	20	20	10	10	40	20	10	10	20
Sn	n.d.	n.d.	n.d.	n.d.	n.d.	n.d.	n.d.	n.d.	n.d.	n.d.	n.d.	n.d.	n.d.	n.d.	n.d.
Mo	n.d.	n.d.	n.d.	n.d.	n.d.	n.d.	n.d.	n.d.	n.d.	n.d.	n.d.	n.d.	n.d.	n.d.	n.d.
S	0.14	0.30	0.11	0.05	0.11	0.13	0.05	0.08	0.03	0.02	0.08	0.14	0.02	0.03	0.14
As	n.d.	n.d.	n.d.	n.d.	n.d.	n.d.	n.d.	n.d.	n.d.	n.d.	n.d.	n.d.	n.d.	n.d.	n.d.
Rb	n.d.	n.d.	n.d.	n.d.	n.d.	n.d.	n.d.	n.d.	n.d.	n.d.	n.d.	n.d.	n.d.	n.d.	n.d.
Ba	n.d.	n.d.	n.d.	n.d.	n.d.	n.d.	n.d.	n.d.	n.d.	n.d.	n.d.	n.d.	n.d.	n.d.	n.d.
Sr	n.d.	n.d.	n.d.	n.d.	n.d.	n.d.	n.d.	n.d.	n.d.	n.d.	n.d.	n.d.	n.d.	n.d.	n.d.
Ga	n.d.	n.d.	n.d.	n.d.	n.d.	n.d.	n.d.	n.d.	n.d.	n.d.	n.d.	n.d.	n.d.	n.d.	n.d.
Nb	n.d.	n.d.	n.d.	n.d.	n.d.	n.d.	n.d.	n.d.	n.d.	n.d.	n.d.	n.d.	n.d.	n.d.	n.d.
Zr	n.d.	n.d.	n.d.	n.d.	n.d.	n.d.	n.d.	n.d.	n.d.	n.d.	n.d.	n.d.	n.d.	n.d.	n.d.
Y	n.d.	n.d.	n.d.	n.d.	n.d.	n.d.	n.d.	n.d.	n.d.	n.d.	n.d.	n.d.	n.d.	n.d.	n.d.
Th	n.d.	n.d.	n.d.	n.d.	n.d.	n.d.	n.d.	n.d.	n.d.	n.d.	n.d.	n.d.	n.d.	n.d.	n.d.
La	n.d.	n.d.	n.d.	n.d.	n.d.	n.d.	n.d.	n.d.	n.d.	n.d.	n.d.	n.d.	n.d.	n.d.	n.d.
Ce	n.d.	n.d.	n.d.	n.d.	n.d.	n.d.	n.d.	n.d.	n.d.	n.d.	n.d.	n.d.	n.d.	n.d.	n.d.
Cl	n.d.	n.d.	n.d.	n.d.	n.d.	n.d.	n.d.	n.d.	n.d.	n.d.	n.d.	n.d.	n.d.	n.d.	n.d.

Appendix 1. Continued 8/22.

Occurrence	KOLKANRANTA							LEVÄN.	LUMPEINEN						
Sample	108	109	110	111	112	113	114	115	116	117	118	119	120	121	122
Lithology	GB	GB	GB	GB	GB	GB	GB	UMAF	PRD	PRD	PRD	PRD	PRD	PRD	PRD
SiO2	52.52	57.46	58.08	59.54	59.43	61.33	65.48	50.32	42.94	41.75	42.60	42.22	46.30	44.01	44.39
TiO2	1.27	1.06	1.17	1.06	1.04	0.93	0.78	0.65	0.21	0.30	0.55	0.43	0.41	0.31	0.34
Al2O3	14.88	15.05	15.48	16.01	16.00	15.74	15.91	7.78	2.01	6.34	3.75	6.23	4.02	2.79	2.83
FeOtot	10.61	8.26	8.52	7.94	7.66	6.89	5.88	10.01	17.23	17.05	16.53	17.44	16.32	15.03	14.56
MnO	0.15	0.11	0.12	0.10	0.10	0.09	0.07	0.16	0.25	0.24	0.25	0.26	0.25	0.23	0.23
MgO	7.00	6.00	5.49	4.95	4.94	4.65	3.43	21.35	34.55	31.20	29.47	29.32	29.25	28.58	28.36
CaO	8.46	6.02	5.77	5.29	5.18	5.24	3.89	8.81	2.81	3.05	6.27	3.03	2.87	8.78	8.97
Na2O	2.47	3.24	2.53	2.56	3.33	2.81	2.77	0.58	0.00	0.00	0.34	0.56	0.09	0.19	0.12
K2O	2.22	2.38	2.45	2.18	1.98	1.97	1.55	0.19	0.00	0.00	0.21	0.44	0.51	0.07	0.18
P2O5	0.42	0.41	0.38	0.36	0.35	0.35	0.24	0.14	0.00	0.07	0.03	0.07	0.00	0.02	0.02
Cr	230	240	220	190	190	180	120	2400	>1100	>130	1024	>71	>230	1471	1312
Ni	60	110	130	90	90	90	80	120	710	480	364	420	440	309	346
V	n.d.	n.d.	n.d.	n.d.	n.d.	n.d.	n.d.	n.d.	n.d.	n.d.	205	n.d.	n.d.	181	178
Cu	140	20	70	60	50	50	90	54	200	150	101	98	280	40	85
Pb	n.d.	n.d.	n.d.	n.d.	n.d.	n.d.	n.d.	n.d.	n.d.	n.d.	<20	n.d.	n.d.	<20	<20
Zn	50	70	100	70	70	60	70	<10	85	120	119	120	120	97	99
Co	20	20	50	20	20	20	30	24	160	160	133	150	150	112	114
Sn	n.d.	n.d.	n.d.	n.d.	n.d.	n.d.	n.d.	n.d.	n.d.	n.d.	<20	n.d.	n.d.	<20	<20
Mo	n.d.	n.d.	n.d.	n.d.	n.d.	n.d.	n.d.	n.d.	n.d.	n.d.	<10	n.d.	n.d.	<10	<10
S	0.04	0.03	0.14	0.08	0.10	0.04	0.09	0.01	0.52	0.40	0.52	0.27	1.12	0.17	0.23
As	n.d.	n.d.	n.d.	n.d.	n.d.	n.d.	n.d.	n.d.	n.d.	n.d.	<30	n.d.	n.d.	<30	<30
Rb	n.d.	n.d.	n.d.	n.d.	n.d.	n.d.	n.d.	n.d.	n.d.	n.d.	<10	n.d.	n.d.	<10	<10
Ba	n.d.	n.d.	n.d.	n.d.	n.d.	n.d.	n.d.	n.d.	n.d.	n.d.	57	n.d.	n.d.	90	43
Sr	n.d.	n.d.	n.d.	n.d.	n.d.	n.d.	n.d.	n.d.	n.d.	n.d.	49	n.d.	n.d.	33	29
Ga	n.d.	n.d.	n.d.	n.d.	n.d.	n.d.	n.d.	n.d.	n.d.	n.d.	n.d.	n.d.	n.d.	n.d.	n.d.
Nb	n.d.	n.d.	n.d.	n.d.	n.d.	n.d.	n.d.	n.d.	n.d.	n.d.	<10	n.d.	n.d.	<10	<10
Zr	n.d.	n.d.	n.d.	n.d.	n.d.	n.d.	n.d.	n.d.	n.d.	n.d.	<10	n.d.	n.d.	<10	10
Y	n.d.	n.d.	n.d.	n.d.	n.d.	n.d.	n.d.	n.d.	n.d.	n.d.	<10	n.d.	n.d.	<10	<10
Th	n.d.	n.d.	n.d.	n.d.	n.d.	n.d.	n.d.	n.d.	n.d.	n.d.	<10	n.d.	n.d.	<10	<10
La	n.d.	n.d.	n.d.	n.d.	n.d.	n.d.	n.d.	n.d.	n.d.	n.d.	<30	n.d.	n.d.	<30	<30
Ce	n.d.	n.d.	n.d.	n.d.	n.d.	n.d.	n.d.	n.d.	n.d.	n.d.	<30	n.d.	n.d.	<30	<30
Cl	n.d.	n.d.	n.d.	n.d.	n.d.	n.d.	n.d.	n.d.	n.d.	n.d.	769	n.d.	n.d.	527	692

Appendix 1. Continued 9/22.

Occurrence	LUMPEINEN														
Sample	123	124	125	126	127	128	129	130	131	132	133	134	135	136	137
Lithology	PRD	PRD	PRD	PRD	PRD	PRD	PRD	PRD	PRD	PRD	PRD	PRD	PRD	PRD	PRD
SiO2	44.57	44.98	44.91	47.41	44.51	46.78	45.17	45.43	47.19	48.63	47.72	46.95	48.08	50.29	49.06
TiO2	0.35	0.33	0.38	0.37	0.42	0.46	0.41	0.48	0.40	0.43	0.44	0.59	0.54	0.46	0.65
Al2O3	2.83	2.74	4.36	3.42	6.78	4.37	4.16	3.75	4.47	3.45	4.11	4.49	4.11	3.84	6.30
FeOtot	15.19	14.78	14.46	12.26	14.52	13.45	13.75	14.01	13.67	11.41	13.08	11.76	10.10	8.94	8.77
MnO	0.22	0.21	0.22	0.22	0.23	0.22	0.22	0.24	0.22	0.19	0.22	0.20	0.18	0.18	0.17
MgO	28.12	27.63	26.36	26.30	25.47	25.41	24.98	24.63	24.17	24.10	22.65	20.71	20.34	19.90	17.07
CaO	8.30	8.99	8.66	9.54	6.98	9.11	10.94	10.85	9.80	11.71	11.70	14.81	16.22	16.08	16.87
Na2O	0.26	0.22	0.42	0.29	0.58	0.10	0.26	0.40	0.00	0.00	0.08	0.38	0.33	0.10	0.81
K2O	0.14	0.09	0.19	0.15	0.45	0.00	0.08	0.18	0.00	0.04	0.00	0.09	0.08	0.22	0.25
P2O5	0.03	0.02	0.04	0.04	0.06	0.09	0.04	0.04	0.08	0.03	0.00	0.02	0.02	0.00	0.05
Cr	1309	2130	1297	1843	>600	>890	1184	1141	>720	>1200	>860	2235	2402	>1800	2530
Ni	331	524	489	369	360	440	365	242	430	450	380	400	366	340	169
V	170	176	171	179	n.d.	n.d.	219	285	n.d.	n.d.	n.d.	290	280	n.d.	323
Cu	83	196	219	77	110	200	172	111	200	220	180	159	191	140	42
Pb	<20	<20	<20	<20	n.d.	n.d.	<20	<20	<10	n.d.	n.d.	<20	<20	n.d.	<20
Zn	104	108	89	93	100	85	83	103	86	73	87	76	64	57	53
Co	126	131	135	125	130	130	124	101	130	120	120	99	86	92	64
Sn	<20	<20	<20	<20	n.d.	n.d.	<20	<20	n.d.	n.d.	n.d.	<20	<20	n.d.	<20
Mo	<10	<10	<10	<10	n.d.	n.d.	<10	<10	n.d.	n.d.	n.d.	<10	<10	n.d.	<10
S	0.20	0.44	0.46	0.38	0.35	0.48	0.38	0.61	0.52	0.62	0.44	0.38	0.43	0.59	0.17
As	<30	<30	<30	<30	n.d.	n.d.	<30	<30	n.d.	n.d.	n.d.	<30	<30	n.d.	<30
Rb	<10	<10	<10	<10	n.d.	n.d.	<10	<10	n.d.	n.d.	n.d.	<10	<10	n.d.	<10
Ba	32	29	57	47	n.d.	n.d.	44	42	n.d.	n.d.	n.d.	46	53	n.d.	74
Sr	33	30	59	46	n.d.	n.d.	50	50	n.d.	n.d.	n.d.	58	50	n.d.	88
Ga	n.d.	n.d.	n.d.	n.d.	n.d.	n.d.	n.d.	n.d.	n.d.	n.d.	n.d.	n.d.	n.d.	n.d.	n.d.
Nb	<10	<10	<10	<10	n.d.	n.d.	<10	<10	n.d.	n.d.	n.d.	<10	<10	n.d.	<10
Zr	<10	<10	15	16	n.d.	n.d.	12	12	n.d.	n.d.	n.d.	18	14	n.d.	29
Y	<10	<10	<10	<10	n.d.	n.d.	<10	<10	n.d.	n.d.	n.d.	13	11	n.d.	13
Th	<10	<10	<10	<10	n.d.	n.d.	<10	<10	n.d.	n.d.	n.d.	<10	<10	n.d.	<10
La	<30	<30	<30	<30	n.d.	n.d.	<30	<30	n.d.	n.d.	n.d.	<30	<30	n.d.	<30
Ce	<30	<30	<30	<30	n.d.	n.d.	<30	<30	n.d.	n.d.	n.d.	<30	<30	n.d.	<30
Cl	681	544	892	538	n.d.	n.d.	885	445	n.d.	n.d.	n.d.	207	163	n.d.	145

Appendix 1. Continued 10/22.

Occurrence	MYLLYNKYLÄ		NIINIMÄKI												
Sample	138	139	140	141	142	143	144	145	146	147	148	149	150	151	152
Lithology	UMAF	UMAF	PRD	PRD	PRD	PRD	PRD	PRD	PRD	PRD	PRD	PRD	PRD	PRD	PRD
SiO2	45.04	47.04	43.13	42.10	42.62	43.54	43.80	42.68	43.78	42.35	42.83	41.90	44.63	45.35	43.69
TiO2	1.01	1.07	0.18	0.21	0.30	0.37	0.28	0.29	0.19	0.37	0.18	0.17	0.20	0.31	0.33
Al2O3	9.04	8.30	3.89	3.63	3.52	3.96	4.52	4.61	4.66	4.11	5.35	3.84	4.79	4.50	5.02
FeOtot	12.23	11.39	13.85	15.81	15.68	14.18	13.13	14.12	13.12	15.66	13.56	17.50	13.13	13.39	14.36
MnO	0.19	0.19	0.19	0.18	0.18	0.19	0.18	0.19	0.18	0.20	0.17	0.18	0.17	0.18	0.19
MgO	21.66	20.87	36.59	36.08	35.64	35.11	35.10	35.00	34.99	34.85	34.74	34.53	33.79	33.46	33.33
CaO	9.37	9.74	1.91	1.71	1.66	2.03	2.42	2.42	1.87	2.02	2.45	1.31	1.63	2.16	2.41
Na2O	1.22	1.11	0.06	0.08	0.08	0.16	0.19	0.11	0.14	0.14	0.37	0.07	0.03	0.25	0.20
K2O	0.13	0.17	0.18	0.15	0.17	0.33	0.30	0.46	1.02	0.17	0.29	0.35	1.56	0.31	0.30
P2O5	0.11	0.12	0.03	0.06	0.16	0.12	0.08	0.12	0.06	0.13	0.05	0.13	0.07	0.10	0.18
Cr	1400	1600	3574	2665	3272	3491	3419	2820	3468	2491	3367	2575	2701	2509	2131
Ni	670	530	1356	1419	1175	1884	1077	1054	1036	1194	1035	2539	1128	2155	1400
V	n.d.	n.d.	61	76	84	81	77	62	61	79	54	50	53	72	77
Cu	66	74	205	277	77	394	98	144	62	148	<20	793	133	575	436
Pb	21	18	<20	<30	<30	<20	<20	<20	<20	<30	<20	<30	<20	<20	<30
Zn	21	18	148	163	156	143	120	152	140	154	153	237	161	113	157
Co	62	47	n.d.	n.d.	n.d.	n.d.	n.d.	n.d.	n.d.	n.d.	n.d.	n.d.	n.d.	n.d.	n.d.
Sn	n.d.	n.d.	<20	<20	<20	<20	<20	<20	<20	<20	<20	<20	<20	<20	<20
Mo	n.d.	n.d.	<10	<10	<10	<10	<10	<10	<10	<10	<10	<10	<10	<10	<10
S	0.01	0.03	0.26	0.41	0.17	0.55	0.13	0.30	0.10	0.28	0.06	1.04	0.30	0.93	0.63
As	n.d.	n.d.	<30	<30	<30	<30	<30	<30	<30	<30	<30	<30	<30	<30	<30
Rb	n.d.	n.d.	<10	<10	<10	13	11	34	53	<10	<10	12	90	10	<10
Ba	n.d.	n.d.	47	118	84	109	94	64	80	89	98	102	158	110	104
Sr	n.d.	n.d.	69	50	72	105	130	108	68	87	107	80	61	91	104
Ga	n.d.	n.d.	<20	<20	<20	<20	<20	<20	<20	<20	<20	<20	<20	<20	<20
Nb	n.d.	n.d.	<10	<10	<10	<10	<10	<10	<10	<10	<10	<10	<10	<10	<10
Zr	n.d.	n.d.	12	20	40	30	27	33	21	32	14	39	18	32	38
Y	n.d.	n.d.	<10	<10	<10	<10	<10	<10	<10	<10	<10	<10	<10	<10	<10
Th	n.d.	n.d.	<10	<10	<10	<10	<10	<10	<10	<10	<10	<10	<10	<10	<10
La	n.d.	n.d.	<30	<30	<30	<30	<30	<30	<30	<30	<30	<30	<30	<30	<30
Ce	n.d.	n.d.	<30	n.d.	n.d.	<30	<30	<30	<30	n.d.	<30	n.d.	<30	<30	n.d.
Cl	n.d.	n.d.	2052	740	801	1861	2425	1156	1578	1088	1855	1100	723	873	826

Appendix 1. Continued 11/22.

Occurrence	NIINIMÄKI														
Sample	153	154	155	156	157	158	159	160	161	162	163	164	165	166	167
Lithology	PRD	PRD	PRD	PRD	PRD	GB	GB	PRD	GB	GB	GB	GB	GB	GB	GB
SiO2	44.42	44.96	43.80	45.17	45.80	50.93	50.75	51.41	51.31	50.50	45.90	43.63	52.77	51.51	52.46
TiO2	0.26	0.58	0.22	0.48	0.28	0.43	0.60	0.28	0.42	0.62	0.81	0.79	0.46	0.76	0.33
Al2O3	5.45	5.20	6.35	5.67	6.97	7.79	8.96	7.01	5.68	10.27	12.81	16.72	8.54	8.55	11.13
FeOtot	13.74	14.10	13.91	16.10	14.73	13.86	11.63	11.61	15.82	12.24	13.11	15.58	10.36	11.98	9.35
MnO	0.17	0.18	0.18	0.20	0.20	0.15	0.08	0.13	0.11	0.13	0.19	0.17	0.18	0.20	0.17
MgO	32.54	32.13	31.76	29.06	27.89	24.94	24.91	24.37	23.94	23.34	23.11	22.76	22.21	20.86	20.77
CaO	2.57	2.53	2.91	2.83	3.66	1.52	1.97	4.73	1.25	2.75	3.68	0.24	4.14	4.41	4.57
Na2O	0.44	0.20	0.45	0.22	0.31	0.00	0.03	0.29	0.18	0.00	0.08	0.00	0.50	0.53	0.63
K2O	0.36	0.07	0.37	0.14	0.10	0.31	0.97	0.09	1.21	0.05	0.11	0.00	0.79	0.99	0.54
P2O5	0.06	0.06	0.04	0.12	0.06	0.06	0.10	0.09	0.07	0.10	0.19	0.11	0.05	0.20	0.05
Cr	2889	2599	3263	2198	2467	2606	2717	3347	2027	2903	1905	2047	2538	1954	1807
Ni	1070	1830	1152	3582	996	1546	532	1681	4121	564	619	516	1383	465	434
V	67	117	72	82	77	129	163	85	120	158	204	146	143	168	122
Cu	102	597	94	1193	156	458	22	436	858	101	127	25	525	61	132
Pb	<30	<30	<30	<30	<20	<30	<30	<30	<30	39	<30	<30	<30	<30	<20
Zn	126	137	148	193	139	157	36	138	404	145	165	290	110	139	106
Co	n.d.	n.d.	n.d.	n.d.	n.d.	n.d.	n.d.	n.d.	n.d.	n.d.	n.d.	n.d.	n.d.	n.d.	n.d.
Sn	<20	<20	<20	<20	<20	<20	<20	<20	<20	<20	<20	<20	<20	<20	<20
Mo	<10	<10	<10	<10	<10	<10	<10	<10	28	<10	<10	<10	<10	<10	<10
S	0.14	1.07	0.15	2.06	0.30	0.28	0.03	0.52	2.96	0.18	0.10	0.00	0.62	0.13	0.39
As	<30	<30	<30	<30	<30	<30	<30	<30	<30	<30	<30	<30	<30	<30	<30
Rb	<10	<10	<10	10	<10	22	64	<10	57	<10	<10	<10	56	62	22
Ba	137	28	130	62	30	62	184	49	124	32	38	27	138	241	97
Sr	120	33	120	58	86	16	84	74	17	19	23	<10	125	108	246
Ga	<20	<20	<20	<20	<20	<20	<20	<20	<20	23	21	21	<20	<20	<20
Nb	<10	<10	<10	<10	<10	<10	<10	<10	<10	<10	10	<10	<10	<10	<10
Zr	39	28	27	39	21	30	44	31	29	40	85	85	27	78	18
Y	10	12	<10	11	<10	12	17	<10	<10	15	28	12	15	23	<10
Th	<10	<10	<10	<10	<10	<10	<10	<10	<10	<10	<10	<10	<10	<10	<10
La	<30	<30	<30	<30	<30	<30	<30	<30	33	<30	<30	<30	<30	<30	<30
Ce	n.d.	n.d.	n.d.	n.d.	<30	n.d.	n.d.	n.d.	n.d.	n.d.	n.d.	n.d.	n.d.	n.d.	<30
Cl	642	386	576	341	362	38	145	61	151	46	43	33	79	61	60

Appendix 1. Continued 12/22.

Occurrence	NIINIMÄKI											PAKINMAA		PIHLAJASALO	
Sample	168	169	170	171	172	173	174	175	176	177	178	179	180	181	182
Lithology	GB	GB	GB	GB	GB	GB	GB	GB	GB	GB	GN	UMAF	UMAF	PRD	PRD
SiO2	52.21	44.70	51.60	49.62	51.71	50.88	51.07	50.71	52.95	0.29	66.38	46.39	45.66	43.67	45.32
TiO2	0.28	0.37	0.41	0.63	0.75	0.86	1.10	0.86	0.30	0.74	0.75	0.90	1.03	0.16	0.16
Al2O3	12.04	21.89	12.51	14.98	12.48	12.48	13.79	16.33	17.41	19.73	16.49	8.72	9.86	2.63	2.76
FeOtot	8.63	10.36	10.24	9.43	10.77	12.82	11.35	9.61	7.12	8.17	6.12	11.68	12.28	11.72	11.60
MnO	0.16	0.17	0.17	0.12	0.18	0.19	0.19	0.13	0.13	0.14	0.10	0.18	0.20	0.18	0.15
MgO	20.65	18.62	17.77	17.05	16.48	15.48	13.96	13.47	12.83	9.21	3.00	24.84	22.95	37.84	36.43
CaO	4.93	1.69	5.89	6.31	5.05	3.81	6.01	5.83	7.01	9.44	1.83	6.33	6.93	3.56	3.35
Na2O	0.52	0.50	0.78	0.90	1.39	1.50	1.55	1.67	1.38	1.78	3.47	0.73	0.90	0.12	0.17
K2O	0.54	1.64	0.45	0.77	0.99	1.57	0.62	1.16	0.84	0.40	1.74	0.13	0.12	0.08	0.03
P2O5	0.04	0.08	0.17	0.19	0.21	0.42	0.37	0.24	0.05	0.10	0.11	0.11	0.08	0.03	0.03
Cr	2112	604	1548	1272	1217	1215	972	1067	700	482	136	2200	1800	4080	4230
Ni	461	174	314	457	355	349	180	175	159	79	53	510	480	718	725
V	116	106	151	158	169	141	194	162	106	196	137	n.d.	n.d.	100	100
Cu	109	<20	<20	197	170	24	<20	<20	77	231	<20	<10	140	<10	<10
Pb	<20	<30	<30	<30	<30	<30	<30	<30	<20	<30	<30	n.d.	n.d.	n.d.	n.d.
Zn	95	115	118	109	135	214	145	136	78	111	98	<10	10	101	121
Co	n.d.	n.d.	n.d.	n.d.	n.d.	n.d.	n.d.	n.d.	n.d.	n.d.	n.d.	42	43	104	108
Sn	<20	<20	<20	<20	<20	<20	<20	<20	<20	<20	<20	n.d.	n.d.	n.d.	n.d.
Mo	<10	<10	<10	<10	<10	<10	<10	<10	<10	<10	<10	n.d.	n.d.	n.d.	n.d.
S	0.28	0.00	0.01	0.45	0.30	0.10	0.05	0.18	0.14	0.05	0.00	0.00	0.01	0.02	0.01
As	<30	<30	<30	<30	<30	<30	<30	<30	<30	<30	<30	n.d.	n.d.	n.d.	n.d.
Rb	24	83	30	40	63	98	37	56	76	15	68	n.d.	n.d.	n.d.	n.d.
Ba	92	435	98	194	283	395	362	379	137	226	920	n.d.	n.d.	n.d.	n.d.
Sr	328	167	249	211	201	183	320	294	563	353	259	n.d.	n.d.	n.d.	n.d.
Ga	<20	21	<20	21	<20	<20	21	20	<20	<20	22	n.d.	n.d.	n.d.	n.d.
Nb	<10	<10	<10	<10	<10	<10	<10	11	<10	<10	13	n.d.	n.d.	n.d.	n.d.
Zr	12	22	30	73	100	14	148	84	21	47	187	n.d.	n.d.	n.d.	n.d.
Y	<10	10	14	16	21	13	27	15	<10	17	32	n.d.	n.d.	n.d.	n.d.
Th	<10	<10	<10	<10	<10	<10	<10	<10	<10	<10	11	n.d.	n.d.	n.d.	n.d.
La	<30	<30	<30	<30	<30	<30	<30	<30	<30	<30	50	n.d.	n.d.	n.d.	n.d.
Ce	<30	n.d.	n.d.	n.d.	n.d.	n.d.	n.d.	n.d.	<30	n.d.	n.d.	n.d.	n.d.	n.d.	n.d.
Cl	60	45	46	59	49	120	59	59	73	97	65	n.d.	n.d.	n.d.	n.d.

Appendix 1. Continued 13/22.

Occurrence	PIHLAJASALO														
Sample	183	184	185	186	187	188	189	190	191	192	193	194	195	196	197
Lithology	PRD	PRD	PRD	PRD	PRD	PRD	PRD	PRD	PRD	PRD	PRD	PRD	PRD	GB	GB
SiO2	44.55	44.93	44.58	45.32	43.50	45.80	46.56	47.15	45.11	44.87	45.16	45.13	46.82	52.33	50.95
TiO2	0.15	0.21	0.17	0.20	0.22	0.21	0.20	0.17	0.24	0.34	0.26	0.37	0.44	0.74	1.73
Al2O3	2.79	3.72	3.03	2.20	3.71	3.15	3.20	3.25	4.32	5.16	4.34	4.59	5.98	7.57	15.31
FeOtot	12.53	11.58	12.12	11.76	12.42	10.73	11.87	11.89	11.70	11.09	12.38	12.66	10.66	9.83	12.50
MnO	0.15	0.18	0.17	0.19	0.19	0.18	0.17	0.19	0.17	0.18	0.18	0.20	0.18	0.17	0.18
MgO	36.00	35.65	35.40	34.84	34.33	32.92	32.21	31.97	31.39	31.10	30.99	30.69	27.58	17.03	7.64
CaO	3.51	3.11	4.24	5.21	5.23	6.68	5.28	4.78	6.37	6.62	6.09	5.87	7.80	11.10	7.39
Na2O	0.15	0.18	0.16	0.18	0.19	0.22	0.33	0.30	0.36	0.40	0.36	0.31	0.38	0.00	2.18
K2O	0.13	0.40	0.08	0.06	0.15	0.08	0.17	0.28	0.28	0.19	0.19	0.13	0.12	1.19	1.56
P2O5	0.05	0.04	0.05	0.05	0.06	0.03	0.02	0.02	0.05	0.05	0.07	0.05	0.06	0.03	0.58
Cr	4360	4000	4100	3860	3200	3380	3330	3450	3600	2900	2990	2980	2500	1500	270
Ni	746	656	731	620	628	539	657	642	630	588	623	551	504	190	130
V	90	90	120	130	120	180	140	110	160	170	150	160	200	n.d.	n.d.
Cu	<10	<10	<10	<10	<10	22	29	41	44	28	35	33	32	120	80
Pb	n.d.	n.d.	n.d.	n.d.	n.d.	n.d.	n.d.	n.d.	n.d.	n.d.	n.d.	n.d.	n.d.	n.d.	n.d.
Zn	105	133	116	116	101	97	112	127	105	89	112	117	87	30	60
Co	106	91	111	100	103	92	109	108	100	93	102	96	82	40	30
Sn	n.d.	n.d.	n.d.	n.d.	n.d.	n.d.	n.d.	n.d.	n.d.	n.d.	n.d.	n.d.	n.d.	n.d.	n.d.
Mo	n.d.	n.d.	n.d.	n.d.	n.d.	n.d.	n.d.	n.d.	n.d.	n.d.	n.d.	n.d.	n.d.	n.d.	n.d.
S	0.03	0.02	0.02	0.04	0.04	0.09	0.12	0.17	0.11	0.13	0.12	0.31	0.39	0.13	0.14
As	n.d.	n.d.	n.d.	n.d.	n.d.	n.d.	n.d.	n.d.	n.d.	n.d.	n.d.	n.d.	n.d.	n.d.	n.d.
Rb	n.d.	n.d.	n.d.	n.d.	n.d.	n.d.	n.d.	n.d.	n.d.	n.d.	n.d.	n.d.	n.d.	n.d.	n.d.
Ba	n.d.	n.d.	n.d.	n.d.	n.d.	n.d.	n.d.	n.d.	n.d.	n.d.	n.d.	n.d.	n.d.	n.d.	n.d.
Sr	n.d.	n.d.	n.d.	n.d.	n.d.	n.d.	n.d.	n.d.	n.d.	n.d.	n.d.	n.d.	n.d.	n.d.	n.d.
Ga	n.d.	n.d.	n.d.	n.d.	n.d.	n.d.	n.d.	n.d.	n.d.	n.d.	n.d.	n.d.	n.d.	n.d.	n.d.
Nb	n.d.	n.d.	n.d.	n.d.	n.d.	n.d.	n.d.	n.d.	n.d.	n.d.	n.d.	n.d.	n.d.	n.d.	n.d.
Zr	n.d.	n.d.	n.d.	n.d.	n.d.	n.d.	n.d.	n.d.	n.d.	n.d.	n.d.	n.d.	n.d.	n.d.	n.d.
Y	n.d.	n.d.	n.d.	n.d.	n.d.	n.d.	n.d.	n.d.	n.d.	n.d.	n.d.	n.d.	n.d.	n.d.	n.d.
Th	n.d.	n.d.	n.d.	n.d.	n.d.	n.d.	n.d.	n.d.	n.d.	n.d.	n.d.	n.d.	n.d.	n.d.	n.d.
La	n.d.	n.d.	n.d.	n.d.	n.d.	n.d.	n.d.	n.d.	n.d.	n.d.	n.d.	n.d.	n.d.	n.d.	n.d.
Ce	n.d.	n.d.	n.d.	n.d.	n.d.	n.d.	n.d.	n.d.	n.d.	n.d.	n.d.	n.d.	n.d.	n.d.	n.d.
Cl	n.d.	n.d.	n.d.	n.d.	n.d.	n.d.	n.d.	n.d.	n.d.	n.d.	n.d.	n.d.	n.d.	n.d.	n.d.

Appendix 1. Continued 14/22.

Occurrence	PIHLAJASALO													RAHIJÄRVI	
Sample	198	199	200	201	202	203	204	205	206	207	208	209	210	211	212
Lithology	GB	GB	GB	GB	GB	GB	GB	GB	GB	GB	GB	GB	GB	GB	GB
SiO2	49.44	48.04	49.25	49.24	55.56	55.69	60.52	54.53	61.23	56.49	56.53	57.10	54.81	52.36	49.50
TiO2	1.21	2.70	2.65	1.77	1.42	2.07	1.01	2.34	0.95	2.23	2.32	2.12	2.95	0.89	0.76
Al2O3	19.21	14.22	16.16	18.05	17.41	17.50	17.71	17.62	17.48	17.30	17.26	17.26	14.94	8.84	20.68
FeOtot	10.95	10.87	12.81	12.86	8.55	9.37	6.78	9.82	6.76	9.14	8.86	9.04	9.84	12.23	8.05
MnO	0.17	0.14	0.17	0.20	0.09	0.12	0.08	0.13	0.06	0.11	0.11	0.11	0.15	0.19	0.14
MgO	7.59	6.27	6.02	5.62	4.82	3.73	3.64	3.60	3.31	3.21	3.10	3.01	2.45	20.01	8.04
CaO	8.08	10.01	8.48	8.47	6.27	6.72	5.32	6.73	4.89	6.19	6.44	6.11	6.25	2.34	9.18
Na2O	2.30	2.10	2.36	2.65	3.17	2.41	2.42	2.70	3.22	1.90	2.83	2.12	3.17	0.43	1.99
K2O	0.86	4.02	1.21	0.88	2.18	1.72	2.14	1.55	1.84	2.49	1.55	2.23	3.95	2.53	1.43
P2O5	0.21	1.62	0.88	0.28	0.52	0.65	0.37	0.98	0.26	0.93	1.00	0.92	1.50	0.18	0.23
Cr	86	150	110	48	110	32	99	23	100	24	25	25	51	1784	362
Ni	69	120	30	52	50	20	40	10	30	10	20	10	20	793	115
V	n.d.	n.d.	n.d.	n.d.	n.d.	n.d.	n.d.	n.d.	n.d.	n.d.	n.d.	n.d.	n.d.	151	175
Cu	44	50	30	44	50	20	20	20	20	20	30	40	30	<20	44
Pb	n.d.	n.d.	n.d.	n.d.	n.d.	n.d.	n.d.	n.d.	n.d.	n.d.	n.d.	n.d.	n.d.	<20	<20
Zn	120	130	50	150	80	60	80	70	80	80	100	90	180	188	134
Co	71	40	20	71	20	20	20	20	20	20	20	20	20	n.d.	n.d.
Sn	n.d.	n.d.	n.d.	n.d.	n.d.	n.d.	n.d.	n.d.	n.d.	n.d.	n.d.	n.d.	n.d.	<20	<20
Mo	n.d.	n.d.	n.d.	n.d.	n.d.	n.d.	n.d.	n.d.	n.d.	n.d.	n.d.	n.d.	n.d.	<10	<10
S	0.13	0.48	0.10	0.15	0.13	0.07	0.07	0.10	0.05	0.07	0.14	0.10	0.48	0.00	0.37
As	n.d.	n.d.	n.d.	n.d.	n.d.	n.d.	n.d.	n.d.	n.d.	n.d.	n.d.	n.d.	n.d.	30	<30
Rb	n.d.	n.d.	n.d.	n.d.	n.d.	n.d.	n.d.	n.d.	n.d.	n.d.	n.d.	n.d.	n.d.	262	130
Ba	n.d.	n.d.	n.d.	n.d.	n.d.	n.d.	n.d.	n.d.	n.d.	n.d.	n.d.	n.d.	n.d.	858	278
Sr	n.d.	n.d.	n.d.	n.d.	n.d.	n.d.	n.d.	n.d.	n.d.	n.d.	n.d.	n.d.	n.d.	37	580
Ga	n.d.	n.d.	n.d.	n.d.	n.d.	n.d.	n.d.	n.d.	n.d.	n.d.	n.d.	n.d.	n.d.	<20	21
Nb	n.d.	n.d.	n.d.	n.d.	n.d.	n.d.	n.d.	n.d.	n.d.	n.d.	n.d.	n.d.	n.d.	16	<10
Zr	n.d.	n.d.	n.d.	n.d.	n.d.	n.d.	n.d.	n.d.	n.d.	n.d.	n.d.	n.d.	n.d.	210	41
Y	n.d.	n.d.	n.d.	n.d.	n.d.	n.d.	n.d.	n.d.	n.d.	n.d.	n.d.	n.d.	n.d.	32	13
Th	n.d.	n.d.	n.d.	n.d.	n.d.	n.d.	n.d.	n.d.	n.d.	n.d.	n.d.	n.d.	n.d.	<10	<10
La	n.d.	n.d.	n.d.	n.d.	n.d.	n.d.	n.d.	n.d.	n.d.	n.d.	n.d.	n.d.	n.d.	47	<30
Ce	n.d.	n.d.	n.d.	n.d.	n.d.	n.d.	n.d.	n.d.	n.d.	n.d.	n.d.	n.d.	n.d.	80	44
Cl	n.d.	n.d.	n.d.	n.d.	n.d.	n.d.	n.d.	n.d.	n.d.	n.d.	n.d.	n.d.	n.d.	102	160

Appendix 1. Continued 15/22.

Occurrence	RAHIJÄRVI													
Sample	213	214	215	216	217	218	219	220	221	222	223	224	225	226
Lithology	GB	GB	GB	GB	GB	GB	GB	GB	GB	GB	GB	GB	GB	GB
SiO2	49.33	46.28	46.97	48.79	46.24	54.30	49.62	48.30	47.02	49.33	46.35	47.70	48.07	49.41
TiO2	0.73	1.80	1.44	0.90	1.71	0.50	1.08	1.78	2.72	2.02	2.03	1.29	0.97	2.01
Al2O3	18.72	17.25	19.50	21.36	18.26	19.02	22.30	19.17	21.50	21.30	21.87	23.22	23.33	21.99
FeOtot	9.55	12.89	11.05	10.47	12.90	8.11	8.43	11.66	11.40	9.83	11.28	8.62	10.47	10.32
MnO	0.15	0.17	0.14	0.18	0.16	0.13	0.06	0.17	0.13	0.11	0.12	0.11	0.12	0.12
MgO	7.73	7.10	6.88	6.48	6.27	6.03	5.98	5.05	5.04	4.88	4.64	4.50	3.45	2.75
CaO	11.38	11.55	11.54	9.69	11.79	9.44	4.52	10.60	7.96	7.46	8.17	10.98	8.72	7.83
Na2O	1.76	2.17	1.64	1.27	1.68	1.34	3.70	2.31	2.40	2.69	2.40	2.03	2.64	3.61
K2O	0.60	0.56	0.60	0.47	0.40	1.00	4.22	0.45	1.58	1.93	2.18	1.18	1.62	1.21
P2O5	0.06	0.23	0.24	0.38	0.58	0.12	0.09	0.51	0.27	0.45	0.95	0.39	0.63	0.76
Cr	324	204	183	363	116	242	229	108	109	124	90	141	138	55
Ni	31	23	35	30	25	47	173	25	66	51	48	33	30	25
V	237	558	282	232	400	122	251	313	262	279	309	268	119	175
Cu	88	58	<20	<20	68	62	240	79	223	120	62	38	53	41
Pb	<20	<20	<20	<20	<20	21	28	<20	<20	22	<20	<20	<20	<20
Zn	97	129	121	137	161	116	294	173	126	139	133	114	134	138
Co	n.d.	n.d.	n.d.	n.d.	n.d.	n.d.	n.d.	n.d.	n.d.	n.d.	n.d.	n.d.	n.d.	n.d.
Sn	<20	<20	<20	<20	34	<20	<20	<20	<20	<20	<20	<20	<20	<20
Mo	<10	<10	<10	<10	<10	<10	12	<10	<10	<10	<10	<10	<10	<10
S	0.11	0.20	0.05	0.01	0.26	0.13	4.12	0.32	0.47	0.24	0.15	0.17	0.13	0.08
As	<30	<30	<30	<30	<30	<30	<30	<30	<30	<30	<30	<30	<30	<30
Rb	31	<10	28	46	<10	63	252	22	59	82	53	75	57	53
Ba	477	273	386	255	248	729	794	695	1026	1881	3352	745	4961	2873
Sr	573	541	875	467	578	597	466	544	743	638	894	749	777	886
Ga	22	24	24	27	27	22	27	27	27	31	23	28	29	25
Nb	<10	<10	<10	<10	<10	<10	17	<10	11	18	<10	11	<10	<10
Zr	85	86	74	23	104	337	165	111	216	237	148	153	1352	1752
Y	13	13	13	<10	15	15	15	17	11	15	14	21	<10	16
Th	<10	<10	<10	<10	<10	<10	12	<10	<10	<10	<10	<10	<10	<10
La	32	31	45	<30	43	62	60	46	45	50	71	41	66	94
Ce	42	59	69	43	71	106	102	83	72	93	116	104	99	156
Cl	50	151	79	51	81	52	1434	169	119	150	85	109	55	96

Appendix 1. Continued 16/22.

Occurrence	RANTALA														
Sample	227	228	229	230	231	232	233	234	235	236	237	238	239	240	241
Lithology	UMAF	UMAF	UMAF	UMAF	UMAF	UMAF	UMAF	GB	GB	GB	GB	M.DYKE	GB	GB	GB
SiO2	45.82	45.94	49.34	47.63	48.85	50.27	50.80	50.17	47.02	47.46	49.74	47.85	49.81	50.12	49.92
TiO2	0.31	0.37	0.57	0.50	0.49	0.69	0.62	0.63	2.00	1.43	0.60	1.75	0.58	0.64	0.75
Al2O3	6.89	7.05	7.16	7.96	7.75	8.04	9.63	10.22	11.68	12.35	17.73	15.03	17.87	17.97	17.66
FeO	13.81	13.54	10.41	11.49	10.13	9.21	9.41	11.68	12.98	12.45	8.44	12.72	8.63	8.78	9.59
MnO	0.24	0.22	0.19	0.20	0.17	0.16	0.19	0.22	0.21	0.21	0.15	0.19	0.15	0.15	0.17
MgO	26.18	25.22	21.88	20.52	18.24	18.04	16.36	15.66	13.51	13.03	10.63	10.52	9.52	9.20	9.19
CaO	5.73	6.82	9.34	10.53	13.21	11.90	11.75	9.80	10.54	10.30	10.15	9.53	10.79	10.00	9.35
Na2O	0.86	0.66	0.83	0.93	0.91	1.36	0.96	1.12	1.07	0.80	1.77	0.53	2.03	2.51	1.09
K2O	0.11	0.14	0.23	0.19	0.18	0.26	0.24	0.47	0.78	1.79	0.76	1.62	0.56	0.56	2.21
P2O5	0.04	0.05	0.05	0.04	0.06	0.07	0.04	0.03	0.21	0.18	0.05	0.26	0.05	0.07	0.07
Cr	980	1297	2580	2106	2110	2200	1248	939	853	761	305	560	206	178	263
Ni	1300	974	1638	2368	2416	2600	408	385	349	396	83	187	71	60	53
V	n.d.	152	244	282	306	n.d.	544	397	287	322	305	333	314	278	291
Cu	490	239	567	1064	1324	1300	148	938	152	24	78	32	32	25	49
Pb	n.d.	<20	<20	<20	22	n.d.	<20	<20	<20	<20	<20	20	<20	<20	<20
Zn	<10	75	98	68	66	n.d.	65	125	119	113	66	131	70	77	84
Co	100	118	109	158	151	34	77	90	85	83	50	61	52	46	55
Sn	n.d.	<20	<20	<20	<20	n.d.	<20	<20	<20	<20	<20	<20	<20	<20	<20
Mo	n.d.	<10	<10	<10	<10	n.d.	<10	<10	<10	<10	<10	<10	<10	<10	<10
S	0.60	0.31	1.05	1.37	1.59	1.72	0.26	0.76	0.22	0.03	0.19	0.11	0.09	0.09	0.12
As	n.d.	<30	<30	<30	<30	n.d.	<30	<30	<30	<30	<30	<30	<30	<30	<30
Rb	n.d.	<10	<10	<10	<10	n.d.	<10	13	27	<10	27	76	19	19	73
Ba	n.d.	30	29	39	41	n.d.	49	74	119	220	88	147	62	78	127
Sr	n.d.	92	28	83	95	n.d.	115	84	167	92	251	139	294	280	214
Ga	n.d.	n.d.	n.d.	n.d.	n.d.	n.d.	n.d.	n.d.	n.d.	n.d.	n.d.	n.d.	n.d.	n.d.	n.d.
Nb	n.d.	<10	<10	<10	<10	n.d.	<10	<10	23	25	<10	16	<10	<10	<10
Zr	n.d.	26	37	33	33	n.d.	34	41	163	96	38	150	47	53	61
Y	n.d.	<10	10	<10	11	n.d.	13	13	23	22	<10	27	12	13	16
Th	n.d.	<10	<10	<10	<10	n.d.	<10	<10	<10	<10	<10	<10	<10	<10	<10
La	n.d.	<30	<30	<30	<30	n.d.	<30	<30	<30	<30	<30	<30	<30	<30	<30
Ce	n.d.	<30	<30	<30	<30	n.d.	<30	<30	53	54	<30	52	<30	<30	30
Cl	n.d.	245	90	117	90	n.d.	39	75	91	212	86	70	33	62	112

Appendix 1. Continued 17/22.

Occurrence	RANTALA		RANTAVUORI					RAUTJÄRVI						
Sample	242	243	244	245	246	247	248	249	250	251	252	253	254	255
Lithology	MARG.	GB	GB	GB	GB	GB	GB	UMAF	UMAF	UMAF	UMAF	UMAF	UMAF	UMAF
SiO2	48.97	54.77	52.77	51.33	57.83	53.95	60.00	50.27	51.30	50.10	49.96	49.76	50.89	51.57
TiO2	1.36	1.24	1.56	1.47	1.28	1.51	0.84	0.62	0.64	0.78	0.76	0.78	0.73	0.71
Al2O3	16.27	17.14	17.58	17.00	18.44	19.34	20.26	7.39	6.60	8.07	7.77	8.10	7.79	7.71
FeO	13.48	10.74	8.64	8.84	7.17	7.79	4.33	9.38	9.49	10.45	10.61	10.96	10.10	10.26
MnO	0.21	0.16	0.12	0.09	0.08	0.10	0.05	0.15	0.16	0.18	0.18	0.18	0.18	0.17
MgO	8.45	5.87	4.46	4.02	3.24	3.06	1.93	21.92	20.89	20.78	20.71	20.28	19.86	19.28
CaO	9.99	6.14	6.75	7.00	6.01	5.46	3.91	9.22	9.86	8.57	9.22	9.04	8.60	8.56
Na2O	0.89	2.29	3.86	4.13	3.70	4.85	5.95	0.81	0.85	0.66	0.49	0.58	0.44	0.48
K2O	0.26	1.54	2.33	3.31	1.82	2.88	2.38	0.09	0.09	0.23	0.15	0.17	1.29	1.12
P2O5	0.11	0.10	1.92	2.81	0.42	1.06	0.35	0.15	0.13	0.18	0.15	0.14	0.14	0.14
Cr	370	145	51	22	50	13	31	2100	2400	1900	1800	2000	2000	2300
Ni	204	529	30	30	10	<10	10	460	670	410	420	340	340	220
V	282	224	n.d.	n.d.	n.d.	n.d.	n.d.	n.d.	n.d.	n.d.	n.d.	n.d.	n.d.	n.d.
Cu	64	659	40	10	<10	20	10	71	85	42	92	57	<10	<10
Pb	21	22	n.d.	n.d.	n.d.	n.d.	n.d.	n.d.	n.d.	n.d.	n.d.	n.d.	n.d.	n.d.
Zn	106	143	60	100	60	70	70	<10	<10	<10	<10	<10	20	<10
Co	62	68	20	20	10	20	20	39	49	29	42	31	29	25
Sn	<20	<20	n.d.	n.d.	n.d.	n.d.	n.d.	n.d.	n.d.	n.d.	n.d.	n.d.	n.d.	n.d.
Mo	<10	<10	n.d.	n.d.	n.d.	n.d.	n.d.	n.d.	n.d.	n.d.	n.d.	n.d.	n.d.	n.d.
S	0.15	0.89	0.18	0.07	0.06	0.25	0.11	0.13	0.27	0.11	0.17	0.09	0.00	0.00
As	<30	<30	n.d.	n.d.	n.d.	n.d.	n.d.	n.d.	n.d.	n.d.	n.d.	n.d.	n.d.	n.d.
Rb	<10	63	n.d.	n.d.	n.d.	n.d.	n.d.	n.d.	n.d.	n.d.	n.d.	n.d.	n.d.	n.d.
Ba	77	262	n.d.	n.d.	n.d.	n.d.	n.d.	n.d.	n.d.	n.d.	n.d.	n.d.	n.d.	n.d.
Sr	215	239	n.d.	n.d.	n.d.	n.d.	n.d.	n.d.	n.d.	n.d.	n.d.	n.d.	n.d.	n.d.
Ga	n.d.	n.d.	n.d.	n.d.	n.d.	n.d.	n.d.	n.d.	n.d.	n.d.	n.d.	n.d.	n.d.	n.d.
Nb	<10	11	n.d.	n.d.	n.d.	n.d.	n.d.	n.d.	n.d.	n.d.	n.d.	n.d.	n.d.	n.d.
Zr	79	94	n.d.	n.d.	n.d.	n.d.	n.d.	n.d.	n.d.	n.d.	n.d.	n.d.	n.d.	n.d.
Y	22	14	n.d.	n.d.	n.d.	n.d.	n.d.	n.d.	n.d.	n.d.	n.d.	n.d.	n.d.	n.d.
Th	<10	<10	n.d.	n.d.	n.d.	n.d.	n.d.	n.d.	n.d.	n.d.	n.d.	n.d.	n.d.	n.d.
La	<30	33	n.d.	n.d.	n.d.	n.d.	n.d.	n.d.	n.d.	n.d.	n.d.	n.d.	n.d.	n.d.
Ce	40	52	n.d.	n.d.	n.d.	n.d.	n.d.	n.d.	n.d.	n.d.	n.d.	n.d.	n.d.	n.d.
Cl	58	73	n.d.	n.d.	n.d.	n.d.	n.d.	n.d.	n.d.	n.d.	n.d.	n.d.	n.d.	n.d.

Appendix 1. Continued 18/22.

Occurrence	RIETSALO														
Sample	256	257	258	259	260	261	262	263	264	265	266	267	268	269	270
Lithology	GB	GB	GB	GB	GB	GB	GB	GB	GB	GB	GB	GB	GB	GB	GB
SiO2	51.15	52.67	53.01	52.02	52.20	53.51	57.45	53.24	52.69	52.92	52.86	46.06	48.40	57.26	57.03
TiO2	0.77	1.00	0.99	0.94	1.08	1.08	1.13	1.52	1.53	1.58	1.58	3.67	1.58	1.22	1.23
Al2O3	15.76	13.70	14.28	15.70	16.07	17.80	15.89	16.81	17.74	18.83	17.77	17.93	21.65	17.97	17.91
FeO	8.84	10.80	10.28	10.92	10.16	9.12	9.10	10.05	9.30	9.57	11.09	11.20	12.09	7.74	8.45
MnO	0.15	0.16	0.14	0.15	0.14	0.13	0.12	0.15	0.12	0.13	0.16	0.18	0.11	0.10	0.11
MgO	11.96	11.47	10.94	9.70	8.93	6.62	6.61	6.53	5.55	5.36	5.25	5.05	5.03	4.68	4.59
CaO	7.86	6.38	6.84	8.01	7.84	7.94	5.75	8.13	7.28	7.45	8.50	10.75	4.48	5.68	6.09
Na2O	1.42	2.23	1.90	1.31	2.00	2.62	1.46	0.70	1.90	2.33	1.44	2.26	3.07	2.88	2.54
K2O	1.84	1.39	1.37	0.91	1.29	0.91	1.72	2.21	2.59	1.41	0.95	0.76	3.54	2.09	1.72
P2O5	0.27	0.22	0.24	0.33	0.29	0.28	0.78	0.64	1.31	0.43	0.41	2.15	0.06	0.38	0.33
Cr	870	590	630	440	350	150	230	140	81	130	45	38	180	160	160
Ni	100	140	250	2740	110	60	100	60	50	40	30	80	90	60	50
V	n.d.	n.d.	n.d.	n.d.	n.d.	n.d.	n.d.	n.d.	n.d.	n.d.	n.d.	n.d.	n.d.	n.d.	n.d.
Cu	<10	80	160	1010	60	50	<10	30	60	40	60	360	100	60	30
Pb	n.d.	n.d.	n.d.	n.d.	n.d.	n.d.	n.d.	n.d.	n.d.	n.d.	n.d.	n.d.	n.d.	n.d.	n.d.
Zn	40	30	30	30	30	30	70	60	80	50	30	20	150	70	50
Co	20	20	30	90	20	20	20	30	30	20	20	50	30	20	20
Sn	n.d.	n.d.	n.d.	n.d.	n.d.	n.d.	n.d.	n.d.	n.d.	n.d.	n.d.	n.d.	n.d.	n.d.	n.d.
Mo	n.d.	n.d.	n.d.	n.d.	n.d.	n.d.	n.d.	n.d.	n.d.	n.d.	n.d.	n.d.	n.d.	n.d.	n.d.
S	0.08	0.09	0.15	1.43	0.13	0.13	0.04	0.16	0.19	0.09	0.13	0.90	0.20	0.17	0.09
As	n.d.	n.d.	n.d.	n.d.	n.d.	n.d.	n.d.	n.d.	n.d.	n.d.	n.d.	n.d.	n.d.	n.d.	n.d.
Rb	n.d.	n.d.	n.d.	n.d.	n.d.	n.d.	n.d.	n.d.	n.d.	n.d.	n.d.	n.d.	n.d.	n.d.	n.d.
Ba	n.d.	n.d.	n.d.	n.d.	n.d.	n.d.	n.d.	n.d.	n.d.	n.d.	n.d.	n.d.	n.d.	n.d.	n.d.
Sr	n.d.	n.d.	n.d.	n.d.	n.d.	n.d.	n.d.	n.d.	n.d.	n.d.	n.d.	n.d.	n.d.	n.d.	n.d.
Ga	n.d.	n.d.	n.d.	n.d.	n.d.	n.d.	n.d.	n.d.	n.d.	n.d.	n.d.	n.d.	n.d.	n.d.	n.d.
Nb	n.d.	n.d.	n.d.	n.d.	n.d.	n.d.	n.d.	n.d.	n.d.	n.d.	n.d.	n.d.	n.d.	n.d.	n.d.
Zr	n.d.	n.d.	n.d.	n.d.	n.d.	n.d.	n.d.	n.d.	n.d.	n.d.	n.d.	n.d.	n.d.	n.d.	n.d.
Y	n.d.	n.d.	n.d.	n.d.	n.d.	n.d.	n.d.	n.d.	n.d.	n.d.	n.d.	n.d.	n.d.	n.d.	n.d.
Th	n.d.	n.d.	n.d.	n.d.	n.d.	n.d.	n.d.	n.d.	n.d.	n.d.	n.d.	n.d.	n.d.	n.d.	n.d.
La	n.d.	n.d.	n.d.	n.d.	n.d.	n.d.	n.d.	n.d.	n.d.	n.d.	n.d.	n.d.	n.d.	n.d.	n.d.
Ce	n.d.	n.d.	n.d.	n.d.	n.d.	n.d.	n.d.	n.d.	n.d.	n.d.	n.d.	n.d.	n.d.	n.d.	n.d.
Cl	n.d.	n.d.	n.d.	n.d.	n.d.	n.d.	n.d.	n.d.	n.d.	n.d.	n.d.	n.d.	n.d.	n.d.	n.d.

Appendix 1. Continued 19/22.

Occurrence	RIETSALO											SIIKAVESI			
Sample	271	272	273	274	275	276	277	278	279	280	281	282	283	284	285
Lithology	GB	GB	GB	GB	GB	GB	GB	GB	GB	GB	GB	GB	GB	GB	GB
SiO2	57.72	58.47	58.43	60.44	57.75	58.67	58.78	59.29	59.68	55.45	50.80	53.19	51.01	51.23	51.98
TiO2	1.15	1.20	1.04	1.03	1.16	1.15	1.19	1.24	1.37	1.12	3.69	0.50	1.15	0.40	0.45
Al2O3	18.38	18.32	18.74	17.30	18.05	18.34	18.40	17.71	17.38	20.34	13.78	10.60	9.29	15.13	16.74
FeO	8.25	8.29	7.43	6.88	7.99	7.52	7.26	7.08	7.76	7.29	11.24	11.69	16.01	10.00	8.49
MnO	0.09	0.07	0.09	0.10	0.09	0.08	0.08	0.09	0.10	0.06	0.13	0.18	0.20	0.15	0.14
MgO	4.59	4.42	4.41	4.33	3.91	3.77	3.75	3.58	3.54	3.28	3.10	16.68	14.08	13.97	11.23
CaO	5.44	4.65	6.33	6.06	5.49	4.86	5.47	5.94	5.66	5.19	7.29	5.31	5.38	7.60	8.27
Na2O	2.48	2.25	0.45	1.84	3.05	2.99	2.44	2.37	2.03	4.43	2.02	0.91	0.65	0.40	1.26
K2O	1.90	2.17	2.81	1.75	2.08	2.49	2.44	2.34	2.14	2.59	5.81	0.95	2.00	1.05	1.31
P2O5	0.00	0.17	0.27	0.28	0.46	0.13	0.19	0.37	0.34	0.25	2.14	0.00	0.23	0.07	0.12
Cr	170	150	91	120	110	150	92	110	89	110	26	1300	1100	880	510
Ni	60	70	40	40	40	50	40	40	30	50	10	50	4620	170	60
V	n.d.	n.d.	n.d.	n.d.	n.d.	n.d.	n.d.	n.d.	n.d.	n.d.	n.d.	n.d.	n.d.	n.d.	n.d.
Cu	70	80	20	10	30	50	50	10	10	50	40	<10	450	110	60
Pb	n.d.	n.d.	n.d.	n.d.	n.d.	n.d.	n.d.	n.d.	n.d.	n.d.	n.d.	n.d.	n.d.	n.d.	n.d.
Zn	70	90	80	60	80	90	80	70	80	120	140	20	100	20	20
Co	20	30	30	20	20	20	20	20	20	30	20	10	220	40	30
Sn	n.d.	n.d.	n.d.	n.d.	n.d.	n.d.	n.d.	n.d.	n.d.	n.d.	n.d.	n.d.	n.d.	n.d.	n.d.
Mo	n.d.	n.d.	n.d.	n.d.	n.d.	n.d.	n.d.	n.d.	n.d.	n.d.	n.d.	n.d.	n.d.	n.d.	n.d.
S	0.15	0.21	0.03	0.07	0.06	0.10	0.16	0.07	0.06	0.24	0.33	0.05	2.80	0.29	0.13
As	n.d.	n.d.	n.d.	n.d.	n.d.	n.d.	n.d.	n.d.	n.d.	n.d.	n.d.	n.d.	n.d.	n.d.	n.d.
Rb	n.d.	n.d.	n.d.	n.d.	n.d.	n.d.	n.d.	n.d.	n.d.	n.d.	n.d.	n.d.	n.d.	n.d.	n.d.
Ba	n.d.	n.d.	n.d.	n.d.	n.d.	n.d.	n.d.	n.d.	n.d.	n.d.	n.d.	n.d.	n.d.	n.d.	n.d.
Sr	n.d.	n.d.	n.d.	n.d.	n.d.	n.d.	n.d.	n.d.	n.d.	n.d.	n.d.	n.d.	n.d.	n.d.	n.d.
Ga	n.d.	n.d.	n.d.	n.d.	n.d.	n.d.	n.d.	n.d.	n.d.	n.d.	n.d.	n.d.	n.d.	n.d.	n.d.
Nb	n.d.	n.d.	n.d.	n.d.	n.d.	n.d.	n.d.	n.d.	n.d.	n.d.	n.d.	n.d.	n.d.	n.d.	n.d.
Zr	n.d.	n.d.	n.d.	n.d.	n.d.	n.d.	n.d.	n.d.	n.d.	n.d.	n.d.	n.d.	n.d.	n.d.	n.d.
Y	n.d.	n.d.	n.d.	n.d.	n.d.	n.d.	n.d.	n.d.	n.d.	n.d.	n.d.	n.d.	n.d.	n.d.	n.d.
Th	n.d.	n.d.	n.d.	n.d.	n.d.	n.d.	n.d.	n.d.	n.d.	n.d.	n.d.	n.d.	n.d.	n.d.	n.d.
La	n.d.	n.d.	n.d.	n.d.	n.d.	n.d.	n.d.	n.d.	n.d.	n.d.	n.d.	n.d.	n.d.	n.d.	n.d.
Ce	n.d.	n.d.	n.d.	n.d.	n.d.	n.d.	n.d.	n.d.	n.d.	n.d.	n.d.	n.d.	n.d.	n.d.	n.d.
Cl	n.d.	n.d.	n.d.	n.d.	n.d.	n.d.	n.d.	n.d.	n.d.	n.d.	n.d.	n.d.	n.d.	n.d.	n.d.

Appendix 1. Continued 20/22.

Occurrence	SIIKAVESI											SIIKASAARI			
Sample	286	287	288	289	290	291	292	293	294	295	296	297	298	299	300
Lithology	GB	GB	GB	GB	GB	GB	GB	GB	GB	GB	GB	GB	GB	GB	GB
SiO2	53.12	51.31	50.60	50.25	50.54	46.96	51.68	52.25	53.59	49.05	64.52	59.47	59.70	58.52	60.15
TiO2	0.78	0.29	1.38	0.30	1.49	3.06	1.02	1.28	1.33	3.01	0.73	0.97	1.04	1.07	1.05
Al2O3	16.72	21.15	17.75	22.94	19.04	13.77	19.78	18.70	19.31	16.89	17.93	17.35	17.41	18.16	17.86
FeO	9.38	6.39	10.63	5.51	9.64	16.12	8.44	10.80	9.89	13.79	4.55	7.70	7.82	7.25	7.13
MnO	0.15	0.10	0.17	0.08	0.15	0.25	0.14	0.13	0.09	0.21	0.05	0.10	0.09	0.08	0.09
MgO	9.21	7.52	6.49	6.16	5.67	5.49	5.47	5.06	4.46	3.37	2.15	4.16	3.90	3.81	3.54
CaO	6.50	10.13	9.00	11.87	9.16	9.52	9.39	7.07	4.28	8.84	5.07	5.73	4.51	4.80	4.81
Na2O	1.91	2.10	2.15	1.66	2.82	1.77	2.51	3.06	3.54	2.92	3.20	2.74	3.21	3.57	3.01
K2O	1.74	0.94	1.47	1.15	1.06	1.12	1.31	1.37	3.36	0.78	1.63	1.48	2.15	2.37	2.10
P2O5	0.49	0.07	0.36	0.07	0.42	1.95	0.26	0.29	0.15	1.14	0.17	0.30	0.18	0.36	0.27
Cr	350	280	110	200	78	13	95	110	130	16	20	130	97	140	110
Ni	100	50	20	70	10	10	20	40	70	<10	10	30	50	40	30
V	n.d.	n.d.	n.d.	n.d.	n.d.	n.d.	n.d.	n.d.	n.d.	n.d.	n.d.	n.d.	n.d.	n.d.	n.d.
Cu	30	30	40	30	30	80	40	10	70	60	<10	30	50	20	60
Pb	n.d.	n.d.	n.d.	n.d.	n.d.	n.d.	n.d.	n.d.	n.d.	n.d.	n.d.	n.d.	n.d.	n.d.	n.d.
Zn	40	20	30	20	30	50	30	50	110	40	50	50	80	70	70
Co	20	10	20	20	10	30	20	20	30	20	10	20	20	20	20
Sn	n.d.	n.d.	n.d.	n.d.	n.d.	n.d.	n.d.	n.d.	n.d.	n.d.	n.d.	n.d.	n.d.	n.d.	n.d.
Mo	n.d.	n.d.	n.d.	n.d.	n.d.	n.d.	n.d.	n.d.	n.d.	n.d.	n.d.	n.d.	n.d.	n.d.	n.d.
S	0.13	0.09	0.18	0.12	0.12	0.45	0.18	0.07	0.27	0.51	0.06	0.09	0.13	0.10	0.15
As	n.d.	n.d.	n.d.	n.d.	n.d.	n.d.	n.d.	n.d.	n.d.	n.d.	n.d.	n.d.	n.d.	n.d.	n.d.
Rb	n.d.	n.d.	n.d.	n.d.	n.d.	n.d.	n.d.	n.d.	n.d.	n.d.	n.d.	n.d.	n.d.	n.d.	n.d.
Ba	n.d.	n.d.	n.d.	n.d.	n.d.	n.d.	n.d.	n.d.	n.d.	n.d.	n.d.	n.d.	n.d.	n.d.	n.d.
Sr	n.d.	n.d.	n.d.	n.d.	n.d.	n.d.	n.d.	n.d.	n.d.	n.d.	n.d.	n.d.	n.d.	n.d.	n.d.
Ga	n.d.	n.d.	n.d.	n.d.	n.d.	n.d.	n.d.	n.d.	n.d.	n.d.	n.d.	n.d.	n.d.	n.d.	n.d.
Nb	n.d.	n.d.	n.d.	n.d.	n.d.	n.d.	n.d.	n.d.	n.d.	n.d.	n.d.	n.d.	n.d.	n.d.	n.d.
Zr	n.d.	n.d.	n.d.	n.d.	n.d.	n.d.	n.d.	n.d.	n.d.	n.d.	n.d.	n.d.	n.d.	n.d.	n.d.
Y	n.d.	n.d.	n.d.	n.d.	n.d.	n.d.	n.d.	n.d.	n.d.	n.d.	n.d.	n.d.	n.d.	n.d.	n.d.
Th	n.d.	n.d.	n.d.	n.d.	n.d.	n.d.	n.d.	n.d.	n.d.	n.d.	n.d.	n.d.	n.d.	n.d.	n.d.
La	n.d.	n.d.	n.d.	n.d.	n.d.	n.d.	n.d.	n.d.	n.d.	n.d.	n.d.	n.d.	n.d.	n.d.	n.d.
Ce	n.d.	n.d.	n.d.	n.d.	n.d.	n.d.	n.d.	n.d.	n.d.	n.d.	n.d.	n.d.	n.d.	n.d.	n.d.
Cl	n.d.	n.d.	n.d.	n.d.	n.d.	n.d.	n.d.	n.d.	n.d.	n.d.	n.d.	n.d.	n.d.	n.d.	n.d.

Appendix 1. Continued 21/22.

Occurrence	SIIKASAARI		SYÖMÄJÄRVI				TURUNEN				VEKARAINEN				
Sample	301	302	303	304	305	306	307	308	309	310	311	312	313	314	315
Lithology	GB	GB	GB	GB	GB	GB	PRD	PRD	PRD	PRD	GB	GB	GB	GB	GB
SiO2	61.23	60.32	52.36	55.21	51.64	53.95	44.43	43.82	45.88	48.82	51.49	50.64	54.15	50.09	50.39
TiO2	1.09	1.11	1.13	0.74	1.89	0.61	0.23	0.25	0.43	0.66	0.65	0.68	0.90	0.90	1.12
Al2O3	17.72	18.11	17.41	16.96	17.15	19.04	2.73	3.79	5.36	5.03	14.40	15.91	16.64	18.18	18.11
FeO	6.61	6.77	9.71	7.93	11.02	8.79	15.92	15.23	14.38	12.24	10.24	10.62	10.58	11.62	10.79
MnO	0.08	0.08	0.14	0.13	0.18	0.16	0.24	0.22	0.22	0.20	0.17	0.17	0.16	0.18	0.15
MgO	3.50	3.19	7.77	7.13	6.56	6.34	30.28	30.19	23.49	20.57	13.44	11.84	8.95	8.53	8.09
CaO	5.20	5.50	9.09	9.11	9.76	7.70	6.18	6.50	9.84	11.57	7.17	7.33	5.75	7.22	8.11
Na2O	2.54	3.31	1.51	1.35	0.51	1.80	0.00	0.00	0.30	0.68	0.93	0.98	0.90	1.49	1.71
K2O	1.70	1.29	0.76	1.29	0.73	1.39	0.00	0.00	0.09	0.18	1.25	1.46	1.64	1.34	1.20
P2O5	0.31	0.33	0.11	0.16	0.55	0.22	0.00	0.00	0.00	0.05	0.26	0.38	0.35	0.45	0.34
Cr	78	54	460	490	300	350	>390	>660	>570	>650	690	520	460	280	250
Ni	40	20	40	10	10	20	670	740	610	620	100	110	90	80	60
V	n.d.	n.d.	n.d.	n.d.	n.d.	n.d.	n.d.	n.d.	n.d.	n.d:	n.d.	n.d.	n.d.	n.d.	n.d.
Cu	30	40	50	<10	20	<10	260	180	130	190	50	70	60	50	40
Pb	n.d.	n.d.	n.d.	n.d.	n.d.	n.d.	n.d.	n.d.	n.d.	n.d.	n.d.	n.d.	n.d.	n.d.	n.d.
Zn	60	50	30	30	20	50	110	120	130	100	20	30	40	30	20
Co	20	10	20	10	10	20	170	170	130	120	30	30	30	20	20
Sn	n.d.	n.d.	n.d.	n.d.	n.d.	n.d.	n.d.	n.d.	n.d.	n.d.	n.d.	n.d.	n.d.	n.d.	n.d.
Mo	n.d.	n.d.	n.d.	n.d.	n.d.	n.d.	n.d.	n.d.	n.d.	n.d.	n.d.	n.d.	n.d.	n.d.	n.d.
S	0.08	0.09	0.04	0.05	0.04	0.03	0.37	0.25	0.27	0.20	0.18	0.30	0.21	0.14	0.14
As	n.d.	n.d.	n.d.	n.d.	n.d.	n.d.	n.d.	n.d.	n.d.	n.d.	n.d.	n.d.	n.d.	n.d.	n.d.
Rb	n.d.	n.d.	n.d.	n.d.	n.d.	n.d.	n.d.	n.d.	n.d.	n.d.	n.d.	n.d.	n.d.	n.d.	n.d.
Ba	n.d.	n.d.	n.d.	n.d.	n.d.	n.d.	n.d.	n.d.	n.d.	n.d.	n.d.	n.d.	n.d.	n.d.	n.d.
Sr	n.d.	n.d.	n.d.	n.d.	n.d.	n.d.	n.d.	n.d.	n.d.	n.d.	n.d.	n.d.	n.d.	n.d.	n.d.
Ga	n.d.	n.d.	n.d.	n.d.	n.d.	n.d.	n.d.	n.d.	n.d.	n.d.	n.d.	n.d.	n.d.	n.d.	n.d.
Nb	n.d.	n.d.	n.d.	n.d.	n.d.	n.d.	n.d.	n.d.	n.d.	n.d.	n.d.	n.d.	n.d.	n.d.	n.d.
Zr	n.d.	n.d.	n.d.	n.d.	n.d.	n.d.	n.d.	n.d.	n.d.	n.d.	n.d.	n.d.	n.d.	n.d.	n.d.
Y	n.d.	n.d.	n.d.	n.d.	n.d.	n.d.	n.d.	n.d.	n.d.	n.d.	n.d.	n.d.	n.d.	n.d.	n.d.
Th	n.d.	n.d.	n.d.	n.d.	n.d.	n.d.	n.d.	n.d.	n.d.	n.d.	n.d.	n.d.	n.d.	n.d.	n.d.
La	n.d.	n.d.	n.d.	n.d.	n.d.	n.d.	n.d.	n.d.	n.d.	n.d.	n.d.	n.d.	n.d.	n.d.	n.d.
Ce	n.d.	n.d.	n.d.	n.d.	n.d.	n.d.	n.d.	n.d.	n.d.	n.d.	n.d.	n.d.	n.d.	n.d.	n.d.
Cl	n.d.	n.d.	n.d.	n.d.	n.d.	n.d.	n.d.	n.d.	n.d.	n.d.	n.d.	n.d.	n.d.	n.d.	n.d.

Appendix 1. Continued 22/22.

Occurrence	VEKARAINEN					VIRMAANLAHTI						
Sample	316	317	318	319	320	321	322	323	324	325	326	327
Lithology	GB	GB	GB	GB	GB	GB	GB	GB	GB	GB	GB	GB
SiO2	51.68	49.41	48.65	51.74	57.29	53.53	54.24	55.88	53.16	52.06	54.73	52.92
TiO2	1.10	1.16	1.74	1.11	0.65	0.54	0.55	0.52	0.62	0.74	0.81	0.63
Al2O3	17.23	19.03	20.07	16.69	18.45	8.13	8.01	8.76	10.35	11.83	12.01	15.11
FeO	10.93	9.90	15.27	11.32	6.87	13.12	13.38	12.48	12.14	10.96	10.51	8.84
MnO	0.13	0.12	0.19	0.13	0.09	0.19	0.19	0.18	0.18	0.16	0.15	0.13
MgO	7.18	7.00	6.92	6.49	5.61	19.15	18.53	16.99	16.03	14.13	12.84	9.99
CaO	7.01	7.65	4.78	6.61	6.51	4.05	3.92	3.86	5.86	7.37	6.89	9.48
Na2O	1.90	2.23	1.05	2.28	2.33	0.00	0.14	0.17	0.48	1.22	0.30	1.64
K2O	1.96	2.47	1.26	1.56	1.77	1.12	0.87	1.02	1.02	1.05	1.47	1.04
P2O5	0.89	1.03	0.07	0.06	0.43	0.18	0.17	0.14	0.17	0.48	0.29	0.22
Cr	210	130	230	170	110	1900	1800	1700	1500	1500	980	690
Ni	60	30	130	100	40	900	820	390	340	100	160	70
V	n.d.	n.d.	n.d.	n.d.	n.d.	n.d.	n.d.	n.d.	n.d.	n.d.	n.d.	n.d.
Cu	50	20	120	100	20	290	280	110	120	10	110	40
Pb	n.d.	n.d.	n.d.	n.d.	n.d.	n.d.	n.d.	n.d.	n.d.	n.d.	n.d.	n.d.
Zn	40	50	60	50	40	30	30	30	20	30	30	20
Co	20	30	40	30	20	70	60	40	30	10	30	10
Sn	n.d.	n.d.	n.d.	n.d.	n.d.	n.d.	n.d.	n.d.	n.d.	n.d.	n.d.	n.d.
Mo	n.d.	n.d.	n.d.	n.d.	n.d.	n.d.	n.d.	n.d.	n.d.	n.d.	n.d.	n.d.
S	0.17	0.19	0.43	0.38	0.08	0.75	0.50	0.25	0.24	0.06	0.20	0.10
As	n.d.	n.d.	n.d.	n.d.	n.d.	n.d.	n.d.	n.d.	n.d.	n.d.	n.d.	n.d.
Rb	n.d.	n.d.	n.d.	n.d.	n.d.	n.d.	n.d.	n.d.	n.d.	n.d.	n.d.	n.d.
Ba	n.d.	n.d.	n.d.	n.d.	n.d.	n.d.	n.d.	n.d.	n.d.	n.d.	n.d.	n.d.
Sr	n.d.	n.d.	n.d.	n.d.	n.d.	n.d.	n.d.	n.d.	n.d.	n.d.	n.d.	n.d.
Ga	n.d.	n.d.	n.d.	n.d.	n.d.	n.d.	n.d.	n.d.	n.d.	n.d.	n.d.	n.d.
Nb	n.d.	n.d.	n.d.	n.d.	n.d.	n.d.	n.d.	n.d.	n.d.	n.d.	n.d.	n.d.
Zr	n.d.	n.d.	n.d.	n.d.	n.d.	n.d.	n.d.	n.d.	n.d.	n.d.	n.d.	n.d.
Y	n.d.	n.d.	n.d.	n.d.	n.d.	n.d.	n.d.	n.d.	n.d.	n.d.	n.d.	n.d.
Th	n.d.	n.d.	n.d.	n.d.	n.d.	n.d.	n.d.	n.d.	n.d.	n.d.	n.d.	n.d.
La	n.d.	n.d.	n.d.	n.d.	n.d.	n.d.	n.d.	n.d.	n.d.	n.d.	n.d.	n.d.
Ce	n.d.	n.d.	n.d.	n.d.	n.d.	n.d.	n.d.	n.d.	n.d.	n.d.	n.d.	n.d.
Cl	n.d.	n.d.	n.d.	n.d.	n.d.	n.d.	n.d.	n.d.	n.d.	n.d.	n.d.	n.d.

Appendix 2. Microprobe analyses of olivine and orthopyroxene. PRD=peridotite, GB=gabbro, UMAF=ultramafic lava and sill. Fo and En in m-%, Ni, Co and Cu in ppm.										
Occurrence	**Sample**	**Lithology**	**Fo**	**Ni(ol)**	**Co(ol)**	**Cu(ol)**	**En**	**Ni(opx)**	**Co(opx)**	**Cu(opx)**
KEKONEN	1	PRD	75.40	1120	260		80.02	230	190	
	2	PRD	72.83	1340	340		77.75	220	110	
	3	PRD	72.59	800			76.20	200		
	4	PRD	71.63	780			78.14	170		
KIISKILÄNKANGAS	5	GB	80.27	150			82.52	<100		
	6	PRD	77.28	280			83.73	<100		
	7	PRD	76.68	880	260					
	8	PRD	75.44	230			80.36	<100		
	9	PRD	75.12	330	320		80.40	<100	160	
	10	PRD	74.89	480			78.94	110		
	11	PRD					80.14	<100		
LEVÄNOMAINEN	12	UMAF	73.27	2500			78.67	500		
LUMPEINEN	13	PRD	77.95	470	<100	260				
	14	PRD	77.72	380	290					
	15	PRD	77.51	550						
	16	PRD	77.18	430						
	17	PRD	76.61	410						
	18	PRD	76.55	360						
	19	PRD	76.34	310		<100				
	20	PRD	76.26	260						
	21	PRD	76.19	380						
	22	PRD	76.14	360						
	23	PRD	75.92	340						
	24	PRD	75.83	310						
	25	PRD	75.72	360						
	26	PRD	75.53	320						
	27	PRD	75.51	270						
	28	PRD	75.44	650						
	29	PRD	75.36	270						
	30	PRD	75.08	310						
	31	PRD	74.72	260						
	32	PRD	74.70	370						
	33	PRD	74.62	330						
	34	PRD	74.35	290						
	35	PRD	73.91	180	320					
	36	PRD	73.79	260	280					
	37	PRD	73.65	280	310					
	38	PRD	73.65	340						
	39	PRD	73.49	250						
	40	PRD	73.39	250						
	41	PRD	73.35	300						
	42	PRD	73.28	300						
	43	PRD	73.15	320						
	44	PRD	73.02	220	230					
	45	PRD	72.93	290						
	46	PRD	72.68	320	330					
	47	PRD	72.62	310						
	48	PRD	72.42	340						
	49	PRD	72.07	310	340					
	50	PRD	71.86	310						
	51	PRD	71.80	310	250					
	52	PRD	71.57	270						
	53	PRD	71.43	270						

Appendix 2. Continued 2/4.										
Occurrence	Sample	Lithology	Fo	Ni(ol)	Co(ol)	Cu(ol)	En	Ni(opx)	Co(opx)	Cu(opx)
LUMPEINEN	54	PRD	71.36	260						
	55	PRD	70.84	280						
	56	PRD	70.18	140						
	57	PRD	69.22	410						
	58	PRD	68.89	330						
	59	PRD	66.12	300						
MYLLYNKYLÄ	60	UMAF	71.23	2080	330					
	61	UMAF	68.03	1670						
NIINIMÄKI E	62	PRD	82.11	940		220	83.40	260		<100
	63	PRD	81.85	1270			83.56	350		320
	64	PRD	81.64	960		140	83.38	220		210
	65	PRD	81.49	1170						
	66	PRD	81.28	990		190	82.96	270		330
	67	PRD	81.25	1060		420	82.58	210		230
	68	PRD	81.04	1060		<100	82.53	200		320
	69	PRD	80.22	890						
	70	PRD	77.73	970			80.35	360		120
NIINIMÄKI W	71	PRD	80.32	560			82.51	260		
	72	PRD	80.21	530			82.31	160		
	73	PRD	79.70	770						
	74	PRD	79.36	860			81.31	<100		180
	75	PRD	78.58	750	210					
	76	PRD	77.49	950	130					
PAKINMAA	77	UMAF	76.16	2520			80.40	410		
	78	UMAF	73.98	2090	290		78.16	340	140	
PIHLAJASALO	79	PRD	84.78	900						
	80	PRD	84.63	1010						
	81	PRD	84.31	990						
	82	PRD	84.19	930	210					
	83	PRD	83.07	930	200					
	84	PRD	82.03	900						
	85	PRD	81.84	690	210					
	86	PRD	81.70	690						
	87	PRD	81.37	650						
	88	PRD	81.24	640						
	89	PRD	81.09	780	240					
	90	PRD	80.23	1360	310					
	91	PRD	80.22	380						
	92	PRD	79.44	800						
	93	PRD	78.87	210						
	94	PRD	78.86	460	230					
	95	PRD	76.68	760						
RANTALA	96	UMAF	78.67	580			81.21	100		
	97	UMAF	74.00	630						
	98	UMAF	72.41	700			79.10	120		
	99	UMAF	70.09	570						
	100	UMAF	67.97	760	<100		76.61	120	160	
	101	UMAF	65.85	730	410					
	102	UMAF					93.79	<100		
RAUTJÄRVI	103	UMAF	73.28	1190			78.88	250		
	104	UMAF	69.94	1090			77.21	210		
	105	UMAF	69.77	1100	350		76.20	210	120	
	106	UMAF	69.01	1020			76.53	210		
	107	UMAF					73.50	310		

Appendix 2. Continued 3/4.										
Occurrence	Sample	Lithology	Fo(m-%)	Ni(ol)	Co(ol)	Cu(ol)	En	Ni(opx)	Co(opx)	Cu(opx)
RAUTJÄRVI	108	UMAF					76.82	190		
	109	UMAF					73.31	410		
SAARIJÄRVI N	110	PRD	79.45	810			80.65	210		
	111	PRD	78.67	1270			81.65	260		
	114	PRD	78.48	1180						
	115	PRD	78.27	1090			81.39	200		
	116	PRD	78.24	1090			81.35	220		
	117	PRD	78.22	1020			82.14	180		
	121	PRD	78.00	1190			82.46	230		
	124	PRD	77.71	1100	300		81.21	210	170	
	126	PRD	77.61	1120						
	127	PRD	77.58	890			80.71	150		
	128	PRD	77.55	1080						
	129	PRD	77.49	1000			80.95	220		
	133	PRD	77.44	900	310	120	81.03	180	110	<100
	134	PRD	77.43	900	290		81.07	180	<100	
	135	PRD	77.39	1120			80.67	260		
	136	PRD	77.36	960			80.60	220		
	139	PRD	77.12	1020			82.44	280		
	140	PRD	76.99	1070			80.58	220		
	141	PRD	76.87	1100	220	130	82.42	220	140	170
	143	PRD	76.68	1220			80.87	250		
	147	PRD	76.51	1330			81.47	290		
	148	PRD	76.45	900			80.38	170		
	149	PRD	76.44	930						
	150	PRD	76.40	1100			79.92	200		
	151	PRD	76.31	1360			80.26	300		
	154	PRD	76.23	1180			79.45	260		
	157	PRD	76.09	1020			80.00	190		
	159	PRD	75.90	1250			79.79	240		
	160	PRD	75.83	900			79.98	160		
	162	PRD	74.85	940			78.96	190		
	164	PRD	74.31	1260			78.36	260		
	165	PRD	74.29	1140			79.79	210		
SAARIJÄRVI S	112	PRD	78.66	1300			82.50	260		
	113	PRD	78.59	1340	290		83.75	340	110	
	118	PRD	78.12	1340			83.49	380		180
	119	PRD	78.09	1310			80.97	220		
	120	PRD	78.00	1390			83.06	300		
	122	PRD	77.81	1270			82.80	340		
	123	PRD	77.74	1370			82.22	300		390
	125	PRD	77.67	1520			83.29	340		
	130	PRD	77.46	1230			80.26	230		
	131	PRD	77.46	1310			80.75	270		260
	132	PRD	77.46	1400			83.04	310		
	137	PRD	77.31	1250			80.73	220		
	138	PRD	77.19	1020			79.65	320		180
	142	PRD	76.84	1300			80.22	230		
	144	PRD	76.67	1230	250		82.36	280	140	
	145	PRD	76.63	1350			79.61	260		
	146	PRD	76.56	1240		660	81.45	260		130
	152	PRD	76.30	1360			81.99	260		
	153	PRD	76.26	1140			79.43	210		
	155	PRD	76.18	1290		140	79.96	220		<100

Appendix 2. Continued 4/4.										
Occurrence	**Sample**	**Lithology**	**Fo(m-%)**	**Ni(ol)**	**Co(ol)**	**Cu(ol)**	**En**	**Ni(opx)**	**Co(opx)**	**Cu(opx)**
SAARIJÄRVI S	156	PRD	76.12	1390			81.75	330		
	158	PRD	75.99	1300		<100	80.20	250		<100
	161	PRD	75.67	1070			80.67	210		
	163	PRD	74.80	1050	350		79.35	220	130	
	166	PRD					81.93	290		
TURUNEN	167	PRD	75.31	620	330					
	168	PRD	74.83	780	330					
	169	PRD	69.25	860	370					
	170	PRD	69.12	780	410					

Appendix 3. Whole rock REE-analyses (ppm). GB=gabbro, PRD=peridotite, MARG.=chilled margin, !=below detection limit.

Occurrence	RIETSALO						TURUNEN		PIHLAJASALO				KEKONEN					
Sample	1	2	3	4	5	6	7	8	9	10	11	12	13	14	15	16	17	18
Lithology	GB	GB	GB	GB	GB	GB	PRD	PRD	GB	GB	PRD	PRD	GB	GB	GB	GB	GB	GB
Ce	52.90	37.50	39.90	36.70	31.00	41.00	8.01	3.23	31.80	46.50	6.46	4.82	13.80	21.20	19.30	14.50	11.50	20.80
Dy	4.89	3.25	3.52	3.26	2.98	3.16	1.80	0.55	4.43	6.05	0.90	0.62	2.18	3.08	2.94	2.26	1.27	1.51
Er	2.76	1.83	2.06	1.84	1.69	1.71	0.91	0.29	2.57	3.54	0.51	0.34	1.38	1.81	1.77	1.34	0.84	0.73
Eu	1.98	1.37	1.40	1.20	1.10	1.34	0.59	0.18	1.46	1.70	0.25	0.18	0.64	1.00	0.88	0.72	0.50	0.94
Gd	6.05	4.04	4.47	4.13	4.04	3.99	2.17	0.57	4.43	6.19	0.89	0.67	2.43	3.43	3.24	2.52	1.72	2.02
Ho	0.96	0.65	0.76	0.71	0.65	0.60	0.32	0.11	0.93	1.27	0.19	0.13	0.47	0.65	0.62	0.46	0.30	0.29
La	24.00	17.50	18.20	16.40	13.50	18.70	3.12	1.47	14.00	20.40	2.86	2.10	6.03	9.59	8.67	6.15	5.16	10.30
Lu	0.34	0.25	0.26	0.25	0.24	0.22	0.11	0.04!	0.35	0.54	0.07!	0.06!	0.19	0.27	0.24	0.19	0.11	0.12
Nd	29.10	20.50	22.80	20.40	18.60	22.30	6.37	2.05	17.50	25.70	3.78	2.85	8.61	12.40	11.70	8.86	6.80	10.30
Pr	6.98	4.83	5.17	4.81	4.29	5.22	1.27	0.46	4.11	5.99	0.87	0.68	1.91	2.74	2.55	1.98	1.49	2.58
Sm	5.59	3.96	4.36	4.17	3.71	4.12	1.92	0.55	3.60	5.56	0.88	0.59	1.99	2.97	2.70	2.01	1.46	2.03
Tb	0.88	0.59	0.65	0.57	0.59	0.57	0.34	0.10!	0.66	0.98	0.15	0.11	0.38	0.53	0.51	0.38	0.26	0.28
Tm	0.38	0.25	0.30	0.29	0.26	0.23	0.11	0.04!	0.37	0.53	0.07	0.04!	0.20	0.25	0.25	0.18	0.12	0.11
Yb	2.49	1.66	1.91	1.90	1.62	1.51	0.77	0.32	2.53	3.61	0.49	0.28	1.19	1.60	1.64	1.33	0.83	0.72

Occurrence	RANTALA					KIISKILÄNKANGAS		LUMPEINEN		NIINIMÄKI				SAARIJÄRVI				VENETEKEMÄ	
Sample	19	20	21	22	23	24	25	26	27	28	29	30	31	32	33	34	35	36	37
Lithology	M.DYKE	UMAF	GB	GB	MARG.	PRD	GB	PRD	PRD	GB	PRD	PRD	GB	PRD	PRD	PRD	PRD	PRD	PRD
Ce	37.40	7.01	9.03	12.10	18.20	16.90	12.40	2.78	4.63	10.40	13.10	5.24	9.85	24.80	21.60	19.30	12.50	4.29	8.02
Dy	4.77	1.54	2.31	2.36	4.17	1.24	1.60	1.14	1.73	0.96	1.07	0.37	0.80	2.40	1.80	1.66	1.09	0.62	0.70
Er	2.35	0.88	1.43	1.42	2.28	0.74	1.20	0.54	0.97	0.55	0.60	0.21	0.47	1.24	0.94	0.81	0.61	0.31	0.43
Eu	1.54	0.26	0.54	0.77	1.19	0.52	0.47	0.29	0.62	0.43	0.34	0.23	0.39	0.64	0.55	0.57	0.46	0.22	0.29
Gd	5.86	1.36	2.19	2.44	4.32	1.67	1.75	1.22	2.04	1.12	1.18	0.42	0.86	3.22	2.35	2.13	1.47	0.72	0.99
Ho	0.93	0.31	0.45	0.53	0.83	0.24	0.37	0.22	0.39	0.18	0.22	0.06!	0.16	0.46	0.34	0.32	0.21	0.12	0.16
La	14.90	2.94	3.80	5.08	6.90	7.84	6.15	1.01	1.52	5.05	6.12	2.67	5.30	11.20	9.95	8.55	6.14	1.91	3.77
Lu	0.35	0.14	0.19	0.23	0.33	0.10	0.17	0.07!	0.12	0.09!	0.09!	0.03!	0.09!	0.18	0.11	0.11	0.09!	0.03!	0.04!
Nd	23.80	4.43	6.06	7.48	13.20	9.01	6.45	2.57	4.88	5.20	6.00	2.12	4.25	14.00	11.60	9.96	6.64	2.90	4.37
Pr	5.33	1.01	1.30	1.68	2.78	2.14	1.55	0.47	0.89	1.37	1.56	0.60	1.15	3.24	2.77	2.48	1.57	0.57	0.98
Sm	5.44	1.16	1.63	1.88	3.31	1.60	1.33	0.99	1.57	1.21	1.24	0.39	0.92	3.06	2.15	2.12	1.47	0.71	0.91
Tb	0.82	0.24	0.34	0.38	0.66	0.25	0.26	0.18	0.34	0.18	0.19	0.07!	0.13	0.47	0.33	0.30	0.22	0.11	0.13
Tm	0.37	0.13	0.20	0.20	0.31	0.09	0.18	0.08	0.13	0.08	0.09	0.02!	0.09	0.18	0.13	0.13	0.10	0.05	0.06
Yb	2.21	0.88	1.23	1.34	2.22	0.66	1.08	0.51	0.87	0.62	0.52	0.12!	0.65	1.15	0.83	0.85	0.57	0.32	0.34

LITHOLOGICAL MAP OF THE JUVA AREA

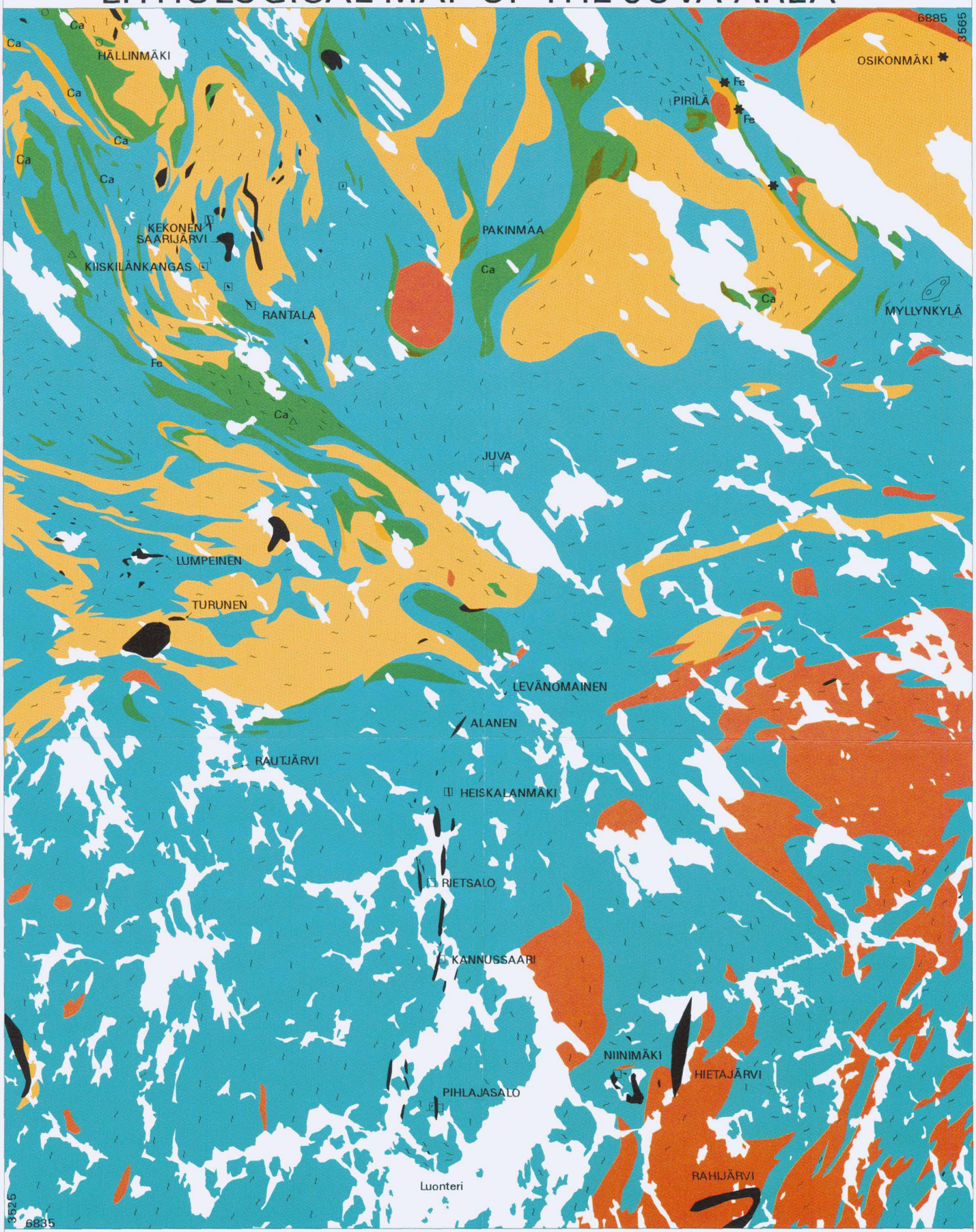

- Granite and pegmatite/foliated
- Tonalite, quartz diorite, granodiorite/foliated
- Ultramafic volcanics and hybabyssal rocks
- Gabbro and peridotite
- Mafic and intermediate volcanics
- Felsic volcanics and quartz-feldspar gneiss
- Marble
- Mica gneiss and mica schist/conglomerate

5 km

- Fe Iron Formation
- Ca Calsic interlayers
- □ Ni-Cu-occurrence
- ○ Cu-occurrence
- ✱ Au-occurrence
- △ Zn-occurrence

The map is modified after the 1 : 100 000 scale geological maps published by the Geological Survey of Finland.

ISBN 951-690-630-3

Compiled by H. V. Makkonen 1996

Tätä julkaisua myy

GEOLOGIAN
TUTKIMUSKESKUS (GTK)
Julkaisumyynti
02150 Espoo
☎ (90) 46 931
Teleksi: 123185 geolo fi
Telekopio: (90) 462 205

GTK, Väli-Suomen
aluetoimisto
Kirjasto
PL 1237
70211 Kuopio
☎ (971) 205 111
Telekopio: (971) 205 215

GTK, Pohjois-Suomen
aluetoimisto
Kirjasto
PL 77
96101 Rovaniemi
☎ (960) 3297 111
Teleksi: 37295 geolo fi
Telekopio: (960) 3297 289

Denna publikation säljes av

GEOLOGISKA
FORSKNINGSCENTRALEN (GFC)
Publikationsförsäljning
02150 Esbo
☎ (90) 46 931
Telex: 123185 geolo fi
Telefax: (90) 462 205

GFC, Distriktsbyrån för
Mellersta Finland
Biblioteket
PB 1237
70211 Kuopio
☎ (971) 205 111
Telefax: (971) 205 215

GFC, Distriktsbyrån för
Norra Finland
Biblioteket
PB 77
96101 Rovaniemi
☎ (960) 3297 111
Telex: 37295 geolo fi
Telefax: (960) 3297 289

This publication can be obtained
from
GEOLOGICAL SURVEY
OF FINLAND (GSF)
Publication sales
FIN-02150 Espoo, Finland
☎ +358 0 46 931
Telex: 123185 geolo fi
Telefax: +358 0 462 205

GSF, Regional office for
Mid-Finland
Library
P.O. Box 1237
FIN-70211 Kuopio, Finland
☎ +358 71 205 111
Telefax: +358 71 205 215

GSF, Regional office for
Northern Finland
Library
P.O. Box 77
FIN-96101 Rovaniemi
☎ +358 60 3297 111
Telex: 37295 geolo fi
Telefax: +358 60 3297 289

E-mail: info@gsf.fi
WWW-address: http://www.gsf.fi

ISBN 951-690-630-3
ISSN 0367-522X